
Doctoral Dissertations

Student Theses and Dissertations

Fall 2018

Part I: Design, synthesis, and studies of novel age-inhibitors and age-breakers; Part II: Novel synthetic methods for organofluorine compound

Jatin Mehta

Follow this and additional works at: https://scholarsmine.mst.edu/doctoral_dissertations

 Part of the [Analytical Chemistry Commons](#), and the [Organic Chemistry Commons](#)

Department: Chemistry

Recommended Citation

Mehta, Jatin, "Part I: Design, synthesis, and studies of novel age-inhibitors and age-breakers; Part II: Novel synthetic methods for organofluorine compound" (2018). *Doctoral Dissertations*. 3136.
https://scholarsmine.mst.edu/doctoral_dissertations/3136

This thesis is brought to you by Scholars' Mine, a service of the Missouri S&T Library and Learning Resources. This work is protected by U. S. Copyright Law. Unauthorized use including reproduction for redistribution requires the permission of the copyright holder. For more information, please contact scholarsmine@mst.edu.

PART I: DESIGN, SYNTHESIS, AND STUDIES OF NOVEL AGE-INHIBITORS
AND AGE-BREAKERS; PART II: NOVEL SYNTHETIC METHODS FOR
ORGANOFLUORINE COMPOUNDS

by

JATIN MEHTA

A DISSERTATION

Presented to the Faculty of the Graduate School of the
MISSOURI UNIVERSITY OF SCIENCE AND TECHNOLOGY

In Partial Fulfillment of the Requirements for the Degree

DOCTOR OF PHILOSOPHY

in

CHEMISTRY

2018

Approved by:

Dr. V. Prakash Reddy, Advisor
Dr. Nuran Ercal
Dr. Yinfa Ma
Dr. Jeffrey G. Winiarz
Dr. K. Chandrashekhara

© 2018

Jatin Mehta

All Rights Reserved

ABSTRACT

Novel small molecule inhibitors and breakers of advanced glycation end-products (AGEs) have been synthesized and their *in-vitro* inhibitory activities have been studied by ^{13}C NMR, fluorescence, and UV-visible spectroscopy. We have demonstrated that these AGE-inhibitors and AGE-breakers were found to be more effective in their sequestration of AGE intermediates, such as dehydroascorbate (DHA) than the state-of-the-art phenacylthiazolium bromide (PTB)-based AGE-inhibitors and AGE-breakers. Citric acid and other polyphenolic antioxidants have substantial AGE inhibitory effects in the D-glucose/leucine or benzylamine Maillard reaction model systems, and thus they are suitable as dietary additives for ameliorating AGE-induced complications.

Organofluorine compounds have found numerous applications as pharmaceutically interesting compounds, and toward developing novel synthetic methods for organofluorine compounds, we have investigated synthetic strategies for *gem*-difluoro and trifluoromethyl compounds. *gem*-Difluorination of 1,3-dithiolanes, obtained from the corresponding ketones, form *gem*-difluoromethylene compounds through the photoredox catalysis, using photocatalyst 9-fluorenone in the presence of visible light (household bulb 13W CFL). This reaction proceeds under mild conditions and is applicable to *gem*-difluorination of variously substituted diaryl 1,3-dithiolanes. We have also developed a novel NHC-catalyzed trifluoromethylation of aromatic *N*-tosyl aldimines with electron-withdrawing as well as electron-donating groups on the aryl ring. We have synthesized a series of novel purine-based triazole derivatives as potential CDK-inhibitors and characterized their structures using high-field ^1H - and ^{13}C -NMR spectroscopy.

ACKNOWLEDGMENTS

First and foremost, I would like to thank my advisor, Dr. V. Prakash Reddy for his continuous guidance and support during my pursuit of graduate studies at Missouri University of Science and Technology. He shaped the researcher in me by giving me the freedom to think and work independently. Moreover, I admire his compassion and discipline, which inspired me to be passionate and hard-working. I want to thank Dr. Jeffrey G. Winiarz, Dr. Nuran Ercal, Dr. Yinfa Ma, and Dr. K. Chandrashekhara for being part of my advisory committee.

I would like to thank my former and current lab members Dr. Avinash Raju Vadapalli, Puspa Aryal, and all undergraduates for their help and expertise in helping complete my research work. I would like to thank the Department of Chemistry at the Missouri University of Science and Technology for the financial support provided through teaching assistantships and other resources. I am also thankful to all teaching and non-teaching staff, and students of the Department of Chemistry for their help with course work and making my stay comfortable at Missouri University of Science and Technology.

Words cannot render the love, appreciation and gratefulness I have towards my family; beloved wife Meenakshi and son Tavish for the unconditional love and support they have extended to me during my research.

TABLE OF CONTENTS

	Page
ABSTRACT.....	iii
ACKNOWLEDGMENTS	iv
LIST OF ILLUSTRATIONS.....	ix
LIST OF TABLES	xvii
NOMENCLATURE	xviii
 SECTION	
1. INTRODUCTION.....	1
2. DESIGN, SYNTHESIS AND STUDIES OF NOVEL AGE-INHIBITORS AND AGE-BREAKERS	4
2.1. BACKGROUND	4
2.1.1. Effects of AGEs on Human Health.....	6
2.1.2. AGE-Inhibitors and AGE-Breakers.	7
2.1.2.1. Naturally occurring AGE-inhibitors and their inhibitory effects.....	8
2.1.2.2. Synthetic AGE-inhibitors and their inhibitory effects.....	8
2.1.2.3. AGE-breakers and their inhibitory effects.....	12
2.2. RESULTS AND DISCUSSION.....	15
2.2.1. Synthesis of N-phenacylthiazolium Halide (PTB) and its Derivatives.	21
2.2.2. Synthesis of N-phenacyl-3-methylimidazolium Halide and its Nitro Derivative	24
2.2.3. Synthesis of Dimers of Phenacylthiazolium (PTB) and Phenacylimidazolium Halides	24

2.2.4. Reactivity Study of AGE-Inhibitors and AGE-Breakers by ¹³ C NMR Spectroscopy	26
2.2.4.1. In situ PTB-DHA adduct formation.....	27
2.2.4.2. In situ adduct formation of DHA with novel AGE-inhibitors and AGE-breakers	27
2.3. EXPERIMENTAL	31
2.3.1. Materials and Methods	31
2.3.2. Preparation of Dehydroascorbic Acid (DHA) and its Reaction with AGE-Inhibitors and-Breakers	31
2.3.3. Synthesis and Properties of Products	32
2.3.4. NMR Spectra of the Products.....	44
3. POLYPHENOLIC ANTIOXIDANTS AND CITRIC ACID AS INHIBITORS OF THE ADVANCED GLYCATION ENDPRODUCTS: A ¹³ C NMR SPECTROSCOPIC STUDY	64
3.1. BACKGROUND	64
3.2. MATERIALS AND METHODS.....	67
3.2.1. Glycation Studies Using D-glucose/L-leucine Model System.....	67
3.2.2. Fluorescence Measurements.....	68
3.2.3. Glycation Studies Using D-glucose/Benzylamine Model System	68
3.3. RESULTS AND DISCUSSION.....	68
3.3.1. D-glucose and L-leucine Model System.	68
3.3.2. D-glucose and Benzylamine Model System	74
4. A NOVEL PHOTOREDOX-CATALYZED gem-DIFLUORINATION OF 1,3-DITHIOLANES	79
4.1. BACKGROUND	79
4.1.1. Direct Fluorination	80

4.1.2. Insertion of Functionalized Difluorinated Building Blocks	82
4.1.3. Photoredox Catalysis and Fluorination.	85
4.1.3.1. Photoredox catalyzed selective C-H gem-difluorination.....	85
4.1.3.2. Photoredox catalyzed gem-difluoromethylation through in-situ generated difluoromethylene (CF ₂) group.....	87
4.1.3.3. Photoredox-catalyzed decarboxylative aliphatic fluorination. .	88
4.2. RESULTS AND DISCUSSION	89
4.3. EXPERIMENTAL.....	93
4.3.1. Materials and Methods	93
4.3.2. General Synthetic Procedure for the Preparation of gem- Difluoromethylene Compounds	94
4.3.3. Synthesis and Properties of Products..	94
4.3.4. NMR Spectra of the Products.....	96
5. N-HETEROCYCLIC CARBENE-CATALYZED TRIFLUORO- METHYLATION OF AROMATIC TOSYLALDIMINES.....	102
5.1. BACKGROUND	102
5.2. RESULTS AND DISCUSSION	105
5.3. EXPERIMENTAL.....	109
5.3.1. Materials and Methods	109
5.3.2. General Procedure for the Preparation of Aromatic N-tosylaldimines.	109
5.3.3. General Procedure for Trifluoromethylation of Aromatic N-tosylaldimines.	109
5.3.4. Synthesis and Properties of Products.	110
5.3.5. NMR Spectra of the Products.....	113
6. SYNTHESIS OF NOVEL PURINE - BASED KINASE INHIBITORS.....	119
6.1. BACKGROUND	119

6.1.1. Purine-Based Kinase Inhibitors.....	120
6.2. RESULTS AND DISCUSSION.....	122
6.3. EXPERIMENTAL.....	128
6.3.1. Material and Methods.....	128
6.3.2. Synthesis and Properties of Products..	129
6.3.3. NMR Spectra of the Products.....	140
7. CONCLUSION	151
REFERENCES	153
VITA.....	177

LIST OF ILLUSTRATIONS

Figure	Page
2.1. Formation of AGEs by different pathways; Maillard Reaction, autooxidation of reducing sugars, and glycooxidation of Amadori product.....	5
2.2. Structures of early and advanced glycation end-products.	6
2.3. AGEs induced biological effects and correlated diseases.....	7
2.4. Chemical structures of naturally occurring AGE-inhibitors.....	9
2.5. Chemical structures of synthetic AGE-inhibitors.....	11
2.6. Aminoguanidine as a carbonyl trap.	11
2.7. Chemical structures of AGE-breakers.....	12
2.8. Proposed mechanism of action of AGE-breakers.....	14
2.9. Proposed mechanism for the trapping of ketoaldehydes by ALT-711.	15
2.10. Cleavage of phenylglyoxal to benzoic acid by N-heterocyclic carbenes.	16
2.11. Chemical structures of bis-2-aminoimidazole derivatives.....	18
2.12. Synthesis of methylene linked bis-2-aminoimidazoles (2.1).....	18
2.13. Synthesis of aminoacid-derived bis-2-aminoimidazoles (2.9-2.14).	19
2.14. Examples of starting compounds for anticancer and antidiabetic drugs.....	19
2.15. Examples of drugs having nitrogen-substituted morpholine.	20
2.16. Examples of antioxidants having morpholine moiety.	20
2.17. Synthesis of phenacylthiazolium bromide (2.16) and 4-nitro phenacylthiazolium bromide (2.18).....	21
2.18. Synthesis of phenacylthiazolium compounds, 2.21 and 2.24.	22
2.19. Synthesis of phenacylthiazolium compounds, 2.27, 2.30, and 2.33.	23
2.20. Synthesis of N-phenacylimidazolium halides, 2.35 and 2.37.....	24

2.21. Synthesis of phenacylimidazolium compounds, 2.40 and 2.41.....	25
2.22. Chemical structures of DHA adducts of flavanols, EC, EGC, ECG, and EGCG... 26	
2.23. Schematic representation of the oxidation of dehydroascorbic acid (DHA), followed by its further degradation in human lens.....	27
2.24. In-situ PTB-DHA adduct formation at 5, 15, 30, 240, 480 min. and 5 days.	28
2.25. Chemical structures of the four possible stereoisomers from the reaction of DHA with PTB.....	29
2.26. In situ adduct formation between DHA and novel AGE-inhibitors and AGE- breakers (compounds 2.30, 2.33, 2.40, and 2.41) by ¹³ C NMR spectroscopy.....	31
2.27. Stability of Dehydroascorbic acid in water.....	32
2.28. ¹ H NMR spectrum of compound 2.16.	45
2.29. ¹³ C- H decoupled NMR spectrum of compound 2.16.....	45
2.30. ¹³ C- H coupled NMR spectrum of compound 2.16.	46
2.31. ¹³ C- APT NMR spectrum of compound 2.16.	46
2.32. ¹³ C NMR spectrum of compound 2.18.	47
2.33. ¹ H NMR spectrum of compound 2.20.	47
2.34. ¹³ C NMR spectrum of compound 2.20.	48
2.35. ¹ H NMR spectrum of compound 2.21.	48
2.36. ¹³ C NMR spectrum of compound 2.21.	49
2.37. ¹³ C- APT NMR spectrum of compound 2.21.	49
2.38. ¹ H NMR spectrum of compound 2.23.	50
2.39. ¹³ C NMR spectrum of compound 2.23.	50
2.40. ¹³ C- APT NMR spectrum of compound 2.23.	51
2.41. ¹ H NMR spectrum of compound 2.24.	51
2.42. ¹³ C NMR spectrum of compound 2.24.	52
2.43. ¹³ C- APT NMR spectrum of compound 2.24.	52

2.44. ^1H NMR spectrum of compound 2.26.	53
2.45. ^{13}C NMR spectrum of compound 2.26.	53
2.46. ^1H NMR spectrum of compound 2.27.	54
2.47. ^{13}C NMR spectrum of compound 2.27.	54
2.48. ^1H NMR spectrum of compound 2.29.	55
2.49. ^{13}C NMR spectrum of compound 2.29.	55
2.50. ^1H NMR spectrum of compound 2.30.	56
2.51. ^{13}C NMR spectrum of compound 2.30.	56
2.52. ^1H NMR spectrum of compound 2.32.	57
2.53. ^{13}C NMR spectrum of compound 2.32.	57
2.54. ^1H NMR spectrum of compound 2.33.	58
2.55. ^{13}C NMR spectrum of compound 2.33.	58
2.56. ^1H NMR spectrum of compound 2.35.	59
2.57. ^{13}C NMR spectrum of compound 2.35.	59
2.58. ^{13}C NMR spectrum of compound 2.37.	60
2.59. ^1H NMR spectrum of compound 2.39.	60
2.60. ^{13}C NMR spectrum of compound 2.39.	61
2.61. ^1H NMR spectrum of compound 2.40.	61
2.62. ^{13}C NMR spectrum of compound 2.40.	62
2.63. ^1H NMR spectrum of compound 2.41.	62
2.64. ^{13}C NMR spectrum of compound 2.41.	63
3.1. Chemical structures of citric acid and other polyphenolic compounds.	66

- 3.2. Partial 100 MHz ^{13}C NMR spectrum for the reaction mixtures of the D-glucose and leucine, heated at 100 °C for 4 h (in 0.1 M phosphate buffer; pH = 7.4), in the absence (bottom trace) and presence of varied concentration of citric acid; the asterisks correspond to the absorptions for the AGE precursors and all the other signals correspond to the C₁-C₆ carbons of the anomeric mixtures of D-glucose. Signals for L-leucine are outside the range shown ($\delta^{13}\text{C}$ 21.1, 22.2, 24.3, 40.1, 53.8, 175.9).....71
- 3.3. Partial 100 MHz ^{13}C NMR spectrum for the reaction mixtures of the D-glucose and L-leucine, heated at 100 °C for 4 h (in 0.1 M phosphate buffer; pH = 7.4), in the absence (bottom trace) and presence of varied concentration of epigallocatechin; the asterisks correspond to the absorptions for the AGE precursors and all the other signals correspond to the C₁-C₆ carbons of the anomeric mixtures of D-glucose. Signals for L-leucine are outside the range shown ($\delta^{13}\text{C}$ 21.1, 22.2, 24.3, 40.1, 53.8, 175.9).....72
- 3.4. Partial 100 MHz ^{13}C NMR spectrum for the reaction mixtures of the D-glucose and L-leucine, heated at 100 °C for 4 h (in 0.1 M phosphate buffer; pH = 7.4), in the absence (bottom trace) and presence of varied concentration of phloroglucinol; the asterisks correspond to the absorptions for the AGE precursors and all the other signals correspond to the C₁-C₆ carbons of the anomeric mixtures of D-glucose. Signals for L-leucine are outside the range shown ($\delta^{13}\text{C}$ 21.1, 22.2, 24.3, 40.1, 53.8, 175.9).....73
- 3.5. Partial 100 MHz ^{13}C NMR spectrum for the reaction mixtures of the D-glucose and L-leucine, heated at 100 °C for 4 h (in 0.1 M phosphate buffer; pH = 7.4)..... 74
- 3.6. Florescence spectrum, showing the formation of the Maillard products in the D-glucose and L-leucine model system (blue trace), and the absence of AGE fluorescence in the presence of 50 mol% citric acid (orange trace), upon heating at 100 °C in phosphate buffer (0.1M, pH = 7.4; λ_{exc} at 355 nm and λ_{em} at 400-500 nm)..... 74
- 3.7. Partial 100 MHz ^{13}C NMR spectrum for the reaction mixtures of the D-glucose and benzylamine, heated at 80 °C for 4 h (in 0.1 M phosphate buffer; pH = 7.4), in the absence (bottom trace) and presence of various antiglycating agents (ferulic acid, phloroglucinol, EGCG, and citric acid); the asterisks correspond to the absorptions for the AGE precursors, (notably less in concentration in the reaction mixtures treated with polyphenolic compounds or citric acid) and all the other signals correspond to the C₁-C₆ carbons of the anomeric mixtures of D-glucose.....76

3.8. Partial 100 MHz ^{13}C NMR spectrum for the reaction mixtures of the D-glucose and benzylamine, heated at 80 °C for 4 h (in 0.1 M phosphate buffer; pH = 7.4), in the absence (bottom trace) and presence of varied concentration of citric acid (100, 50, 25, 20, 15, and 10 mol %); the asterisks correspond to the absorptions for the AGE precursors and all the other signals correspond to the $\text{C}_1\text{-C}_6$ carbons of the anomeric mixtures of D-glucose. The signals for benzylamine are outside the range shown ($\delta^{13}\text{C}$ 133.8, 129.2, 128.9, 128.8, 128.7, 43.4).....	77
3.9. Effect of various additives (10 mol% concentration) used as antiglycating agents on the formation of AGEs in D-glucose and benzylamine model system, upon heating at 80 °C in phosphate buffer (0.1M, pH = 7.4) for 4 h.....	78
3.10. Effect of various additives (20 mol% concentration) used as antiglycating agents on the formation of AGEs in D-glucose and benzylamine model system, upon heating at 80 °C in phosphate buffer (0.1M, pH = 7.4) for 4 h.....	78
4.1. Bioisosterism of CF_2 Fragment.....	80
4.2. Oxidative desulfurization- difluorination: gem-difluorination of dithioacetals.....	81
4.3. gem-difluorination of dicarbonyls using fluoroiodane.	81
4.4. gem- difluorination of styrene using fluoroiodane.	81
4.5. Difluorination using ionic liquids; a.) Synthesis of [bdmim][F] (4.5) b.) gem-difluorination of dithiocarbonate c.) gem- difluorination of xanthate.	82
4.6. Difluoromethylation of alkyl and vinyl iodides.....	83
4.7. Palladium-Silver dual co-operative catalysed difluoromethylation of biologically relevant compounds.	84
4.8. Nucleophilic difluoromethylation of aldehydes by using TMSCF_3	85
4.9. Visible light-promoted C-H activation; a.) Photoredox-catalyzed benzylic monofluorination and gem-difluorination b.) Mechanism of visible light-promoted C-H fluorination.	86
4.10. Photoredox-catalyzed gem-difluorination of tetrahydroisoquinoline.....	88
4.11. Possible mechanism of gem-difluorination of tetrahydroisoquinoline.....	88
4.12. Photoredox catalyzed decarboxylative fluorination of aliphatic carboxylic acids. ..	89
4.13. Photoredox catalyzed gem-difluorination of 1,3-dithiolane.	91
4.14. Proposed mechanism of photoredox gem-difluorination of 1,3-dithiolanes.	93

4.15. ^1H NMR spectrum of compound 4.9.	97
4.16. ^{13}C -H decoupled NMR spectrum of compound 4.9.....	97
4.17. ^{13}C -H coupled NMR spectrum of compound 4.9.	98
4.18. ^{13}C -APT NMR spectrum of compound 4.9.	98
4.19. ^{19}F NMR spectrum of compound 4.9.....	99
4.20. ^{19}F NMR spectrum of compound 4.11.....	99
4.21. ^{19}F NMR spectrum of compound 4.13.....	100
4.22. ^{19}F NMR spectrum of compound 4.15.....	100
4.23. ^{19}F NMR spectrum of compound 4.17.....	101
5.1. Nucleophilic trifluoromethylation of N-tosyl aldimines using TMSCF_3 and TBAT.	103
5.2. NHC catalyzed nucleophilic trifluoromethylation of carbonyl compounds.	105
5.3. Structures of NHC-1 and NHC-2.....	106
5.4. Optimization of trifluoromethylation of N-tosylbenzaldimine in the presence of in situ generated NHC-1.	107
5.5. ^1H NMR spectrum of compound 5.2.	113
5.6. ^{13}C NMR spectrum of compound 5.2.	113
5.7. ^{19}F NMR spectrum of compound 5.2.....	114
5.8. ^1H NMR spectrum of compound 5.4.	114
5.9. ^{13}C NMR spectrum of compound 5.4.	115
5.10. ^{19}F NMR spectrum of compound 5.4.....	115
5.11. ^{19}F NMR spectrum of compound 5.6.....	116
5.12. ^{19}F NMR spectrum of compound 5.8.....	116
5.13. ^{19}F NMR spectrum of compound 5.10.....	117
5.14. ^{19}F NMR spectrum of compound 5.12.....	117

5.15. ^{19}F NMR spectrum of compound 5.14.....	118
6.1. Chemical structures of Imatinib and other related small molecule kinase inhibitors.	120
6.2. Purine based protein kinase inhibitors in pre-clinical/clinical trials.	121
6.3. Synthesis of purine-based fluoroalkyl triazoles.....	124
6.4. Synthesis of aniline derivative of purine-based fluoroalkyl triazoles.....	125
6.5. Synthesis of dimeric version of purine-based fluoroalkyl triazole.	126
6.6. Synthesis of pyridyl ring derivative of purine-based fluoroalkyl triazole.	127
6.7. Synthesis of biarylmethylamine derivative of purine-based fluoroalkyl triazole... ..	128
6.8. ^1H NMR spectrum of compound 6.14.	140
6.9. ^{13}C NMR spectrum of compound 6.14.	141
6.10. ^{19}F NMR spectrum of compound 6.14.....	141
6.11. ^1H NMR spectrum of compound 6.18.	142
6.12. ^{13}C NMR spectrum of compound 6.18.	142
6.13. ^{19}F NMR spectrum of compound 6.18.....	143
6.14. ^1H NMR spectrum of compound 6.20.	143
6.15. ^1H NMR spectrum of compound 6.21.	144
6.16. ^{13}C NMR spectrum of compound 6.21.	144
6.17. ^1H NMR spectrum of compound 6.22.	145
6.18. ^{13}C NMR spectrum of compound 6.22	145
6.19. ^{19}F NMR spectrum of compound 6.22.....	146
6.20. ^1H NMR spectrum of compound 6.25	146
6.21. ^{13}C NMR spectrum of compound 6.25	147
6.22. ^1H NMR spectrum of compound 6.26.	147
6.23. ^{13}C NMR spectrum of compound 6.26.	148

6.24. ^1H NMR spectrum of compound 6.27	148
6.25. ^{13}C NMR spectrum of compound 6.27.	149
6.26. ^1H NMR spectrum of compound 6.28.	149
6.27. ^{13}C NMR spectrum of compound 6.28.	150
6.28. ^{19}F NMR spectrum of compound 6.28.....	150

LIST OF TABLES

Table	Page
2.1. ^{13}C NMR chemical shifts (experimental and theoretical) of four possible stereoisomers of PTB-DHA adducts.....	30
4.1. ^{19}F NMR chemical shifts in ppm for the conversion of diaryldithiolanes into their corresponding gem-difluorocompounds. a.) Estimated yield by ^{19}F NMR (Isolated yield). Yields are not optimized.....	92
5.1. NHC-1 catalyzed trifluoromethylation of aromatic N-tosylaldimines.	108

NOMENCLATURE

Symbol	Description
AGEs	Advanced glycation end-products
CML	N _ε -carboxymethyllysine
RAGE	Receptor for AGEs
ROS	Reactive oxygen species
RCS	Reactive dicarbonyls
EGCG	Epigallocatechin gallate
EGC	Epigallocatechin
TF3	Theaflavin-3-3'-digallate
AG	Aminoguanidine
PTB	Phenacylthiazolium bromide
ALT-711	Alagebrium chloride
MGO	Methylglyoxal
NHC	N-heterocyclic carbene
2-AI	bis-2-aminoimidazole
Boc	tert-butyloxycarbonyl
PEG	Polyethylene glycol
Na ₂ HPO ₄	Disodium hydrogen phosphate
NaH ₂ PO ₄	Sodium dihydrogen phosphate
PBS	Phosphate buffer solution
TBAB	Tetrabutylammonium bromide
TEA	Triethylamine

DHAA	Dehydroascorbic acid
ASA	Ascorbic acid
APT	Attached proton test
<i>gem</i>	Geminal
PET	Positron emission tomography
SF ₄	Sulfur tetrafluoride
Selectfluor	1-chloromethyl-4-fluoro-1, 4-diazoniahicyclo [2.2.2] octane bis(tetrafluoroborate)
HF	Hydrofluoric acid
NFSI	N-fluorobenzenesulfonimide
DAST	Diethyliminosulfur trifluoride
TMSCF ₃	Trimethylsilyl trifluoromethane
Zn (SO ₂ CF ₂ H) ₂	Zinc difluoromethanesulfinate
Selectfluor II	Fluoro-4-methyl-1,4-diazoniabicyclo[2.2.2]octane tetrafluoroborate
CFL	Compact fluorescent lamp
DDQ	2,3-Dichloro,5,6-dicyano-1,4-benzoquino
[Ru(bpy) ₃]Cl ₂	Tris (bipyridine) ruthenium (II) chloride
BF ₃ . OEt	Boron trifluoride diethyl etherate
TBAT	Tetrabutylammonium (triphenylsilyl) difluoride
TBAF	Tetrabutylammonium fluoride
Ts	<i>p</i> -toluenesulfonyl
TDAE	Tetrakis(dimethylamino) ethylene
KO <i>t</i> -Bu	Potassium <i>tert</i> -butoxide
RTK	Receptor tyrosine kinase

ATP	Adenosine triphosphate
SAR	Structure activity relationship
CDKs	Cyclin dependent kinases
TLC	Thin layer chromatography
Pd(PPh ₃) ₄	Tetrakis(triphenylphosphine)palladium(0)

1. INTRODUCTION

Advanced glycation end-products (AGEs) are formed in the body by non-enzymatic glycation (Maillard reaction), which involves the reaction between carbonyl groups of reducing sugars and amino groups of proteins to form an unstable Schiff base intermediate, which rearranges to form a more stable Amadori product and a small part of Amadori products slowly undergo oxidation to form AGEs.¹ Reactive dicarbonyl intermediates such as methylglyoxal (MG), glyoxal, and 3-deoxyglucosone (3DG), which are generated from glucose-derived glycolytic intermediates², lipid peroxidation and oxidative stress³⁻⁴ play an important role in AGEs formation. AGEs play an important role in pathogenesis of diseases such as diabetes, Alzheimer's disease, atherosclerosis, inflammatory arthritis and cataracts. Due to these harmful effects of AGEs on human health, it is interesting to explore novel AGE-inhibitors and AGE-breakers which would be effective in retarding the AGE-induced complications. We synthesized novel AGE-inhibitors and AGE-breakers and studied their dicarbonyl trapping by ¹³C NMR, UV-vis, and fluorescence spectroscopy, and demonstrated their AGE-inhibitory and AGE-breaking effects. We also studied the effect of citric acid and several polyphenolic antioxidants on glycation (Maillard reaction) by UV-fluorescence and ¹³C NMR spectroscopy.

Organofluorine compounds have important role as pharmaceuticals, agrochemicals, materials, and radiotracers for positron emission tomography (PET).⁵ Incorporation of fluorine and trifluoromethyl group changes the chemical, physical, and biological properties of the parent compound. Difluorocompounds have unique

applications in drug design due to the ability of the difluoromethyl group to serve as a hydrogen bond donor.⁶ In recent years, novel synthetic methods for organofluorine compounds are of great interest^{5, 7-9} and among those, visible-light promoted fluorination has proved to be a mild and most effective synthetic method for the preparation of monofluoro and *gem*-difluorocompounds.¹⁰⁻¹² α -Trifluoromethyl substituted amines and their related fluorinated derivatives also have unique applications in pharmaceutical, agrochemical and material industry. Basicity of amino moiety in α -trifluoromethylamines is attenuated due to the strong electron-withdrawing effect of the trifluoromethyl group, which enhances the pharmacokinetic properties such as lipophilicity, cell-permeability, and metabolic stability of α -trifluoromethylamines.¹³ Several synthetic methods for the preparation of α -trifluoromethylamines have been reported to date¹⁴⁻¹⁶, and recently, the direct preparation of α -trifluoromethylamines by nucleophilic trifluoromethylation of imines has received renewed attention.¹⁷⁻¹⁸ *N*-heterocyclic carbenes (NHC) have received a considerable interest in recent years as a catalyst for nucleophilic trifluoromethylation, perfluorophenylation, and cyanosilylation of carbonyl compounds.¹⁹⁻²¹ In this thesis, we presented a novel photoredox-catalyzed synthetic method for the preparation of *gem*-difluoro compounds from 1,3 dithiolanes using a commercially available Selectfluor as fluorine source and 9-fluorenone as a cheap and readily available photocatalyst. We also developed NHC-catalyzed trifluoromethylation of *N*-tosylimines, using TMSCF₃ (Ruppert-Prakash reagent) and the readily available *N*-heterocyclic carbene (NHC) derived from its corresponding imidazolium salt.¹³

Protein kinases play an important role in controlling the cellular processes in the human body by phosphorylation of amino acids and play a critical role in tumor cell proliferation as well as survival and migration of neoplasia. Therefore kinase inhibition is

very important strategy in treatment of cancers. Kinase inhibitors target the adenosine-triphosphate (ATP) binding pocket and block the action of protein kinases. Imatinib was the first FDA approved tyrosine kinase inhibitor, and the clinical success of this drug led to the discovery of various new kinase inhibitors. Purine analogues are effective anticancer (acute leukemias), antiviral, antitumor, bronchodilator, immunosuppressive therapeutics, and a variety of purine-based kinase inhibitors are in pre-clinical and clinical trials.²² In this study, we have synthesized various derivatives of an earlier reported fluorinated purine-based triazole lead compound.²³⁻²⁵ The structural characterization of these novel derivatives was accomplished by high field ¹H NMR and ¹³C NMR spectroscopy.

2. DESIGN, SYNTHESIS AND STUDIES OF NOVEL AGE-INHIBITORS AND AGE-BREAKERS

2.1. BACKGROUND

Advanced (glycation end products AGEs) are a large group of protein-crosslink-derived compounds, generated both exogenously (*in vitro*) and endogenously (*in vivo*) by a series of very slow complex non-enzymatic reactions (also known as Maillard reaction) between reducing sugars and amino groups in proteins, lipids, and nucleic acids.²⁶⁻²⁸ This process is also known as protein glycation.²⁷ The glycation is initiated through a non-enzymatic reaction of amino groups of proteins, lipids or nucleic acids with the carbonyl groups of reducing sugars²⁹, resulting in the formation of an unstable Schiff base intermediate.³⁰⁻³¹ A Schiff base undergoes very slow chemical transformations over a period of weeks to form a highly reversible and stable ketoamine intermediate (also known as Amadori product).^{31,32-34} Finally, Amadori products undergo dehydration and rearrangements to form AGE precursors (reactive dicarbonyls), which cause protein aggregation by developing a crosslink between adjacent proteins and lead to the formation of advanced glycation end products (AGEs).³⁵ Oxidation of sugars (autooxidative glycation), ketoamines-Amadori product (glycooxidation), lipids, and amino acids in the presence of transition metals and oxygen can also generate very reactive dicarbonyls³⁶⁻³⁸ as AGE precursors that can covalently bind to proteins and lead to the formation of AGEs (Figure 2.1). These AGE- bound proteins can also interact with other proteins in the body to finally form AGE-protein crosslinking. This is advanced stage of glycation and leads to the pathogenesis of numerous life threatening diseases.

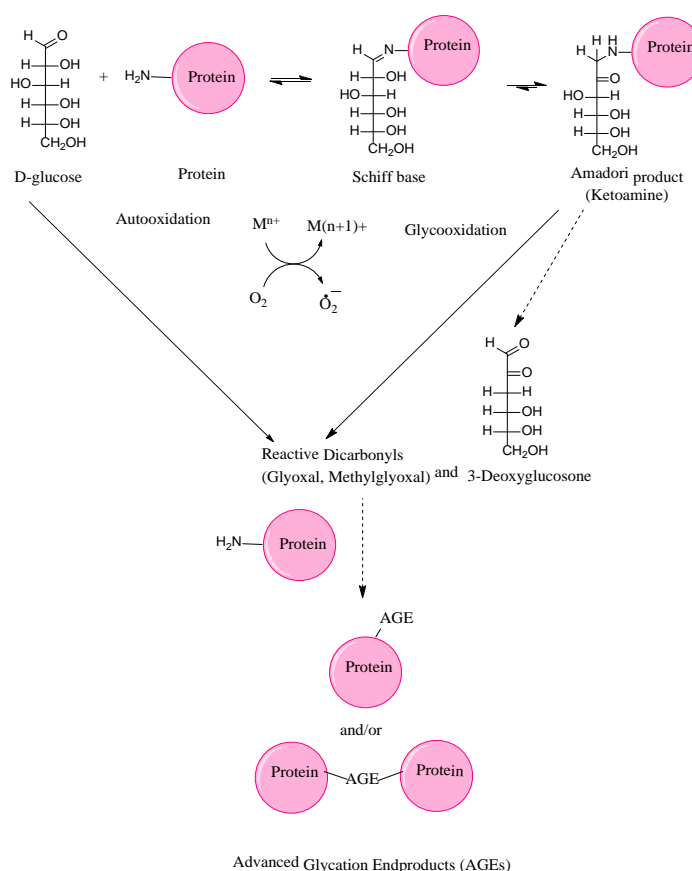


Figure 2.1. Formation of AGEs by different pathways; Maillard Reaction, autooxidation of reducing sugars, and glycooxidation of Amadori product.³¹

Chemical interaction between degradation and fragmentation products of reducing sugars (glucose/fructose) and protein (lysine/arginine) residues also lead to the formation of early glycation products.³⁹ Chemical structures of some early and advanced glycation end-products are shown in Figure 2.2. Of these AGEs, N_ϵ -carboxymethyllysine (CML) was the first discovered AGE⁴⁰ and is used in many studies as the AGE marker. It is also formed by metal catalysed oxidation of polyunsaturated fatty acids.

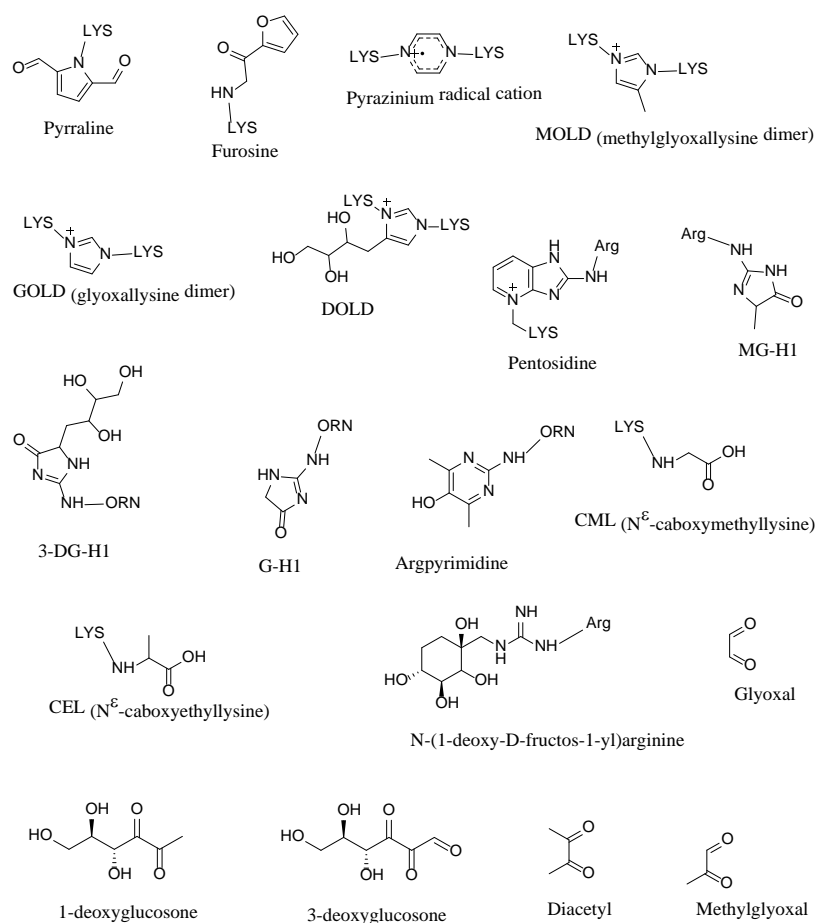


Figure 2.2. Structures of early and advanced glycation end-products.³⁹

2.1.1. Effects of AGEs on Human Health. AGEs have harmful effects on human health through two different physiological functions.⁴¹ AGEs can promote protein cross-linking, protein aggregation and tissue stiffness to lose their original function. AGEs can also bind to proteins (protein-bound AGEs) and activate cell membrane receptors such as receptors for advanced glycation end-products (RAGE) to promote reactive oxygen species (ROS) generation and affect cell physiology. Not all the AGEs form protein adducts and only N^ε-carboxymethyllysine (CML) can bind to RAGE for the activation of specific cellular signaling pathways.⁴¹⁻⁴² Due to these physiological

functions, AGEs promote oxidative stress, affect the immune system, cause chronic inflammation, protein aggregation, alter/or damage the function of tissues and proteins, and cause the pathogenesis of many diseases, such as diabetes cardiovascular disease, rheumatoid arthritis, Alzheimer's disease, dementia, and various kinds of cancer⁴³⁻⁴⁸ as shown in Figure 2.3.

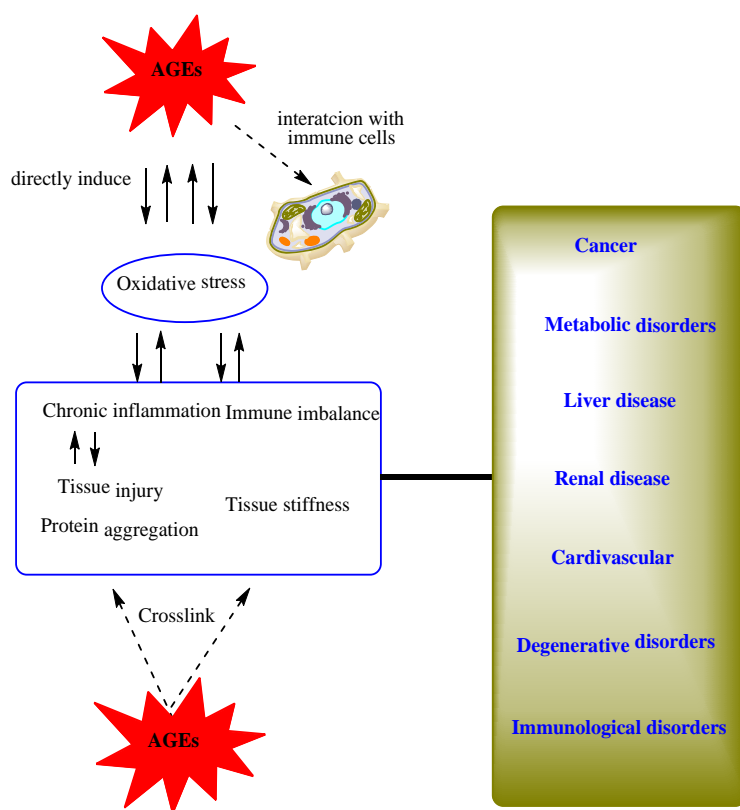


Figure 2.3. AGEs induced biological effects and correlated diseases.⁴⁹

2.1.2. AGE-Inhibitors and AGE-Breakers. A large number of compounds have reached the phase of clinical studies used as therapeutic agents to inhibit the

glycation (AGE-inhibitors)⁵⁰⁻⁵⁴ and break the AGE-protein crosslinking (AGE-breakers)⁵⁵⁻⁵⁹ for the prevention of diseases caused by AGEs. These compounds are collectively known as AGE-inhibitors and- breakers.

2.1.2.1. Naturally occurring AGE-inhibitors and their inhibitory effects.

Polyphenols and flavonoids such as tannins,⁶⁰ rutin,⁶¹ quercetin, cirsilineol,⁶² arbutin, ferulic acid, and hydroxycitric acid⁶³ found in medicinal plants (natural products), vegetables, fruits, teas, cereals, spices, nuts, algae, and polyphenols have proven to be promising agents for AGE inhibition. Structures of some naturally occurring AGE-inhibitors are shown in Figure 2.4. Phenolic compounds inhibit AGE formation through their antioxidant activities by scavenging free radicals formed during Maillard reaction. However, the mechanism of AGE inhibition of these naturally occurring AGE-inhibitors is not completely understood. Flavonoids exhibit inhibition activities through free radical scavenging.⁶⁴ Among flavonoids, flavones have stronger inhibitory effects than flavonols, flavanones and isoflavones.^{63, 65} Based on an in-vitro study, a number of hydroxyl groups and their derivatization in flavonoids are the structural requirements for effective inhibition of AGEs. Tea polyphenols such as epigallocatechin gallate (EGCG), epigallocatechin (EGC), and theaflavin-3-3'-digallate (TF3) not only inhibit AGE formation through their antioxidant activities, but also scavenge reactive dicarbonyl intermediates (AGE precursors) formed in glycation under physiological conditions.⁶⁶

2.1.2.2. Synthetic AGE-inhibitors and their inhibitory effects. Synthetic AGE-inhibitors can also inhibit the AGE formation in the same way as naturally occurring

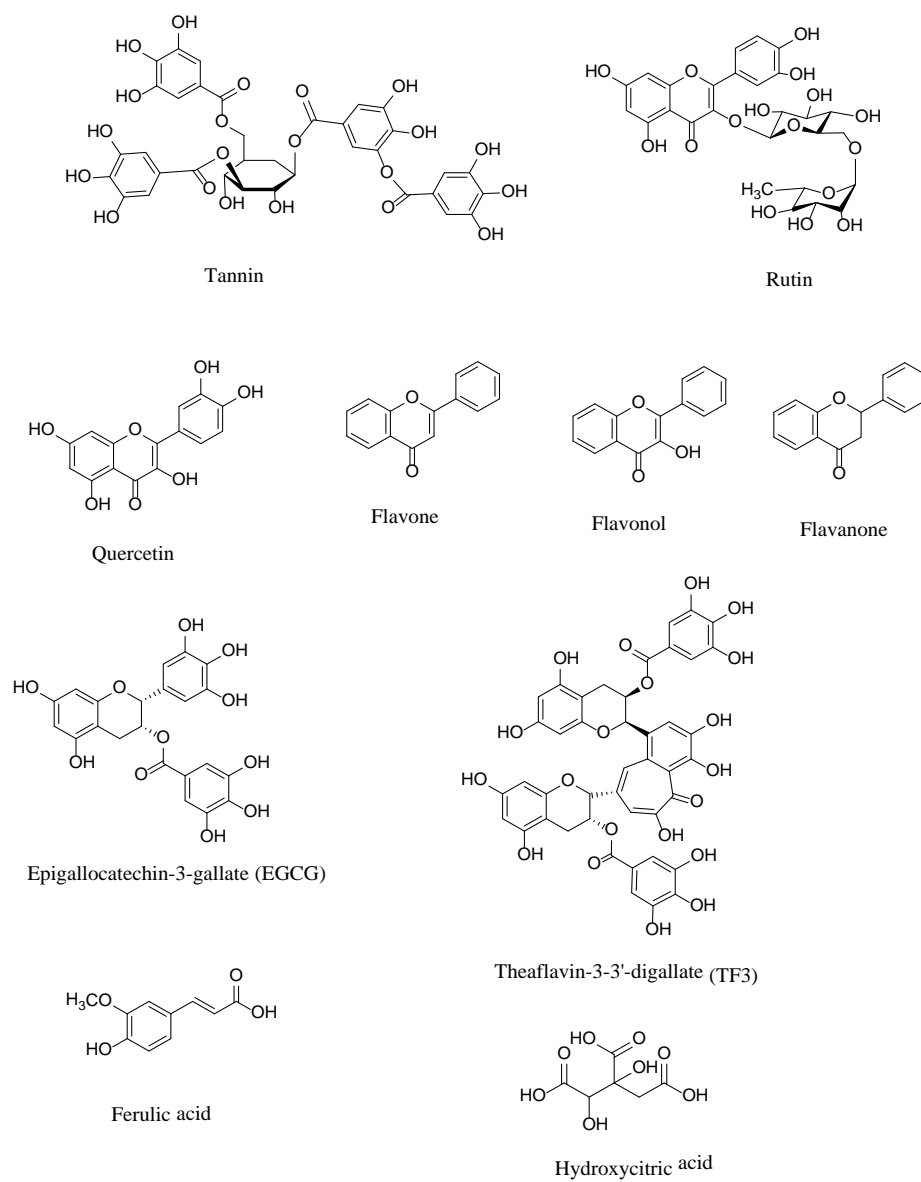


Figure 2.4. Chemical structures of naturally occurring AGE-inhibitors.

AGE-inhibitors, either by blocking the reaction of amino group of proteins with reducing sugars (early glycation) or by trapping reactive dicarbonyls and radical species (RCS/ROS) formed (late glycation) during Maillard reaction but their exact and detailed

mechanism of action also needs to be investigated. On this basis, AGE- inhibitors are divided into two categories; 1.) Inhibitors of early stages of glycation, 2.) Inhibitors of late stages of glycation. For example, aspirin is considered to be an effective inhibitor in early glycation due to its ability to acetylate free amino groups of proteins and inhibit the further glycation reactions to prevent diabetic complications.⁶⁷⁻⁶⁸ Diclofenac, an anti-inflammatory drug, can also bind to proteins by noncovalent bonding to prevent the proteins' interaction with sugars and block glycation sites in human serum albumin.⁶⁹ Pioglitazone, metformin (antidiabetic drug), and pentoxifylline have also been reported to moderate early-stage glycation inhibitors.⁷⁰ Structures of some synthetic AGE-inhibitors are shown in Figure 2.5. Aminoguanidine (AG), pyridoxamine, thiamine pyrophosphate, tenilsetam, pyrrolidine, buformin, quinine, carnosine, amlodipine, kinetin, penicillamine, and ethanol have been reported to be effective AGE-inhibitors in late stages of glycation. These compounds show inhibitory effects by either trapping dicarbonyl compounds or inhibiting Amadori products formation. Ethanol also showed inhibitory effects on AGE formation as it has ability to metabolize into acetaldehyde *in vivo*, which could react with protein-bound Amadori products.⁷¹

The Mechanism of trapping carbonyls by aminoguanidine is shown in Figure 2.6. Aminoguanidine reacts with very toxic hydroxyaldehyde (carbonyl) and 2,3-butanedione (dicarbonyl) to form less toxic hydrazone and triazine, respectively.⁵⁵ Proposed mechanism of action of trapping dicarbonyls by aminoguanidine is based on *in-vitro* model studies. Since the discovery of aminoguanidine, there is no published evidence of trapping AGE precursors by aminoguanidine *in vivo*. The less toxic products hydrazone and triazine formed after the reaction of aminoguanidine with dicarbonyls, shown in

Figure 2.6 have never been detected in urine and plasma of the animal models used in this study.

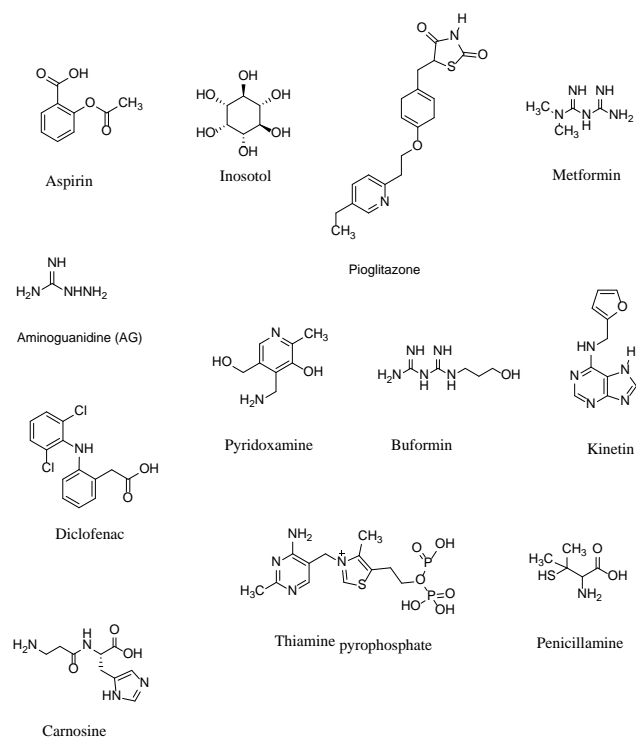


Figure 2.5. Chemical structures of synthetic AGE-inhibitors.

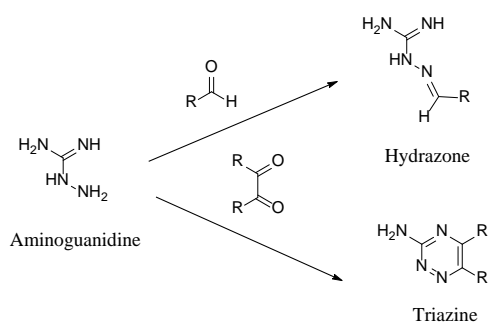


Figure 2.6. Aminoguanidine as a carbonyl trap.⁵⁵

2.1.2.3. AGE-breakers and their inhibitory effects. AGE-breakers such as N-phenacylthiazolium bromide (PTB) and its derivative alagebrium chloride (ALT-711) selectively cleave the established covalent AGE-protein crosslinks *in vivo* and *in vitro*⁵⁸⁻⁵⁹ to restore the original function of proteins and finally combat the adverse effects associated with aging, diabetes, arthritis, Alzheimer's, chronic inflammation, skin, and cardiovascular diseases.⁷²⁻⁷⁵ Besides these two prototypical AGE-breakers, other compounds such as curcumin,⁷⁶ ALT-946,⁷⁷⁻⁷⁸ pyridinium analogs (TRC4186 and TRC4149),⁵⁶⁻⁵⁷ C-16, and C-36⁵⁵ have also been known as potential AGE-breakers having therapeutic effects against the diseases associated with AGE-protein crosslinking. Chemical structures of some AGE-breakers are shown in Figure 2.7.

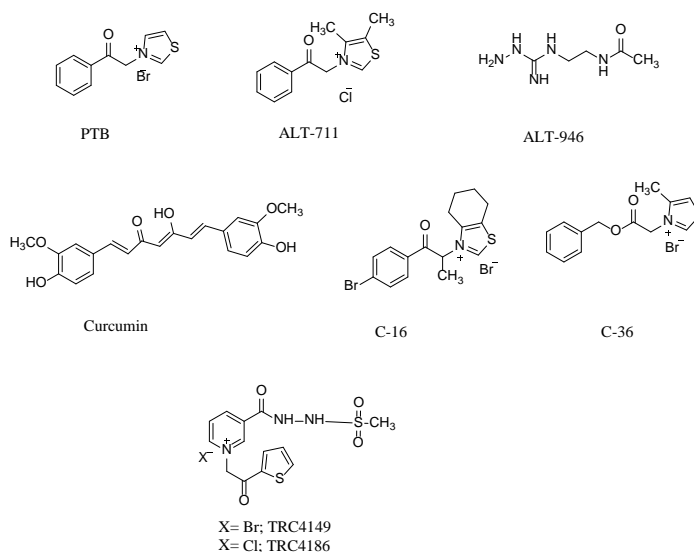


Figure 2.7. Chemical structures of AGE-breakers.

Vasan et al.⁵⁹ were the first to show the mechanism of cleavage of glucose-derived protein crosslinking by phenacylthiazolium bromide (PTB). On this basis, other AGE-breaker therapeutics effective to break protein crosslinking in diabetic rats were designed, and their mechanism of action was supported by release of AGE-albumin from preformed AGE-albumin-collagen complexes, binding of released immunoglobulins with RBCs of diabetic rats, and finally reversal or decrease of collagen crosslinking in diabetic rats.⁵⁶⁻⁵⁷ The proposed mechanism of action of AGE-inhibitors is shown in Figure 2.8. The bifunctional AGE-breaker attacks at dicarbonyl AGE-crosslinking, followed by intramolecular rearrangements to cleave the dicarbonyl bond of crosslinking. After hydrolysis, AGE-breaker is regenerated with the simultaneous removal of chemically inert CML (N_{ϵ} -carboxymethyllysine) on one peptide chain and reactive aldehyde group on another peptide chain involved in crosslinking. It is thus apparent that the target of AGE-breakers would be reactive dicarbonyls- derived crosslinks, in the AGE-modified proteins. AGE-breakers have proven to be very effective in various *in vivo* and *in vitro* studies.

Some AGE-inhibitors, AGE-breakers and their hydrolysis and/or metabolism products have metal chelating activity in the tissues to prevent the formation of harmful AGEs. Alterations in metal homeostasis (copper and iron) in different body tissues is also the cause of diseases such as diabetes, cardiovascular disease, and renal diseases.⁷⁹⁻⁸¹ Antihypertensive drugs have been shown to have chelation as their mechanism of action on AGE formation.⁸²⁻⁸³ Hydrophilic compounds (aminoguanidine and pyridoxamine) act as chelators in high doses while on the other hand, low doses of hydrophobic compounds are required. Although, various synthetic AGE-inhibitors and AGE-breakers described above have very strong therapeutic properties by acting through different mechanism of

action but they have side effects. For example, aminoguanidine (AG) considered to be the gold standard in this area didn't give very promising results in clinical trials and phase II trials were terminated because of adverse side effects observed such as gastrointestinal disturbance, anemia, and flu symptoms.^{53, 84-85}

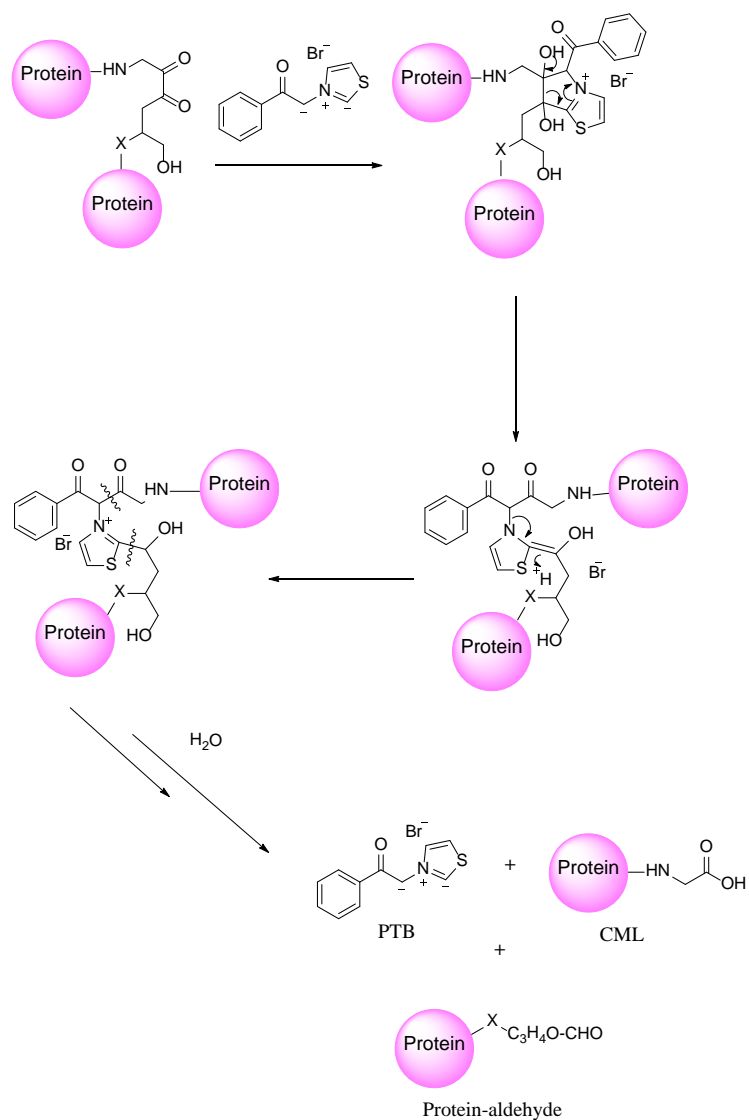


Figure 2.8. Proposed mechanism of action of AGE-breakers.^{55, 59}

2.2. RESULTS AND DISCUSSION

N-phenacylthiazolium bromide (PTB) has been found to cleave and transform the most reactive α -dicarbonyl AGE precursors (1-phenyl-2,3-propanedione) into less reactive compounds (benzoic acid).⁵⁹ Alagebrium (ALT 711) was developed as another stable N-phenacyl-derived thiazolium salt having very good therapeutic effects against diabetes and aging *in vitro*.^{58, 86-88} Both of these compounds can cleave α -dicarbonyls but their mechanism of action as antiaging agents is unclear.⁷² Kim and Spiegel⁸⁹ demonstrated that phenacylthiazolium carbene (ALT-711, PTB) is more reactive than benzylthiazolium carbene towards α -dicarbonyl cleavage in aqueous medium. ALT-711 also reacts with toxic methylglyoxal (MGO) *in vitro* to form ALT-MGO adduct (cyclic diol), which was not observed with benzylthiazolium carbene and thereby rescues the growth of *E. coli*. Proposed mechanism of MGO trapping by ALT-711 form ALT-MGO adduct is shown in Figure 2.9.

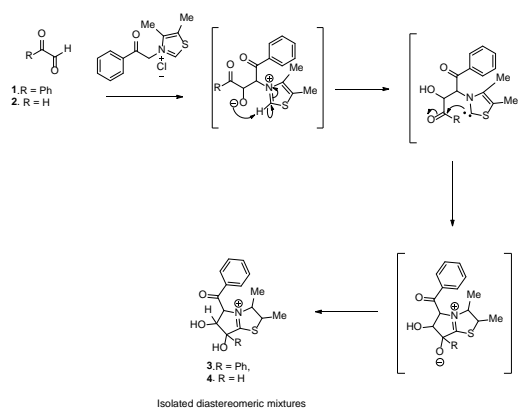
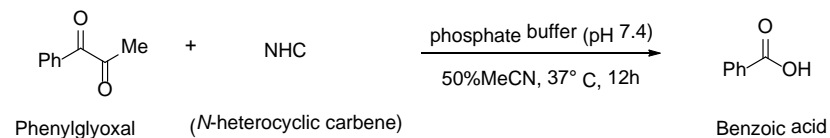


Figure 2.9. Proposed mechanism for the trapping of ketoaldehydes by ALT-711.⁸⁹

Cleavage of α -dicarbonyl compound phenylglyoxal with different carbenes was performed either by modifying Vasan's method⁵⁹ or by using acetonitrile as a co-solvent. Results are summarized in Figure 2.10. Yields of benzoic acid were determined by LC-MS by peak integration with respect to phenylglyoxal.



No.	NHC	Conversion (%)
1.		60
2.		12
3.		14
4.		20
5.		0
6.		0

Figure 2.10. Cleavage of phenylglyoxal to benzoic acid by N-heterocyclic carbenes.⁸⁹

Samuel et al.⁹⁰ have demonstrated that phenacylethylimidazolium halides with electron-donating groups are the most effective oral hypoglycemic agents. A library of compounds by varying heterocyclic moieties, number, and position of different functional groups was synthesized, and their effects in reducing blood glucose levels in diabetic mice were shown. Richardson and Furlani et al.⁹¹⁻⁹² have synthesized and demonstrated by fluorescence assay that second-generation bis-2-aminoimidazole (2-AI) based compounds are more effective AGE-inhibitors and AGE-breakers than the first-generation gold standard known to be aminoguanidine (AG). Bis-2-aminoimidazole derivative with tether linking of 3-carbon chain length 1.1 was shown to be the most effective AGE-inhibitor as well as AGE-breaker even at very low concentration. There were many synthetic challenges to synthesize these compounds, and their chemical structures are shown in Figure 2.11.

Compound **2.1** having tether linking with different carbon chain length ($n = 1-5$) was synthesized in two steps. Corresponding di- α -chloroketone was obtained by Nierstein reaction of di-acid chloride followed by cyclization with Boc-guanidine and subsequent Boc deprotection, as shown in Figure 2.12. Compounds **2.9-2.14** with different amino acid derivatives were synthesized by Akabori reduction followed by cyanamide condensation of corresponding amino acid methyl esters, as shown in Figure 2.13.

Mohammad et al.⁹³ have shown the importance of morpholine moiety in drug candidate. Several anticancer and antidiabetic drugs have starting compounds bearing morpholine moiety, as shown in Figure 2.14. Drug candidates with nitrogen-substituted morpholines shown in Figure 2.15 have a wide spectrum of biological activities.

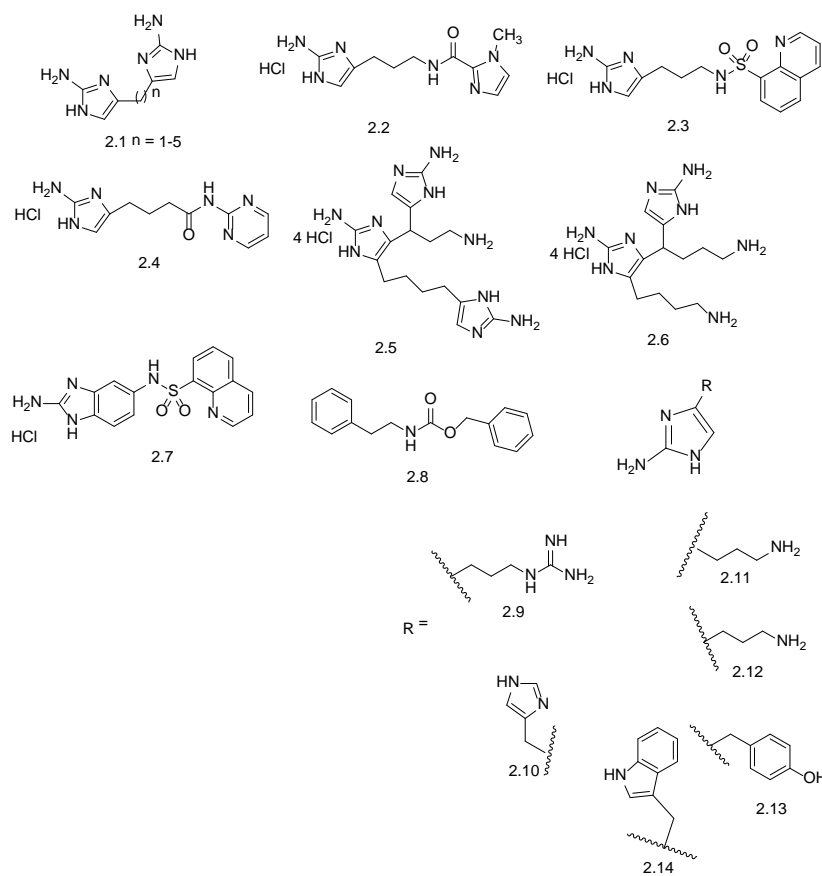


Figure 2.11. Chemical structures of bis-2-aminoimidazole derivatives.

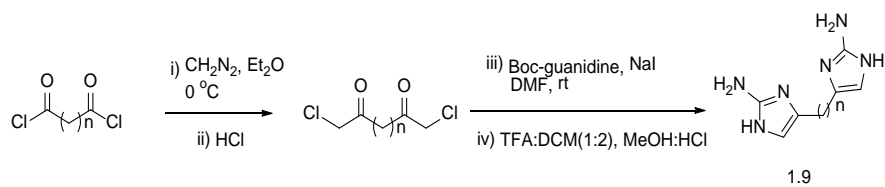


Figure 2.12. Synthesis of methylene linked bis-2-aminoimidazoles (2.1).⁹²

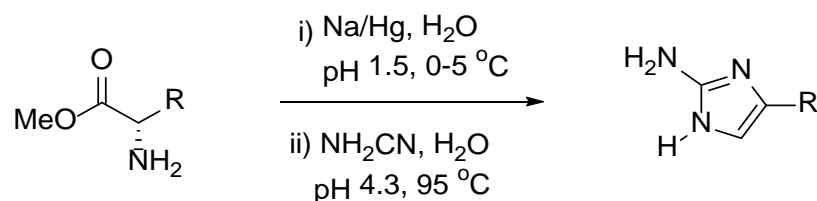


Figure 2.13. Synthesis of aminoacid-derived bis-2-aminoimidazoles (2.9-2.14).⁹²

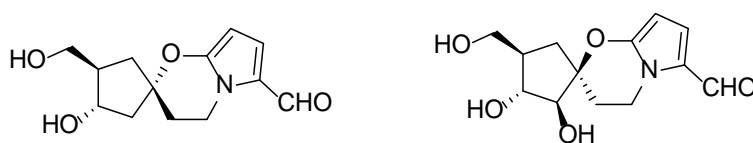


Figure 2.14. Examples of starting compounds for anticancer and antidiabetic drugs.

Drug candidates with nitrogen-substituted morpholines shown in Figure 2.15 have a wide spectrum of biological activities. Antioxidants such as tannins and polyphenols found in fruits, vegetables, teas, and red wines also have morpholine moiety in their structure, as shown in Figure 2.16.⁹⁴ These novel derivatives are found to inhibit the ferrous/ascorbate induced lipid peroxidation of microsomal membrane lipids.⁹⁵

Polyethylene glycol (PEG) is very inexpensive and has been approved by FDA for use as drug delivery and drug modification. It enhances the aqueous solubility of hydrophobic drugs, prolongs circulation time and minimizes non-specific uptake of drugs.⁹⁶⁻⁹⁸

Therefore, specific targetability could be achieved through enhanced permeability and retention effects. PEG prodrugs for anticancer drugs paclitaxel and camptothecin have been prepared and proved that the prodrugs have improved water solubility and *in vivo*

activity.⁹⁹⁻¹⁰¹ Based upon the promising results for the compounds (AGE-inhibitors and-breakers) reported in the literature as described above, we decided to synthesize N-phenacylthiazolium and N-phenacyl-3-methylimidazolium halides, their derivatives, and dimers.

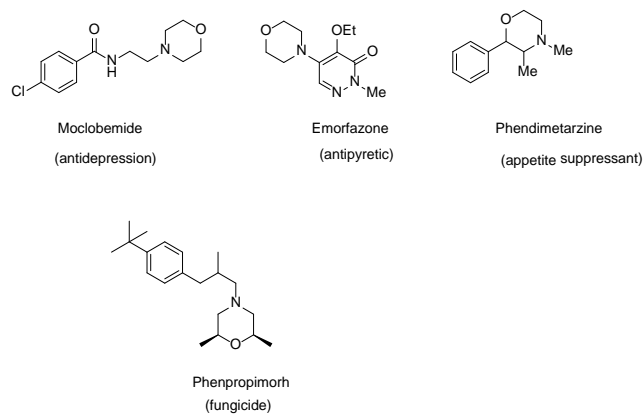


Figure 2.15. Examples of drugs having nitrogen-substituted morpholine.

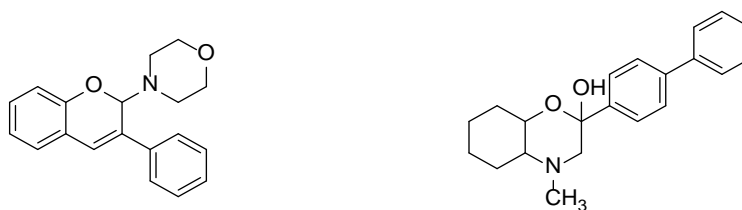


Figure 2.16. Examples of antioxidants having morpholine moiety.

Based upon the promising results for the compounds (AGE-inhibitors and-breakers) reported in the literature as described above, we decided to synthesize N-phenacylthiazolium and N-phenacyl-3-methylimidazolium halides, their derivatives, and dimers.

2.2.1. Synthesis of N-phenacylthiazolium Halide (PTB) and its Derivatives. N-phenacylthiazolium halide (PTB) and its derivatives were synthesized according to literature procedures with modifications¹⁰²⁻¹⁰⁵ as shown in Figure 2.17. N-phenacylthiazolium bromide **2.16** was prepared by reacting bromoacetophenone **2.15** with thiazole in methanol at reflux for 3 h. Recrystallization in methanol and diisopropylether afforded pure compound **2.16** in 50% yield. 4-nitrophenacylthiazolium compound **2.18** was also prepared by the same method in 37% yield.

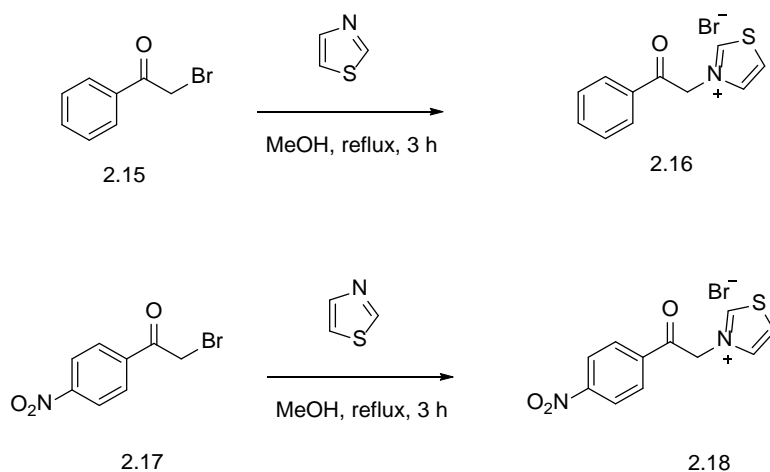


Figure 2.17. Synthesis of phenacylthiazolium bromide (2.16) and 4-nitrophenacylthiazolium bromide (2.18).

Catechol and phloroglucinol derivatives of PTB **2.21** & **2.24** were synthesized in two steps as shown in Figure 2.18. Friedel-Crafts acylation of catechol **2.19** with chloroacetylchloride gave chloroacetylated catechol **2.20** in 71% yield,¹⁰⁶ which was further reacted with thiazole in the presence of catalytic amount of tetrabutylammonium bromide (TBAB) in methanol at reflux for 65 h. Recrystallization in methanol and diisopropylether afforded pure compound **2.21** in 41% yield. Similarly, Friedel-Crafts acylation of phloroglucinol **2.22** with chloroacetylchloride gave chloroacetylated phloroglucinol **2.23** in 34% yield,¹⁰⁷ which was further reacted with thiazole in acetonitrile at reflux for 4 d to afford compound **2.24** in 53% yield.

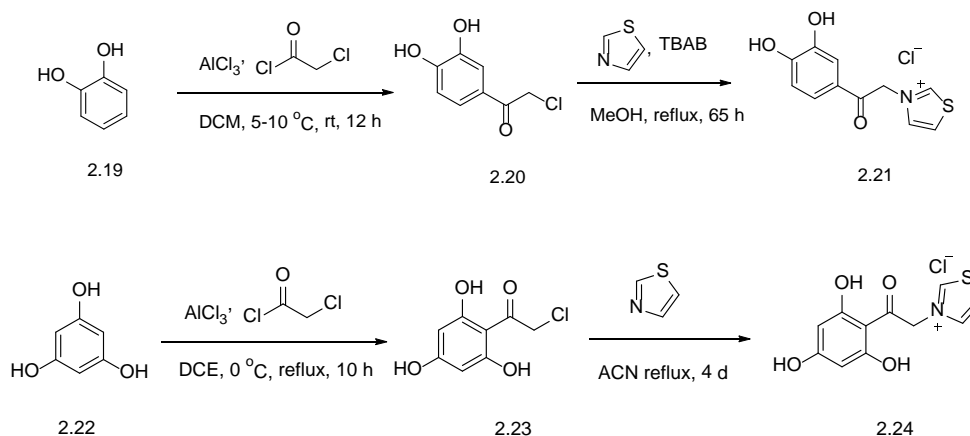


Figure 2.18. Synthesis of phenacylthiazolium compounds, **2.21** and **2.24**.

Similarly, other derivatives such as polyethylene glycol (PEG), benzylamine, and morpholine were also synthesized in two steps as shown in Figure 2.19. To synthesize

PEG-derived PTB **2.27**, PEG-methyl ether **2.25** was reacted with bromoacetylchloride in DCM for 12 h to afford bromoacetyl-derived PEG-methyl ether **2.26** in 89% yield, which was further reacted with thiazole in acetonitrile at reflux for 20 h. Purification by column chromatography afforded pure compound **2.27** in only 10% yield. Synthesis of morpholine-derived PTB **2.30** was also done by first reacting morpholine **2.28** with chloroacetyl chloride in the presence of triethylamine (TEA) in DCM for 45 min. to afford chloroacetylated morpholine **2.29** in 35% yield,¹⁰⁸ which was further reacted with thiazole in acetonitrile under microwave heating for 45 min. to afford pure compound **2.30** in 67% yield. Benzylamine-derived PTB **2.33** was also obtained by first reacting benzylamine **2.31** with chloroacetyl chloride in the presence of triethylamine (TEA) in DCM for 45 min. to afford N-benzyl-2-chloroacetamide **2.32** in 58% yield,¹⁰⁹ which was further reacted with thiazole in acetonitrile under microwave heating for 45 min. to afford pure compound **2.33** in 27% yield.

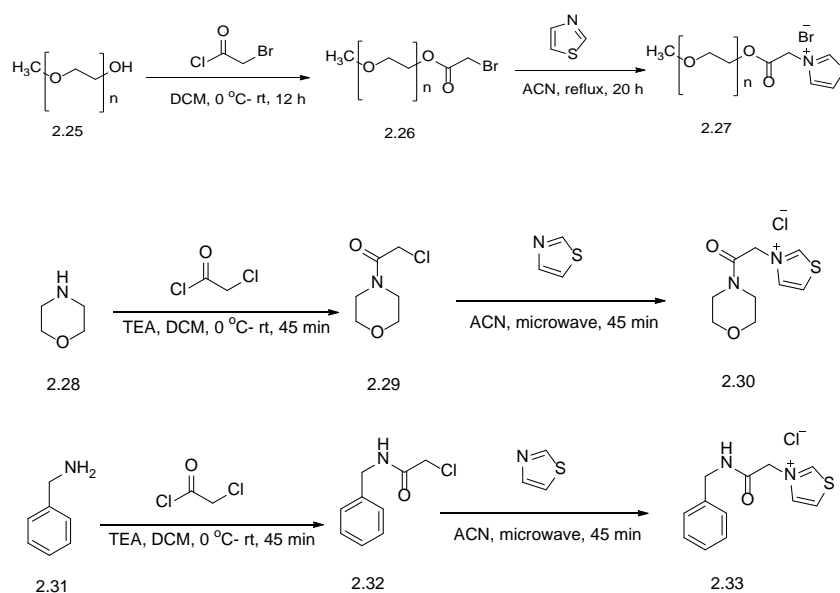


Figure 2.19. Synthesis of phenacylthiazolium compounds, **2.27**, **2.30**, and **2.33**.

2.2.2. Synthesis of N-phenacyl-3-methylimidazolium Halide and its Nitro Derivative. Several methods for the synthesis of phenacyl-methylimidazolium halides have been reported in the literature.^{103, 110-113} N-phenacyl-3-methylimidazolium halide **2.35** and 4-nitrophenacyl-methylimidazolium halide **2.37** were also prepared according to previous procedures with slight modifications^{111, 113} as shown in Figure 2.20. Bromoacetophenone **2.15** and 2-bromo-4'-nitroacetophenone **2.17** were reacted with methylimidazole in THF for 3 h at room temperature to afford pure compounds **2.35** & **2.37** in 80% and 77% yield, respectively.

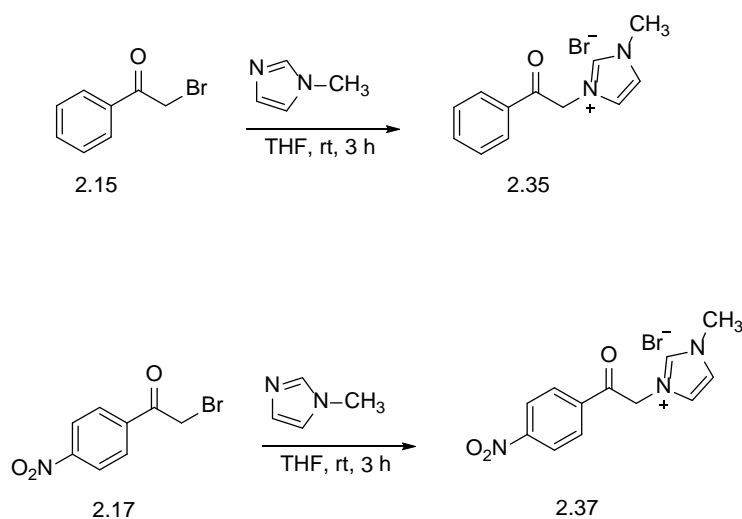


Figure 2.20. Synthesis of N-phenacylimidazolium halides, 2.35 and 2.37.

2.2.3. Synthesis of Dimers of Phenacylthiazolium (PTB) and Phenacylimidazolium Halides. Dimeric versions of PTB and N-phenacylimidazolium

halides were synthesized in two steps, as shown in Figure 2.21. In the first step, chloroacetylated diphenylmethane **2.39** was prepared according to a previous procedure with slight modifications.¹¹⁴ Friedal-Crafts acylation of diphenylmethane **2.38** with chloroacetylchloride gave pure compound **2.39** in 60% yield, which was further used as a starting material for the synthesis of dimeric compounds **2.40** and **2.41**. Compound **2.39** was reacted with thiazole in acetonitrile under microwave heating for 5 h to afford PTB-dimer **2.40** in 80% yield. Similarly, phenacylimidazolium dimer **2.41** was obtained in 43% yield by reacting **2.39** with methylimidazole in acetonitrile under microwave heating for only 45 min. Many synthetic challenges were overcome to synthesize bis-phenacylthiazolium and imidazolium (**2.40**, **2.41**) based derivatives.

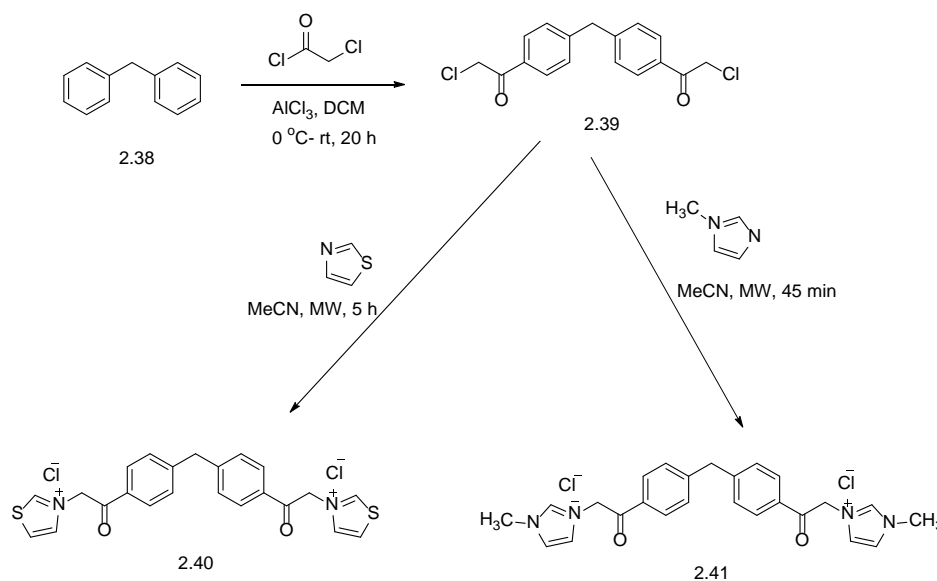


Figure 2.21. Synthesis of phenacylimidazolium compounds, **2.40** and **2.41**.

2.2.4. Reactivity Study of AGE-Inhibitors and AGE-Breakers by ^{13}C NMR Spectroscopy.

Zhu et al.¹¹⁵ have shown by NMR (1D and 2D) and LC-MS in the bovine lens crystalline-DHA assay that four tea flavanols (EC, ECG, EGC, and EGCG) could trap dehydroascorbic acid (DHA) and form conjugates as shown in Figure 2.22 to prevent glycation in the lens. Ascorbic acid (ASA) in the lens present in very high concentration (3mM)¹¹⁶ is oxidized in to a reactive dicarbonyl dehydroascorbic acid (DHA),¹¹⁷ precursor for the formation of AGEs as shown in Figure 2.23, which are known to be causative factors for the diseases such as nephropathy, atherosclerosis, diabetic retinopathy and cataract.^{31, 118}

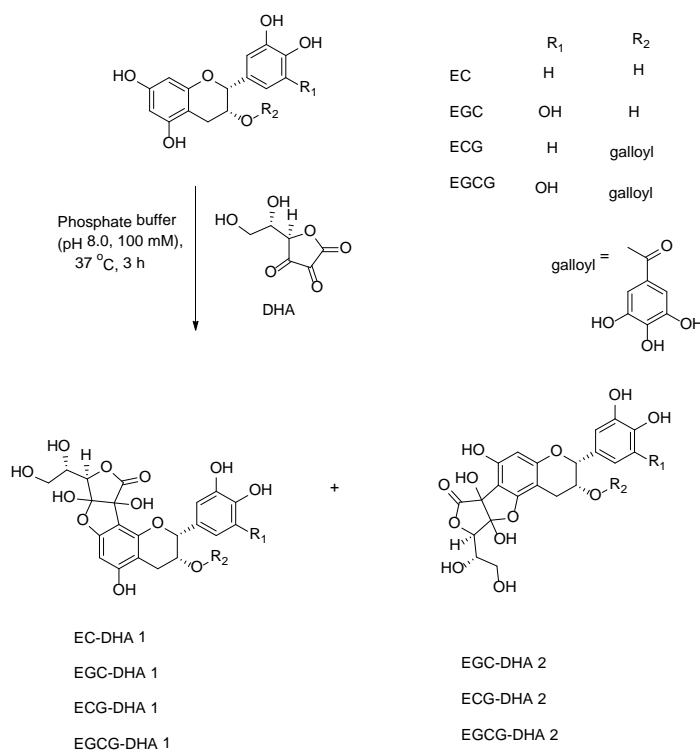


Figure 2.22. Chemical structures of DHA adducts of flavanols, EC, EGC, ECG, and EGCG.

2.2.4.1. In situ PTB-DHA adduct formation. To the best of our knowledge, PTB-DHA adduct formation has not been reported in the literature. We first time demonstrated the in-situ adduct formation in NMR tube between DHA and PTB in deionized water at room temperature at different time intervals by ^{13}C NMR spectroscopy as shown in Figure 2.24.

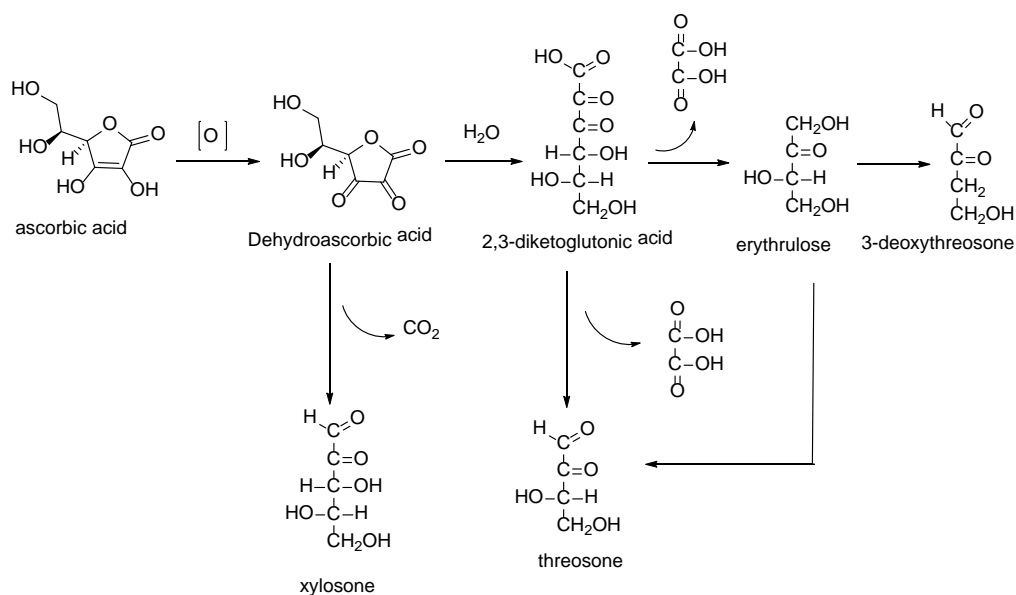


Figure 2.23. Schematic representation of the oxidation of dehydroascorbic acid (DHA), followed by its further degradation in human lens.

Structures of four possible stereoisomers of PTB-DHA adduct are shown in Figure 2.25. Out of these four possible structures, **PTB-DHA 3** adduct is in agreement with the theoretical calculations as shown in Table 2.1.

2.2.4.2. In situ adduct formation of DHA with novel AGE-inhibitors and AGE-breakers. After conforming the PTB-DHA adduct formation by ^{13}C NMR spectroscopy, In situ adduct formation between novel AGE-inhibitors and –breaker

compounds **2.30**, **2.33**, **2.40**, and **2.41** and DHA was studied by ^{13}C NMR as shown in Figure 2.26. Our NMR experiment showed that all of our four AGE- inhibitors **2.30**, **2.33**, **2.40**, and **2.41** can form adducts with DHA and the rate of adduct formation is faster than PTB. As shown in Figure 2.24, PTB-DHA adduct forms in about 30 min. but in case of our novel AGE-inhibitors and AGE-breakers, the adducts are formed within 5 min. and the relative intensities of ^{13}C signals for the adducts are very high even after 5 min., as compared to the signals of the PTB-DHA adduct as shown in Figure 2.26.

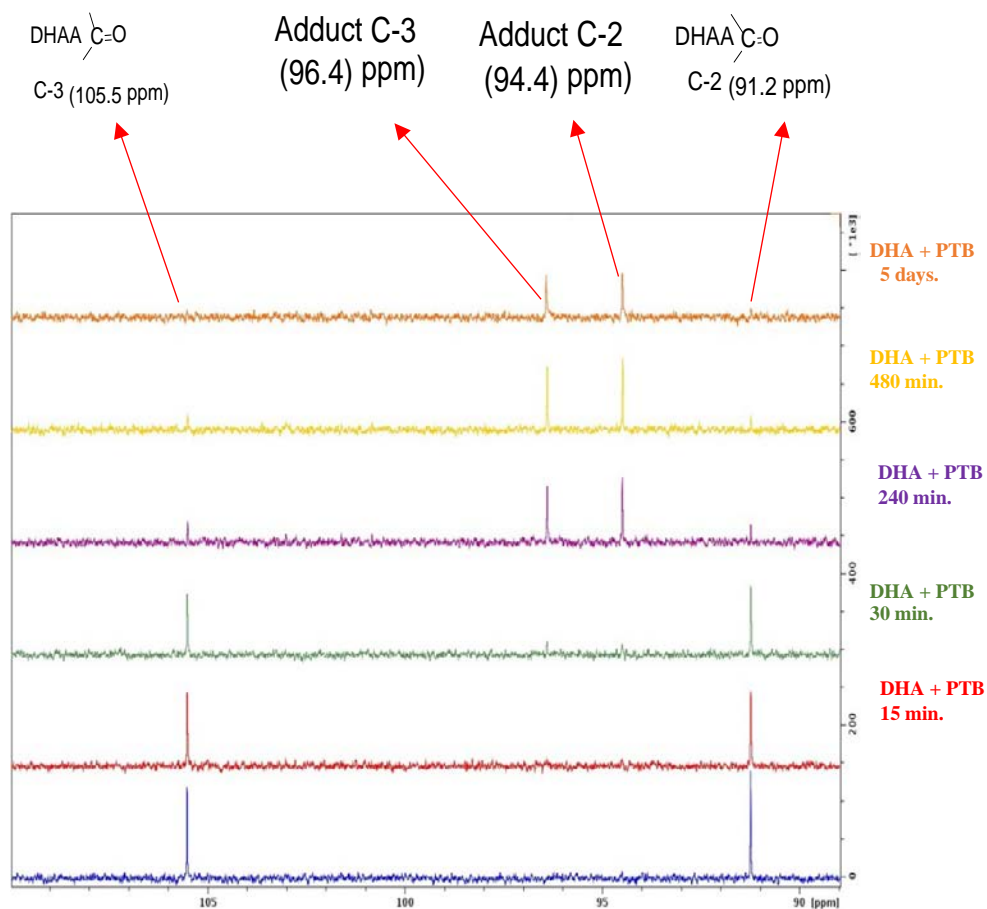


Figure 2.24. In-situ PTB-DHA adduct formation at 5, 15, 30, 240, 480 min. and 5 days.

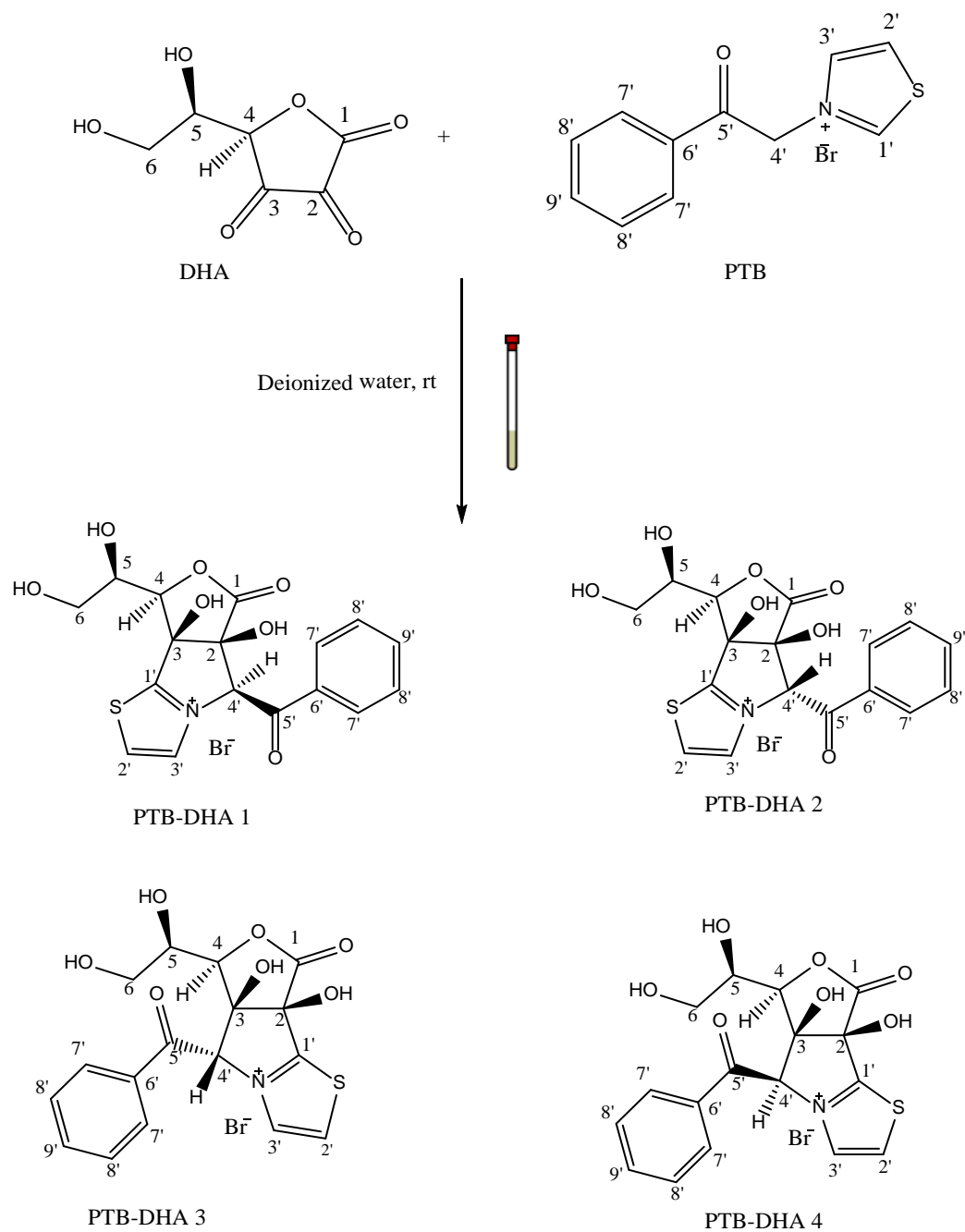


Figure 2.25. Chemical structures of the four possible stereoisomers from the reaction of DHA with PTB.

The structures shown in Figure 2.25 are various possible products of DHA-PTB adducts, and they have not been reported to date.

Table 2.1. ^{13}C NMR chemical shifts (experimental and theoretical) of four possible stereoisomers of PTB-DHA adducts.

Carbon No.	Chemical shifts in ppm				
	Exp.	Calculated			
		PTB-DHA 1	PTB-DHA 2	PTB-DHA 3	PTB-DHA 4
1	173.3	176.1	171.6	169.9	170.1
2	94.4	86.7	89.3	86.4	86.5
3	96.3	88.3	85.9	97.0	94.5
4	87.3	84.5	83.8	82.5	84.7
5	76.0	73.7	74.9	74.8	72.8
6	72.7	64.2	64.3	64.9	65.2
1'	160.0	192.3	186.1	182.9	182.7
2'	125.5	139.7	136.7	140.1	138.2
3'	138.3	133.2	138.0	134.3	136.8
4'	60.5	74.9	80.3	85.3	81.8
5'	191.9	196.7	192.8	192.9	192.9
6'	132.8	136.5	136.7	137.1	140.0
7'	129.3	136.7	135.7	134.4	130.0
8'	128.5	135.6	132.6	135.4	135.2
9'	135.5	146.4	144.8	145.1	143.7

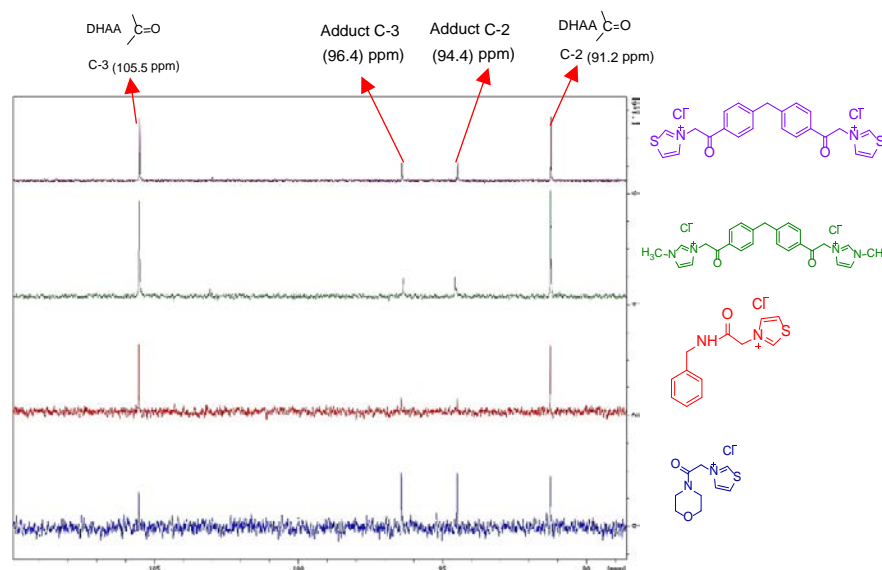


Figure 2.26. In situ adduct formation between DHA and novel AGE-inhibitors and AGE-breakers (compounds 2.30, 2.33, 2.40, and 2.41) by ^{13}C NMR spectroscopy.

2.3. EXPERIMENTAL

2.3.1. Materials and Methods. All reagents were purchased from commercial sources and used as received. Column chromatography was carried out using Merck 60, 230-400 mesh. Thin layer chromatography was carried out using silica gel coated polyester backed sheets. The ^1H and ^{13}C NMR spectrum for CDCl_3 , Acetone- d_6 , and DMSO- d_6 solutions were obtained on an INOVA-Varian 400 MHz spectrometer at 400 and 100 MHz respectively. The ^1H NMR, ^{13}C NMR chemical shifts are referenced to the residual solvents signals or the internal TMS ($\delta = 0.0$).

2.3.2. Preparation of Dehydroascorbic Acid (DHA) and its Reaction with AGE-Inhibitors and-Breakers. Dehydroascorbic acid was prepared by chemical oxidation of ascorbic acid with bromine. Ascorbic acid (3.0 eq.) with respect to PTB and other compounds **2.30**, **2.33**, **2.40**, and **2.41** was dissolved in 1 mL of deionized water at

room temperature to obtain a clear and colorless solution. To this solution, 2 or 3 drops of bromine were added to obtain a light brown colored solution, which was titrated with ascorbic acid to finally obtain a clear and colorless dehydroascorbic acid solution.

Conversion of ascorbic acid into dehydroascorbic acid and its stability in water was confirmed by ^{13}C NMR as shown in Figure 2.27. To this DHA solution, PTB was added and stirred at vortex till dissolution at room temperature. Reactivity study of PTB with DHA to form adduct was done by ^{13}C NMR at various time intervals. Similar method was applied for the reactivity study of compounds **2.30**, **2.33**, **2.40**, and **2.41**.

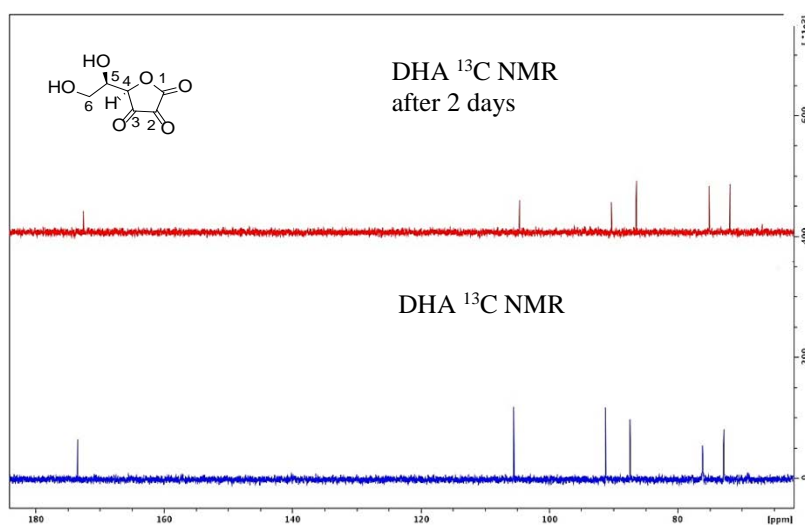
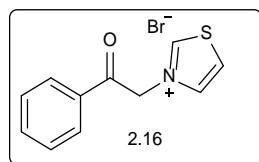
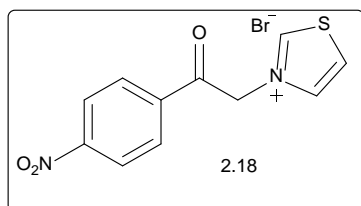


Figure 2.27. Stability of Dehydroascorbic acid in water.

2.3.3. Synthesis and Properties of Products. Synthetic methods and characterization of the compounds prepared are discussed below.

N-Phenacylthiazolium bromide (2.16).¹⁰⁵

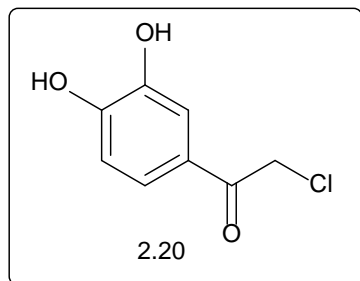
A mixture of bromoacetophenone (2.6 g, 10.06 mmol), and thiazole (1.0 g, 11.76 mmol) in methanol (30 mL) was allowed to stir under reflux for 3 h. After completion of reaction as monitored by TLC, methanol was evaporated under reduced pressure and the residue was triturated with hexane (10 mL) for 30 min. at room temperature. The solid was filtered and product thus obtained was further recrystallized with methanol and diisopropylether to obtain 3-Phenacyl-1, 3-thiazolium bromide **2.16** as a white solid (1.8 g, yield = 50%); ¹H NMR (400 MHz, DMSO-d₆) δ 10.23 (s, thiazole 1H), 8.52 (dd, J = 4.6, 0.96 Hz, thiazole 1H), 8.42 (dd, J = 6.0, 0.92 Hz, thiazole 1H), 8.06 (d, J = 8 Hz, 2H), 7.80 (t, J = 8 Hz, 1H), 7.67 (t, J = 8 Hz, 2H), 6.42 (s, 2H), ; ¹³C NMR (100 MHz, DMSO-d₆) δ 190.6, 161.6, 138.3, 134.6, 133.5, 129.1, 128.1, 126.2, 60.5.

1-(4-nitrophenacyl) thiazolium bromide (2.18).

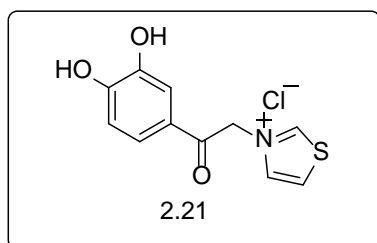
A mixture of 2-bromo-4'-nitroacetophenone (250 mg, 1.02 mmol), and thiazole (80 mg, 0.94 mmol) in methanol (5 mL) was allowed to stir under reflux for 3 h. After the reaction was complete as monitored by TLC, methanol was evaporated under vacuum and the solid obtained was recrystallized with methanol and diisopropyl ether to afford

compound **2.18** (126 mg, yield = 37%); ^{13}C NMR (100 MHz, H_2O) δ 190.5, 159.9, 150.7, 137.8, 137.3, 129.3, 126.7, 123.9, 60.2.

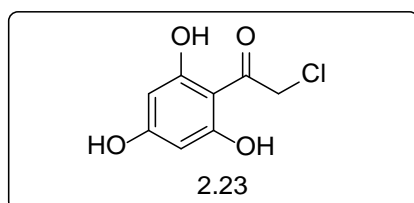
2-chloro-1-(3,4-dihydroxyphenyl)ethan-1-one (2.20).¹⁰⁶



To an oven-dried 50 mL round-bottom flask was added aluminum chloride (3 g, 22.55 mmol) to dichloroethane (10 mL) at 5-10 °C. The reaction mixture was stirred for 10 min. followed by slow addition of catechol (1 g, 9.09 mmol) in small portions over a period of 10 min. After the addition was complete, the reaction mixture was further stirred for 15 min followed by the addition of chloroacetyl chloride (1.1 g, 9.73 mmol) at 5-10 °C. After the addition was complete, the reaction mixture was allowed to come to room temperature and was further stirred overnight. After the reaction was complete as monitored by TLC, the reaction mixture was poured into cold dilute HCl (5 mL of conc. HCl in crushed ice), stirred for 1 h room temperature. The resulting precipitate was filtered, washed with cold water and dried at 120 °C overnight to afford compound **2.20** (1.2 g, yield = 71%); ^1H NMR (400 MHz, Acetone- d_6) δ 8.86 (s, 1OH), 8.43 (s, 1OH), 7.46-7.48 (m, 2H), 6.92 (d, J = 8.0 Hz, 1H), 4.84 (s, 2H); ^{13}C NMR (100 MHz, Acetone- d_6) δ 190.2, 151.8, 146.1, 128.1, 123.2, 116.1, 115.9, 46.9.

3-(2-(3,4-dihydroxyphenyl)-2-oxoethyl)thiazol-3-ium chloride (2.21).

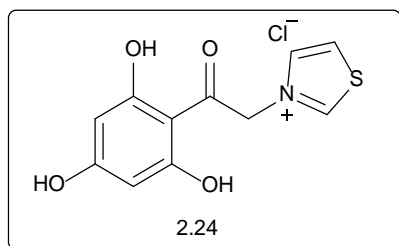
A mixture of 2-chloro-1-(3,4-dihydroxyphenyl)ethan-1-one (1 g, 5.4 mmol), thiazole (594 mg, 7 mmol), tetrabutylammonium bromide (250 mg, 0.77 mmol) in (40 mL) methanol was allowed to stir under reflux for 65 h. After the reaction was complete as monitored by TLC, methanol was evaporated under vacuum. The residue was triturated with acetone, filtered and was further recrystallized with methanol and diethylether to afford pure compound **2.21** (600 mg, yield = 41%); ^1H NMR (400 MHz, DMSO- d_6) δ 10.19 (s, thiazole 1H), 8.47 (dd, $J = 4.88, 1.16$ Hz, thiazole 1H), 8.37 (dd, $J = 6.04, 2.4$ Hz, thiazole 1H), 7.45 (d, $J = 2.16$ Hz, catechol 1H), 7.42 (s, catechol 1H), 6.97 (d, $J = 8$ Hz, catechol 1H), 6.30 (s, 2H); ^{13}C NMR (100 MHz, DMSO- d_6) δ 188.4, 161.4, 152.2, 145.7, 138.4, 125.9, 125.1, 121.6, 115.5, 114.9, 59.9.

2-chloro-1-(2,4,6-trihydroxyphenyl)ethan-1-one (2.23).¹⁰⁷

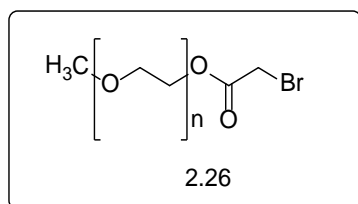
To an oven-dried 100 mL round-bottom flask was sequentially added phloroglucinol (2 g, 15.87 mmol), aluminum chloride (4 g, 30.15 mmol) in dichloroethane (20 mL) at room temperature. The reaction mixture was then cooled to 0 °C, and chloroacetyl chloride (2.2 g, 19.52 mmol) was added to the contents over a period

of 15 min. After the addition was complete, the reaction mixture was refluxed for 10 h. After the reaction was complete as monitored by TLC, the reaction mixture was poured into cold dilute HCl (5 mL of conc. HCl in crushed ice), stirred for 1 h room temperature. The resulting precipitate was filtered, washed with cold water and dried at 120 °C overnight to afford compound **2.23** (1.1 g, yield = 34%); ^1H NMR (400 MHz, Acetone- d_6) δ 11.53 (s, 2OH), 9.36 (s, 1OH), 5.96 (s, 2H), 4.94 (s, 2H); ^{13}C NMR (100 MHz, Acetone- d_6) δ 196, 166.2, 165.2, 103.8, 96, 51.5.

3-(2-oxo-2-(2,4,6-trihydroxyphenyl)ethyl)thiazol-3-ium chloride (2.24).

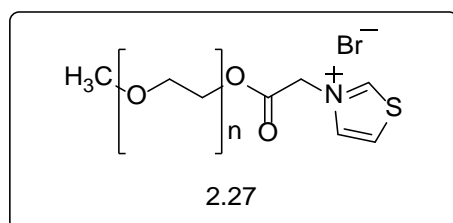


A mixture of 2-chloro-1-(2,4,6-trihydroxyphenyl)ethan-1-one **1.23** (2 g, 9.9 mmol), thiazole (12.87 mmol) in acetonitrile (60 mL) was allowed to stir under reflux for 4 days. After the reaction was complete as monitored by TLC, the reaction mixture was cooled to room temperature. The resulting precipitate was filtered, triturated with acetone, filtered and dried under air to afford 3-(2-oxo-2-(2,4,6-trihydroxyphenyl)ethyl)thiazol-3-ium chloride **2.24**. (1.5g, yield = 53%); ^1H NMR (400 MHz, DMSO- d_6) δ 12.09 (s, 2OH), 10.87 (s, 1OH), 10.17 (s, thiazole 1H), 8.48 (dd, J = 4.8, 0.8 Hz, thiazole 1H), 8.33 (dd, J = 6.0, 2.8 Hz, thiazole 1H), 6.12 (s, 2H), 5.99 (s, 2H); ^{13}C NMR (100 MHz, DMSO- d_6) δ 193.1, 166.5, 164.2, 161.5, 138.7, 125.4, 102.1, 94.9, 62.8.

2,5,8,11,14,17,20-heptaodocosan-22-yl 2-bromoacetate (2.26).

To an oven dried 100 mL round-bottom flask was added bromoacetyl chloride (1.5 mL, 21.42 mmol) to a solution of PEG-OH methyl ether (5.0 g, 14.28 mmol) in dichloromethane (50 mL) at 0 °C. After the addition was complete, reaction mixture was allowed to come to room temperature and was further stirred overnight. After completion of reaction, saturated brine solution was added and the product was extracted by adding dichloromethane (2 x 20 mL). The dichloromethane layer was washed with saturated brine solution and then with deionized water, dried over anhydrous MgSO₄ and evaporated under vacuum to afford 2,5,8,11,14,17,20-heptaodocosan-22-yl 2-bromoacetate **2.26** as a clear colorless oil (6 g, 89%); ¹H NMR (400 MHz, acetone-d₆) δ 4.26 (t, J = 4 Hz, 2H), 4.0 (s, OH), 3.69 (t, J = 4 Hz, PEG-OH, 2H), 3.45 (t, J = 4 Hz, PEG-OCH₃, 2H), 3.47-3.58 (m, PEG-OCH₃, 29 H); ¹³C NMR (100 MHz, acetone-d₆) δ 167.9, 72.6, 71.3, 71.2, 71, 69.3, 65.9, 58.8, 27.1, 27.

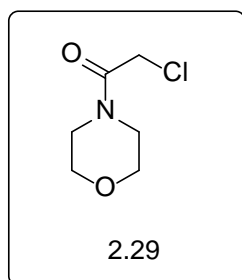
3-(24-oxo-2,5,8,11,14,17,20,23-octaoxapentacosan-25-yl)thiazol-3-ium bromide (2.27).



A mixture of 2,5,8,11,14,17,20-heptaodocosan-22-yl 2-bromoacetate 1.26 (2.0 g, 4.24 mmol), and thiazole (550 mg, 6.47 mmol) in acetonitrile (40 mL) was allowed to

stir under reflux overnight. After completion of reaction as monitored by ^1H NMR, acetonitrile was evaporated under reduced pressure. The residue was further purified by column chromatography by eluting with dichloromethane to afford pure 3-(24-oxo-2,5,8,11,14,17,20,23 octaoxapentacosan-25-yl)thiazol-3-ium bromide **2.27** as a clear yellow oil (250 mg, 10%); ^1H NMR (400 MHz, DMSO- d_6) δ 10.3 (s, thiazole 1H), 8.57 (dd, $J = 4.76, 1.08$ Hz, thiazole 1H), 8.37 (dd, $J = 6.0, 1.04$ Hz, thiazole 1H), 5.58 (s, 2H), 3.21-3.48 (m, PEG-OCH $_3$ 46 H); ^{13}C NMR (100 MHz, DMSO- d_6) δ 167.4, 161.5, 138.2, 126.2, 72.3, 71.3, 69.8, 69.6, 60.2, 58.1, 54.7.

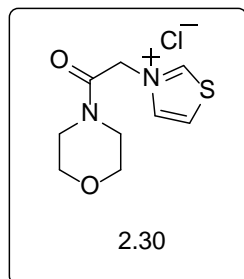
2-chloro-1-morpholinoethan-1-one (2.29).¹⁰⁸



To an oven-dried 50 mL round-bottom flask was added chloroacetyl chloride (1 g, 8.85 mmol) to a solution of morpholine (850 mg, 9.77 mmol), triethylamine (2.4 mL, 17.6 mmol) in dichloromethane (20 mL) at 0 °C. After the addition was complete, reaction mixture was allowed to come to room temperature and was further stirred for 45 min. After completion of reaction as monitored by ^1H NMR, 5% aqueous hydrochloric acid was added and the product was extracted with dichloromethane (2 x 20 mL). The dichloromethane layer was washed with saturated brine solution and then with deionized water, dried over anhydrous MgSO_4 and evaporated under vacuum to afford 2-chloro-1-morpholinoethan-1-one **2.29** as a yellow solid (550 mg, yield = 35%); ^1H NMR (400 MHz, CDCl_3) δ 3.93 (s, 2H), 3.51-3.56 (dt, $J = 20.50, 4.64$ Hz, morpholine 4H), 3.44 (t, J

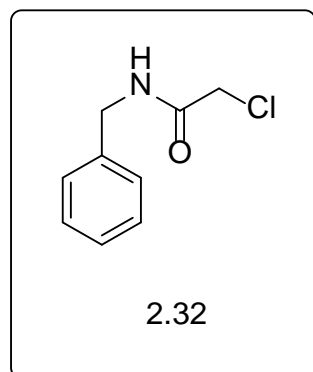
= 4.64 Hz, morpholine 2H), 3.36 (t, J = 4.72, morpholine 2H); ^{13}C NMR (100 MHz, CDCl_3) δ 165, 66.3, 66.2, 46.4, 42.2, 40.5.

3-(2-oxo-2-(1-morpholino) thiazoliumchloride (2.30).



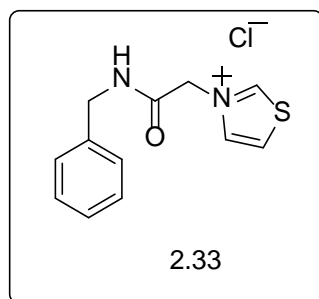
To a microwave reaction vial was sequentially added 2-chloro-1-morpholinoethan-1-one 1.29 (540 mg, 3.312 mmol), thiazole (1.4 g, 16.47 mmol) and acetonitrile (8 mL). The vial was sealed and kept in microwave. After the reaction was complete as monitored by TLC, the resulting precipitate was filtered, then further triturated with diethylether, filtered and air dried to afford compound **2.30** as a brown solid (550 mg, yield = 67%); mp: 215-222 $^{\circ}\text{C}$; ^1H NMR (400 MHz, DMSO-d_6) δ 10.31 (s, thiazole 1H), 8.52 (dd, J = 4.84, 0.84 Hz, thiazole 1H), 8.34 (dd, J = 6.04, 2.48 Hz, thiazole 1H), 5.89 (s, 2H), 3.49-3.70 (m, 4H), 3.43-3.48 (m, 4H); ^{13}C NMR (100 MHz, DMSO-d_6) δ 163.3, 161.7, 138.5, 125.7, 65.8, 65.7, 55.1, 44.8, 42.2.

N-benzyl-2-chloroacetamide (2.32).¹⁰⁹ Prepared according to literature procedure with slight modifications as described below.



To an oven-dried 50 mL round-bottom flask was added chloroacetyl chloride (1.6 g, 14.15 mmol) to a solution of benzylamine (1 g, 9.34 mmol), triethylamine (1.5 mL, 20.4 mmol) in dichloromethane (20 mL) at 0 °C. After the addition was complete, reaction mixture was allowed to come to room temperature and was further stirred overnight. After the reaction was complete, dichloromethane was evaporated under reduced pressure and ice cold water was added. The resulting precipitate was filtered, washed with diethyl ether and dried under vacuum to afford compound **2.32** (1.0 g, yield = 58%); mp: 92-97 °C; ¹H NMR (400 MHz, DMSO-d₆) δ 8.67, 8.25 (s, NH exchange), 7.21-7.30 (m, aromatic 5H), 4.26 (d, J = 5.96 Hz, 2H), 4.07 (s, 2H); ¹³C NMR (100 MHz, DMSO-d₆) δ 165.1, 137.9, 127.4, 126.4, 126, 41.7, 41.5.

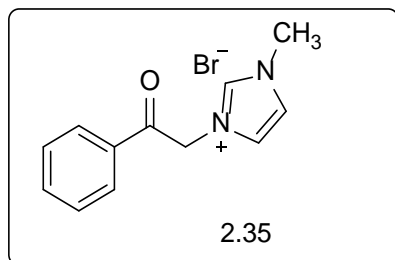
3-(2-oxo-2-benzylamino) thiazolium chloride (2.33).



To a microwave reaction vial was sequentially added N-benzyl-2-chloroacetamide **1.32** (1.0 g, 5.464 mmol), thiazole (2.3 g, 27.058 mmol), and acetonitrile (8 mL). The vial was sealed and kept in microwave. After completion of reaction as monitored by TLC, the resulting precipitate was filtered, then further triturated with acetone and filtered to afford compound **2.33** as an off-white solid (400 mg, 27%); mp: 212-218 °C; ¹H NMR (400 MHz, DMSO-d₆) δ 10.26 (s, thiazole 1H), 9.29 (t, J = 4.0 Hz, NH), 8.52 (dd, J = 4.76, 0.76 Hz, thiazole 1H), 8.32 (dd, J = 6.04, 1.04 Hz, thiazole 1H), 7.26-7.34 (m,

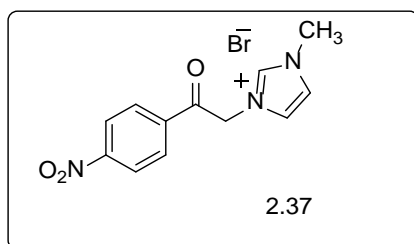
aromatic 5H), 5.52 (s, 2H), 4.34 (s, 2H); ^{13}C NMR (100 MHz, DMSO- d_6) δ 164.2, 161.4, 138.5, 138.4, 128.3, 127.4, 127.0, 125.6, 55.5, 42.5.

N-Phenacyl-3-methylimidazolium bromide (2.35).¹¹⁰



To a stirred solution of 2-bromoacetophenone **1** (2.0 g, 10.05 mmol) in 12 mL of THF was added 1-methylimidazole **2** (0.8 mL; 10.16 mmol) at room temperature. The reaction mixture was stirred at room temperature for 3 h. The solid was filtered, washed with 10 mL of ether and finally dried under vacuum to obtain 1-Phenacyl-3-methylimidazolium bromide **2.35** as a cream colored solid (2.2 g, 80%); ^1H NMR (400 MHz, DMSO- d_6) δ 9.14 (s, thiazole 1H), 8.06 (m, thiazole 2H), 7.61-7.81 (m, aromatic 5H), 6.12 (s, 2H), 3.96 (s, imidazole 3H); ^{13}C NMR (100 MHz, DMSO- d_6) δ 191.4, 137.7, 134.9, 133.7, 129.0, 128.1, 123.9, 123.2, 55.4, 35.9.

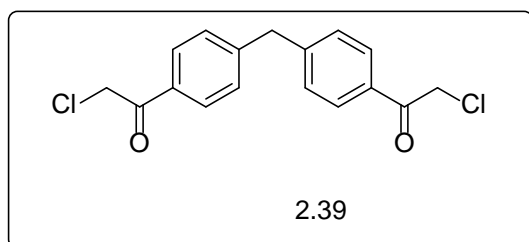
1-(4-nitrophenacyl)-3-methylimidazolium bromide (2.37).¹¹³ Prepared according to literature procedure with slight modifications as described below.



To a solution of 2-bromo-4'-nitroacetophenone (250 mg, 1.02 mmol) in THF (2 mL), N-methylimidazole (85 mg, 1.03 mmol) was added at room temperature. The instantaneously formed precipitate was stirred for 2 h at room temperature. The

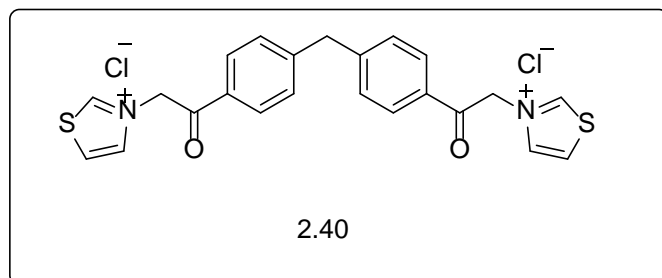
precipitate was filtered, washed with diethylether and dried under air to afford pure compound **2.37** (255 mg, yield = 77%); ^{13}C NMR (100 MHz, H_2O) δ 191.7, 150.6, 137.5, 129.2, 123.9, 123.3, 123.2, 55.1, 35.6.

4,4'-bis(chloroacetyl)diphenylmethane (2.39).¹¹⁴



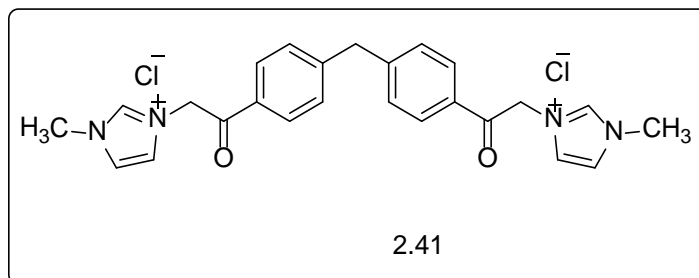
To an oven-dried 100 mL round-bottom flask was sequentially added aluminum chloride (10g, 75.18 mmol) and chloroacetyl chloride (7.5g, 66.3 mmol; solution in dichloromethane (10mL)) at room temperature. Reaction mixture was then cooled to 0 °C, and diphenylmethane (5g, 29.76 mmol; solution in dichloromethane (5mL)) was added to the contents over a period of 10 min. After the addition was complete, reaction mixture was allowed to come to room temperature and was further stirred overnight. After completion of reaction as monitored by TLC, the reaction mixture was poured in to cold dilute HCl (12.5 mL of conc. HCl in 20g of crushed ice), stirred for 15 min at room temperature, and the product was extracted by adding dichloromethane (2x25 mL). The organic layer was washed with 10% NaHCO_3 solution and then with deionized water, dried over anhydrous MgSO_4 and evaporated under vacuum. The resulting yellow solid was further purified by recrystallization in absolute ethanol to afford 4,4'-bis(chloroacetyl)diphenylmethane **2.39** as a light-yellow solid (5.8 g, yield = 60%); ^1H NMR (400 MHz, CDCl_3) δ 7.81-7.83 (m, aromatic 4H), 7.18-7.21 (m, aromatic 4H), 4.59 (s, 4H), 4.03 (s, 2H); ^{13}C NMR (100 MHz, CDCl_3) δ 190.8, 146.5, 132.9, 129.6, 129.2, 45.9, 42.1.

3,3'-((methylenebis(4,1-phenylene))bis(2-oxoethane-2,1-diyl))bis(thiazole-3-ium) dichloride (2.40).



To a microwave reaction vial was sequentially added 4,4'-bis(chloroacetyl)diphenylmethane 1.39 (225 mg, 0.7 mmol), thiazole (660 mg, 7.76 mmol), and acetonitrile (8 mL) The vial was sealed and kept in a microwave (600 Watt power, 20 psi and fan speed =100) for 5 h. After completion of reaction as monitored by ^1H NMR, reaction vial was taken out of microwave and cooled to room temperature prior to opening the cap. The product was obtained as a precipitate from the reaction mixture. The solvent acetonitrile was decanted, and the residual acetonitrile was evaporated under an air pressure. Fresh acetonitrile was added to the contents, and the mixture was stirred overnight at room temperature. The solid was filtered to afford the compound **2.40** as a pure cream colored solid (275 mg, yield = 80%); mp: 200 $^{\circ}\text{C}$ (decomposition); ^1H NMR (400 MHz, DMSO- d_6) δ 10.34 (s, thiazole 2H), 8.55 (dd, $J = 3.91, 0.84$ Hz, thiazole 2H), 8.0 (d, $J = 8.0$ Hz, aromatic 4H), 7.53 (d, $J = 8.0$ Hz, aromatic 4H), 6.52 (s, 4H), 4.23 (s, 2H); ^{13}C NMR (100 MHz, DMSO- d_6) 190.2, 161.6, 147.6, 138.3, 131.8, 129.5, 128.6, 126.1, 60.4, 40.2.

3,3'-((methylenebis(4,1-phenylene))bis(2-oxoethane-2,1-diyl))bis(1-methyl-1H-imidazol-3-ium) dichloride (2.41).



To microwave reaction vial was sequentially added 4,4'-bis(chloroacetyl)diphenylmethane 1.39 (500 mg, 1.55 mmol) 1-methylimidazole (640 mg, 7.80 mmol), and acetonitrile (6 mL) at room temperature. The vial was sealed and kept in a microwave (600 Watt power, 20 psi and fan speed =100) for 45 min. After completion of reaction as monitored by ^1H NMR, reaction vial was taken out of microwave and cooled to room temperature prior to opening the cap. The product was obtained as a precipitate from the reaction mixture. The precipitate was filtered and then triturated with diethyl ether, filtered and further purified by column chromatography by eluting with dichloromethane and methanol. The solvent was evaporated under vacuum and the residue was triturated with diethyl ether to afford a pure light-yellow compound **2.41** (325 mg, yield = 43%); mp: 177-183 $^{\circ}\text{C}$; ^1H NMR (400 MHz, DMSO-d_6) δ 9.24 (s, thiazole 2H), 8.0 (m, thiazole 4H), 7.52-7.80(m, aromatic 8H), 6.14 (s, 4H), 4.21 (s, 2H), 3.95 (s, 6H); ^{13}C NMR (100 MHz, DMSO-d_6) 191, 147.4, 137.8, 131.9, 129.4, 128.6, 123.9, 123.2, 55.2, 40.2, 35.9.

2.3.4. NMR Spectra of the Products. ^1H NMR and ^{13}C NMR spectra of all the compounds are shown in Figures 2.28-2.64.

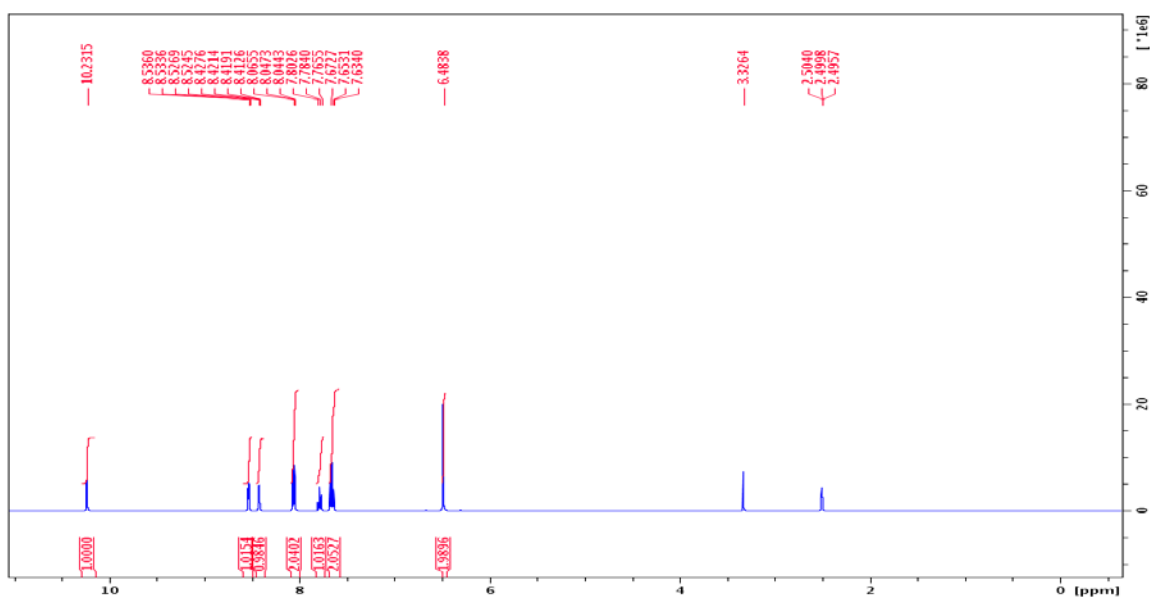


Figure 2.28. ^1H NMR spectrum of compound 2.16.

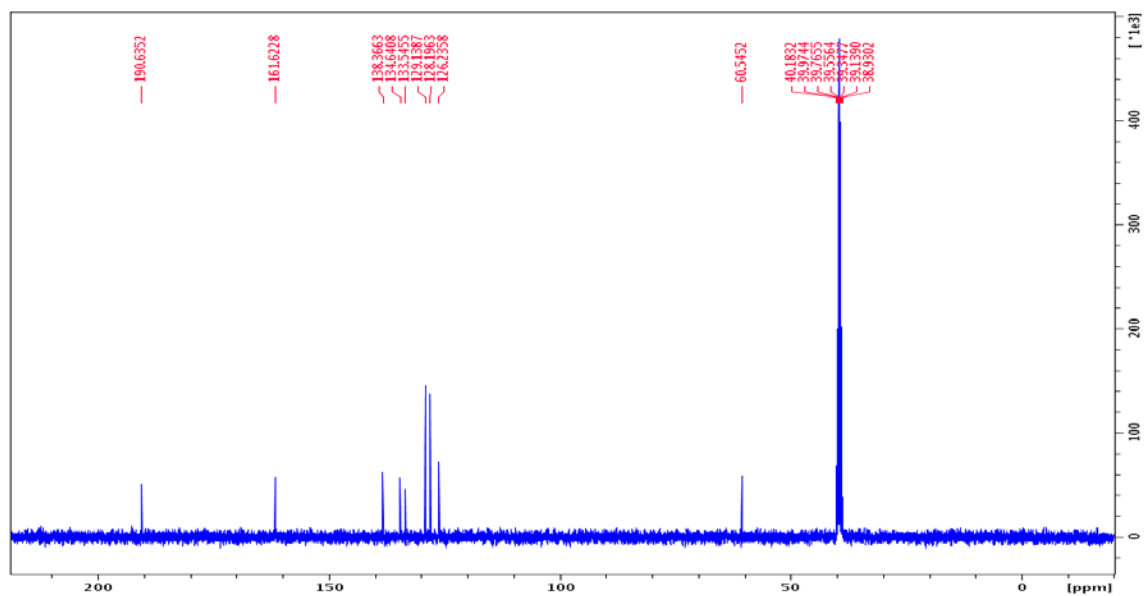


Figure 2.29. ^{13}C - ^1H decoupled NMR spectrum of compound 2.16.

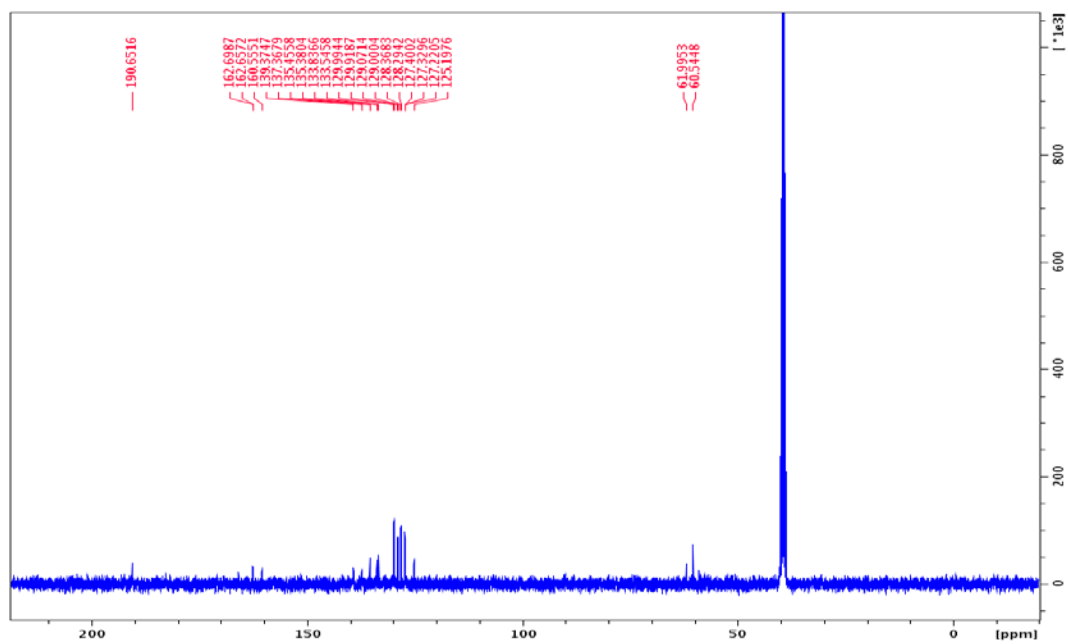


Figure 2.30. ^{13}C -H coupled NMR spectrum of compound 2.16.

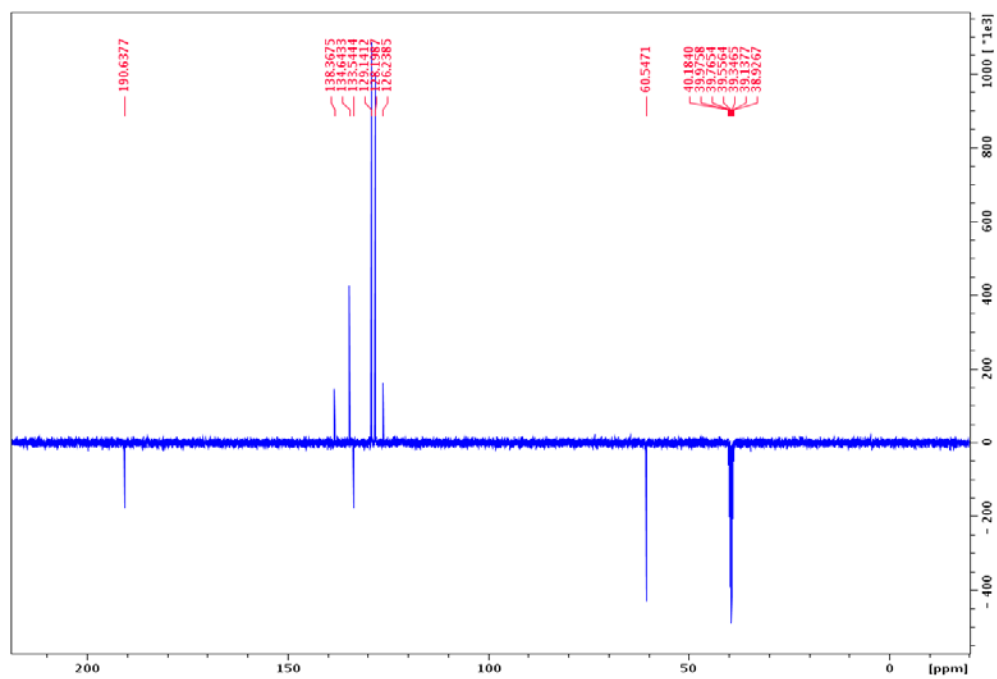


Figure 2.31. ^{13}C -APT NMR spectrum of compound 2.16.

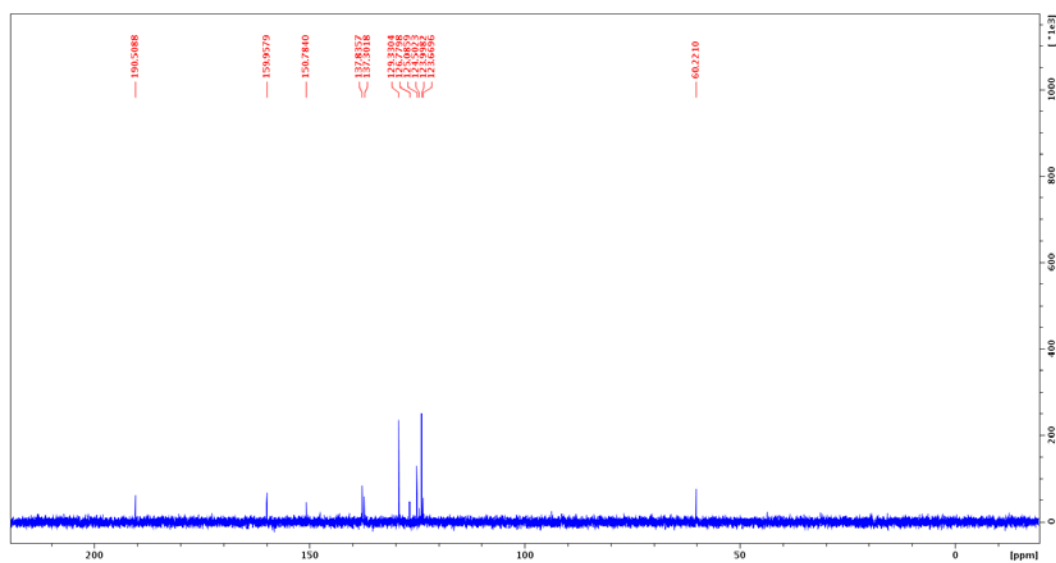


Figure 2.32. ^{13}C NMR spectrum of compound 2.18.

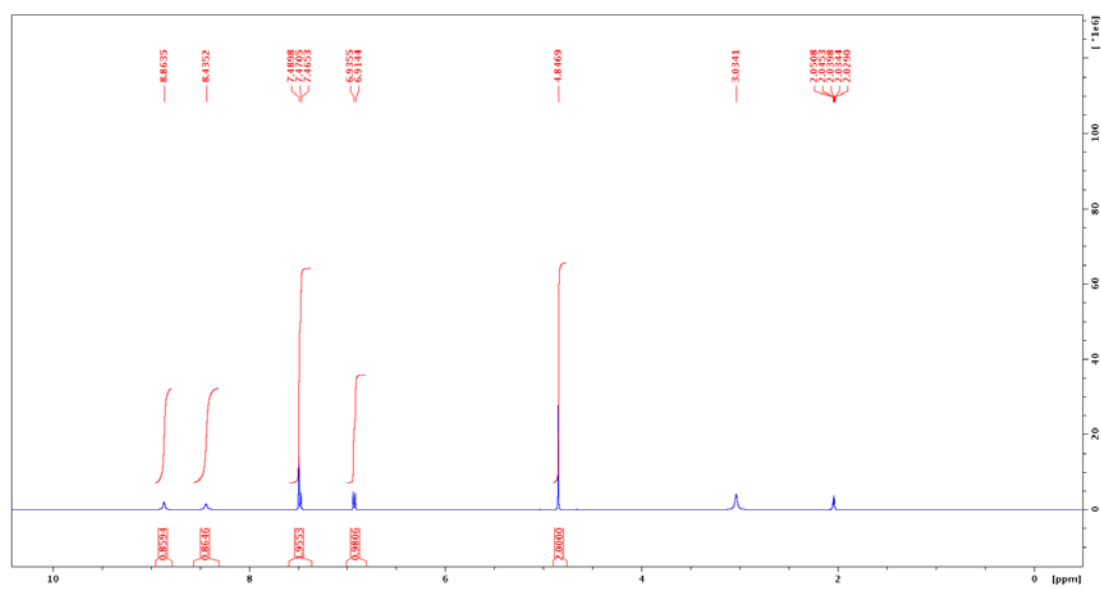


Figure 2.33. ^1H NMR spectrum of compound 2.20.

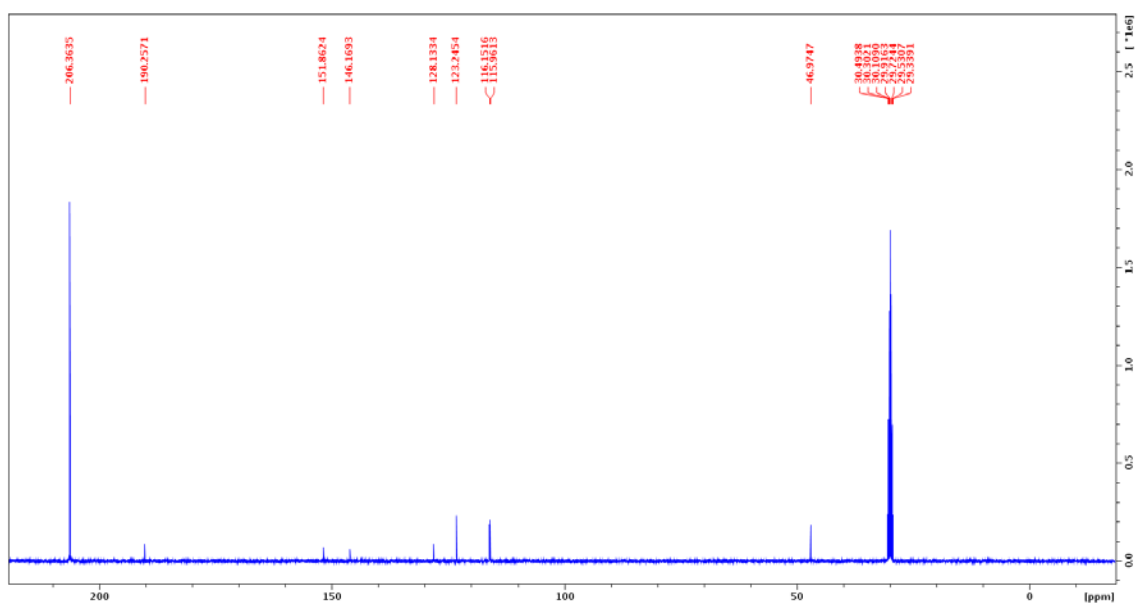


Figure 2.34. ¹³C NMR spectrum of compound 2.20.

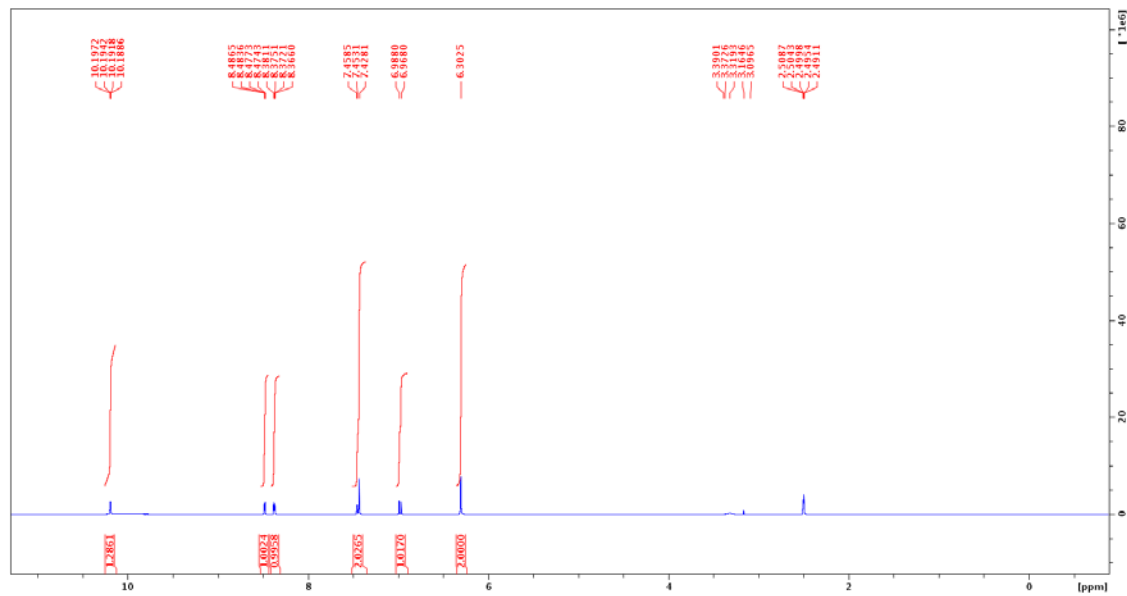


Figure 2.35. ¹H NMR spectrum of compound 2.21.

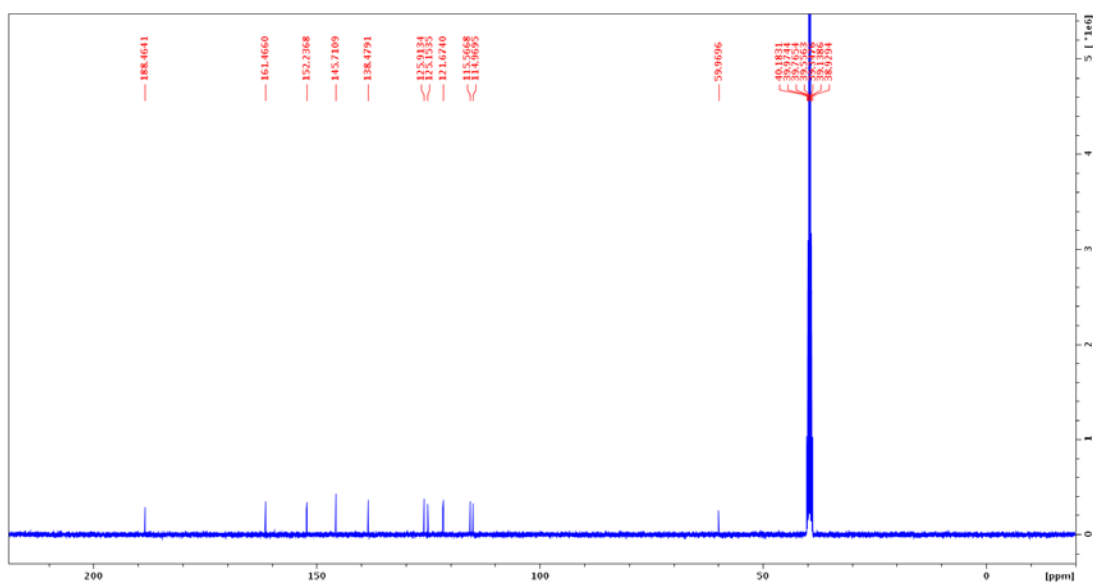


Figure 2.36. ^{13}C NMR spectrum of compound 2.21.

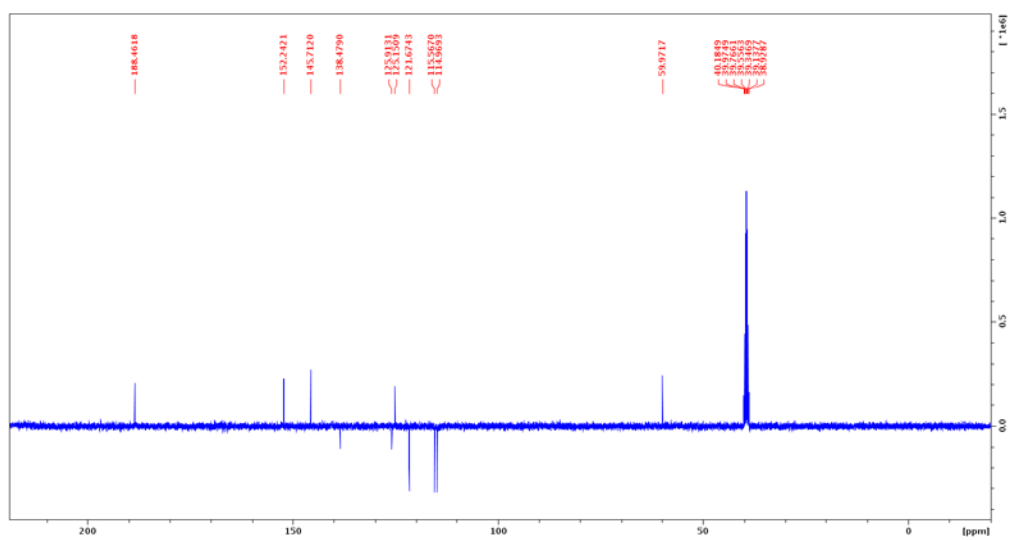


Figure 2.37. ^{13}C -APT NMR spectrum of compound 2.21.

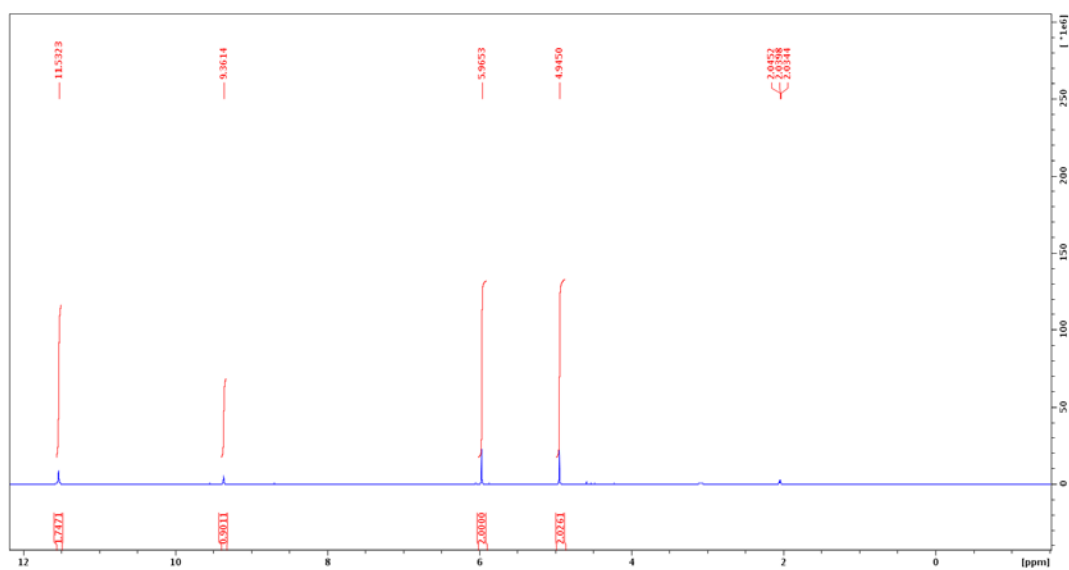


Figure 2.38. ^1H NMR spectrum of compound 2.23.

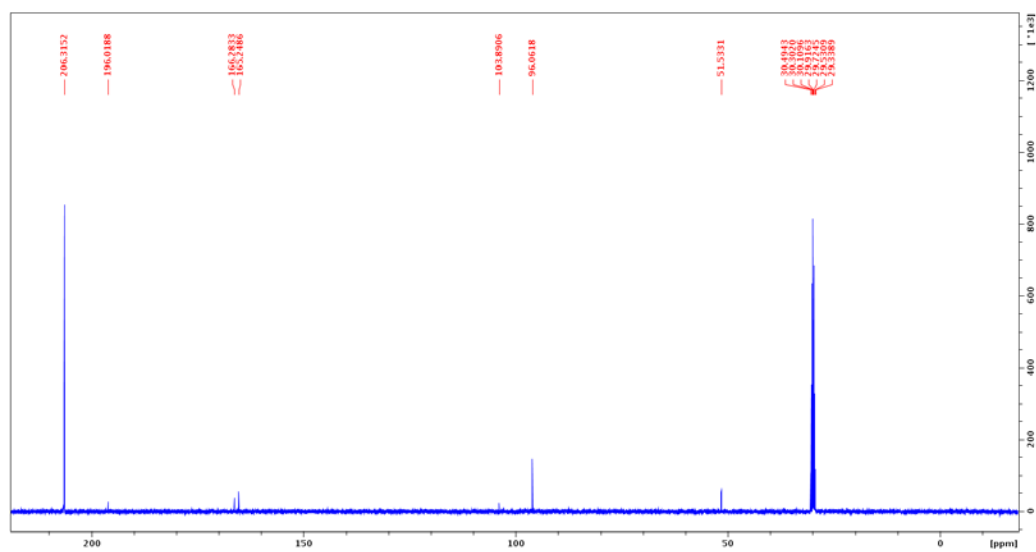


Figure 2.39. ^{13}C NMR spectrum of compound 2.23.

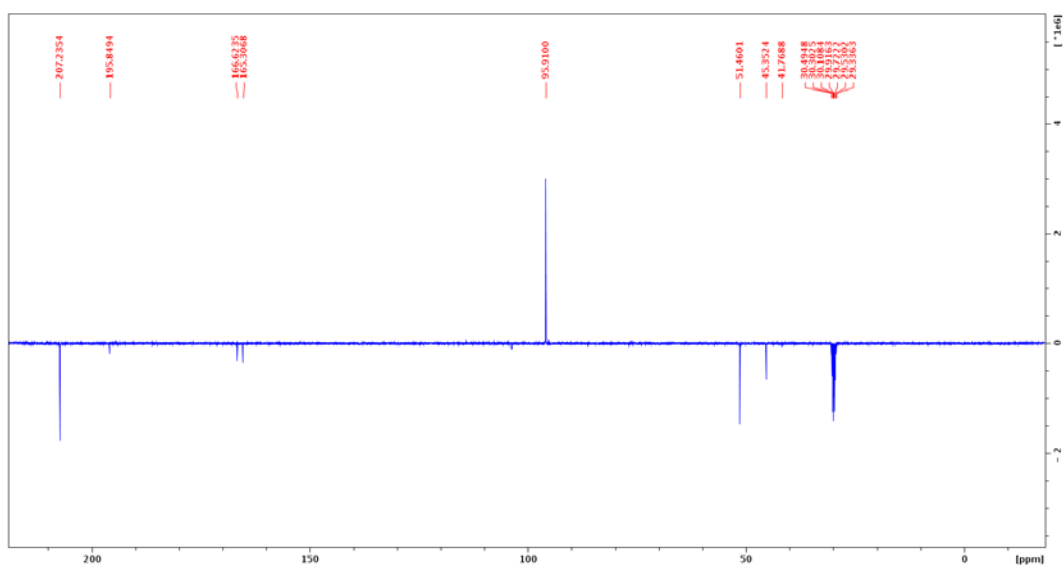


Figure 2.40. ¹³C-APT NMR spectrum of compound 2.23.

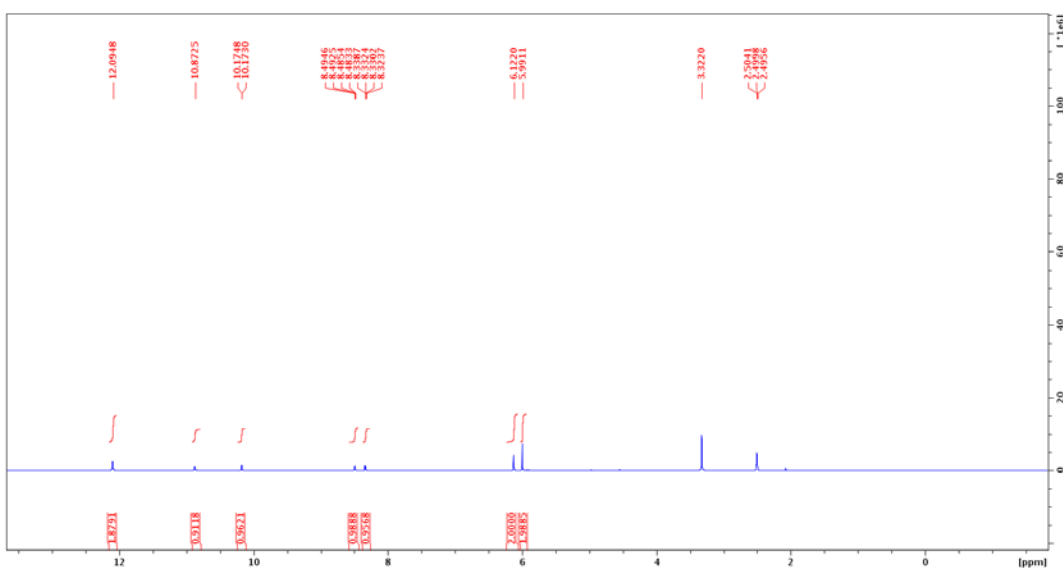
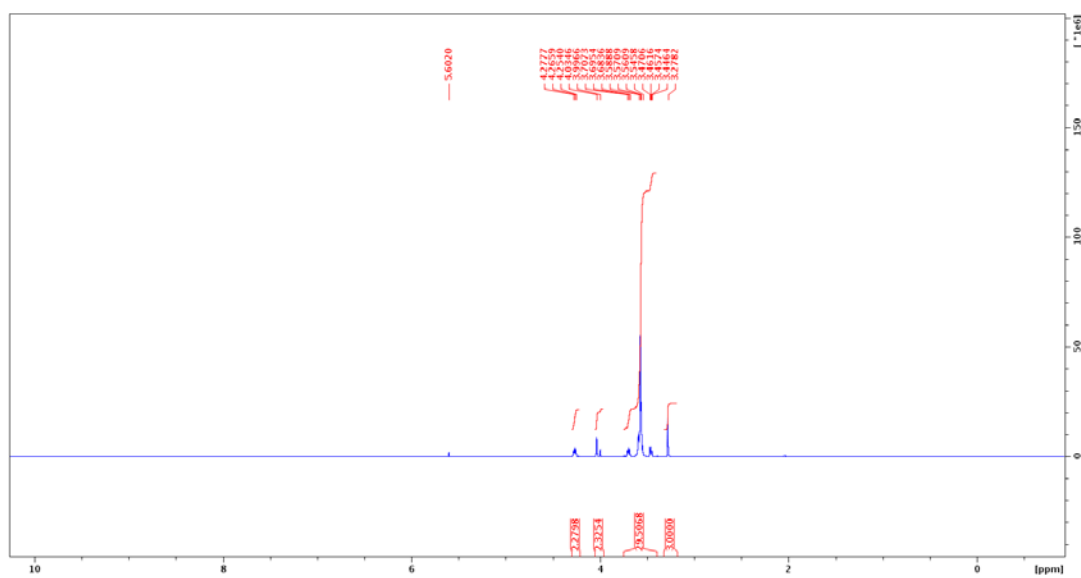
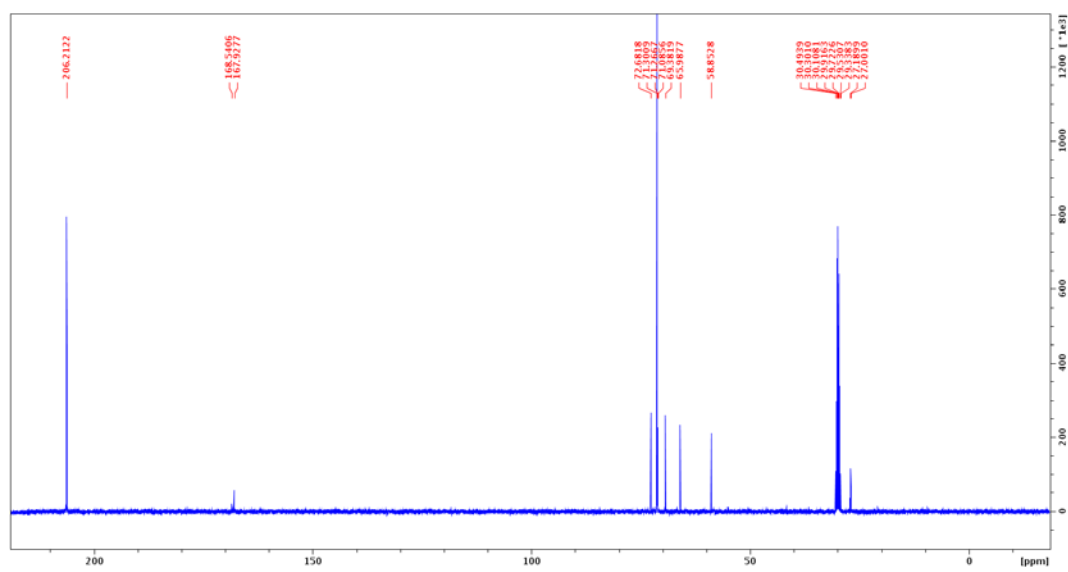
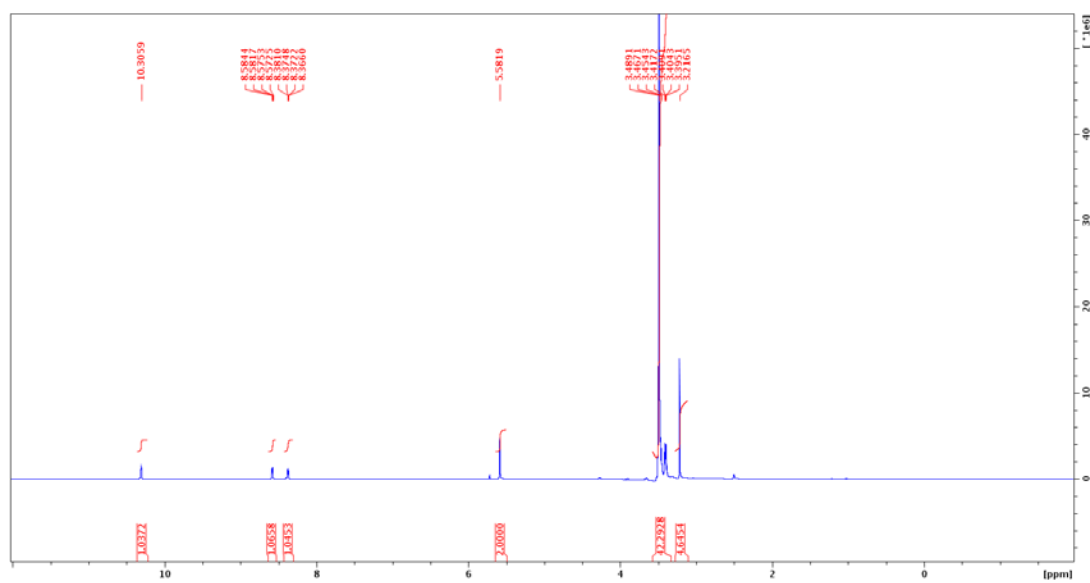
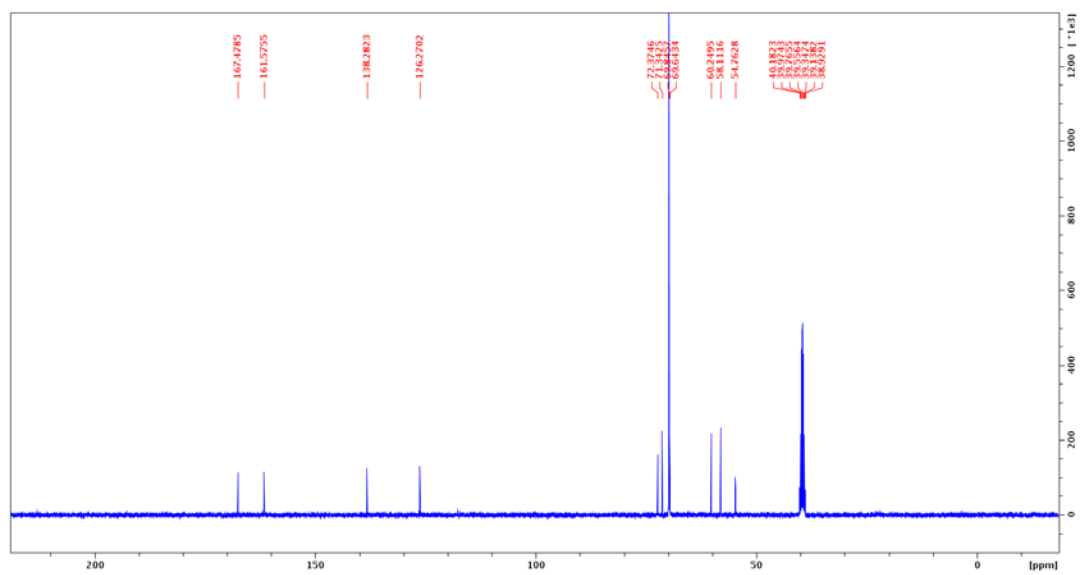


Figure 2.41. ¹H NMR spectrum of compound 2.24.

Figure 2.44. ^1H NMR spectrum of compound 2.26.Figure 2.45. ^{13}C NMR spectrum of compound 2.26.

Figure 2.46. ^1H NMR spectrum of compound 2.27.Figure 2.47. ^{13}C NMR spectrum of compound 2.27.

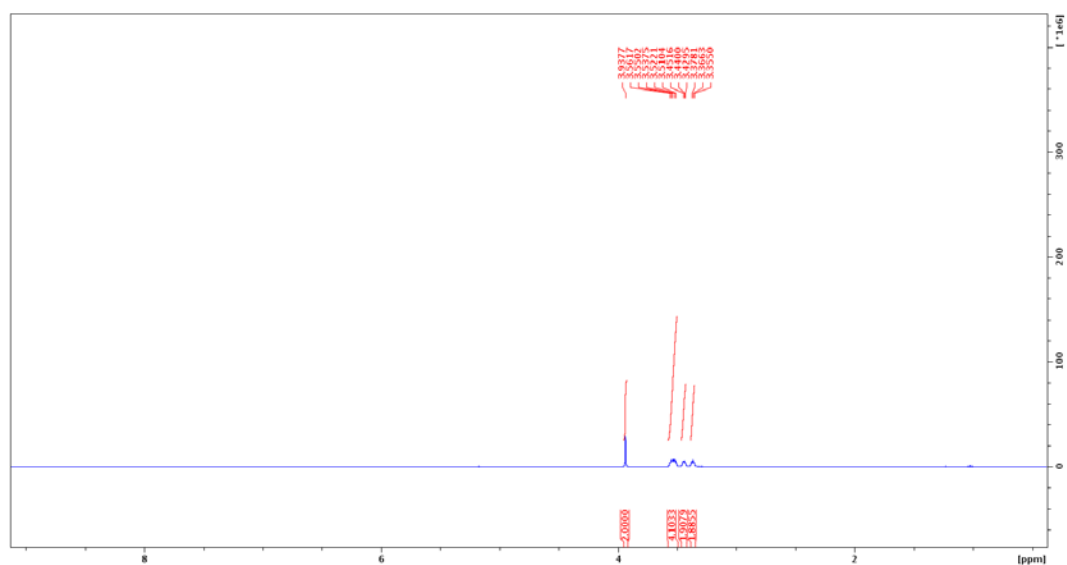


Figure 2.48. ^1H NMR spectrum of compound 2.29.

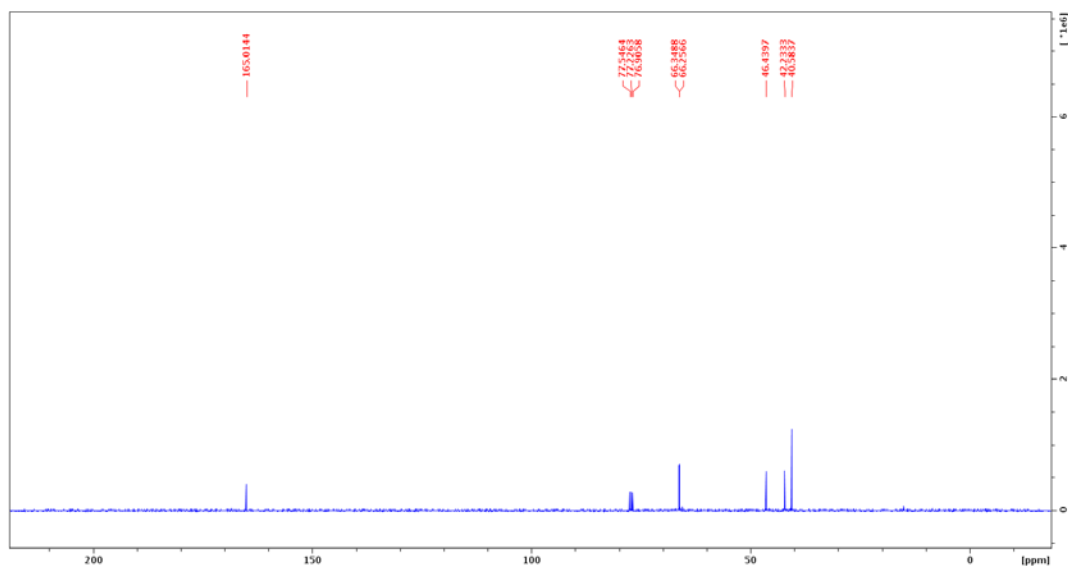
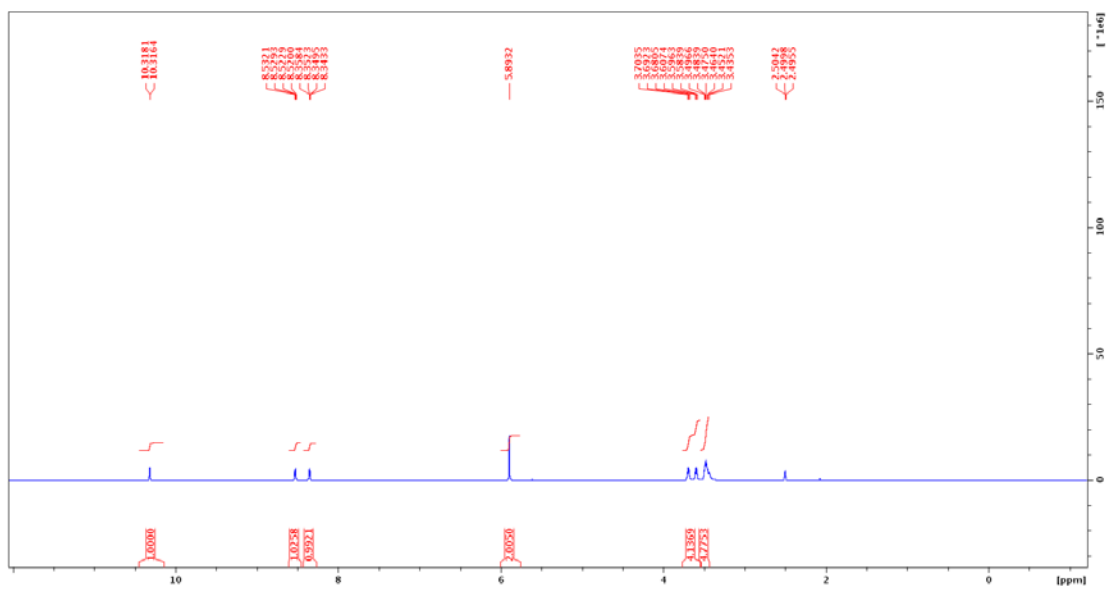
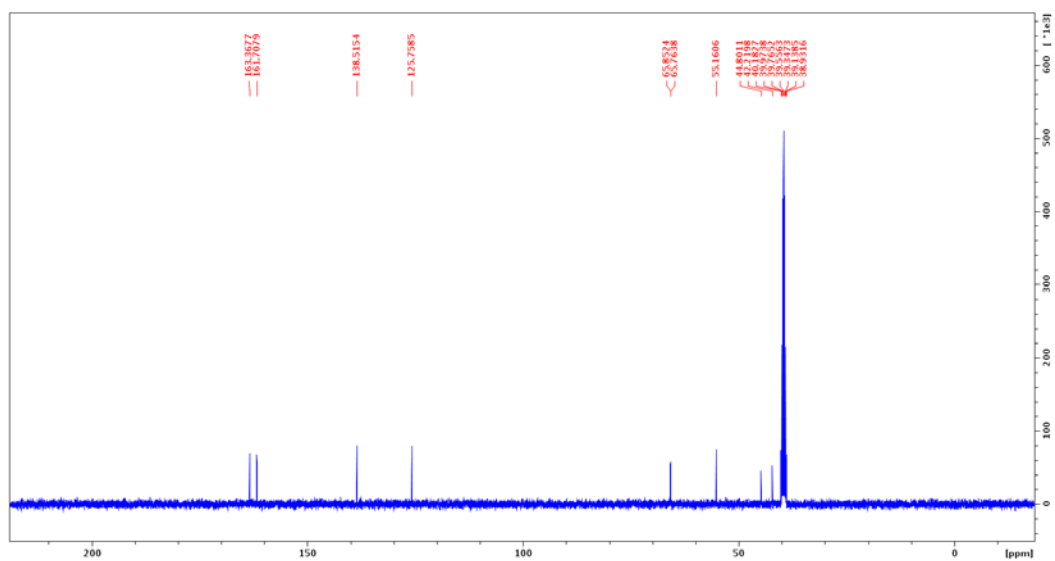
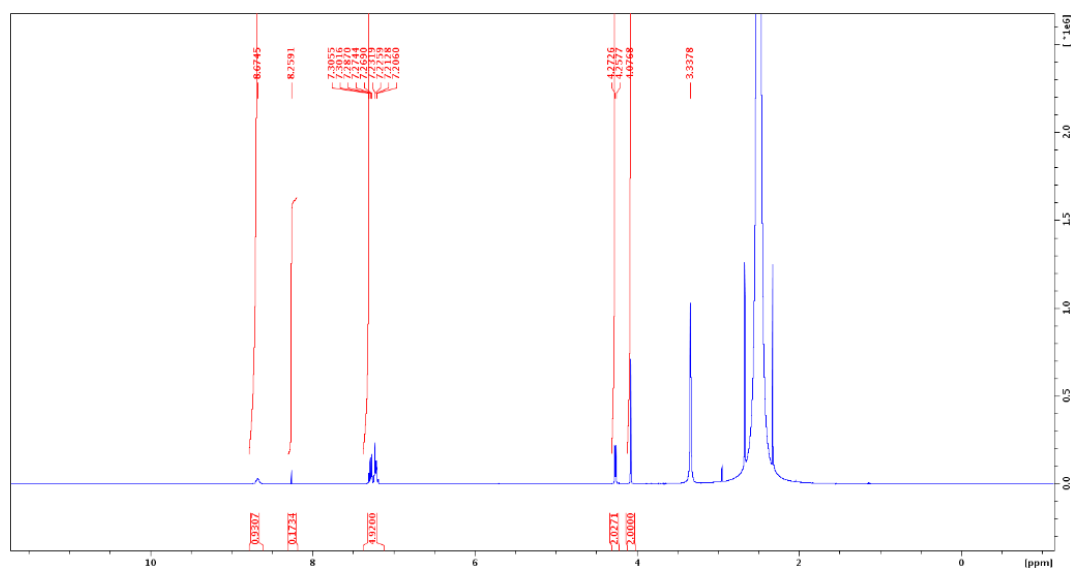
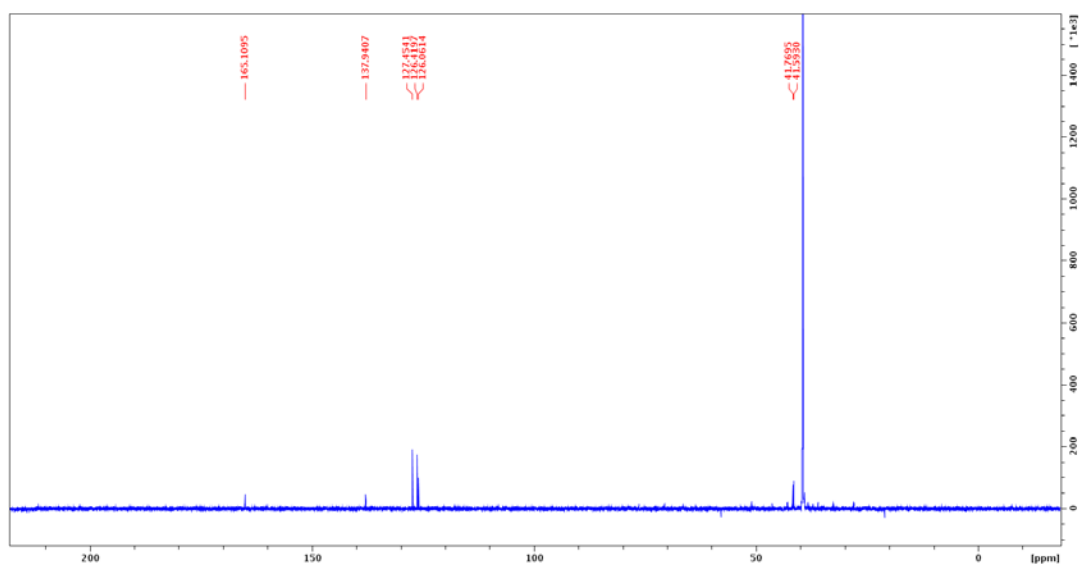
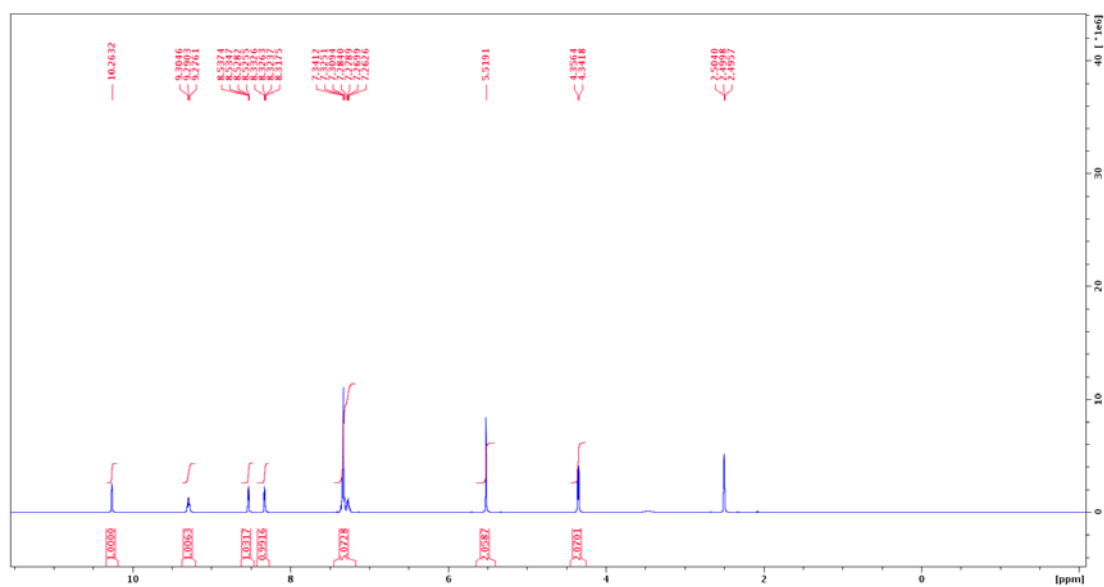
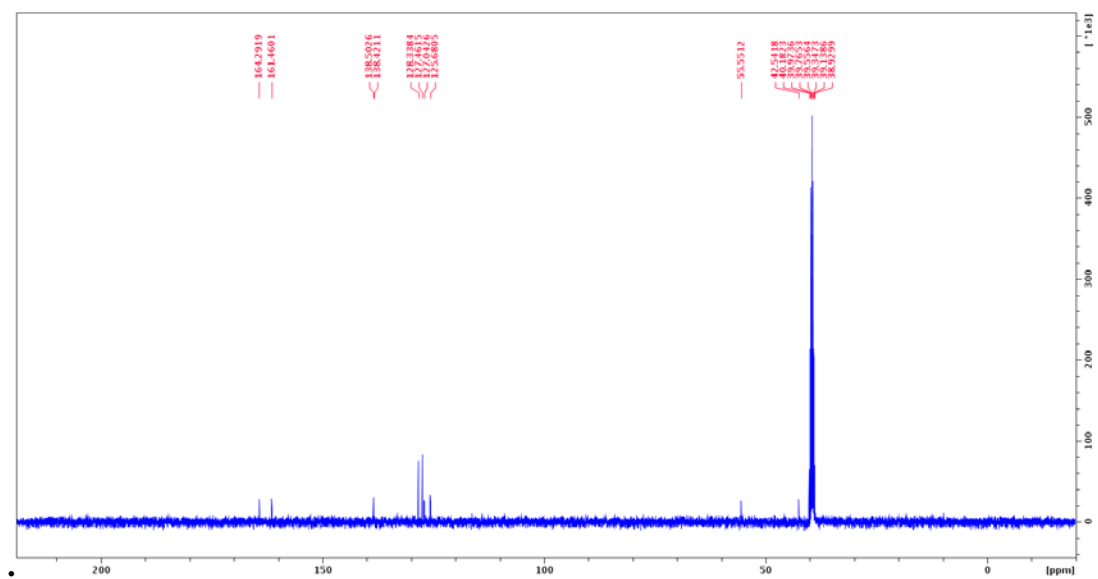
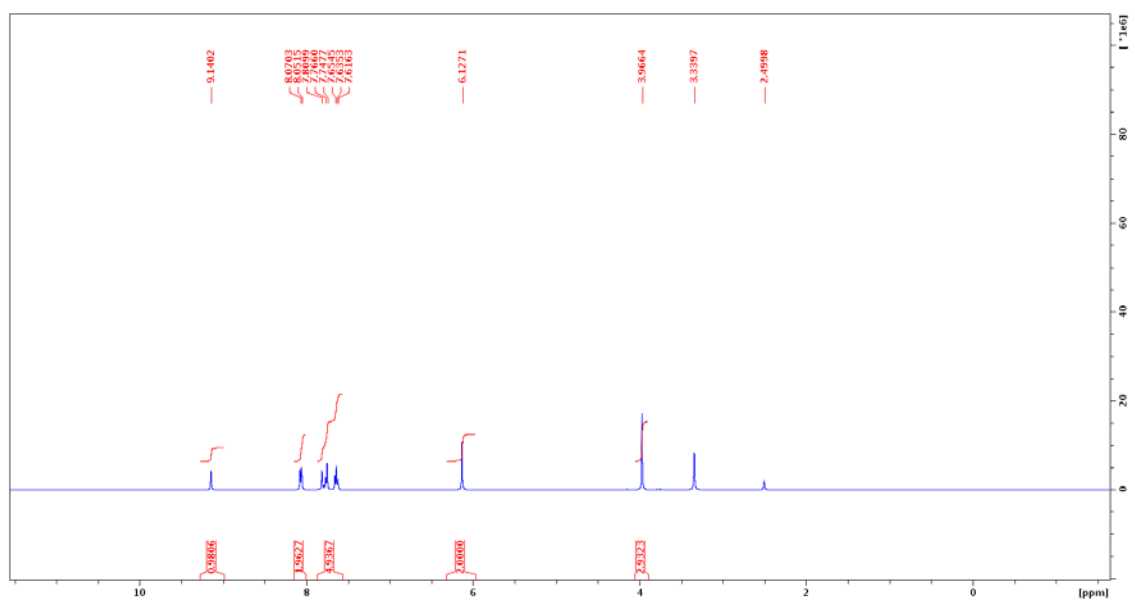
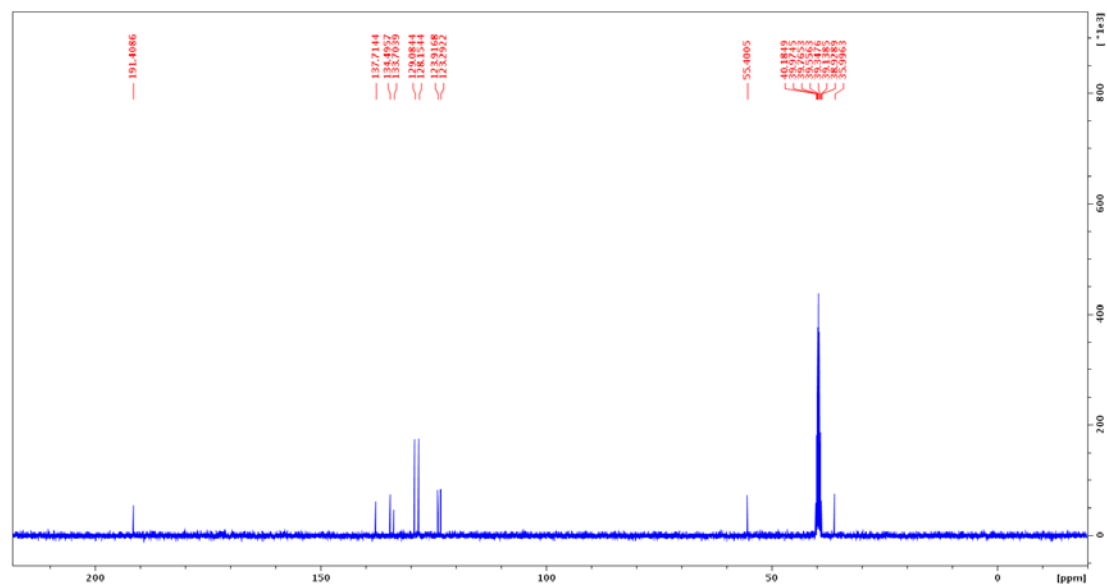


Figure 2.49. ^{13}C NMR spectrum of compound 2.29.

Figure 2.50. ^1H NMR spectrum of compound 2.30.Figure 2.51. ^{13}C NMR spectrum of compound 2.30.

Figure 2.52. ^1H NMR spectrum of compound 2.32Figure 2.53. ^{13}C NMR spectrum of compound 2.32.

Figure 2.54. ¹H NMR spectrum of compound 2.33.Figure 2.55. ¹³C NMR spectrum of compound 2.33.

Figure 2.56. ¹H NMR spectrum of compound 2.35.Figure 2.57. ¹³C NMR spectrum of compound 2.35.

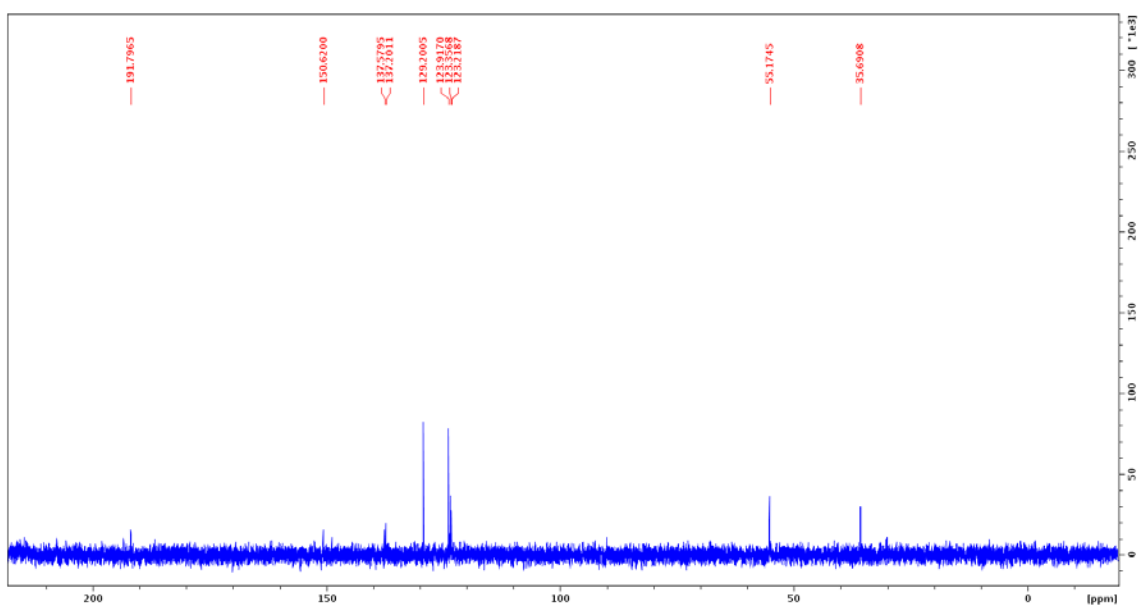


Figure 2.58. ¹³C NMR spectrum of compound 2.37.

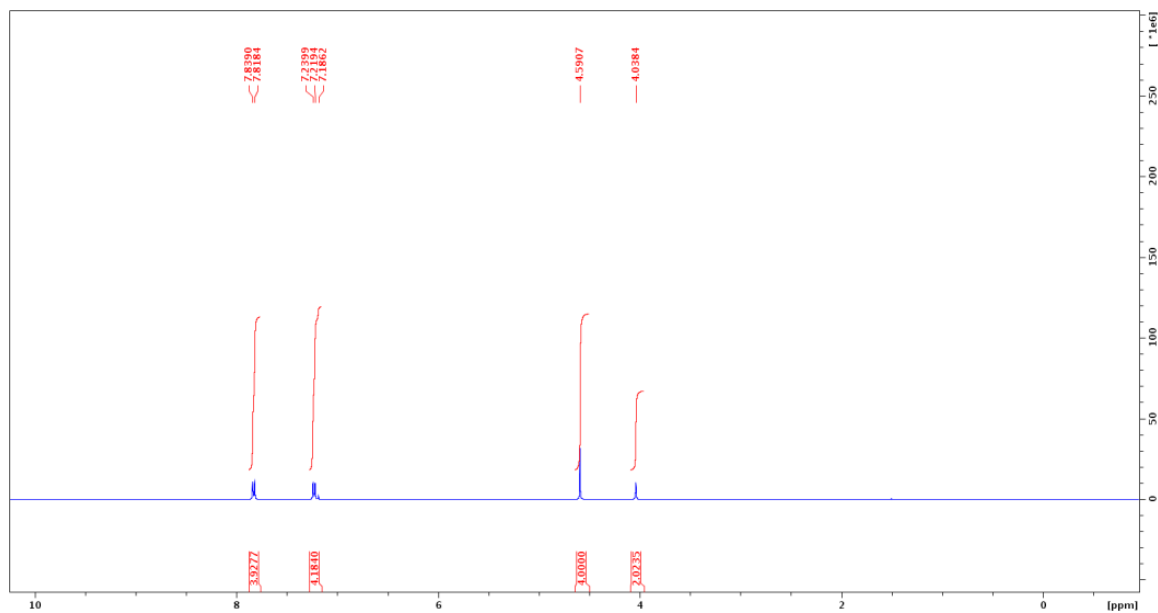


Figure 2.59. ¹H NMR spectrum of compound 2.39.

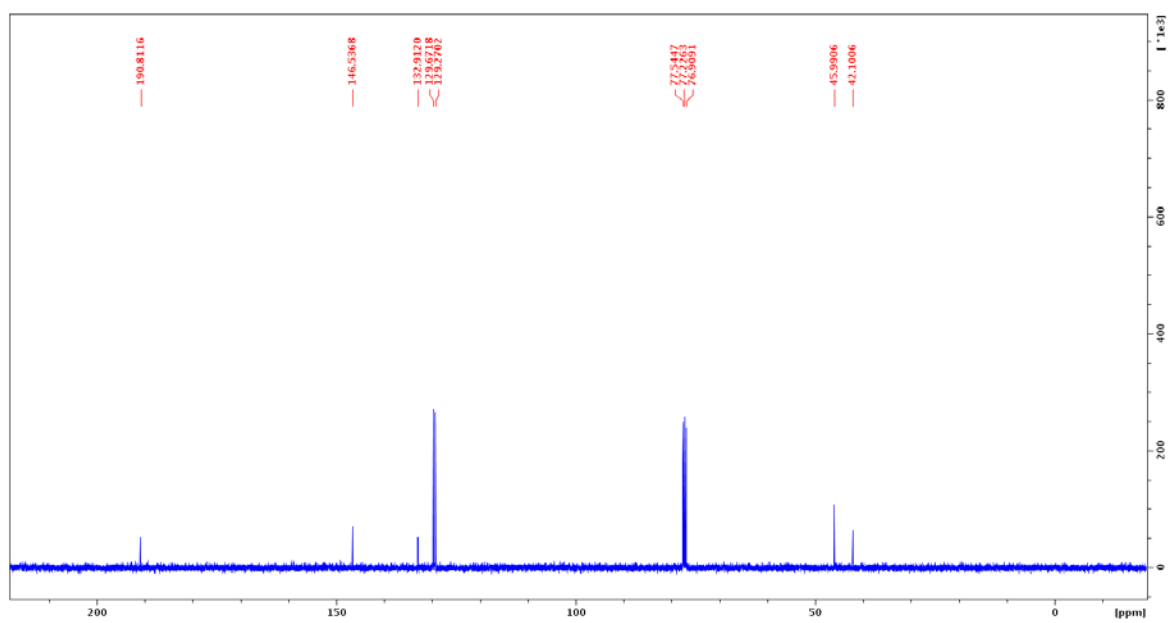


Figure 2.60. ^{13}C NMR spectrum of compound 2.39.

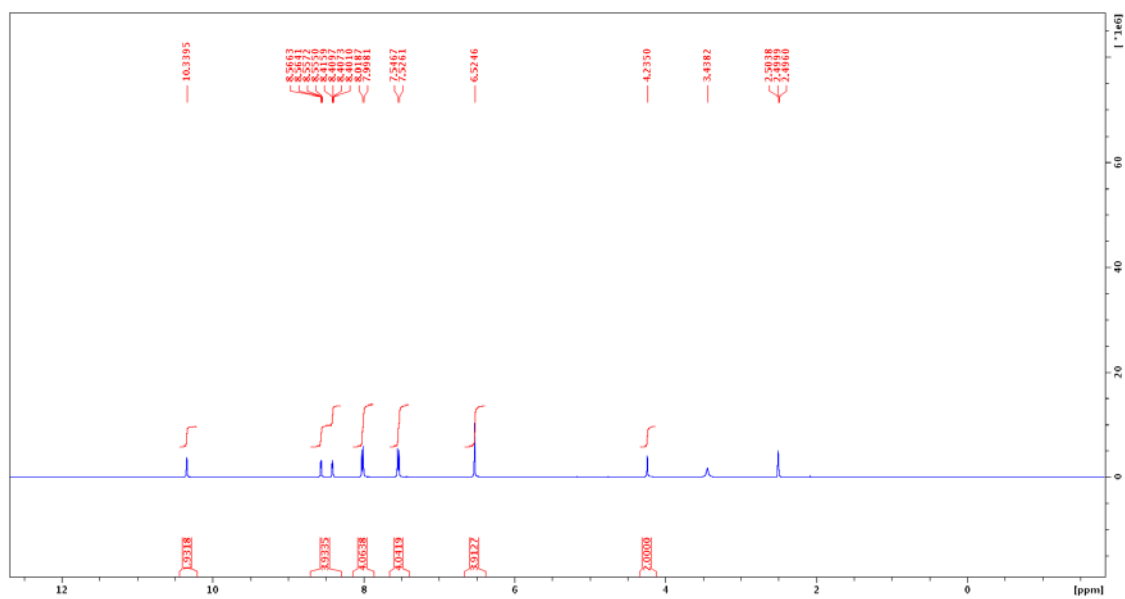


Figure 2.61. ^1H NMR spectrum of compound 2.40.

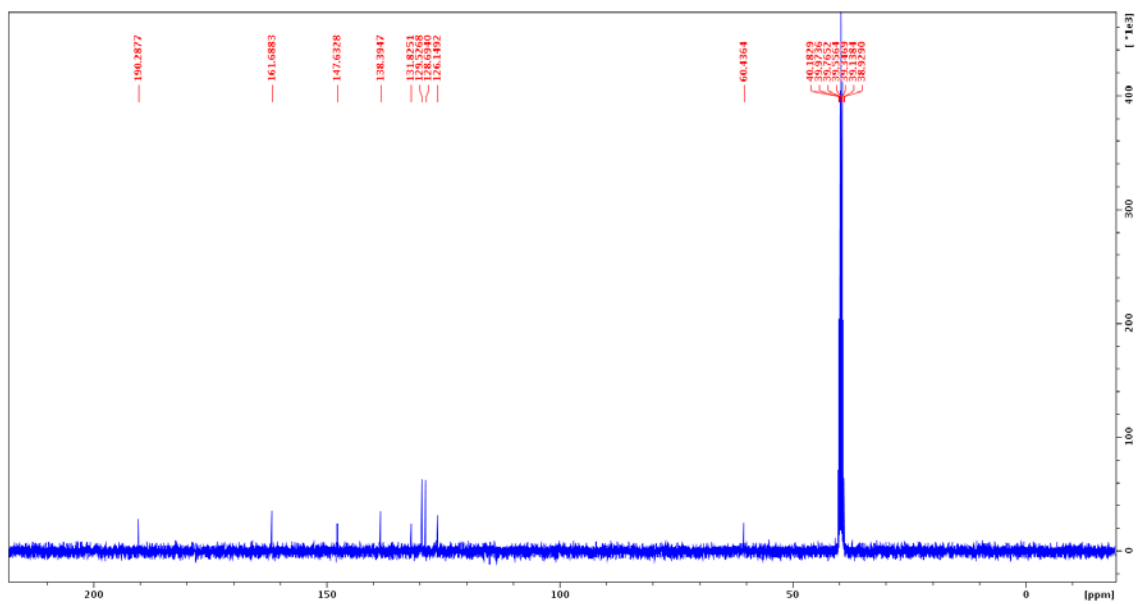


Figure 2.62. ^{13}C NMR spectrum of compound 2.40.

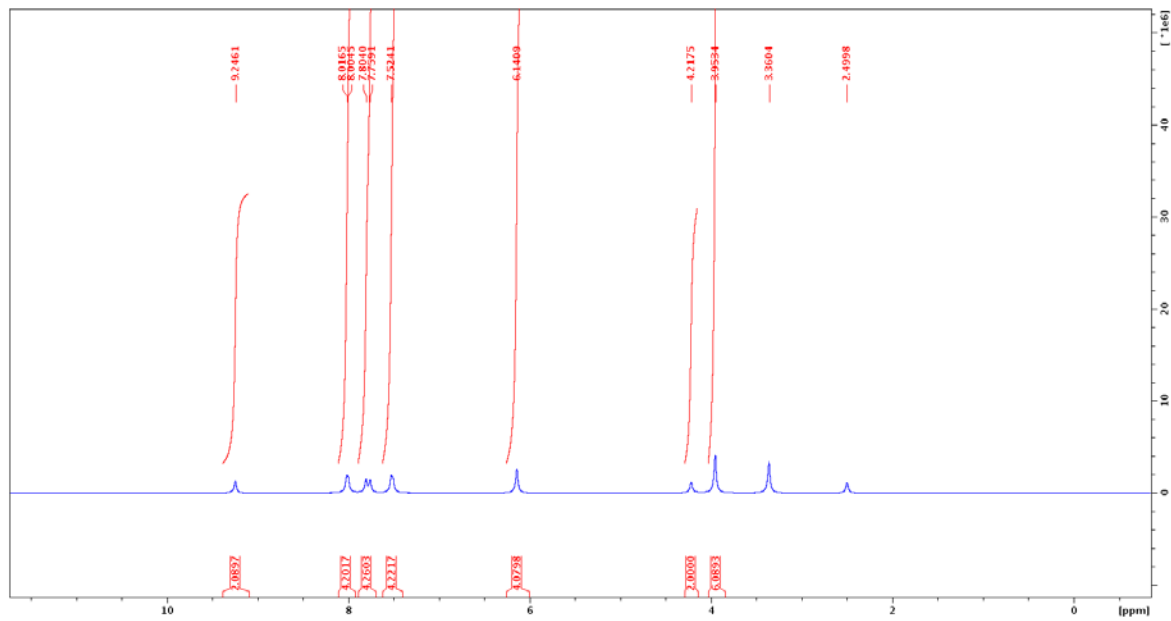


Figure 2.63. ^1H NMR spectrum of compound 2.41.

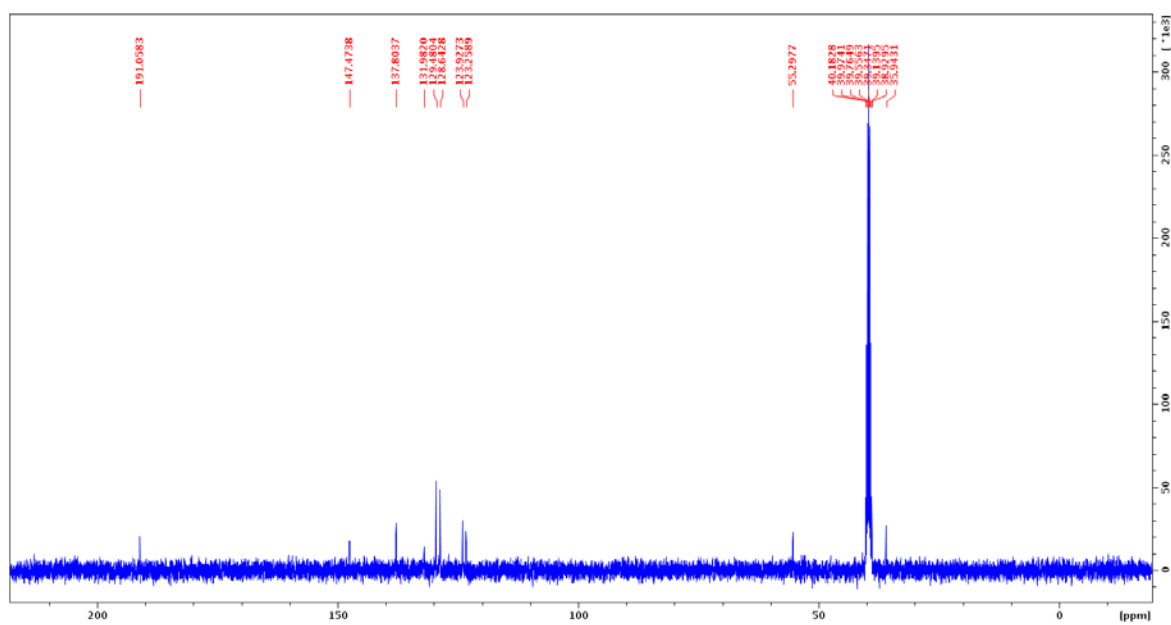


Figure 2.64. ^{13}C NMR spectrum of compound 2.41.

3. POLYPHENOLIC ANTIOXIDANTS AND CITRIC ACID AS INHIBITORS OF THE ADVANCED GLYCATION ENDPRODUCTS: A ¹³C NMR SPECTROSCOPIC STUDY

3.1. BACKGROUND

Advanced glycation end products (AGEs) are formed by a non-enzymatic browning reaction called Maillard reaction between the carbonyl groups of reducing sugars and the amino groups of proteins and amino acids during food processing.^{30, 119-121} The AGEs formed during food processing and storage control food quality parameters, including taste, aroma, color, and flavor. Furthermore, the ingested AGEs along with the endogenously formed AGEs in the human body impact human health and are the causative factors in various pathophysiological effects, including renal failure, diabetes, diabetic nephropathy, diabetic retinopathy, chronic heart failure, atherosclerosis, and Alzheimer's disease.¹²²⁻¹²⁷ There is an emerging interest in the pharmaceutical as well as food industries in developing AGE-inhibitors that would significantly attenuate the formation of the AGE during food processing or under physiological conditions in the human body. Dietary flavonoids and related polyphenols and their analogs are especially attractive targets as antiglycating agents.¹²⁸⁻¹³⁰ In addition to the polyphenolic compounds, the naturally occurring citric acid (a major constituent of lemon and orange juice) is also of interest as an antiglycating agent. Using enzyme-linked immunoassay (ELISA), it has been shown that citric acid inhibits the accumulation of AGEs, N^ε-(carboxyethyl)lysine (CEL) and N^ε-(carboxymethyl)lysine (CML), in lens proteins in animal models of type 1 diabetes.¹³¹ Phenolic acids (hydroxybenzoic acids) are present in higher concentration in food from plants than their concentration in flavonoids. Phenolic acids act as antioxidants and are effective AGE inhibitors in early stages of glycation.¹³²⁻

¹³³ The polyphenolic compound epigallocatechin-3-gallate (EGCG), an abundant constituent of green tea, in addition to its antioxidant properties, acts as a trapping agent for the reactive dicarbonyl species, such as methylglyoxal (MGO) and glyoxal (GO), which are formed as intermediates in Maillard reactions, thus attenuating the AGE formation.¹³⁴⁻¹³⁷ The polyphenol phloroglucinol, isolated from phloretin, a compound found in fruit trees is used by cosmetics and pharmaceutical industries as an antioxidant, and a phloroglucinol derivative, extracted from the brown alga *Eisenia bicyclis*, was demonstrated to have antiglycating effect.¹³⁸ Ferulic acid, 4'-hydroxy-3'-methoxycinnamic acid, is an abundant antioxidant phytochemical, and exhibits antiglycating effects, as demonstrated by fluorescence spectroscopic studies.¹³⁹ Ferulic acid when added to a model bread system reduced the formation of the CML formed by Maillard reactions.¹⁴⁰ Although these polyphenols and citric acid have been demonstrated as antioxidants and AGE-inhibitors by various studies, the relative AGE-inhibitory activities of these compounds have not been determined to date.

Maillard reactions are usually followed by fluorescence spectroscopy and other tedious techniques, such as ELISA and matrix-assisted laser desorption mass spectroscopy (MALDI), which in most cases are not reliable indicators of the extent of AGE formation. ¹³C NMR spectroscopy in aqueous solutions of the reaction mixtures provides direct evidence of the formation of the AGEs, and the extent of AGE formation can be continuously monitored for the same reaction mixture at various time intervals. At the early stages of glycation, the ¹³C NMR spectrum is relatively uncomplicated and the Maillard reaction products (AGEs and AGE-precursors) could be observed as distinct signals (at $\delta^{13}\text{C}$ 98.1, 69.3, 67.7, 64.0, 63.3, 62.8, 60.8, 60.7) in D-glucose/L-leucine and (at $\delta^{13}\text{C}$ 98.2, 69.3, 67.6, 64.0, 63.4, 60.8, 60.6) D-glucose/benzylamine model system

respectively distinct from those of the D-glucose. We have now demonstrated, using this convenient ^{13}C NMR technique, the antiglycating effects of citric acid and other polyphenolic compounds, 3,4-dihydroxybenzoic acid, acetic acid, ethanol, phloroglucinol, 2,3-dihydroxybenzoic acid, ferulic acid, benzoic acid, catechol, epigallocatechin-3-gallate (EGCG), resorcinol and phenol (Figure 3.1), using glucose and leucine/benzylamine model system.

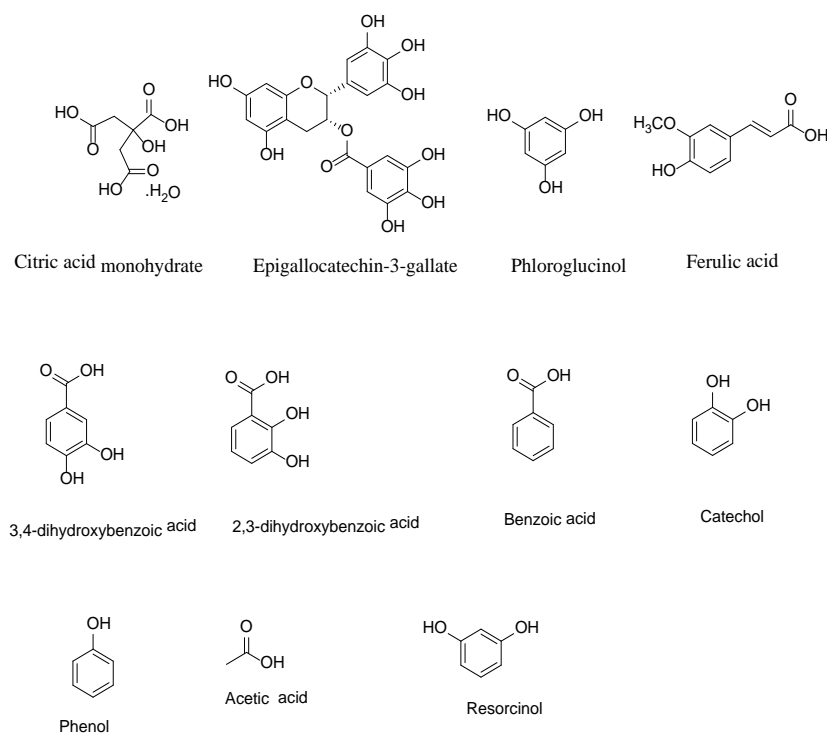


Figure 3.1. Chemical structures of citric acid and other polyphenolic compounds.

3.2. MATERIALS AND METHODS.

D-Glucose, L-leucine, citric acid monohydrate, polyphenolic compounds and other reagents used were obtained from commercial sources. Sodium dihydrogen phosphate ($\text{NaH}_2\text{PO}_4 \cdot 2\text{H}_2\text{O}$) and anhydrous disodium hydrogen phosphate (Na_2HPO_4) were of analytical grade. ^{13}C NMR spectrum were recorded at 100 MHz using a 400 MHz Bruker Avance spectrometer in aqueous solutions, and the chemical shifts were assigned based on the literature values for the starting materials. Fluorescence spectrum were recorded using a Perkin Elmer LS-5 Fluorescence spectrophotometer, with an excitation wavelength of 354 nm.

3.2.1. Glycation Studies Using D-glucose/L-leucine Model System. A solution of 0.5 mmol of glucose and 0.5 mmol of leucine in a phosphate buffer solution (4 mL, 0.1 M, pH 7.4) was placed in a 25-mL round-bottom flask, fitted with a reflux condenser. The reaction mixture was heated at 100 °C for 4 h on a heating mantle, and the aliquots taken at various intervals were investigated using ^{13}C NMR spectroscopy (acquired in unlocked mode; typically 512 scans were required to obtain a reasonable signal-to-noise ratio). In order to determine the effect of citric acid on the formation of AGE, various concentrations of citric acid monohydrate (0.5–0.052 mmol), prepared in phosphate buffer solution (4 mL, 0.1M, pH 7.4), were added to a solution of 0.5 mmol of glucose and 0.5 mmol of leucine prepared in phosphate buffer solution; (4 mL, 0.1 M, pH 7.4), and then the contents were heated at 100 °C for 4 h. In order to determine the antiglycating effects of epigallocatechin-3-gallate (EGCG), phloroglucinol, or ferulic acid, solutions of 0.25 mmol of glucose and 0.25 mmol of leucine, and various concentrations of EGCG (0.125–0.037 mmol), or phloroglucinol (0.125–0.037 mmol), or ferulic acid (0.25–0.062 mmol), prepared in phosphate buffer solution (4 mL, 0.1 M, pH

7.4), were heated at 100 °C for 4 h. Aliquots at various intervals were withdrawn from the reaction mixture and investigated using ^{13}C NMR spectroscopy.

3.2.2. Fluorescence Measurements. Fluorescence measurements of the aliquots from the above Maillard reaction mixtures were achieved using a reported procedure, with minor modifications.¹⁴¹ In brief, the aliquots at various reaction times were diluted to 1:9 v/v in the phosphate buffer, and the fluorescence spectrum were obtained with an excitation wavelength of 354 nm and the fluorescence intensity was monitored at 400–500 nm.

3.2.3. Glycation Studies Using D-glucose/Benzylamine Model System. 0.25 mmol of glucose and 0.25 mmol of benzylamine in a phosphate buffer solution (3 mL, 0.1 M, pH 7.4) was placed in a 4 mL screw capped vial fitted in an aluminum block on a heating mantle, and the aliquots taken at various intervals were investigated using ^{13}C NMR spectroscopy (acquired in unlocked mode; typically 1024 scans were required to obtain a reasonable signal-to-noise ratio). In order to determine the effect of citric acid and other polyphenolic compounds on the formation of AGE, solutions of 0.25 mmol of glucose, 0.25 mmol of benzylamine, and 0.05 mmol of citric acid, or acetic acid, or ethanol, or phenol, or catechol, or phloroglucinol, or resorcinol, or EGCG, or benzoic acid, or 2,3-dihydroxybenzoic acid, or 3,4- dihydroxybenzoic acid, or ferulic acid, prepared in phosphate buffer solution (3mL, 0.1M, pH = 7.4), were heated at 80 °C for 4 h.

3.3. RESULTS AND DISCUSSION

3.3.1. D-glucose and L-leucine Model System. During our attempts in identifying a reliable technique to compare the relative glycating effects of various polyphenols and citric acid, we have found that ^{13}C NMR spectroscopy provides a

convenient analytical probe. Although not as sensitive as fluorescence spectroscopy, ^{13}C NMR shows definitive evidence for the AGEs. Even though integration of the ^{13}C NMR absorptions is not quantitative due to the long relaxation times of the nuclear spins, the relative errors cancel out when the total AGE absorptions are integrated with respect to the D-glucose absorptions, and this method would provide the relative antiglycating effects of various compounds when the Maillard reactions are carried out under similar conditions.

Naturally occurring polyphenolic antioxidants are known to attenuate oxidative stress, and thus these compounds play an important role *in vivo* as AGE-inhibitors in the initial stages of the Maillard reaction. Although these antioxidants exert their AGE-inhibitory effects through alternative pathways, such as sequestering the reactive 1,2-dicarbonyl compounds formed as the intermediates in the Maillard reaction, they would also act as inhibitors of the receptors for AGE (RAGE).¹⁴²⁻¹⁴⁶ Polyphenolic antioxidants, such as resveratrol, were shown to substantially attenuate the Maillard reactions during food storage.¹⁴⁷ Similarly, citric acid, because of its high acidity, would be expected to reversibly protonate the amino groups and thereby attenuate the rates of formation of the Schiff-base adducts from the reaction of the reducing sugars with amines, and thus would be expected to attenuate the AGE formation. Citric acid and polyphenolic antioxidants can also attenuate the AGE formation by sequestering metal ions, and reactive oxygen- and reactive nitrogen species (ROS and RNS).

It has been reported that citric acid inhibits the accumulation of AGEs in lens proteins, and thereby protects against albuminuria and ketosis.¹⁴⁸ In order to probe the relative antiglycating effect of various polyphenolic compounds and citric acid, we have carried out Maillard reactions of D-glucose and L-leucine in the presence of citric acid

and polyphenolic compounds, epigallocatechin-3-gallate, phloroglucinol, and ferulic acid (at various concentrations), and monitored the formation of the AGE-related products, (AGEs as well as AGE-precursor compounds), using ^{13}C NMR and fluorescence spectroscopy.

We have initially focused on the model system of D-glucose and L-leucine for the Maillard reaction in 0.1 M phosphate buffer (pH = 7.4). The formation of the AGEs is typically a slow process, and even at 100 °C, 4 h of reaction time is required in order to observe the signals for the early-stage AGE, with an adequate signal to noise ratio. Under these conditions, new absorptions corresponding to the early stages of glycation appeared (Figure 3.2; bottom trace). We then varied the concentration of citric acid monohydrate to study its optimal effects on inhibition of the AGE, and followed by ^{13}C NMR and fluorescence spectroscopy. Citric acid monohydrate, at concentrations ranging from 100 mol% to 15 mol% effectively inhibited the AGE-formation, and even after 4 h at 100 °C, there were no visible signals for the AGE products in the ^{13}C NMR spectrum (Figure 3.2). Upon further lowering the concentration of citric acid to 10 mol%, relatively low-intensity signals for the AGEs or AGE-precursors could be observed in the ^{13}C NMR spectrum of the reaction mixture (after heating 4 h at 100 °C). These results suggest that citric acid attenuates the formation of AGE at the early stages of glycation, presumably by attenuating the imine formation. Further mechanistic studies are needed to gain insight into whether it is involved in the glycooxidation reactions that would lead to the AGE.

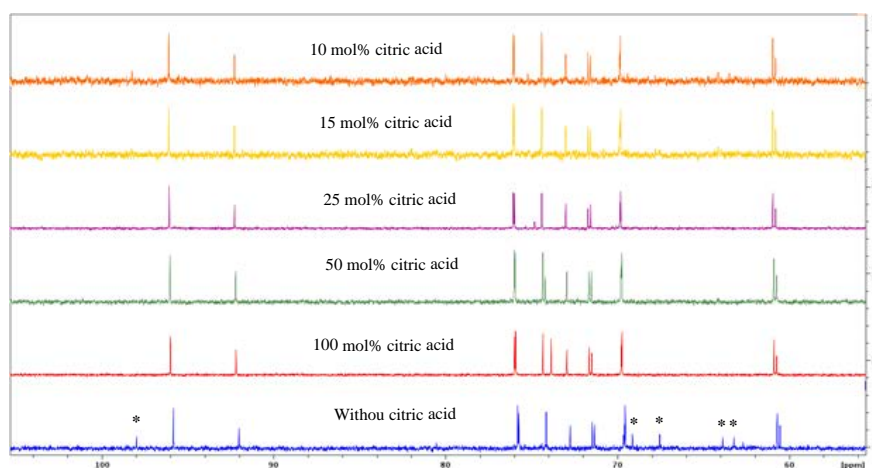


Figure 3.2. Partial 100 MHz ^{13}C NMR spectrum for the reaction mixtures of the D-glucose and L-leucine, heated at 100 °C for 4 h (in 0.1 M phosphate buffer; pH = 7.4), in the absence (bottom trace) and presence of varied concentration of citric acid; the asterisks correspond to the absorptions for the AGE precursors and all the other signals correspond to the $\text{C}_1\text{-C}_6$ carbons of the anomeric mixtures of D-glucose. Signals for L-leucine are outside the range shown ($\delta^{13}\text{C}$ 21.1, 22.2, 24.3, 40.1, 53.8, 175.9).

We have probed the Maillard reaction of L-leucine with D-glucose, in the presence of epigallocatechin-3-gallate (EGCG) additive under the same experimental conditions as that for the citric acid additive. The glycation reaction of D-glucose and L-leucine was carried out using various concentrations (50 mol%–10 mol %) of EGCG in order to optimize the amount of EGCG required for AGE attenuation. Through these experiments, we have demonstrated that, even at 15 mol% of concentration, EGCG is an effective AGE-inhibitor, as shown by the ^{13}C NMR spectrum of the reaction mixture after heating for 4 h at 100 °C (Figure 3.3).

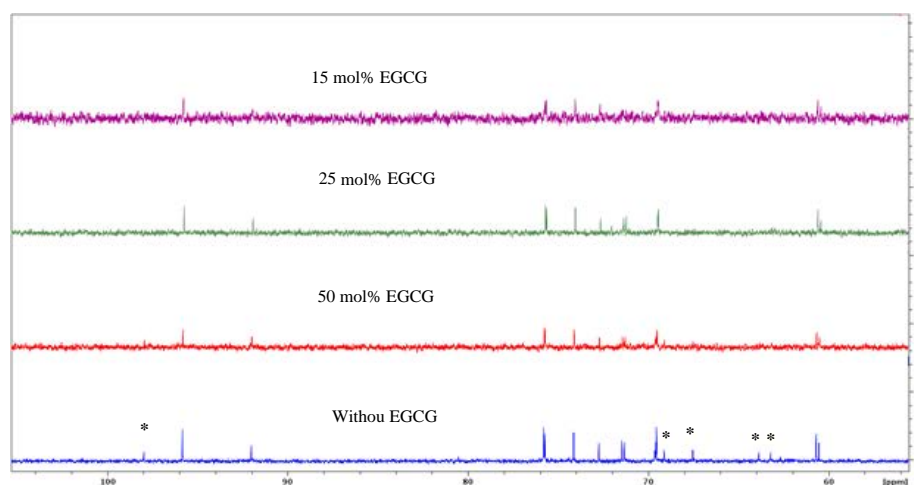


Figure 3.3. Partial 100 MHz ^{13}C NMR spectrum for the reaction mixtures of the D-glucose and L-leucine, heated at 100 °C for 4 h (in 0.1 M phosphate buffer; pH = 7.4), in the absence (bottom trace) and presence of varied concentration of epigallocatechin-3-gallate (EGCG); the asterisks correspond to the absorptions for the AGE precursors and all the other signals correspond to the C₁-C₆ carbons of the anomeric mixtures of D-glucose. Signals for L-leucine are outside the range shown ($\delta^{13}\text{C}$ 21.1, 22.2, 24.3, 40.1, 53.8, 175.9).

Having demonstrated that EGCG is comparable to citric acid in its anti-glycating effects, we then investigated the pharmaceutically interesting polyphenolic antioxidants phloroglucinol and ferulic acid for their AGE-inhibitory effects under our model Maillard reaction conditions. We studied the effect of phloroglucinol as an antiglycating agent at various concentrations (50 mol%–15 mol %). It is evident from the ^{13}C NMR spectrum of the Maillard reaction mixtures (Figure 3.4) that phloroglucinol effectively attenuates the formation of AGE at ≥ 15 mol% concentration. However, AGE-related ^{13}C NMR absorptions began to appear in relatively low intensity when the concentration of phloroglucinol additive was lowered to 15 mol%. In similar experiments, ferulic acid at

100 mol%–25 mol% concentration effectively prevented the AGE formation (4 h at 100 °C in phosphate buffer (pH 7.4)), as shown by the ^{13}C NMR spectrum (Figure 3.5).

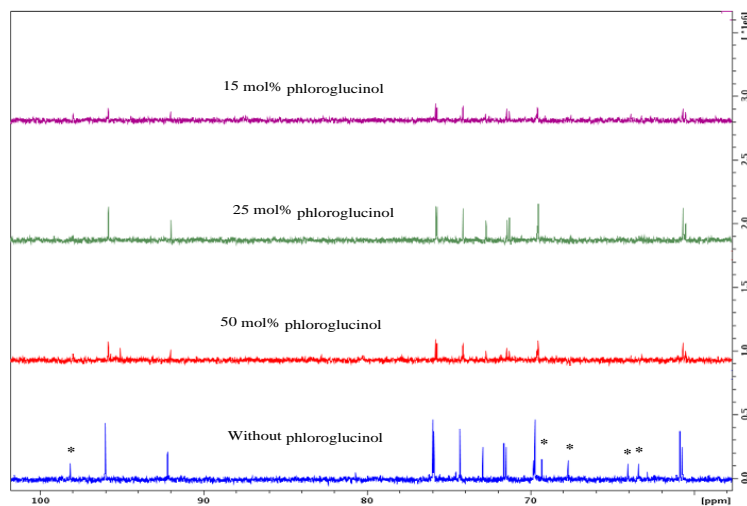


Figure 3.4. Partial 100 MHz ^{13}C NMR spectrum for the reaction mixtures of the D-glucose and L-leucine, heated at 100 °C for 4 h (in 0.1 M phosphate buffer; pH = 7.4), in the absence (bottom trace) and presence of varied concentration of phloroglucinol; the asterisks correspond to the absorptions for the AGE precursors and all the other signals correspond to the C₁–C₆ carbons of the anomeric mixtures of D-glucose. Signals for L-leucine are outside the range shown ($\delta^{13}\text{C}$ 21.1, 22.2, 24.3, 40.1, 53.8, 175.9).

The formation of the AGE, which are typically fluorescent products, is also corroborated by fluorescence spectroscopy studies (Figure 3.6). The fluorescence spectroscopy revealed the formation of the AGE when the Maillard reaction was carried out in the absence of citric acid, with a characteristic fluorescence emission at 400–500 nm for excitation at 355 nm, in agreement with literature reports.¹⁴¹ This fluorescence

emission was completely suppressed in the presence of 50 mol% of citric acid (Figure 3.6).

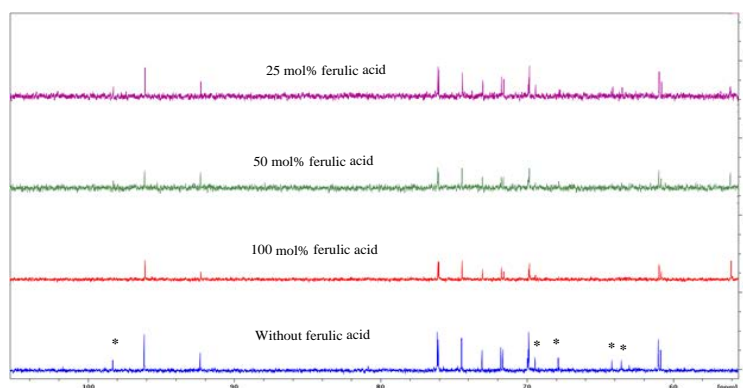


Figure 3.5. Partial 100 MHz ^{13}C NMR spectrum for the reaction mixtures of the D-glucose and L-leucine, heated at 100 °C for 4 h (in 0.1 M phosphate buffer; pH = 7.4).

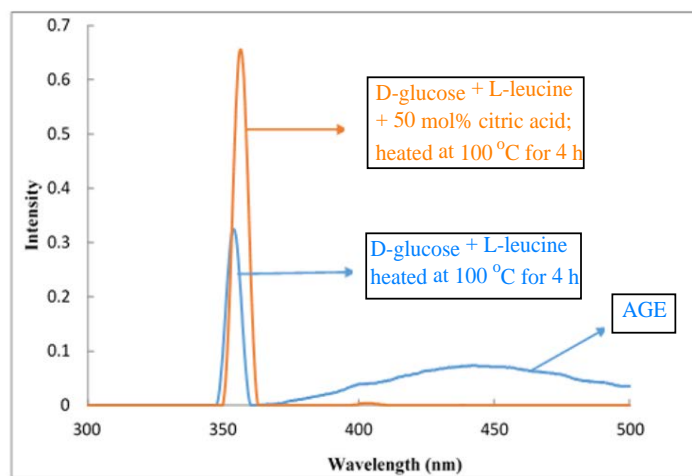


Figure 3.6. Fluorescence spectrum, showing the formation of the Maillard products in the D-glucose and L-leucine model system (blue trace), and the absence of AGE fluorescence in the presence of 50 mol% citric acid (orange trace), upon heating at 100 °C in phosphate buffer (0.1M, pH = 7.4; λ_{exc} at 355 nm and λ_{em} at 400-500 nm).

3.3.2. D-glucose and Benzylamine Model System. We decided to use other amino acids and primary amines instead of L-leucine to enhance the rate of Maillard

reaction. Solutions of D-glucose and lysine, or asparagine, or propylamine, or benzylamine, prepared in phosphate buffer (3mL, 0.1M, pH = 7.4), were heated at 80 oC for 4 h, except for propylamine; solution of D-glucose and propylamine was kept at room temperature because of low boiling point of propylamine, and the aliquots at various intervals were investigated using ^{13}C NMR spectroscopy (acquired in unlocked mode; typically 1024 scans were required to obtain reasonable signal-to-noise ratio). Benzylamine gave desired results, so we decided to do further study by using benzylamine. We started by using citric acid as an additive to inhibit the formation of AGE in D-glucose/benzylamine model system. Concentration of citric acid was varied from 100 mol% to 10 mol% to study its optimal effect on inhibition of the AGE, and followed by ^{13}C NMR spectroscopy. Citric acid, at concentrations ranging from 100 mol% to 20 mol% effectively inhibited the AGE-formation, and even after 4 h at 80 oC, there were no visible signals for the AGE products in the ^{13}C NMR spectrum. Then we used EGCG, phloroglucinol, and ferulic acid to study their effect on the formation of AGEs in glucose/benzylamine model system. The glycation reaction of D-glucose and benzylamine was carried out by using 20 mol% concentration of each additive. We have found that at 20 mol% concentration of citric acid, EGCG, phloroglucinol, and ferulic acid, intensity of AGE signals was relatively less than the intensity seen in the absence of additives. Citric acid was found to be more effective than other antiglycating agents as shown in Figure 3.7.

Upon further lowering the concentration of citric acid to 15 mol%, or 10 mol%, relatively low-intensity signals for the AGEs or AGE-precursors could be observed in the ^{13}C NMR spectrum of the reaction mixture after heating 4 h at 80 oC as shown in Figure 3.8. Other polyphenols such as acetic acid, or ethanol, or phenol, or catechol, or

resorcinol, or benzoic acid, or hydroxyl derivatives of benzoic acid were also used at 10 mol% concentration to study their effect on the formation of AGE products, but ^{13}C NMR results showed that 10 mol% concentration of citric acid and other additives used is not very effective to attenuate the formation of early AGE products as shown in Figure 3.9.

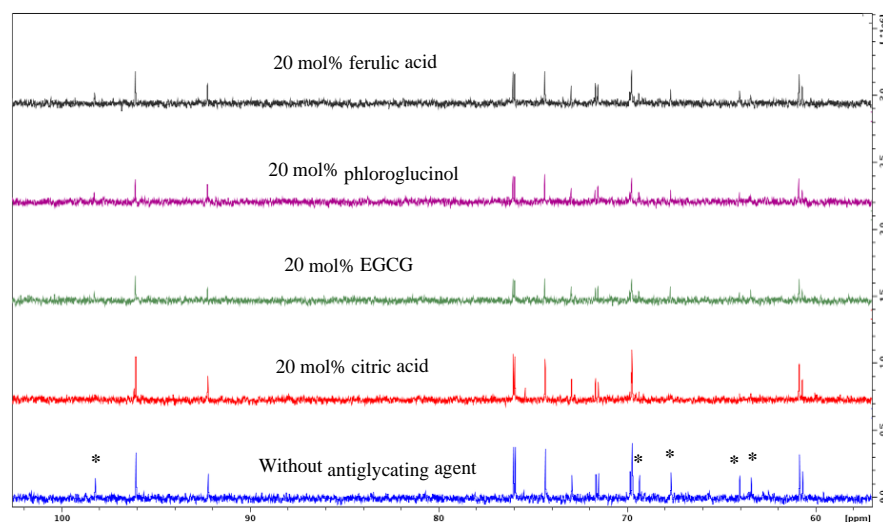


Figure 3.7. Partial 100 MHz ^{13}C NMR spectrum for the reaction mixtures of the D-glucose and benzylamine, heated at 80 °C for 4 h (in 0.1 M phosphate buffer; pH = 7.4), in the absence (bottom trace) and presence of various antiglycating agents (ferulic acid, phloroglucinol, EGCG, and citric acid); the asterisks correspond to the absorptions for the AGE precursors, (notably less in concentration in the reaction mixtures treated with polyphenolic compounds or citric acid) and all the other signals correspond to the C₁-C₆ carbons of the anomeric mixtures of D-glucose.

Having 20 mol% optimal effective concentration of these additives in our hand, various other polyphenols (additives) were used as antiglycating agents to compare their

effect on the inhibition of formation of AGE or AGE-precursors by ^{13}C NMR spectroscopy. Intensities of AGE formation were measured qualitatively by integrating AGE and glucose signals in ^{13}C NMR spectrum. We have found that all the polyphenols used are effective to some extent in inhibition of AGE except phenol since intensity of AGE formation is more than the intensity measured in a system having only glucose and benzylamine, without any additive as shown in Figure 3.10.

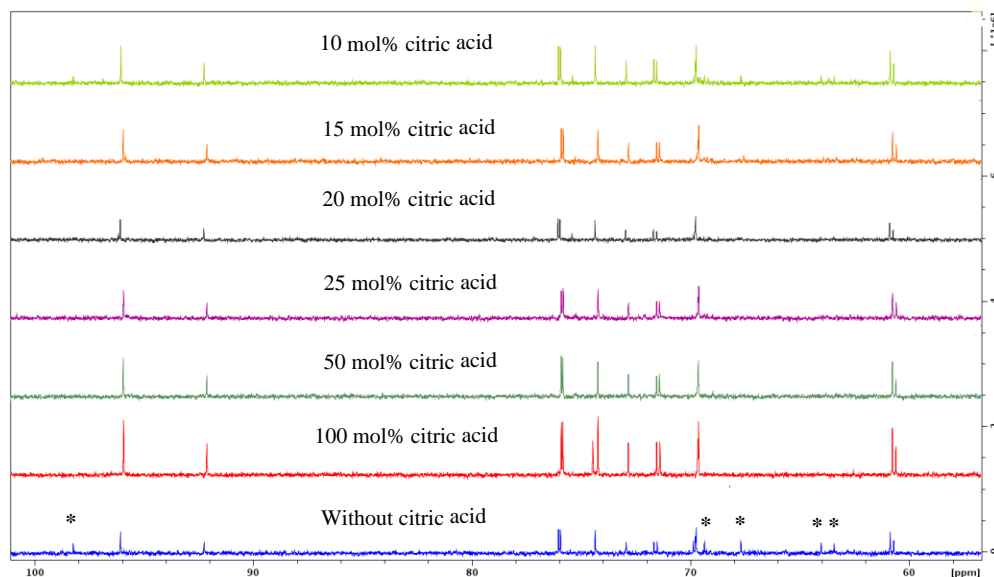


Figure 3.8. Partial 100 MHz ^{13}C NMR spectrum for the reaction mixtures of the D-glucose and benzylamine, heated at 80 °C for 4 h (in 0.1 M phosphate buffer; pH = 7.4), in the absence (bottom trace) and presence of varied concentration of citric acid (100, 50, 25, 20, 15, and 10 mol %); the asterisks correspond to the absorptions for the AGE precursors and all the other signals correspond to the $\text{C}_1\text{-C}_6$ carbons of the anomeric mixtures of D-glucose. The signals for benzylamine are outside the range shown ($\delta^{13}\text{C}$ 133.8, 129.2, 128.9, 128.8, 128.7, 43.4).

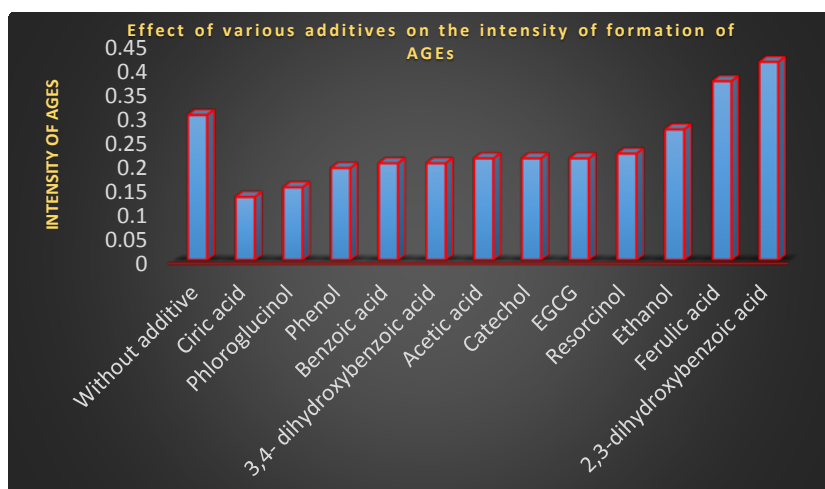


Figure 3.9. Effect of various additives (10 mol% concentration) used as antiglycating agents on the formation of AGEs in D-glucose and benzylamine model system, upon heating at 80 °C in phosphate buffer (0.1M, pH = 7.4) for 4 h.

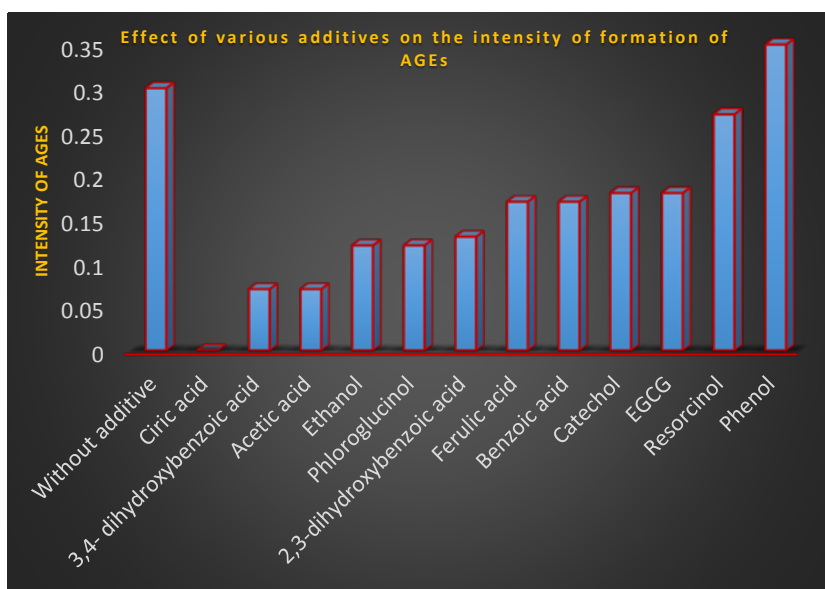


Figure 3.10. Effect of various additives (20 mol% concentration) used as antiglycating agents on the formation of AGEs in D-glucose and benzylamine model system, upon heating at 80 °C in phosphate buffer (0.1M, pH = 7.4) for 4 h.

4. A NOVEL PHOTOREDOX-CATALYZED *gem*-DIFLUORINATION OF 1,3-DITHIOLANES

4.1. BACKGROUND

Organofluorine compounds have important role as pharmaceuticals,¹⁴⁹⁻¹⁵⁸ agrochemicals¹⁵⁹, materials¹⁶⁰⁻¹⁶⁶, and radiotracers for positron emission tomography (PET)¹⁶⁷⁻¹⁷⁰ due to their properties of enhanced lipophilicity and thereby bioavailability.^{152, 158, 171-173} Synthesis of organofluorine compounds is very challenging due to high electronegativity of fluorine and high hydration energy of fluoride ion.^{5, 174} The dehydrofluorination of benzylic hydrogens is a reaction of great interest in both industrial and academic laboratories. Koperniku and et al.⁷ have reviewed base- mediated, transition-metal-catalyzed, and radical-initiated benzylic monofluorination and difluorination. Synthesis of difluoroalkylated molecules is being considered as one of the interesting area of research in drug discovery because CF₂ moiety significantly enhances the activities of biologically active molecules because the difluoromethyl group serves as a lipophilic hydrogen bond donor and there is an isosteric relationship between the CF₂ and ethereal oxygen as shown in Figure 4.1. Difluorocompounds are metabolically more stable than original biologically active molecules and are considered to be potent enzyme inhibitors.¹⁷⁵

Organofluorine compounds can be synthesized in two ways.¹⁷⁶ a.) Direct fluorination, which includes transformation of C-H bond or a functional group into C-F bond by treating with well-known fluorinating agents such as elemental fluorine (F₂), hydrofluoric acid (HF), SF₄, Selectfluor, NFSI, diethyliminosulfur trifluoride (DAST)

etc. b.) Another method includes the introduction of fluorinated small molecules called building blocks into organic molecules.

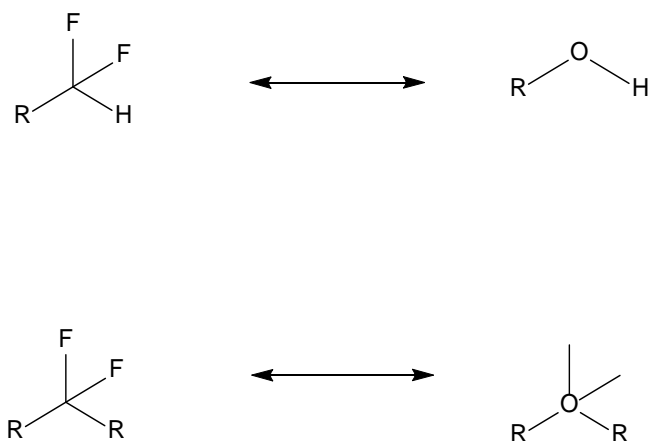


Figure 4.1. Bioisosterism of CF_2 Fragment.¹⁷⁷

4.1.1. Direct Fluorination. Several synthetic methods for direct fluorination have been developed¹⁷⁸ but oxidative desulfurization-fluorination method has been regarded as an efficient method for the synthesis of *gem*-difluoromethylene compounds.^{176, 179} This method has been used extensively to convert cyclic dithioacetals 4.1 derived from aryl and alkyl halides into *gem*-difluoro compounds 4.2 by using reagent combination of an oxidant and Py/HF (Figure 4.2).¹⁸⁰⁻¹⁸⁷ Geary et al.¹⁸⁸ have reported a gram scale synthesis of air and water stable hypervalent iodine reagent fluoroiodane and used as an electrophilic reagent for *gem*-difluorination of dicarbonyl compounds (Figure 4.3).

Authors also investigated the use of fluoroiodane 4.3 as an effective fluorinating reagent for monofluorination of diketesters.

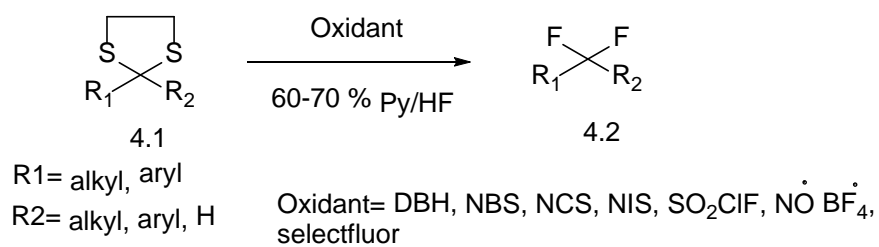


Figure 4.2. Oxidative desulfurization- difluorination: *gem*-difluorination of dithioacetals.

This hypervalent fluorinating reagent was further investigated as a suitable reagent for silver- mediated selective *gem*-difluorination of styrenes under mild conditions (Figure 4.4).¹⁸⁹

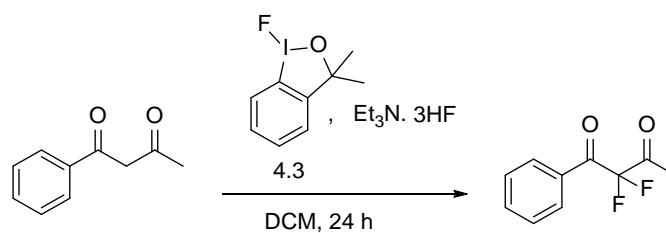


Figure 4.3. *gem*-difluorination of dicarbonyls using fluoroiodane.

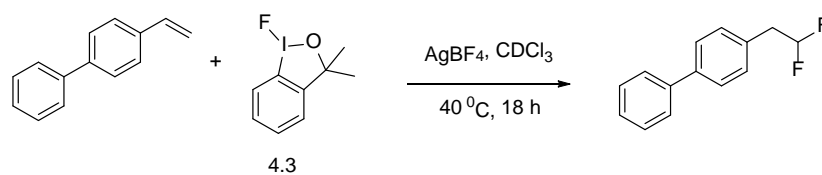


Figure 4.4. *gem*- difluorination of styrene using fluoroiodane.

Bouvet et al.¹⁹⁰ have synthesized and used a novel fluorinated ionic liquid for *gem*-difluorination of xanthates and thiocarbonates (Figure 4.5).

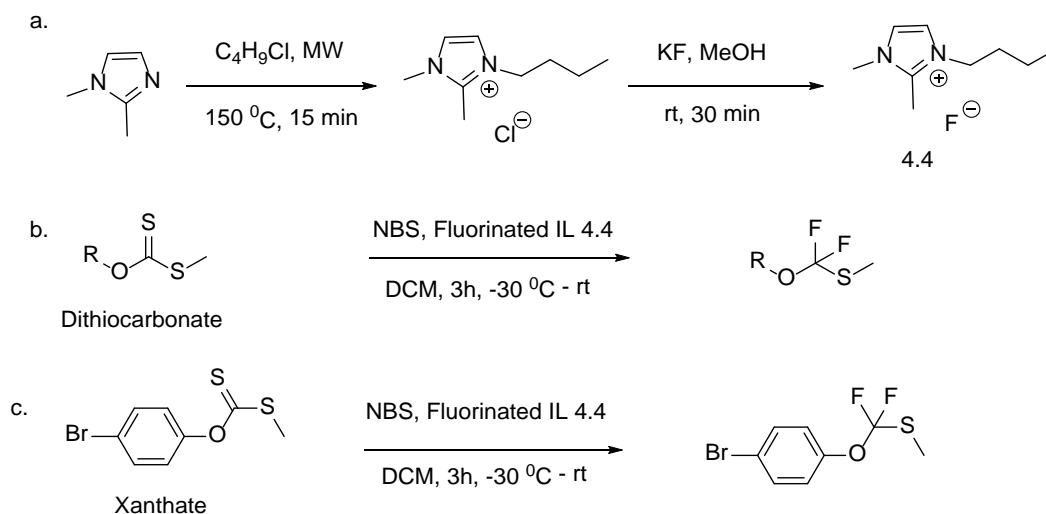


Figure 4.5. Difluorination using ionic liquids; a.) Synthesis of [bdmim][F] (4.5) b.) *gem*-difluorination of dithiocarbonate c.) *gem*-difluorination of xanthate.

4.1.2. Insertion of Functionalized Difluorinated Building Blocks. Belhomme

et al.¹⁹¹ wrote a review on most relevant synthetic methods for the introduction of functionalized difluoromethylated building blocks such as $\text{CF}_2\text{SO}_2\text{R}$, CF_2H , $\text{CF}_2\text{CONR}^1\text{R}^2$, $\text{CF}_2\text{CO}_2\text{R}$, CF_2Br , CF_2R_f and $\text{CF}_2\text{PO}(\text{OR})_2$ onto C (sp^2) and C (sp) centers. Fier and Hartwig¹⁹² have reported a copper-mediated cross coupling of aryl and vinyl iodides with a difluoromethyl group generated by sodium borohydride reduction of Ruppert-Prakash reagent (TMSCF_3) to form difluoromethyl arenes and difluoromethyl-substituted alkenes (Figure 4.6). Prakash et al.¹⁹³ have also reported the

Difluoromethylation of aryl and heteroaryl halides by using $\text{Bu}_3\text{SnCF}_2\text{H}$ and copper iodide.

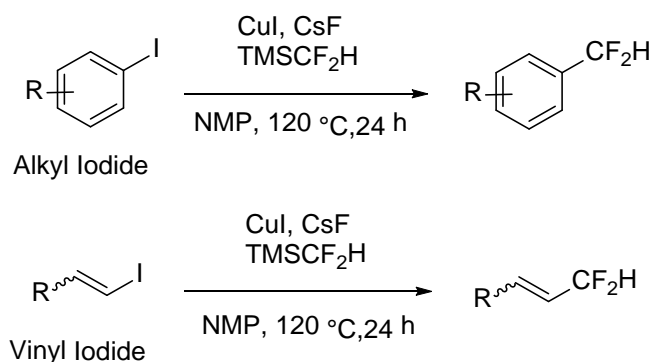


Figure 4.6. Difluoromethylation of alkyl and vinyl iodides.

Fujiwara et al.⁹ have invented a new air stable, difluorinating reagent zinc difluoromethanesulfinate [$\text{Zn}(\text{SO}_2\text{CF}_2\text{H})_2$] and reported its applications in C-H difluoromethylation of heteroarenes and difluoromethylation of thiols and enones. The scope of reaction includes high regioselectivity, ambient reaction temperature, stability towards moisture and air and compatibility with halogen, electron rich or deficient heterocycles. Yang Gu and co-workers¹⁹⁴ reported a dual palladium/silver catalytic system for difluoromethylation of aryl halides. They also showed the application of this dual catalytic system for the difluoromethylation of medicinally relevant compounds (Figure 4.7).

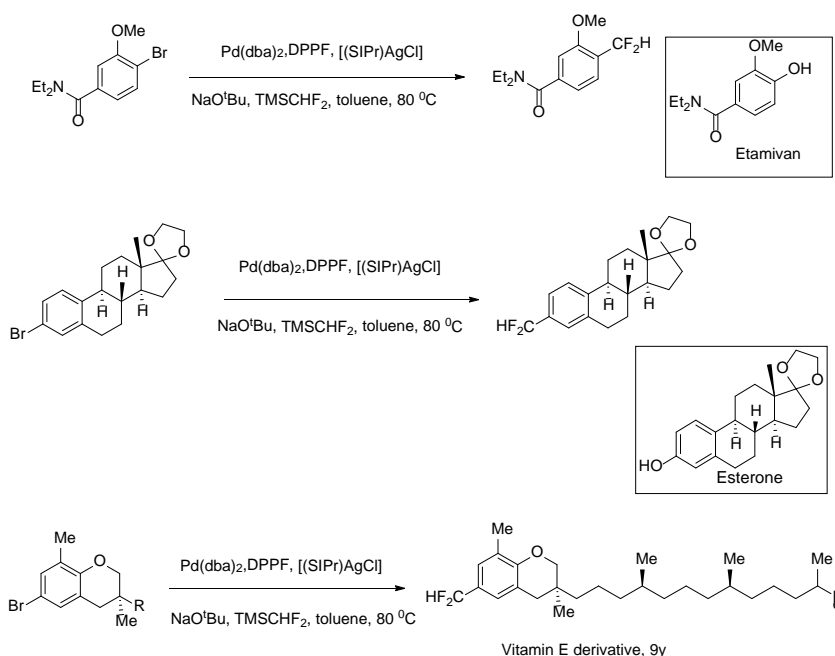


Figure 4.7. Palladium-Silver dual co-operative catalysed difluoromethylation of biologically relevant compounds.

Recently Prakash and co-workers¹⁹⁵ have reported a nucleophilic difluoromethylation of aromatic aldehydes in the presence of lithium iodide, lithium tetrafluoroborate and triphenylphosphine by using Ruppert-Prakash reagent (TMSCHF_3). Difluoromethylated compounds are finally formed by alkaline hydrolysis of *gem*-difluorinated phosphonium salts (Figure 4.8). Recently Dilman and Levin¹⁷⁷ wrote a review on difluorocarbenes as a building block for the synthesis of compounds having difluoromethylene fragment. The difluorocarbene is a singlet carbene, short lived intermediate and its electrophilic nature due to the presence of empty p orbitals makes it more reactive towards nucleophiles for the synthesis of a wide variety of organofluorine compounds.

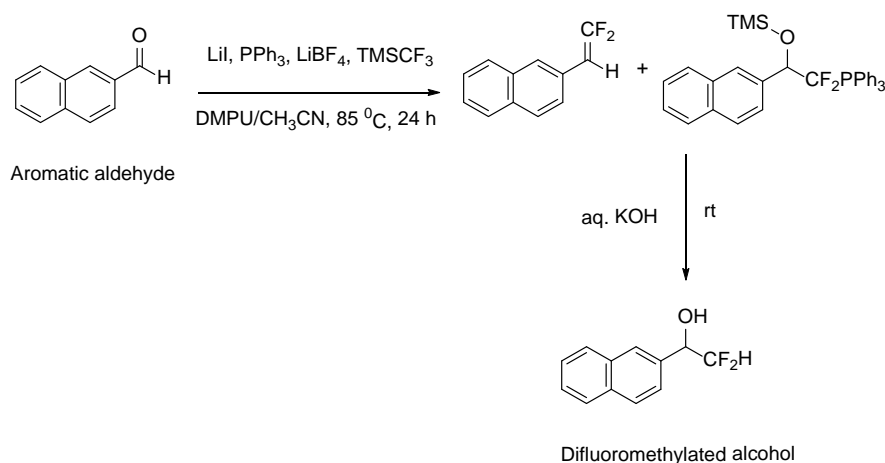


Figure 4.8. Nucleophilic difluoromethylation of aldehydes by using TMSCF_3 .

4.1.3. Photoredox Catalysis and Fluorination. The free radical chemistry in organic synthesis has been widely used over the past few years due to high radical reactivity, substrate scope, mild reaction conditions, and high selectivity. Photoredox catalysis is one of the most rapidly expanding areas of free radical chemistry. Photoredox catalysis is a mild method of attaining unique chemical reactivity and has several applications in organic synthesis.¹⁹⁶

4.1.3.1. Photoredox catalyzed selective C-H *gem*-difluorination. Xia, Zhu, and Chen first time reported the visible light promoted metal free selective benzylic monofluorination and *gem*-difluorination by control of diarylketones (9-fluorenone and xanthone) as photocatalysts and fluorine source (Selectfluor and Selectfluor II) House hold bulb (CFL-19W) as a light source is sufficient enough to abstract hydrogen from benzylic carbon and fluorine radical generated from fluorine source (Selectfluor) attacks the benzylic site to form benzyl fluorides and regenerates the photocatalyst (Figure 4.9).¹¹

Mechanism was proposed that photoexcited ketone abstracts benzylic hydrogen from I to generate benzylic radical II. Subsequent fluorine atom transfer from selectfluor would provide benzylic fluoride III. In 2014, they also reported the photoredox catalyzed fluorination of unactivated C(sp³)-H groups by activation of acetophenone, a monoarylketone by using violet light (375-400 nm) generated by household compact fluorescent bulb (CFL).¹⁹⁷

a.)

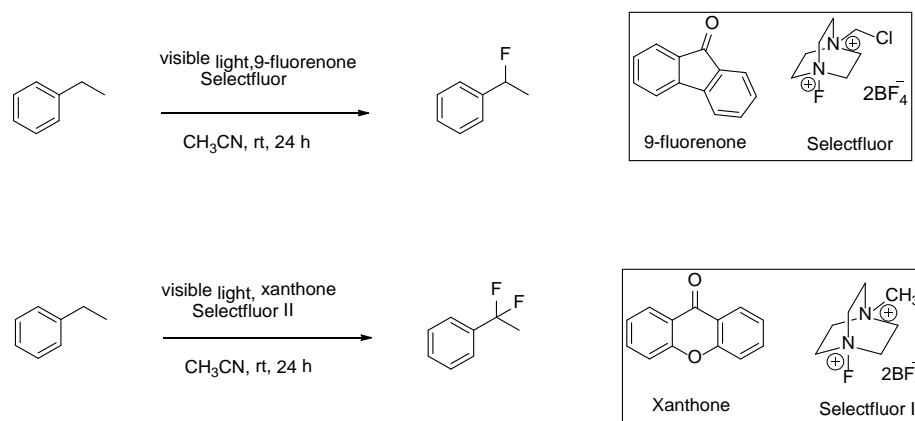


Figure 4.9. Visible light-promoted C-H activation; a.) Photoredox-catalyzed benzylic monofluorination and *gem*-difluorination b.) Mechanism of visible light-promoted C-H fluorination.¹¹

b.)

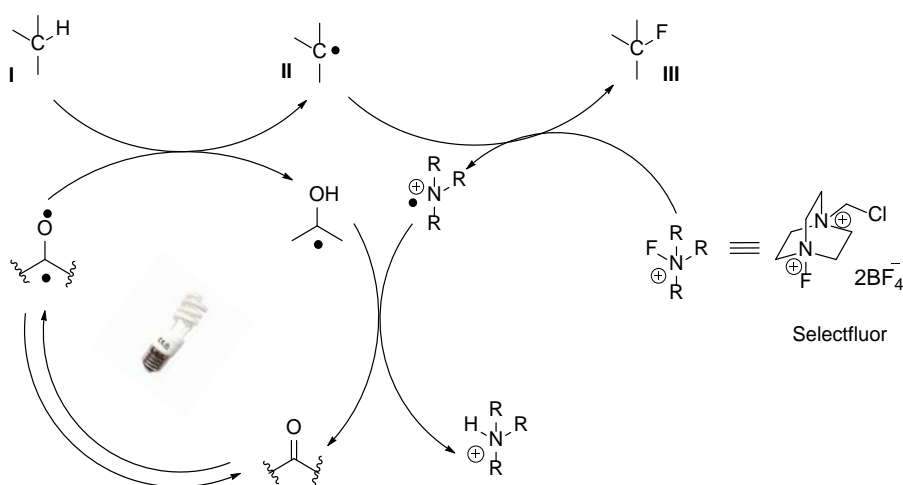


Figure 4.9. Visible light-promoted C-H activation; a.) Photoredox-catalyzed benzylic monofluorination and *gem*-difluorination b.) Mechanism of visible light-promoted C-H fluorination.¹¹ (cont.)

4.1.3.2. Photoredox catalyzed *gem*-difluoromethylation through in-situ generated difluoromethylene (CF₂) group. Li et al.¹⁰ have reported a novel, feasible and effective photoredox catalyzed difluoromethylation to introduce CF₂ group into tertiary amine derivative, tetrahydroisoquinolines through in-situ generated difluoromethylene group from difluoroenolates. N-aryl substituted tetrahydroisoquinoline 4.5 was coupled with α,α -difluorinated *gem*-diol 4.6 in the presence of photocatalyst Ru(bpy)₃Cl₂, CCl₄, and Et₃N in solvent acetonitrile under visible light irradiation at room temperature to form *gem*-difluoromethylated tetrahydroisoquinoline derivatives 4.7 as shown in Figure 4.10. Mechanism of the reaction involves photoexcitation of Ru(bpy)₃(II) by visible light to *Ru(bpy)₃(II), which could reduce the tetrahydroquinoline derivative I to form radical cation II and Ru(bpy)₃(I), which would reduce CCl₄ to

chloride ion and trichloromethyl radical. Trichloromethyl radical abstracts hydrogen atom from radical cation II to generate iminium cation III. α,α -difluorinated *gem*-diol IV in the presence of Et_3N generates difluoroenolate V by the release of trifluoroacetate. Intermediate is very reactive and it could be rapidly trapped by iminium cation to generate difluoromethylated product VI (Figure 4.11).

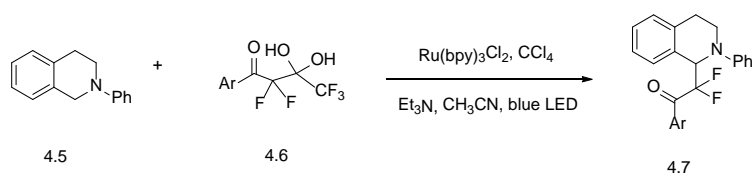


Figure 4.10. Photoredox-catalyzed *gem*-difluorination of tetrahydroisoquinoline.¹⁰

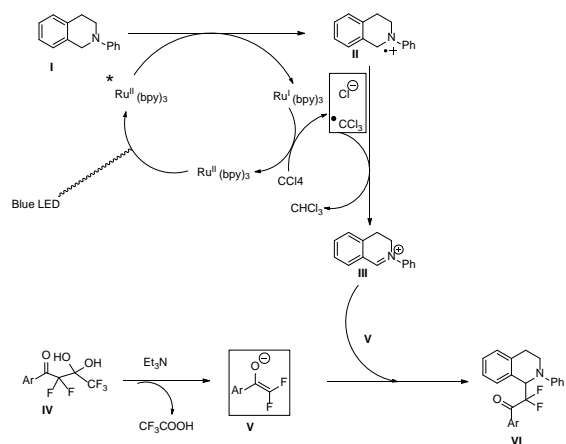


Figure 4.11. Possible mechanism of *gem*-difluorination of tetrahydroisoquinoline.¹⁰

4.1.3.3. Photoredox-catalyzed decarboxylative aliphatic fluorination.

MacMillan and co-workers¹⁹⁸ in 2015 have reported a novel transition metal catalyzed

photoredox decarboxylation of aliphatic carboxylic acids for C-F bond formation (synthesis of fluoroalkanes) by using iridium as a photocatalyst in the presence of disodium hydrogen phosphate (Na_2HPO_4) as a base as shown in Figure 4.12. Wu et al.¹⁹⁹ have also reported a similar type of decarboxylation of aliphatic carboxylic acids to form fluoroalkanes but their method was modified by the use of an organic dye (Mes-AcrClO₄) shown in Figure 4.12 as a photocatalyst instead of transition metal and cesium carbonate as a base.

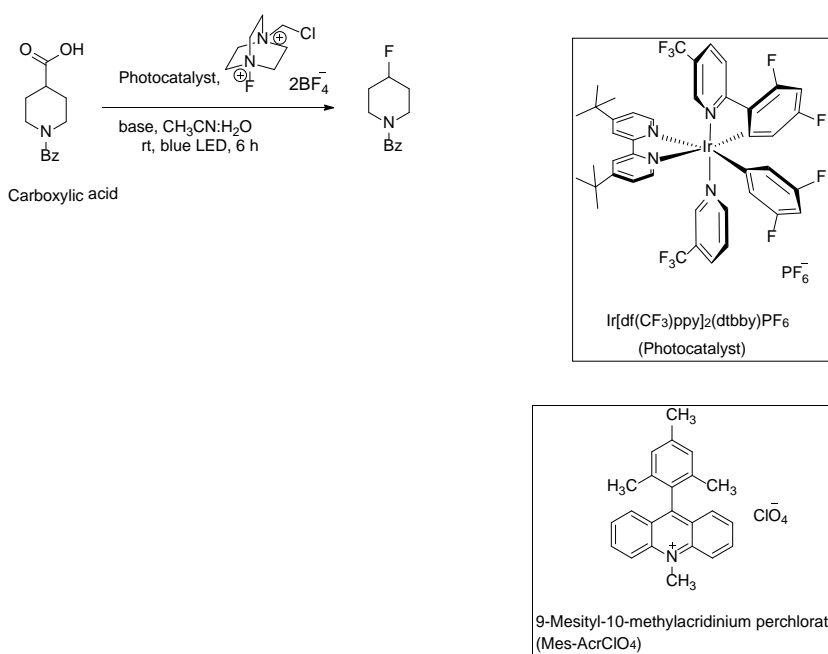


Figure 4.12. Photoredox catalyzed decarboxylative fluorination of aliphatic carboxylic acids.¹⁹⁸⁻¹⁹⁹

4.2. RESULTS AND DISCUSSION

Oxidative desulfurization of cyclic dithioacetals derivatives of aldehydes and ketones to form *gem*-difluoromethylene compounds by using combination of an oxidant and Py/HF has been reported as more convenient synthetic method rather than using

elemental fluorine, iodine, BrF₃, and CF₃OF/HF combination.^{180, 184, 186-187} Reddy and co-workers in 2005 reported a novel synthetic method for conversion of 2,2,-diaryl-1,3-dithiolanes into *gem*-difluorinated compounds by using Selectfluor and Py/HF.¹⁸¹ This method allowed the *gem*-difluorination of dithiolanes in high yields, although the use of Py/HF requires special care of handling in a well ventilated hood with appropriate personal protective equipments (PPE). This is an example of electrophilic fluorination. Ma and co-workers²⁰⁰ have reported a metal-free oxidative persulfate-promoted C-H activation through radical mechanism for the synthesis of *gem*-difluorinated compounds.

We initially attempted *gem*-difluorination of dithiolanes using persulfate as an oxidant and Selectfluor as a fluorinating agent. Difluoro compound was obtained in trace amount as confirmed by ¹⁹F NMR, as expected there was formation of starting aldehyde because of using aqueous conditions, which was also confirmed by ¹H and ¹³C NMR. Visible light promoted photoredox catalysis has emerged in last few years as a mild and most effective synthetic method for various organic transformations.²⁰¹⁻²⁰² Therefore, we switched to photoredox catalysed difluorination of 1,3-dithiolanes. To the best of our knowledge, photoredox-catalysed *gem*-difluorination of 1,3-dithiolanes has not been reported in the literature so far.

2,2-diphenyl-1,3-dithiolane 4.8 was synthesized from 1,2-ethanedithiol and benzophenone using BF₃.Et₂O as a catalyst by reported method.²⁰³ The resulting dithiolane 2.8 was reacted with Selectfluor using 9-fluorenone (photocatalyst), in anhydrous acetonitrile in O₂ free environment under irradiation with 13W CFL at room temperature for 20 h to form *gem*-difluorocompound 4.9 as shown in Figure 4.13. When acetone was used as a solvent in this reaction, unidentified products along with desired product were observed in ¹⁹F NMR. We did not try other solvents for this reaction due to

limited solubility of Selectfluor. We also found that reaction without using 9-fluorenone did not give desired product and when reaction was tried without light source, relatively slow reaction rate was observed. Therefore, 9-fluorenone as a photocatalyst and light source are required for this reaction. We have also explored other photocatalysts such as 2,3-Dichloro,5,6-dicyano-1,4-benzoquinone (DDQ) and Tris (bipyridine)ruthenium (II) chloride ($[\text{Ru}(\text{bpy})_3]\text{Cl}_2$) but relative reaction rates were slow in both cases. Through these studies, 9-fluorenone was found to be a superior photocatalyst for this reaction.

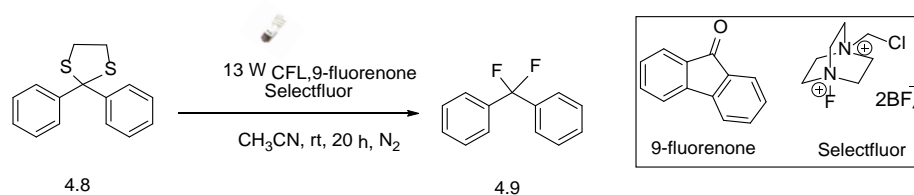
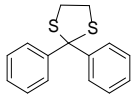
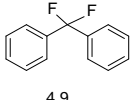
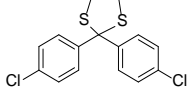
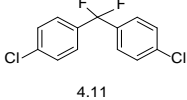
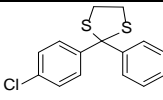
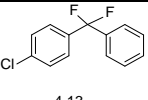
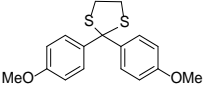
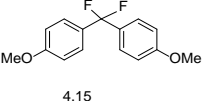
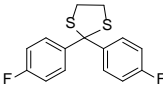
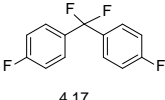
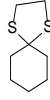
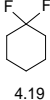


Figure 4.13. Photoredox catalyzed *gem*-difluorination of 1,3-dithiolane.

With this promising result, several diaryl ketones were transformed into their corresponding 1,3-dithiolanes using $\text{BF}_3 \cdot \text{Et}_2\text{O}$ as a catalyst, and the resulting dithiolanes were reacted with Selectfluor in moisture/ O_2 free environment in the presence of 9-fluorenone (photocatalyst) under visible light irradiation for 20 h at room temperature. Various substituted benzophenone dithiolanes with halogens and methyl groups gave only the corresponding *gem*-difluoro compounds, as the single products, confirmed by ^{19}F NMR prior to work up. There was no reaction in case of dithiolane-derived from cyclohexanone because of instability of the radical intermediate involved in the reaction as shown in Table 4.1.

Table 4.1. ^{19}F NMR chemical shifts in ppm for the conversion of diaryldithiolanes into their corresponding *gem*-difluorocompounds. a.) Estimated yield by ^{19}F NMR (Isolated yield). Yields are not optimized.

Entry	Dithiolane	Product	^{19}F NMR Chemical shift (ppm)	% Estimated yield, (isolated yield) ^a
1	 4.8	 4.9	-88.1 (s)	75, (60)
2	 4.10	 4.11	-88.5 (s)	73
3	 4.12	 4.13	-88.7 (s)	67
4	 4.14	 4.15	-86.9 (s)	69
5	 4.16	 4.17	-86.5 (s) and -111.0 (s)	70
6	 4.18	 4.19	N.R.	0

Although the mechanism for this reaction needs to be clarified, we propose free radical mechanism as shown in Figure 4.14. First, the photocatalyst fluorenone undergoes excitation in the presence of visible light and initiates the free radical reaction. Photo excited fluorenone cleaves C-S bond in dithiolane I to form a radical cationic intermediate II, which takes fluorine radical generated by Selectfluor to form monofluorinated radical intermediate III, which undergoes further cleavage of C-S bond

to form another monofluorinated radical cationic intermediate IV. This intermediate finally takes fluorine radical from Selectfluor to form *gem*-difluorinated product V. The proposed mechanism proves that the fluorenone in this process is required in catalytic amount.

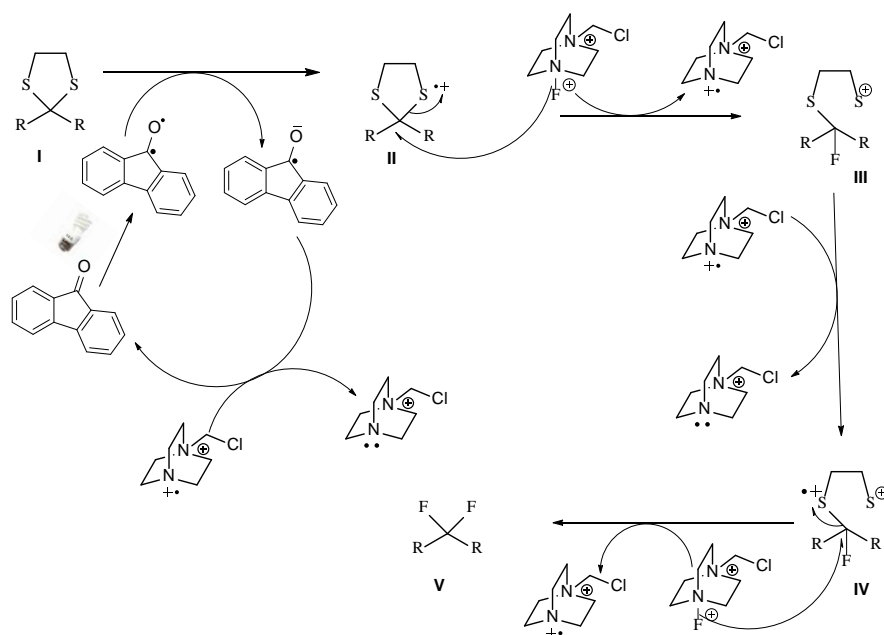


Figure 4.14. Proposed mechanism of photoredox *gem*-difluorination of 1,3-dithiolanes.

4.3. EXPERIMENTAL

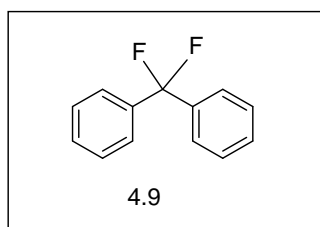
4.3.1. Materials and Methods. All reagents were purchased from commercial sources and used as received. Column chromatography was carried out using Merck 60, 230-400 mesh. Thin layer chromatography was carried out using silica gel coated polyester backed sheets. The ^1H , ^{13}C NMR and ^{19}F NMR spectrum for DMSO- d_6 solutions were obtained on an INOVA-Varian 400 MHz spectrometer at 400, 100, and

376 MHz respectively. The ^1H NMR, ^{13}C NMR chemical shifts referenced to the residual solvents signals or the internal TMS ($\delta = 0.0$). The ^{19}F chemical shifts referenced to the internal CFCl_3 ($\delta^{19}\text{F} = 0.0$).

4.3.2. General Synthetic Procedure for the Preparation of *gem*-Difluoromethylene Compounds. Dithiolane (0.38 mmol.), Selectfluor (1.16 mmol.), and 9-fluorenone (5 mol %) were added to oven dried 25 mL round bottom flask under nitrogen atmosphere at room temperature. To this, anhydrous acetonitrile (6 mL) was added through syringe at room temperature. The reaction mixture was irradiated with 13W CFL for 20 h at room temperature. After completion of reaction as confirmed by ^{19}F NMR, dichloromethane (15 mL) and DI water (8 mL) were added to the reaction mixture and layers were separated. Aqueous layer was extracted with (2 x 5 mL) dichloromethane. The combined dichloromethane layer was washed with DI water (5 mL) and finally dried over MgSO_4 . The solvent was evaporated under reduced pressure and the residue was purified by column chromatography (Silica gel, 30 % ethyl acetate in hexane) to obtain *gem*-difluoromethylene product. The final product obtained was characterized by ^1H , ^{13}C , and ^{19}F NMR spectroscopy and confirmed by NMR chemical shifts reported in literature.

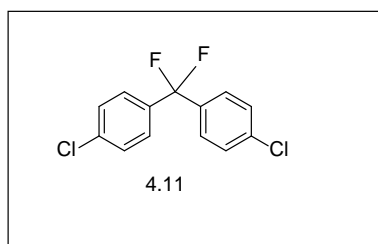
4.3.3. Synthesis and Properties of Products. Synthetic methods and characterization of the prepared compounds are discussed below.

Difluorodiphenylmethane (4.9).



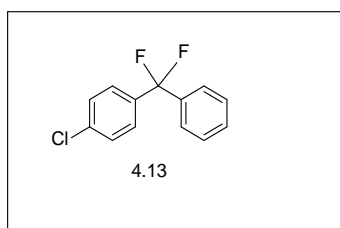
Prepared according to general procedure. Colorless oil (40 mg yield = 60 %); ^1H NMR (400 MHz, DMSO-d_6) δ 7.48-7.53 (m, 10 H); ^{13}C NMR (100 MHz, DMSO-d_6) δ 137.3 (t, $^2J_{\text{C-F}} = 30$ Hz, C1), 130.3 (C3), 128.8 (C4), 125.3 (t, $^3J_{\text{C-F}} = 6$ Hz, C2), 123.2 (t, $^1J_{\text{C-F}} = 240$ Hz, CF_2); ^{19}F NMR (376 MHz, DMSO-d_6) -88.1 (s, 2 F).

bis(4-Chlorophenyl)difluoromethane (4.11).



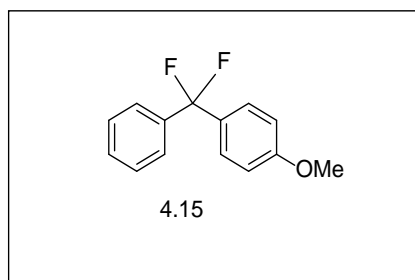
Prepared according to general procedure. ^{19}F NMR (376 MHz, DMSO-d_6) -88.5, (s, 2 F)

1-Chloro-4-(difluoro(phenyl)methyl)benzene (4.13).



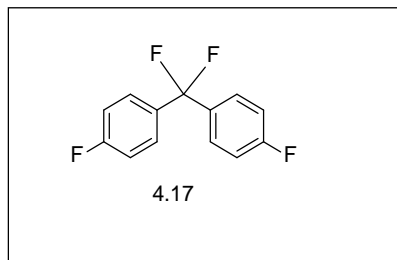
Prepared according to general procedure. ^{19}F NMR (376 MHz, DMSO-d_6) -88.7, (s, 2 F)

1-(Difluoro(phenyl)methyl)-4-methoxybenzene (4.15).



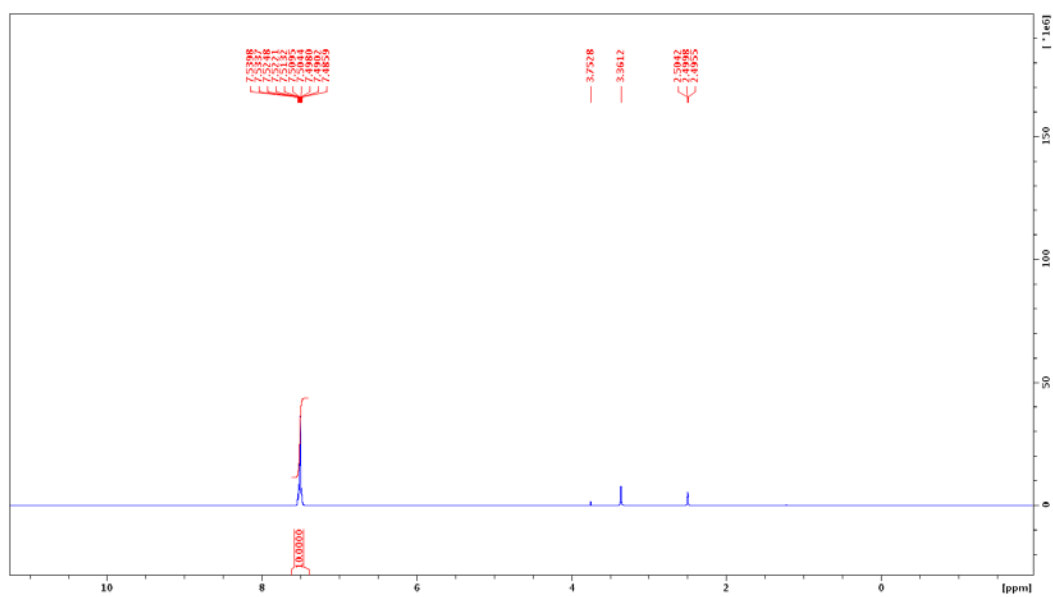
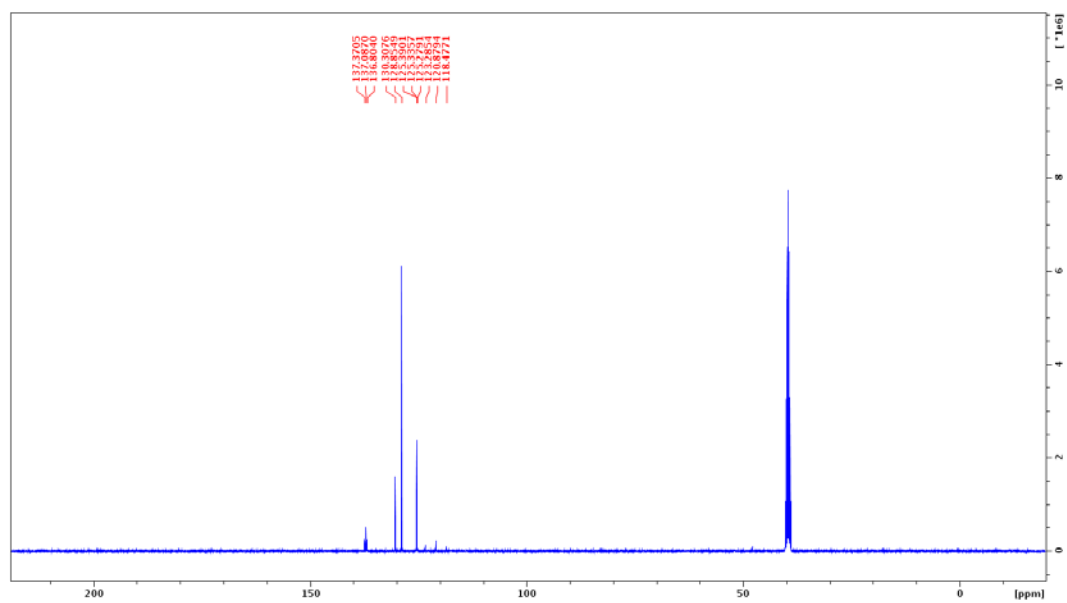
Prepared according to general procedure. ^{19}F NMR (376 MHz, DMSO-d_6) -86.9, (s, 2F)

bis(4-Fluorophenyl)difluoromethane (4.17).



Prepared according to general procedure. ^{19}F NMR (376 MHz, DMSO-d_6) - 86.5, (s, 2F), -111.0 (s, 2F).

4.3.4. NMR Spectra of the Products. The ^1H NMR, ^{13}C NMR, and ^{19}F NMR spectra of the products are shown in Figures 4.15- 4.23. Compound **4.9** was only isolated compound and ^1H NMR, ^{13}C NMR, and ^{19}F NMR spectra of this compound are provided. Only ^{19}F NMR spectra of other compounds are provided and all these spectra were recorded for reaction mixtures to confirm the completion of reaction. The signals for selectfluor in these spectra are outside the range (δ F -151.2 ppm), only partial spectrum for each compound is shown below.

Figure 4.15. ^1H NMR spectrum of compound 4.9.Figure 4.16. ^{13}C -H decoupled NMR spectrum of compound 4.9.

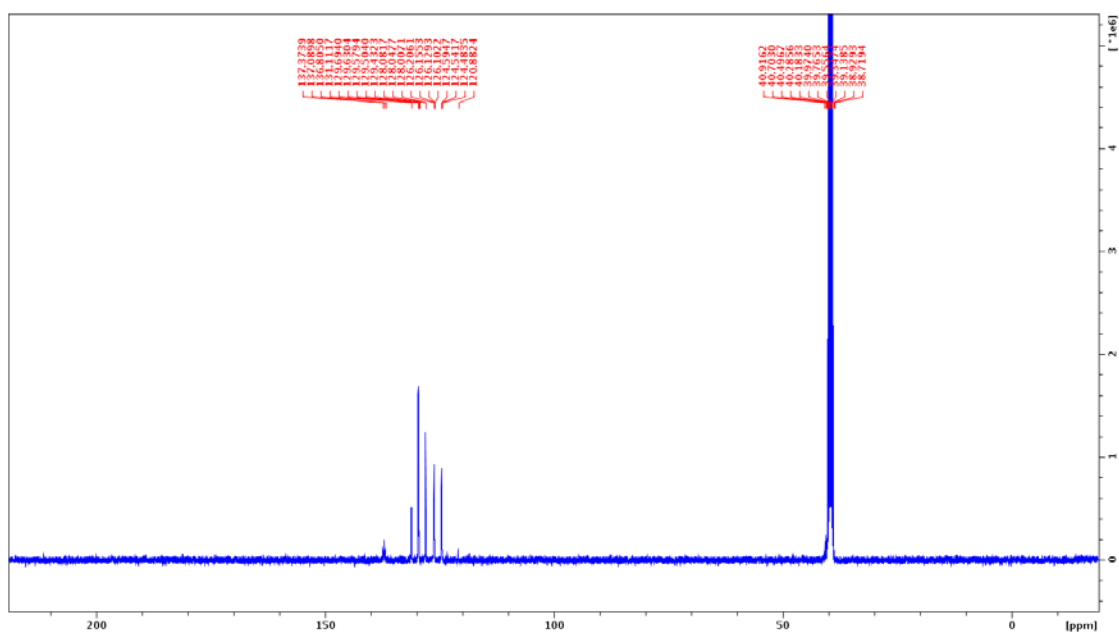


Figure 4.17. ^{13}C -H coupled NMR spectrum of compound 4.9.

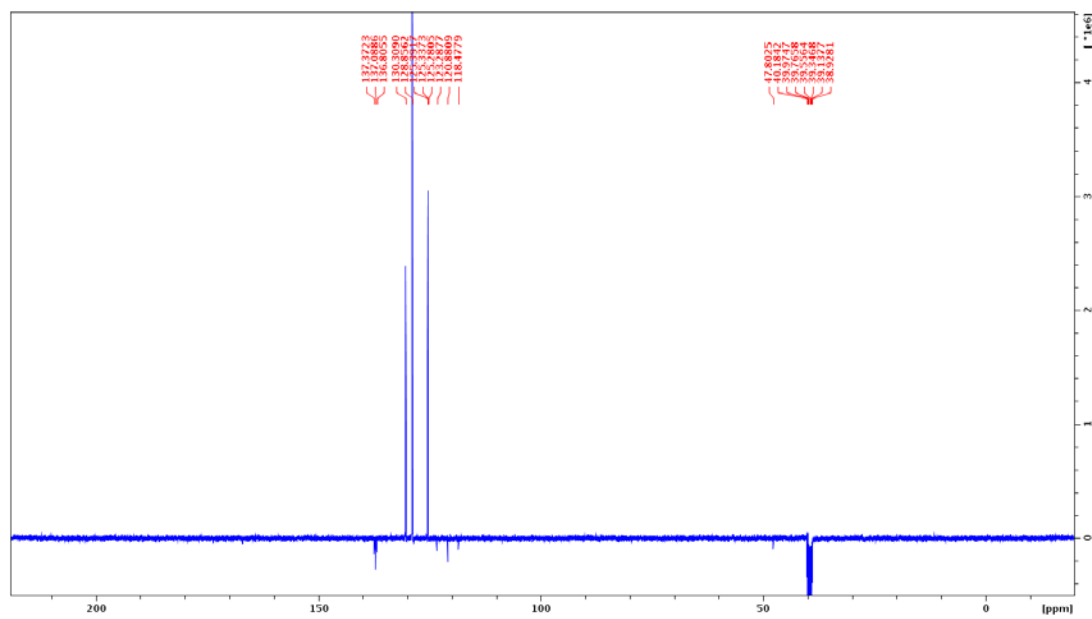


Figure 4.18. ^{13}C -APT NMR spectrum of compound 4.9.

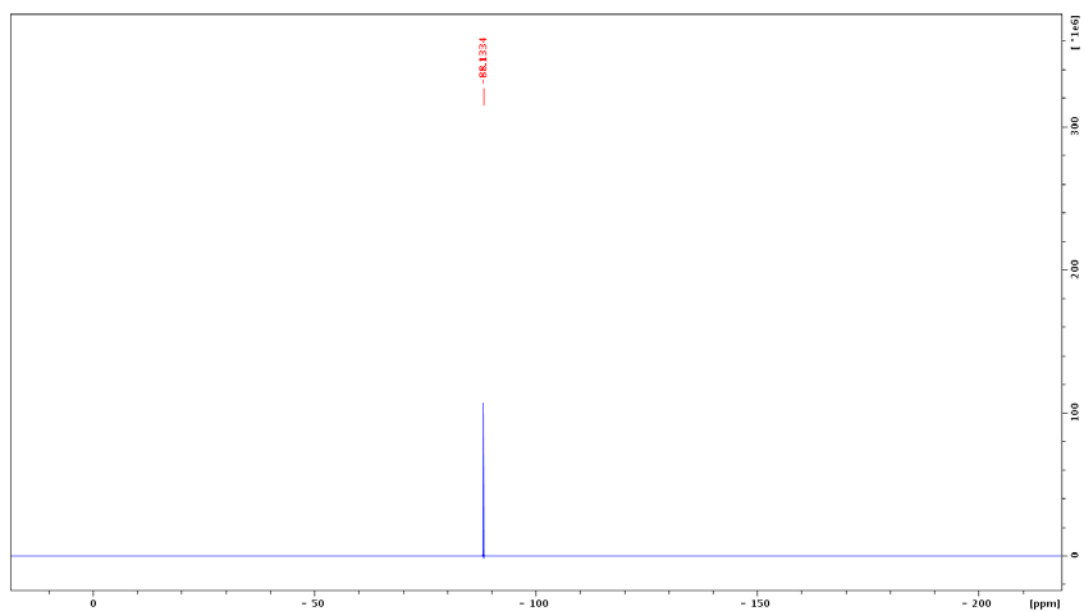


Figure 4.19. ^{19}F NMR spectrum of compound 4.9.

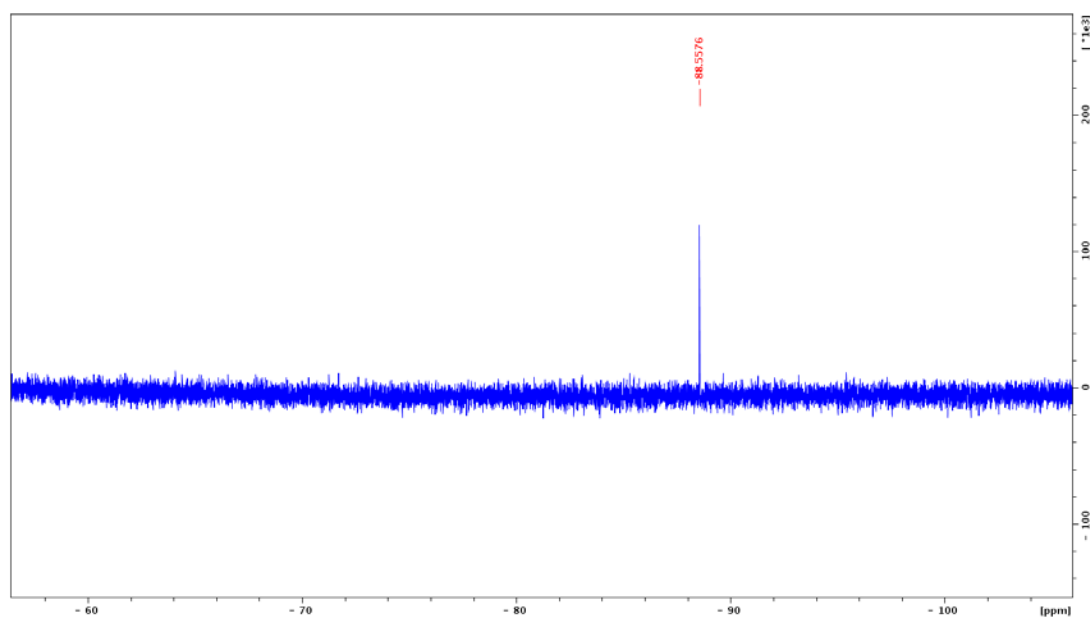


Figure 4.20. ^{19}F NMR spectrum of compound 4.11.

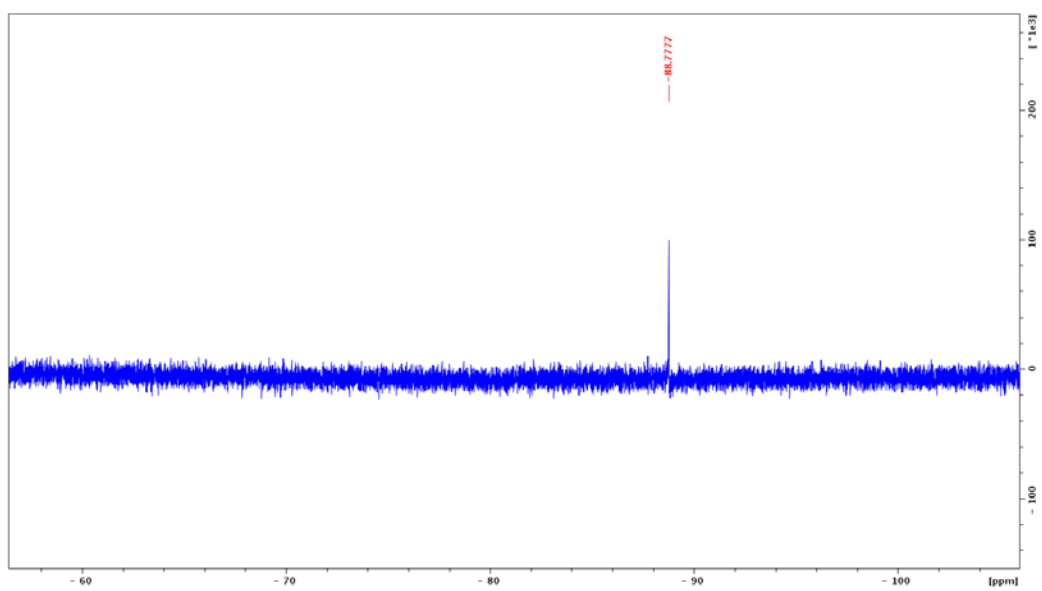


Figure 4.21. ^{19}F NMR spectrum of compound 4.13.

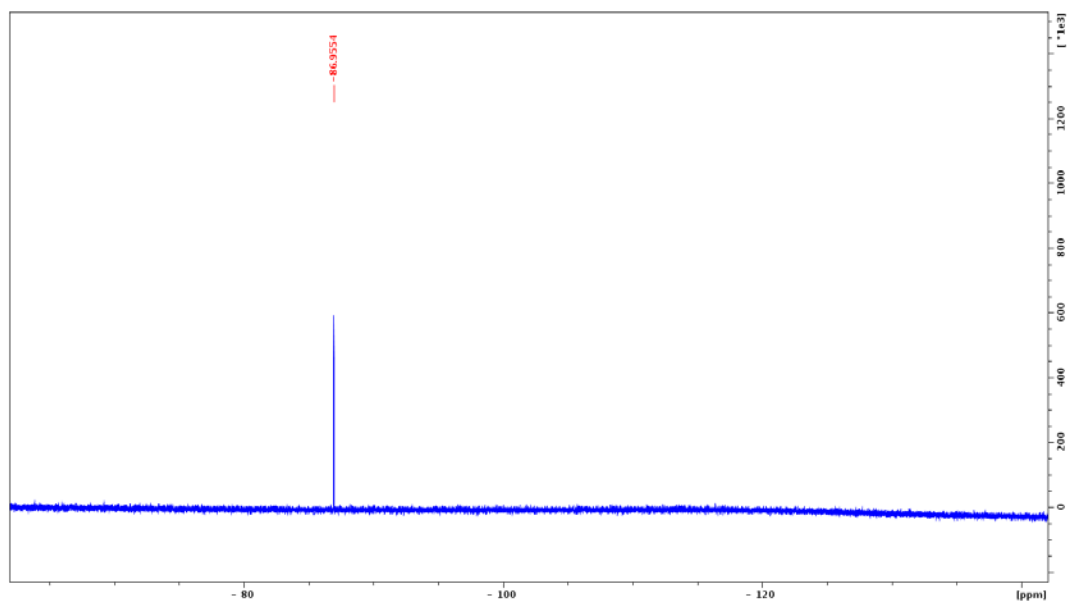


Figure 4.22. ^{19}F NMR spectrum of compound 4.15.

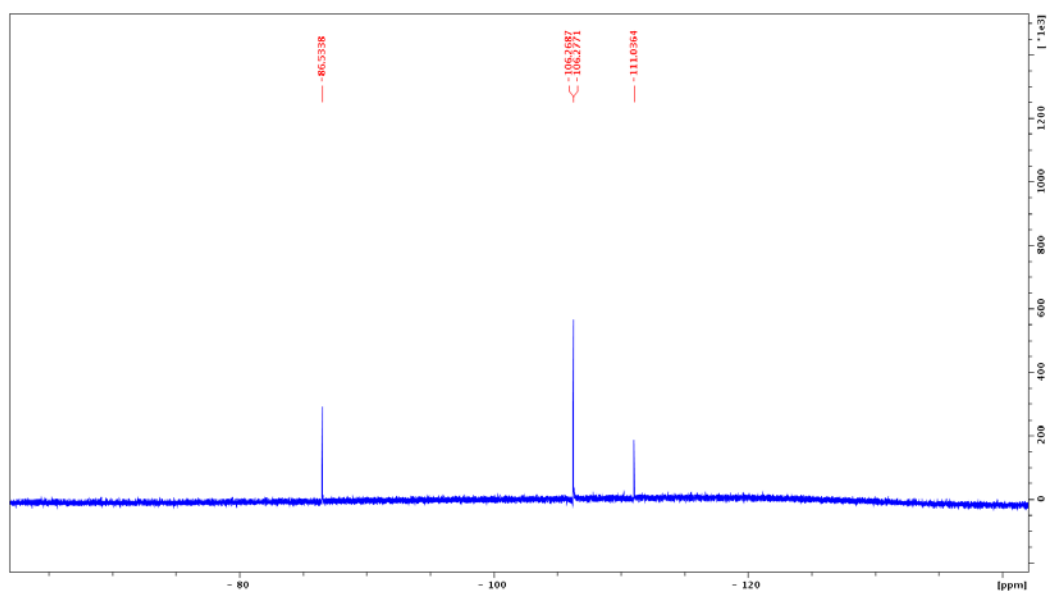


Figure 4.23. ^{19}F NMR spectrum of compound 4.17.

5. N-HETEROCYCLIC CARBENE-CATALYZED TRIFLUOROMETHYLATION OF AROMATIC TOSYLALDIMINES

5.1. BACKGROUND

α -Trifluoromethyl substituted amines and their related fluorinated derivatives have unique applications in areas ranging from pharmaceuticals to agro-chemicals to materials chemistry.^{14, 204-207} Basicity of amino moiety is substantially attenuated in the α -trifluoromethylamines due to the strong electron-withdrawing effect of the trifluoromethyl group, thereby enhancing the lipophilicity, cell-permeability, and metabolic stability of the α -trifluoromethylamines—the favorable pharmacokinetic parameters that are required in the successful drug-design. A variety of methods have been reported for the preparation of α -trifluoromethylamines^{14-16, 208-213}, and recently, the direct preparation of α -trifluoromethylamines by nucleophilic trifluoromethylation of imines has received renewed attention.^{17-18, 214-218} Although nucleophilic trifluoromethylation of the carbonyl compounds has been extensively explored over the last few decades, trifluoromethylation of aldehyde-imines (aldimines) has received relatively less attention. Prakash and co-workers have first reported nucleophilic trifluoromethylation of N-tosyl substituted aromatic aldehyde imines and obtained the corresponding trifluoromethylated products in high yields, using (trifluoromethyl) trimethylsilane (TMSCF₃; Ruppert-Prakash Reagent) and catalytic amounts of tetrabutylammonium (triphenylsilyl) difluoride (TBAT), as the fluoride ion source, for initiation of the reaction as shown in Figure 5.1.²¹⁹⁻²²¹ In these substrates, N-tosyl moiety enhances the electrophilicity of the imines toward the trifluoromethide anion through its electron-withdrawing effect. The use of tetrabutylammonium fluoride (TBAF) initiator at higher concentrations (> 0.5 equiv), however, results in the formation of the corresponding difluoromethylated imines.²²⁰

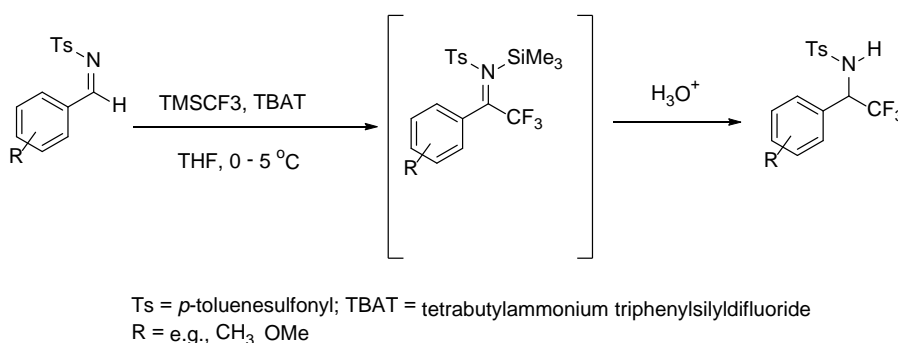


Figure 5.1. Nucleophilic trifluoromethylation of N-tosyl aldimines using TMSCF₃ and TBAT.

Dolbier and co-workers have reported the nucleophilic trifluoromethylation of various aromatic N-tosyl aldimines using in situ generated trifluoromethide anion, formed from the reagent combination CF₃I and tetrakis(dimethylamino) ethylene (TDAE), in good to moderate yields.²²²⁻²²³ The latter reaction gave good yields of the corresponding N-tosyl α -trifluoromethylated benzylamines (with various substituents in the aryl ring, such as 4-OMe, 4-F, and 4-NO₂), although it is not applicable to enolizable imines, such as the imines derived from acetophenone, cyclohexanone, and hexanal. Mukaiyama and co-workers have reported catalytic trifluoromethylation of aldimines with TMSCF₃ in the presence of Lewis bases.²²⁴⁻²²⁵ Lithium carboxylates, such as lithium benzoate, lithium acetate, and lithium pivalate were found to be effective initiators in these reactions, and under these reaction conditions, aromatic aldimines with electron-withdrawing as well as electro-donating groups (e.g., NO₂, Cl, CH₃) afforded the corresponding trifluoromethylated products in good yields.²²⁴⁻²²⁵ Shibata and co-workers have achieved the nucleophilic trifluoromethylation of N-tosyl-substituted aromatic aldimines using TMSCF₃ and stoichiometric amounts of tri(*tert*-butyl)phosphine as the initiating agent.²²⁶

N-Heterocyclic carbenes (NHC) have received considerable interest in recent years as catalysts for a variety of transformations, including nucleophilic trifluoromethylation of carbonyl compounds using TMSCF_3 , nucleophilic perfluorophenylation using pentafluorophenyltrimethylsilane, and cyanosilylation of aldehydes and N-tosylaldimines using trimethylsilylcyanide.^{19-21, 227-230} Song et al.¹⁹ have reported that both enolizable and nonenolizable aldehydes and α -ketoesters undergo facile trifluoromethylation at room temperature in the presence of 0.5–1 mol% of the NHC to afford the corresponding α -trifluoromethyl alcohols in good yields as shown in Figure 5.2. Under NHC catalysis, selective trifluoromethylation of aldehydes over ketones was achieved, and this method offered much greater catalytic efficiency as well as broader substrate scope as compared to the other Lewis base-catalyzed trifluoromethylation methods. NHC have reactivities similar to the Lewis bases such as phosphines and amines, and therefore can activate TMSCF_3 or TMSC_6F_5 towards the trifluoromethylation or perfluorophenylation of carbonyl compounds.¹⁹⁻²⁰ NHC have also been used as efficient catalysts in the silyl-Reformatsky reaction of aldehydes using difluoro(trimethylsilyl)acetate to give the corresponding β -hydroxy *gem*-difluoro esters.²³¹ We have reported the NHC-catalyzed trifluoromethylation of imines, and also investigated the feasibility of the NHC-catalyzed trifluoromethylation of imines, using the N-tosyl substituted aldimines and TMSCF_3 , using the readily available NHC-1 and NHC-2¹³, (Figure 5.3) derived from their corresponding imidazolium salts 1 and 2, respectively.²³²

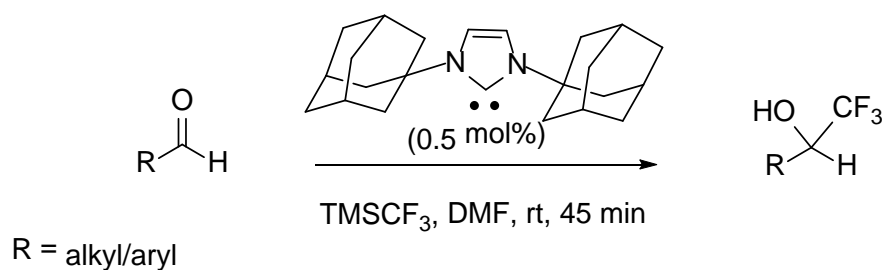


Figure 5.2. NHC catalyzed nucleophilic trifluoromethylation of carbonyl compounds.

5.2. RESULTS AND DISCUSSION

In order to explore the feasibility of NHC-catalyzed trifluoromethylation, *o*-chloroderivative of *N*-tosylbenzaldimine **5.1** was reacted with TMSCF_3 in anhydrous DMF (dried by anhydrous magnesium sulfate), as the solvent in the presence of the in situ generated **NHC-1** (formed in situ in the reaction mixture through the reaction of 1,3-bis(2,4,6-trichloromethylphenyl)imidazolium chloride (**1**; 15 mol% with $\text{KO}t\text{-Bu}$ (13 mol%), 4 Å molecular sieves under nitrogen atmosphere (N_2 balloon) at room temperature. ^1H NMR analysis of the reaction mixture after 20 h showed 92% conversion. In order to test the possibility of the catalysis by any residual potassium tert-butoxide in the reaction mixture, we have independently carried out trifluoromethylation of **5.1** using TMSCF_3 and potassium tert-butoxide in varying ratios, in the absence of the NHC, at room temperature for 20 h. Under these conditions, trifluoromethylation of **5.1** proceeded in 16 and 45% yields, respectively (as monitored by ^1H NMR), in the presence 1 and 16% potassium tert-butoxide. On the other hand, NHC-1 (13 mol%) catalyzed trifluoromethylation of **5.1** under these conditions afforded 92% of the product **5.2**, as monitored by ^1H NMR as shown in Figure 5.4. These control experiments thus demonstrate that the NHC catalysis dramatically enhances the rates of the trifluoromethylation reactions.

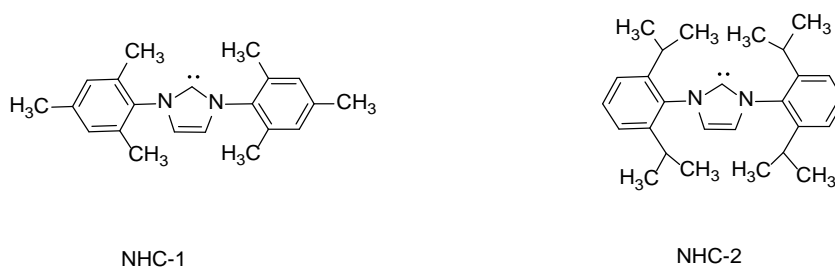


Figure 5.3. Structures of NHC-1 and NHC-2.

Having optimized the NHC-1 catalyzed trifluoromethylation of N-tosylaldimine **5.1**, we have proceeded to explore the scope of this reaction to various other aryl N-tosylaldimines to obtain the corresponding α -trifluoromethylated sulfonamides. Aromatic N-tosylaldimines with electron-withdrawing as well as electron-donating substituents on the aryl ring reacted readily with TMSCF_3 in the presence of NHC-1 to afford the corresponding α -trifluoromethylsulfonamides in moderate to good yields (Table 5.1) as shown below.

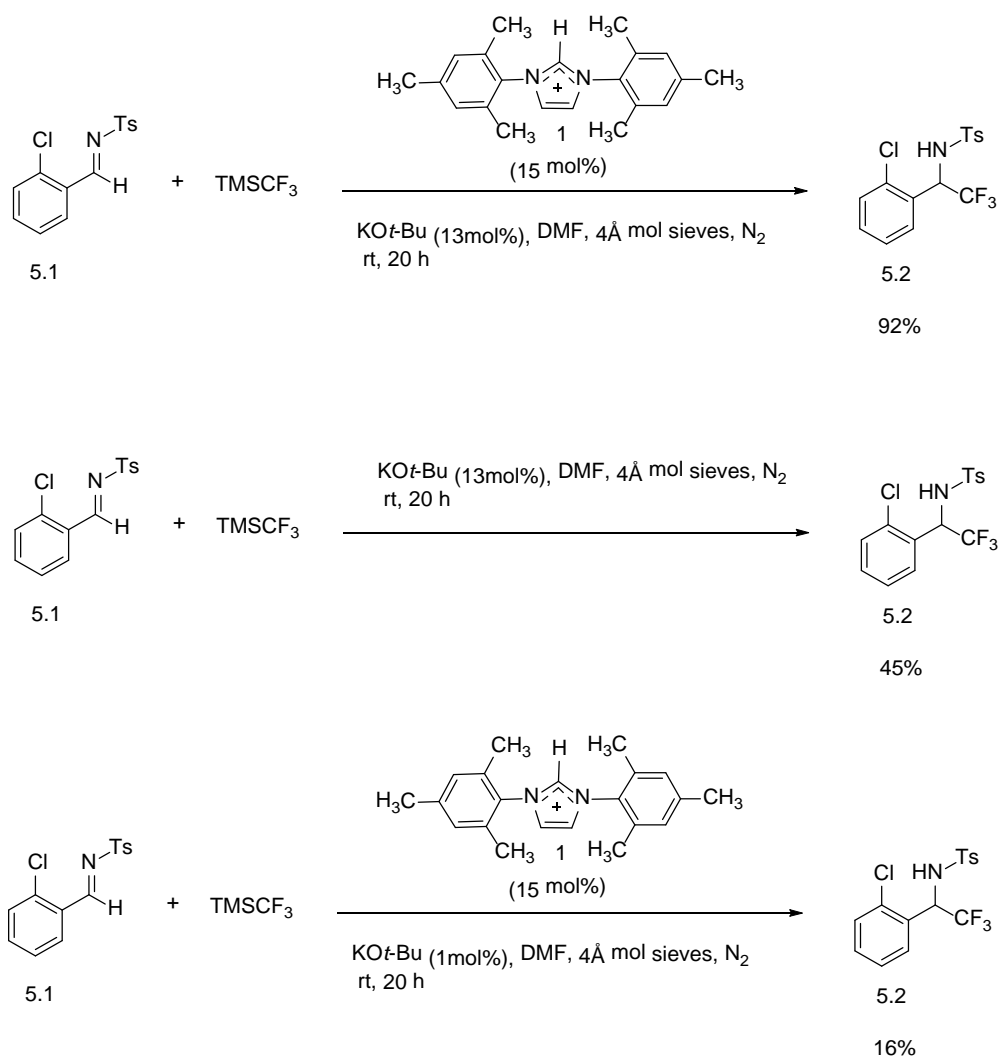
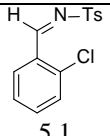
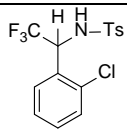
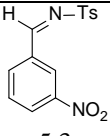
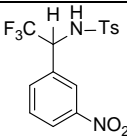
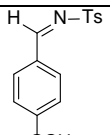
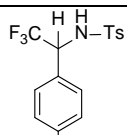
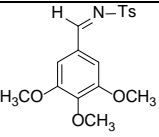
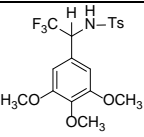
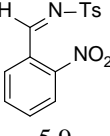
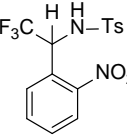
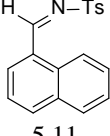
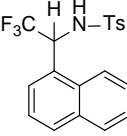
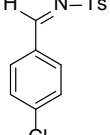
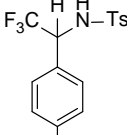


Figure 5.4. Optimization of trifluoromethylation of N-tosylbenzaldehyde in the presence of in situ generated NHC-1.

Table 5.1. NHC-1 catalyzed trifluoromethylation of aromatic N-tosylaldimines.

Entry	Reactant	Product	% Conversion; estimated by ^1H NMR (isolated yield)	^{19}F NMR, δ (ppm)
1	 5.1	 5.2	92 (76)	-74.1
2	 5.3	 5.4	100 (80)	-73.7
3	 5.5	 5.6	52	-74.0
4	 5.7	 5.8	34	-73.6
5	 5.9	 5.10	41	-73.4
6	 5.11	 5.12	35	-73.0
7	 5.13	 5.14	94	-73.8

5.3. EXPERIMENTAL

5.3.1. Materials and Methods. All reagents were purchased from commercial sources and used as received. Column chromatography was carried out using Merck 60, 230-400 mesh. Thin layer chromatography was carried out using silica gel coated polyester backed sheets. The ^1H , ^{13}C NMR and ^{19}F NMR spectrum for DMSO- d_6 solutions were obtained on an INOVA-Varian 400 MHz spectrometer at 400, 100, and 376 MHz respectively. The ^1H NMR, ^{13}C NMR chemical shifts are referenced to the residual solvents signals or the internal TMS ($\delta = 0.0$). The ^{19}F chemical shifts are referenced to the internal CFCl_3 ($\delta^{19}\text{F} = 0.0$).

5.3.2. General Procedure for the Preparation of Aromatic N-tosylaldimines.

Aromatic N-tosylaldimines were prepared according to our convenience by two different methods reported in literature.²³³⁻²³⁴

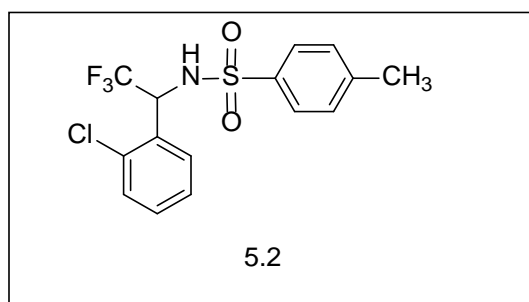
5.3.3. General Procedure for Trifluoromethylation of Aromatic N-

tosylaldimines. To a mixture of imidazolium chloride 1 (18 mg, 0.053 mmol) in 2 mL anhydrous DMF dried over oven dried MgSO_4 and molecular sieves was added potassium tert-butoxide (5 mg, 0.045 mmol) under nitrogen atmosphere (N_2 balloon) at room temperature. After dissolution of imidazolium chloride (~ 20 min.), N-tosylbenzaldimine **5.1** (100 mg, 0.34 mmol) and TMSCF_3 (70 μL , 0.475 mmol) were added to the contents and the solution was stirred under nitrogen atmosphere at room temperature for 20 h. After reaction completion confirmed by ^1H NMR, reaction was quenched by adding water, and the product was extracted by dichloromethane (3 x 10 mL). The organic layers were combined and successively washed with water and brine, dried over Na_2SO_4 , and the solvents were removed in vacuum. The resulting product was

purified by silica gel chromatography (10% ethyl acetate in hexanes) to afford pure trifluoromethylated sulfonamide **5.2** as a white solid (94 mg, 76%).

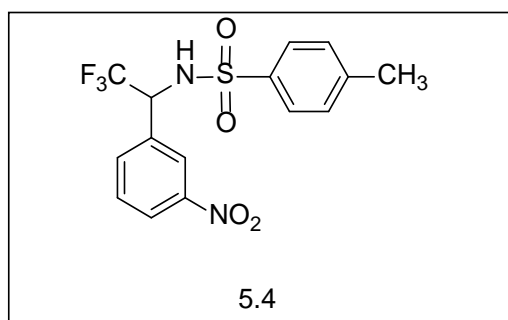
5.3.4. Synthesis and Properties of Products. Synthetic methods and characterization of prepared compounds are discussed below.

N-(1-(2-chlorophenyl)-2,2,2-trifluoroethyl)-4-methylbenzenesulfonamide (5.2).



Prepared according to general procedure. White solid (94 mg, 76%); ^1H NMR (400 MHz, CDCl_3) δ 7.75 (d, $J = 12$ Hz, 2H), 7.21-7.39 (m, 5H), 6.36 (d, $J = 12$ Hz, 1H), 5.66-5.74 (m, 1H), 2.44 (s, 3H); ^{13}C NMR (100 MHz, CDCl_3) δ 144.4, 136.9, 134.6, 130.8, 130.5, 130.2, 130.0, 129.1, 127.9, 127.4, 56.1 (q, q, $J_{\text{C-F}} = 33\text{Hz}$, CF_3), 21.9; ^{19}F NMR (376 MHz, CDCl_3) δ -74.1 (d, $J_{\text{H-F}} = 6.88$ Hz).

4-methyl-N-(2,2,2-trifluoro-1-(3-nitrophenyl)ethyl)benzenesulfonamide (5.4).

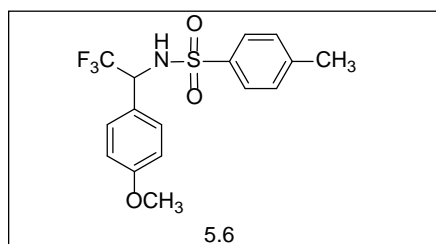


Prepared according to general procedure. White solid (98 mg, 80%); ^1H NMR (400 MHz, CDCl_3) δ 8.18 (dq, $^1J = 9.28$, $^2J = 5.08$, $^3J = 1.08$ Hz, 1H), 7.94 (s, 1H), 7.48-7.61

(m, 4H), 7.17 (d, $J = 8.64$ Hz, 2H), 5.38 (d, $J = 8$ Hz, 1H), 5.08 (m, $J = 7.36$ Hz, 1H), 2.35 (s, 3H); ^{13}C NMR (100 MHz, CDCl_3) δ 148.6, 144.9, 136.9, 134.5, 134.3, 130.5, 130.2, 127.4, 124.7, 123.6, 59.6 (q, $J_{\text{C-F}} = 30$ Hz, CF_3), 21.9; ^{19}F NMR (376 MHz, CDCl_3) δ -73.7 (d, $J_{\text{H-F}} = 7.0$ Hz).

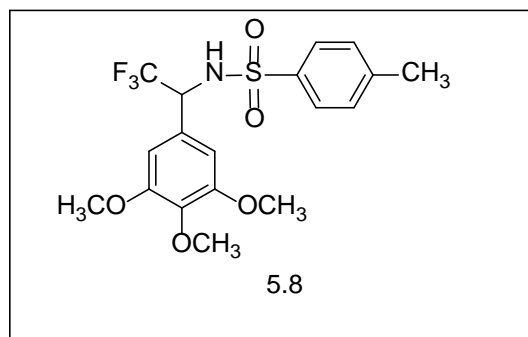
4-methyl-N-(2,2,2-trifluoro-1-(4-methoxyphenyl)ethyl)benzenesulfonamide

(5.6).

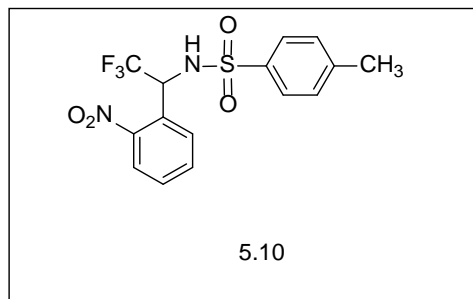


Prepared according to general procedure. ^{19}F NMR (376 MHz, CDCl_3) δ -74.0 (d, $J_{\text{H-F}} = 7.3$ Hz).

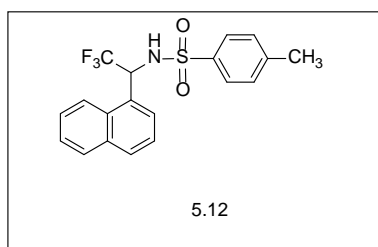
4-methyl-N-(2,2,2-trifluoro-1-(3,4,5-trimethoxyphenyl)ethyl)benzenesulfonamide (5.8).



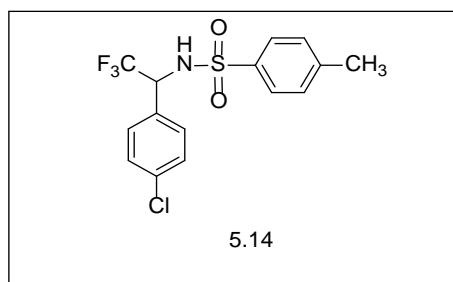
Prepared according to general procedure. ^{19}F NMR (376 MHz, CDCl_3) δ -73.6 (d, $J_{\text{H-F}} = 7.7$ Hz).

4-methyl-N-(2,2,2-trifluoro-1-(2-nitrophenyl)ethyl)benzenesulfonamide**(5.10).**

Prepared according to general procedure. ^{19}F NMR (376 MHz, CDCl_3) δ -73.4 (d, $J_{\text{H-F}} = 6.9$ Hz).

4-methyl-N-(2,2,2-trifluoro-1-(naphthalen-1-yl)ethyl)benzenesulfonamide**(5.12).**

Prepared according to general procedure. ^{19}F NMR (376 MHz, CDCl_3) δ -73.0 (d, $J_{\text{H-F}} = 6.2$ Hz).

N-(1-(4-chlorophenyl)-2,2,2-trifluoroethyl)-4-methylbenzenesulfonamide**(5.14).**

Prepared according to general procedure. ^{19}F NMR (376 MHz, CDCl_3) δ -73.8 (d, $J_{\text{H-F}} = 7.7$ Hz).

5.3.5. NMR Spectra of the Products. The ^1H NMR, ^{13}C NMR, and ^{19}F NMR spectra of the products are shown in Figures 5.5- 5.15.

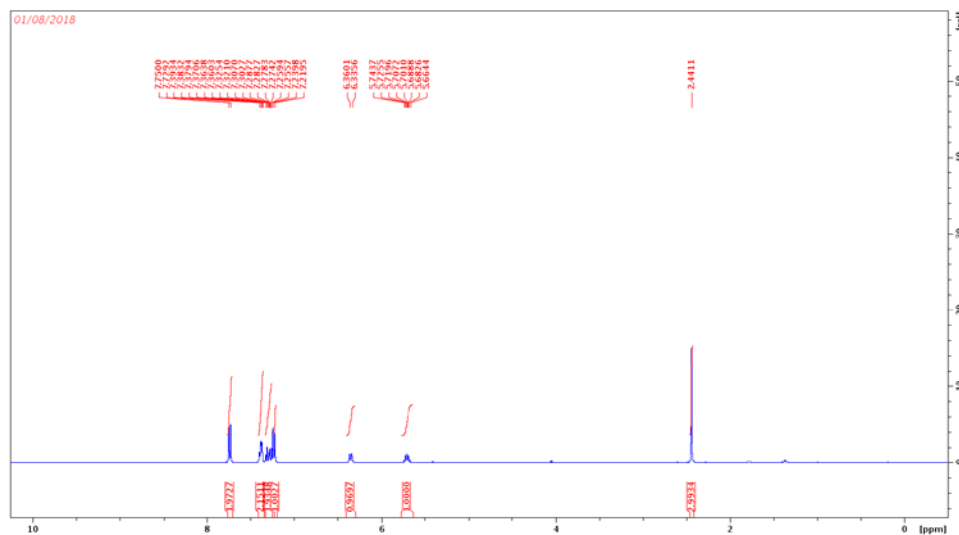


Figure 5.5. ^1H NMR spectrum of compound 5.2.

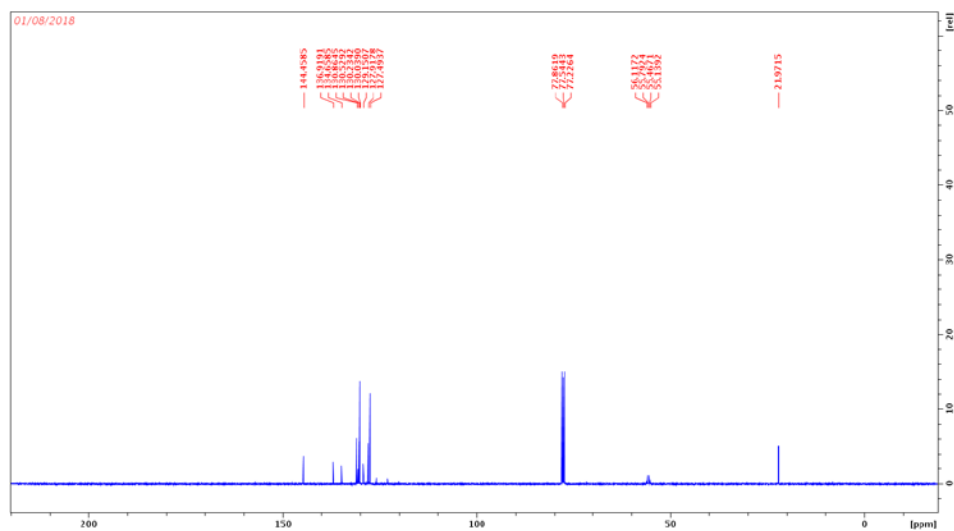


Figure 5.6. ^{13}C NMR spectrum of compound 5.2.

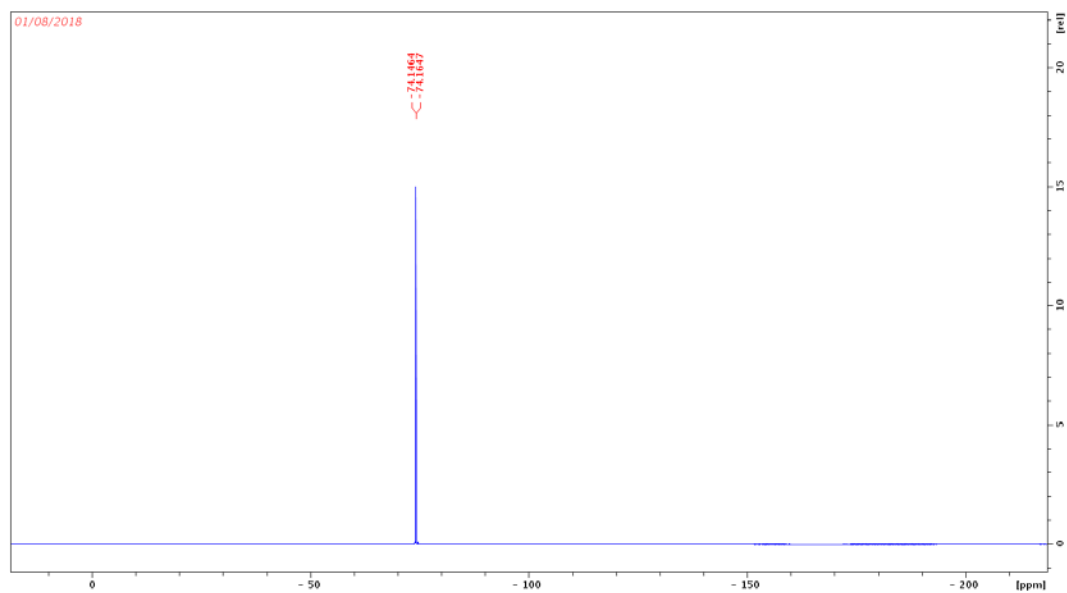


Figure 5.7. ^{19}F NMR spectrum of compound 5.2.

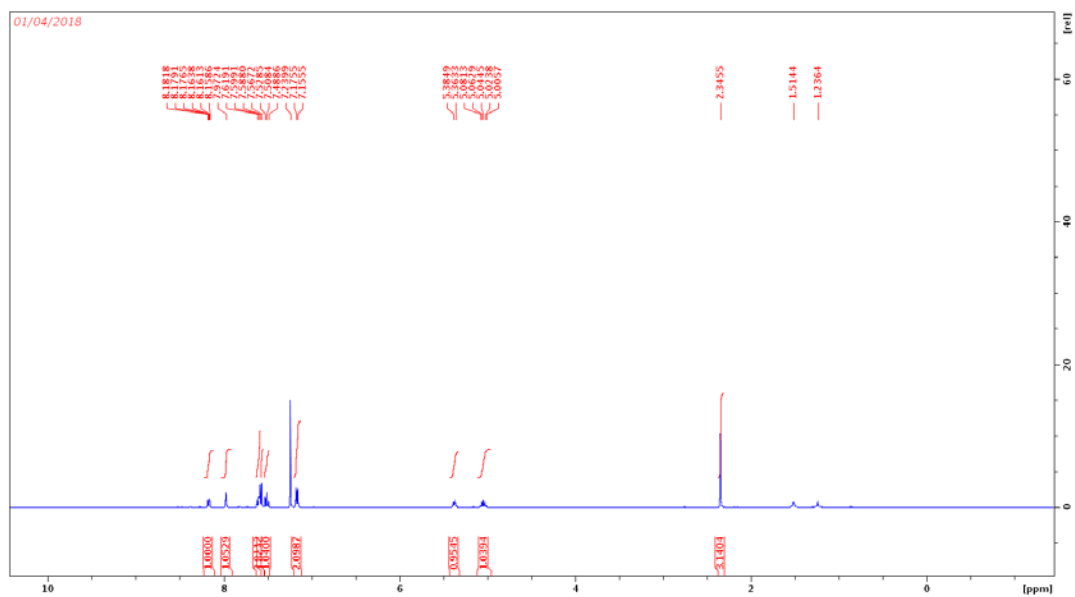


Figure 5.8. ^1H NMR spectrum of compound 5.4.

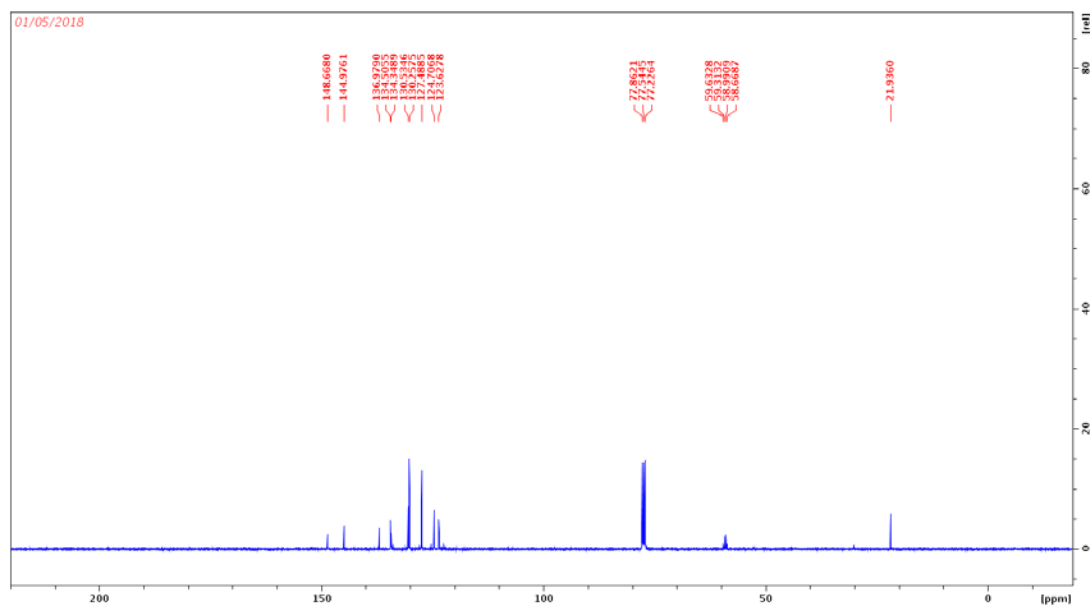


Figure 5.9. ^{13}C NMR spectrum of compound 5.4.

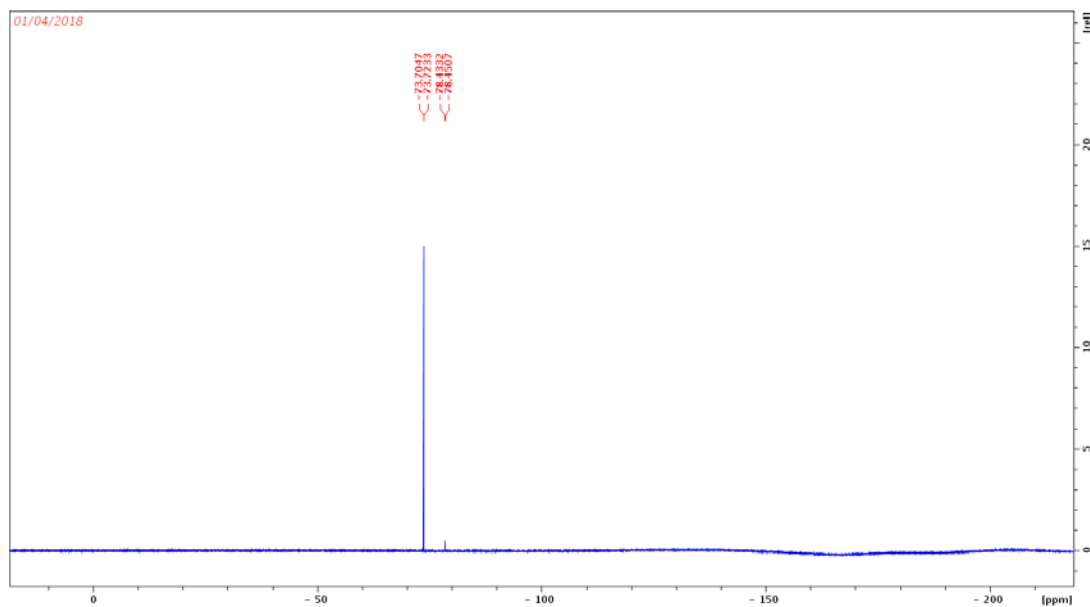


Figure 5.10. ^{19}F NMR spectrum of compound 5.4.

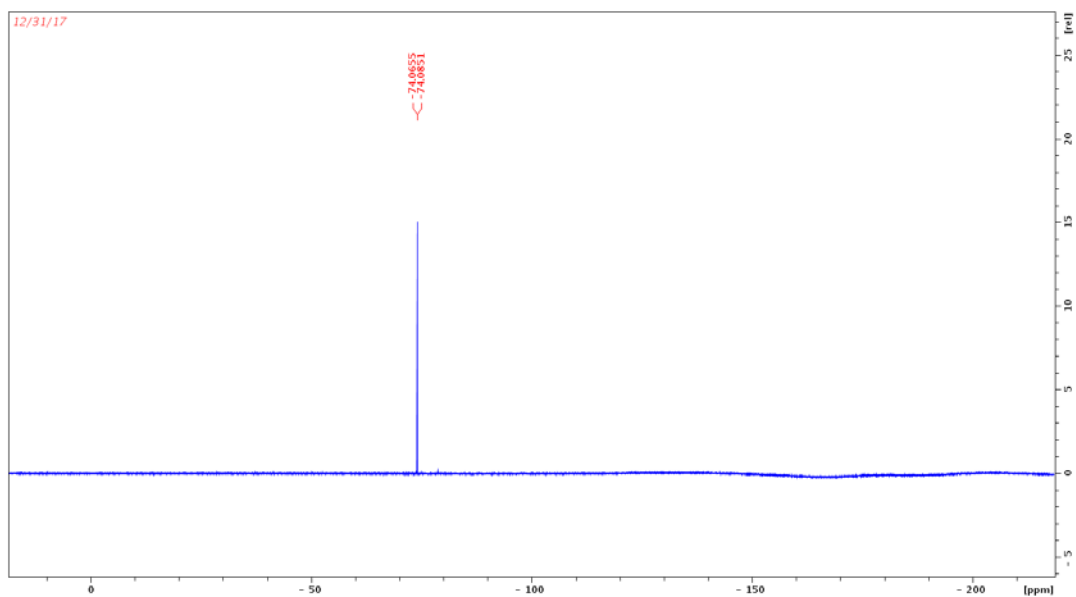


Figure 5.11. ^{19}F NMR spectrum of compound 5.6.

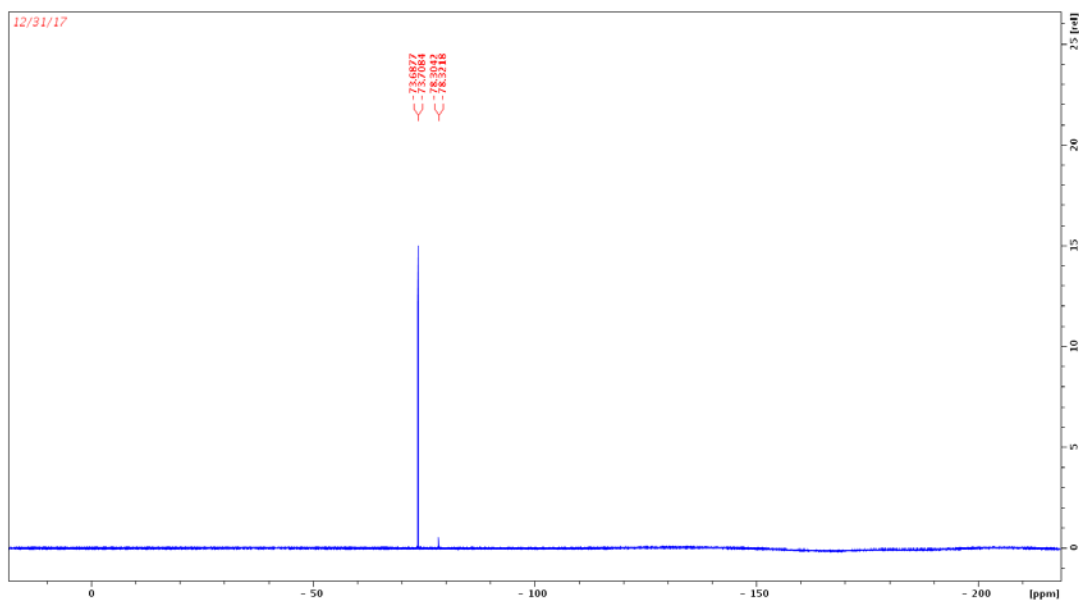


Figure 5.12. ^{19}F NMR spectrum of compound 5.8.

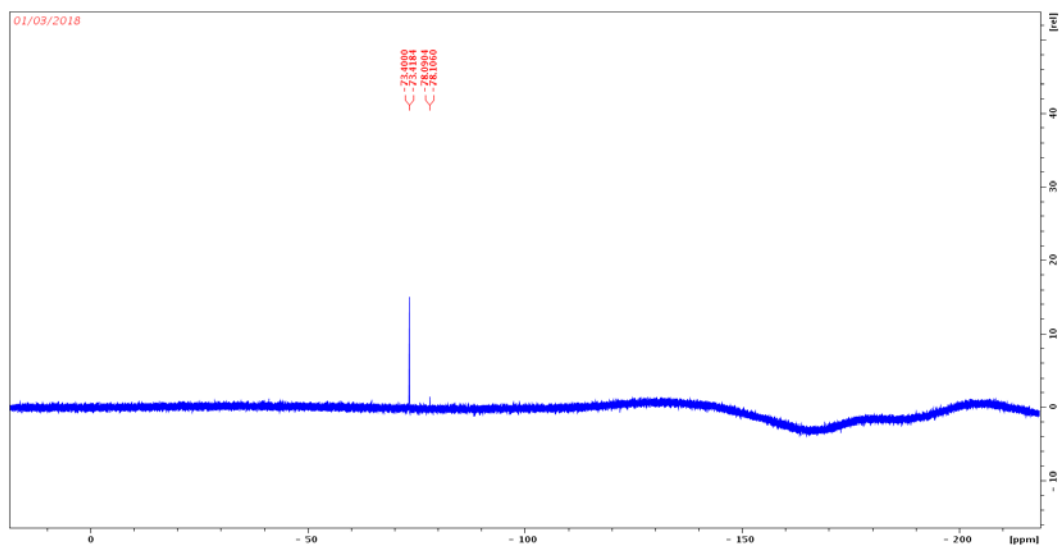


Figure 5.13. ^{19}F NMR spectrum of compound 5.10.

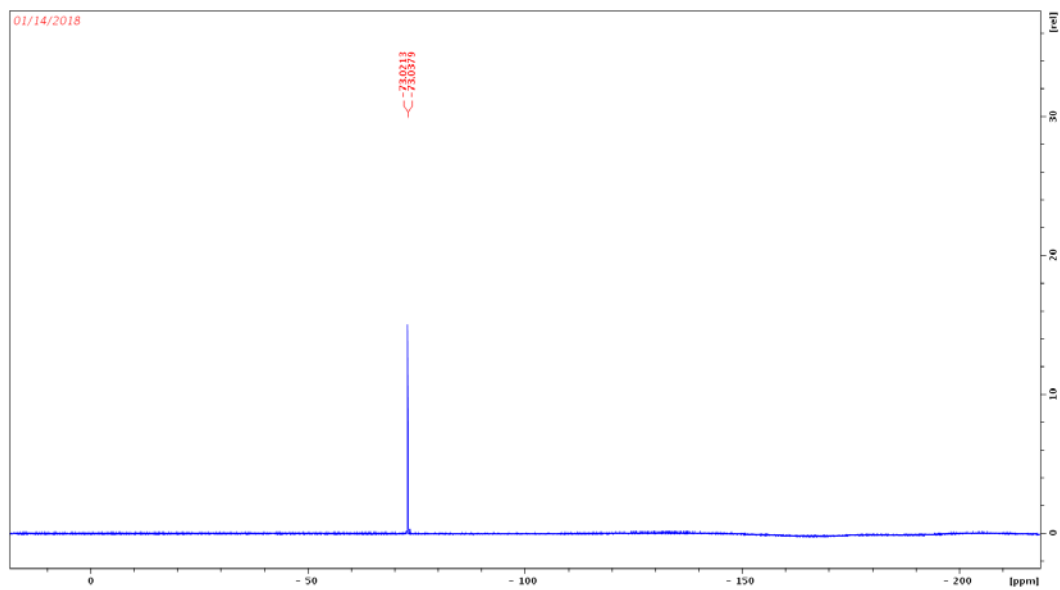


Figure 5.14. ^{19}F NMR spectrum of compound 5.12.

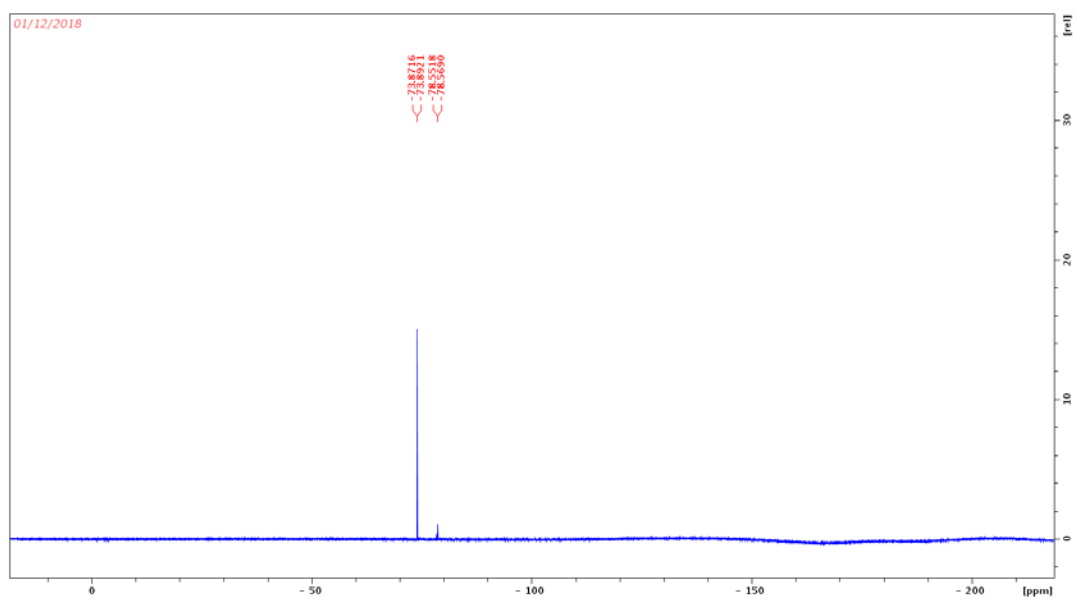


Figure 5.15. ^{19}F NMR spectrum of compound 5.14.

6. SYNTHESIS OF NOVEL PURINE - BASED KINASE INHIBITORS

6.1. BACKGROUND

Kinases have been investigated as promising drug targets²³⁵⁻²⁴³ for the past three decades and 38 kinase inhibitors have been approved till date by FDA.²⁴⁴ These therapeutics are predominantly multitargeted receptor tyrosine kinase (RTK) inhibitors for the treatment of various diseases including neurodegenerative diseases, cardiovascular diseases, diabetes, inflammation and cancers.²⁴⁵⁻²⁵² Kinases control the cellular processes comprising of reversible phosphorylation of proteins.²² Protein phosphorylation is a molecular mechanism to regulate the function of proteins in response to extracellular stimuli in the nervous system. Kinases catalyze the transfer of γ -phosphate group of adenosine triphosphate (ATP) onto to a substrate containing amino acid (serine, threonine or tyrosine) residues²⁵³ to mediate signal transduction and regulate cellular activities²⁵⁴ and deregulation of kinases' activity is the causative factor for the pathogenesis of diseases.²⁵⁵⁻²⁵⁸ Therefore, kinase inhibitor discovery requires extensive research.²⁵⁹⁻²⁶⁰ Many potential therapeutics have been designed so far after understanding the molecular biology of protein kinases and use of structural information. Small molecule kinase inhibitors^{254, 261-262} such as Imatinib (first approved in 2001 by FDA), Afatinib, and Sorafenib have been getting an attention in both academia and pharmaceutical industry research. Imatinib has been used for the treatment of chronic myeloid leukemia (CML)²⁶³ and for various structure activity relationship (SAR) studies to design next generation kinase inhibitors and their binding mechanism.²⁶⁴⁻²⁶⁵ Chemical structures of Imatinib and other related small molecule kinase inhibitors are shown in Figure 6.1.

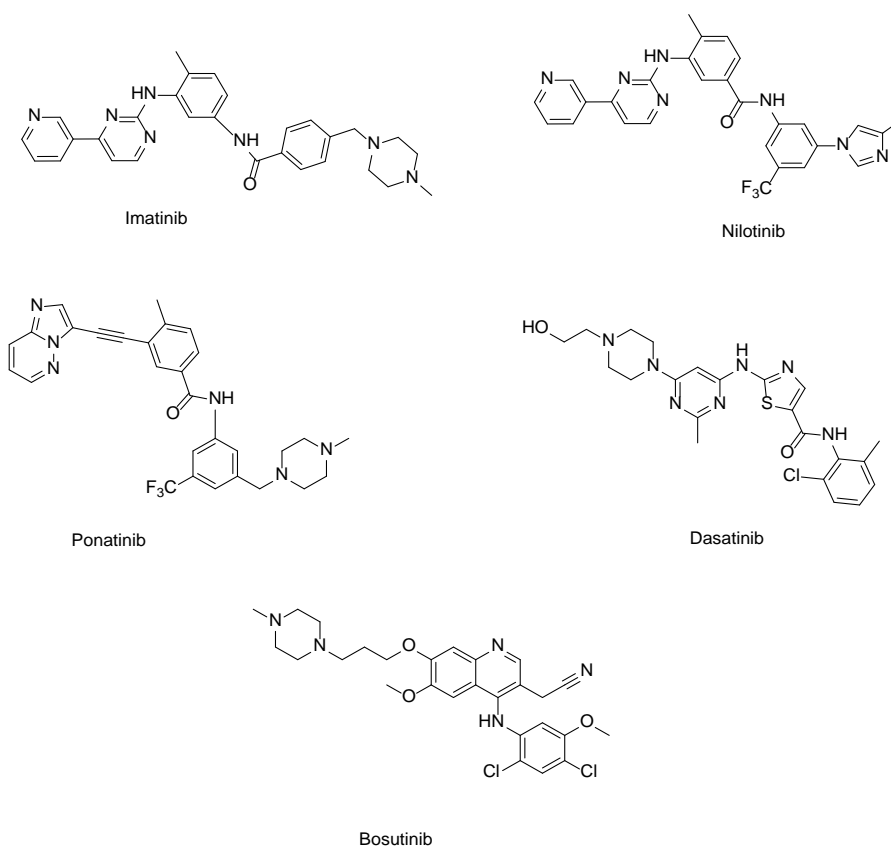


Figure 6.1. Chemical structures of Imatinib and other related small molecule kinase inhibitors.²⁵⁴

6.1.1. Purine-Based Kinase Inhibitors. Purine is a heterocyclic moiety present in chemical structure of many bioactive molecules. Several purine analogs e.g. thiopurines, pentostatin, acyclovir, penciclovir, ganciclovir, azathiopurine, vidarabine and theophylline have been used in the treatment of several diseases including acute leukemias, immunological disorders, tumors and asthma. Purine nucleus has been established as an important pharmacophore in the development of kinase inhibitors. Published research showed the kinase inhibitory activity of purines²⁶⁶⁻²⁷⁰ and 2,6, and 9 substituted purine derivatives showed increased binding affinity and selectivity towards

kinases.²⁷¹ Purine based kinase inhibitors has been classified into tyrosine specific protein, specific protein, dual specificity (tyrosine/specific protein), and miscellaneous kinase inhibitors.²² Although several purine based kinase inhibitors are still in pre-clinical/clinical trials as shown in Figure 6.2, there is still a need of developing novel purine-based kinase inhibitors showing promising inhibitory activities on diverse kinases.

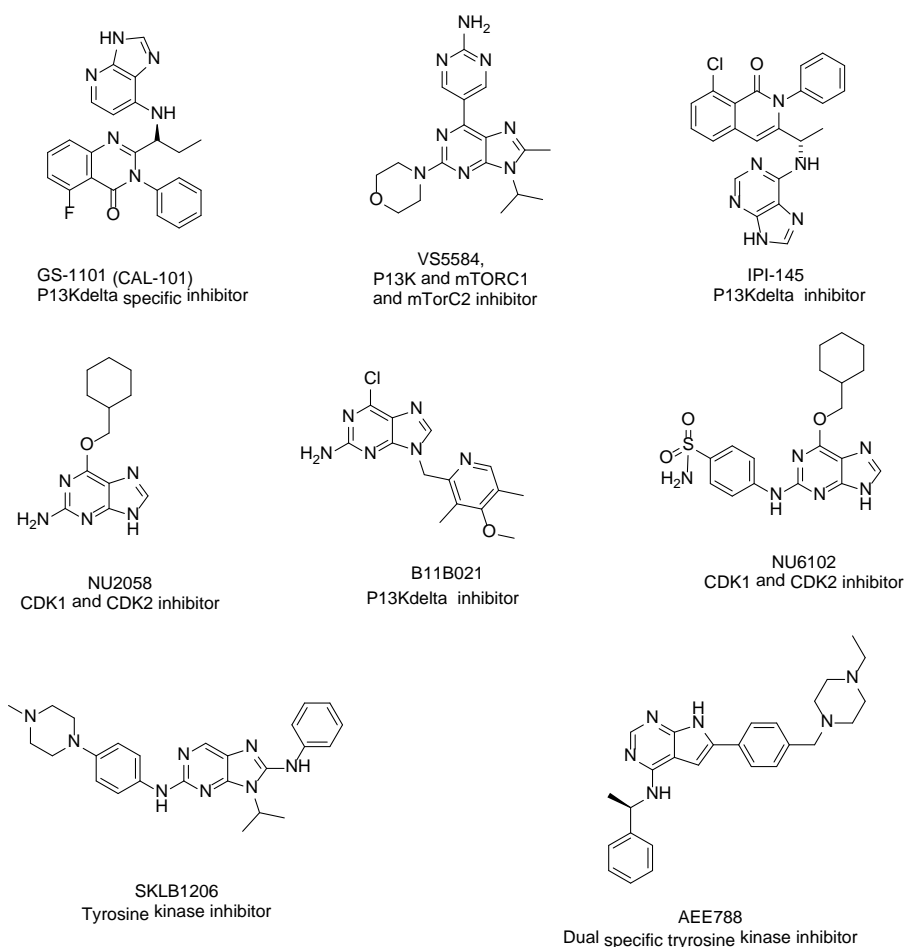
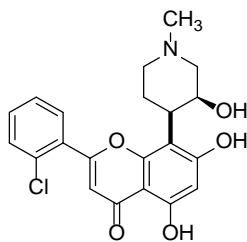


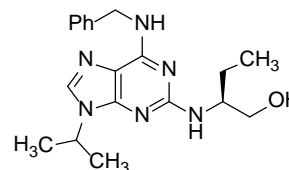
Figure 6.2. Purine based protein kinase inhibitors in pre-clinical/clinical trials.²²

6.2. RESULTS AND DISCUSSION

Cyclin-dependent kinases (CDKs) are the protein kinases responsible for regulation of cellular processes. CDK5 plays an important role in neuronal cell death²⁷²⁻²⁷³ because of overactivation CDK5 by amyloid β (A β) protein.²⁷⁴ Selective CDK5 inhibitors are currently in demand²⁷⁵⁻²⁷⁶ and a variety of structurally diverse compounds including indole²⁷⁷, imidazole²⁷⁸, and purine²⁷⁹⁻²⁸¹ pharmacophore have been tested as CDK5 inhibitors. Flavopiridol and Roscovitin are currently under clinical trials as therapeutics in Alzheimer's disease.



Flavopiridol



Roscovitin

Flavopiridol is highly toxic, whereas the roscovitin exists as an enantiomeric mixture, thereby necessitating synthesis of chirally pure compounds for therapeutic applications. In order to circumvent the toxicity and tedious synthesis of these compound, and towards the goal of developing selective CDK5 kinase inhibitors, Reddy, Nair, and co-workers have synthesized a series of fluorinated purine-based triazoles (Figure 6.3), and developed an effective CDK5 kinase inhibitor that has implications in the treatment

of Alzheimer's disease and various cancers.²³⁻²⁵ In *in vitro* studies in mouse hippocampal cell cultures, using fluorescence electron microscopy, they have demonstrated that the monofluoroaryl-derived triazole is a neuroprotective compound comparable with that of the roscovitin or flavopiridol. The results were substantiated through docking studies.²⁵ The neuroprotecting effects of these compounds are correlated with the number of fluorines in the aryl rings. For example, the pentafluoroaryl- derived triazole **3.10** has nearly no neuroprotective effect. This unexpected result was rationalized as arising from the hydrophobic effects of the polyfluorinated aryl ring.

The synthetic methods for these triazole derivatives were optimized for high-yield and high-purity. Thus, facile aromatic nucleophilic substitution of 2,6-dichloropurine with benzyl amine under mild conditions gives the 2-chloro-6-(N-benzyl)purine **6.3** in 95% yield. Propargylation of the compound **6.3**, in dimethyl sulfoxide at 0 °C resulted in the formation of **6.5** in high yield. Cu(I) catalyzed 1,3-dipolar cycloaddition of compound **6.5** with benzyl bromide, and various fluorinated versions gave the corresponding triazoles in high yield (>80%) and purity. The isomeric homogeneity of these compounds could be readily established through ¹⁹F NMR, as evidenced by characteristic ¹⁹F NMR chemical shifts.

Toward the goal of developing more effective kinase inhibitors, and to study the structure-activity relationship, in this study, we have synthesized various derivatives of the earlier reported parent lead compound monofluoro-aryl-substituted triazole **6.8**,²⁵ replacing the N⁵-benzyl group of the compound **6.8** with various aryl and pyridyl derivatives (**6.22**, **6.28**), and the dimeric version of the compound **6.8** (**6.18**). The synthesis of these compounds was accomplished using essentially the same procedures as reported earlier,²⁵ with slight modifications, as shown in Figures 6.4-6.7. As in the case

of the parent triazole **6.8**, the synthesis of these compounds proceeded in high yields and purity, as shown by their ^1H , ^{13}C , and ^{19}F NMR.

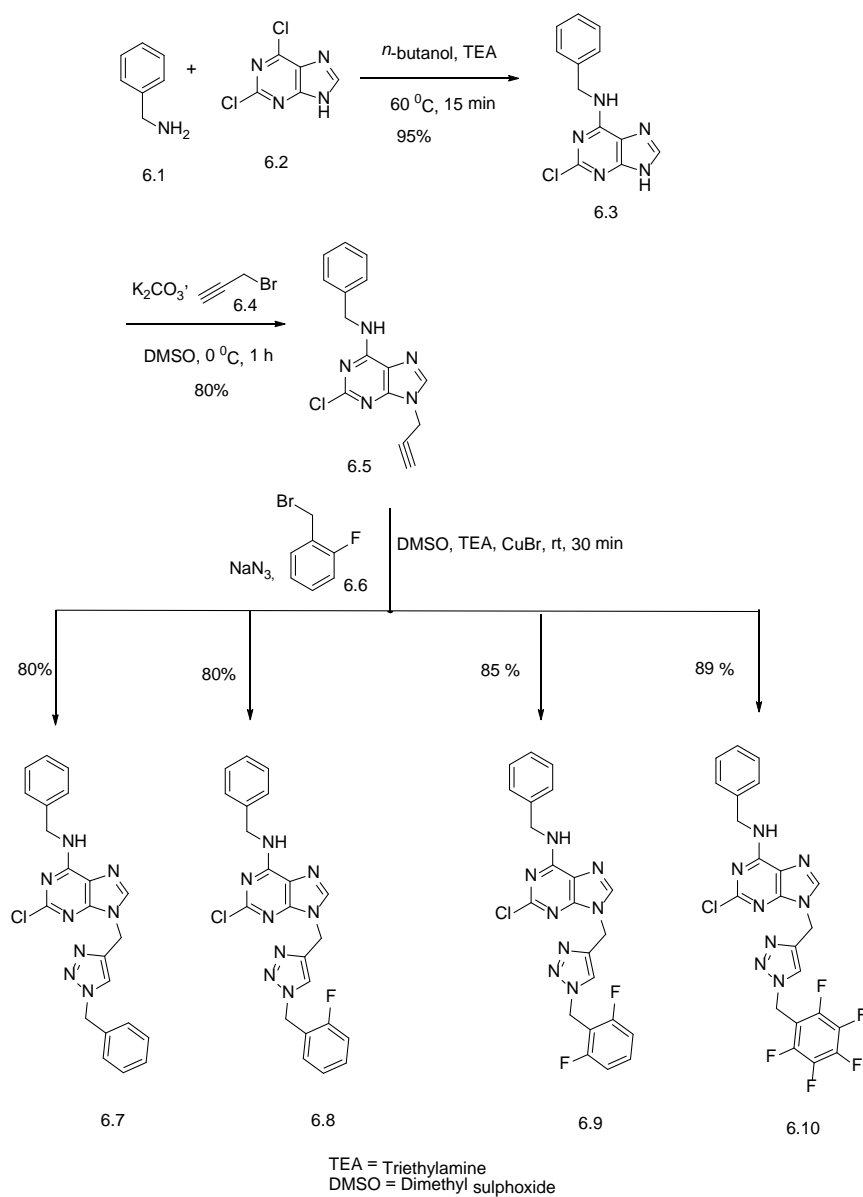


Figure 6.3. Synthesis of purine-based fluoroalkyl triazoles.²⁵

On this basis, we synthesized aniline and its dimer-derived purine-based fluoroalkyl triazoles Figure 6.4 and 6.5 by adopting the same route of synthesis with slight modifications.^{25, 282} Briefly, reaction of commercially available 2,6-dichloropurine **6.2** with corresponding amine **6.11** and/or **6.15** gave compound **6.12** and/or **6.16**. Propargylation of compound **6.12** and/or **6.16**, using propargyl bromide in DMSO in the presence of potassium carbonate at room temperature gave compound **6.13** and/or **6.17**. The Cu(I) catalysed azide-alkyne click reaction of alkynes **6.13** and/or **6.17** with the fluorinated benzyl azide prepared in situ from benzyl bromide gave triazoles **6.14** and/or **6.18**.

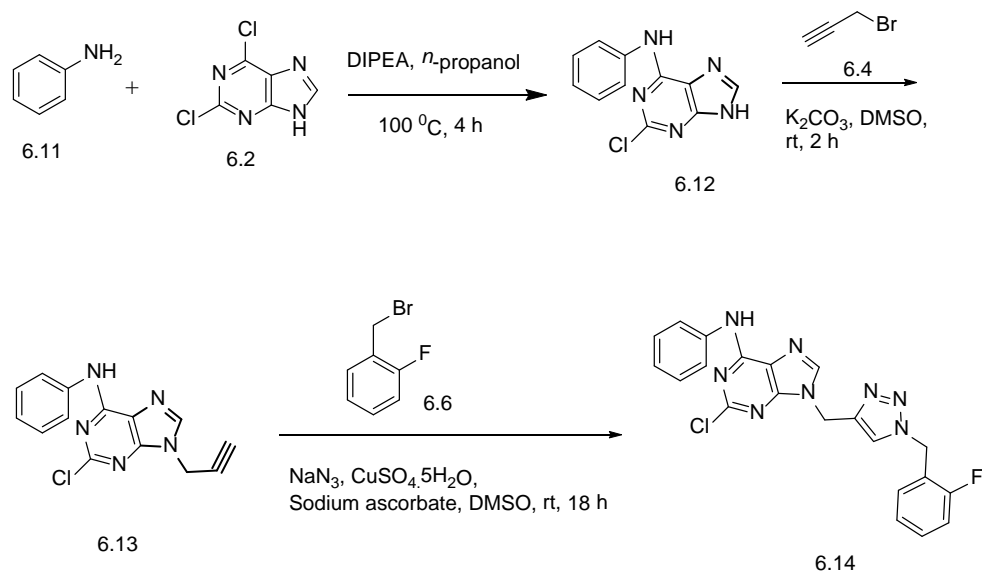


Figure 6.4. Synthesis of aniline derivative of purine-based fluoroalkyl triazoles.

Oumata et al²⁷⁹ have synthesized and shown the promising IC₅₀ values against CDK5 for several Roscovitin derivatives. They found the pyridyl ring derivatives and biaryl amines or biarylmethylamines ring derivatives are most effective CDK5 inhibitors. Wilson et al²⁸³ have also found that pyridyl ring derivatives are the most effective CDK5 inhibitors. On the basis of literature precedence, we also synthesized pyridyl ring and biaryl methylamine-derived purine-based fluoroalkyl triazoles Figure 6.6 and 6.7.

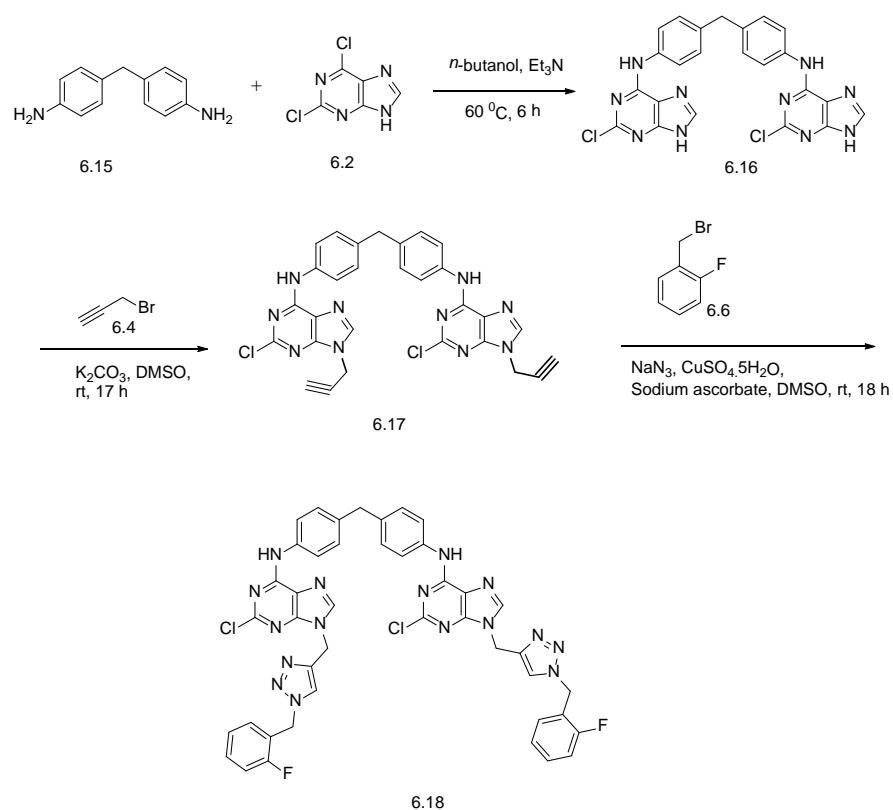


Figure 6.5. Synthesis of dimeric version of purine-based fluoroalkyl triazole.

Compound **6.22** was synthesized by typical synthetic procedure as described above for the synthesis of aniline derivatives. Biarylmethylamine derivative of purine-based fluoroalkyl triazole **6.28** was also prepared by typical synthetic procedure except for the starting material biarylmethylamine **6.25**, which was prepared by reported literature method with slight modifications.²⁸⁴ Briefly, Suzuki coupling of pyridine 3-boronic acid **6.23** with 4-bromobenzylamine **6.24** in the presence of a base at 100 °C under nitrogen atmosphere for 3 h gave compound **6.25**, which was purified by column chromatography for further use in the synthesis.

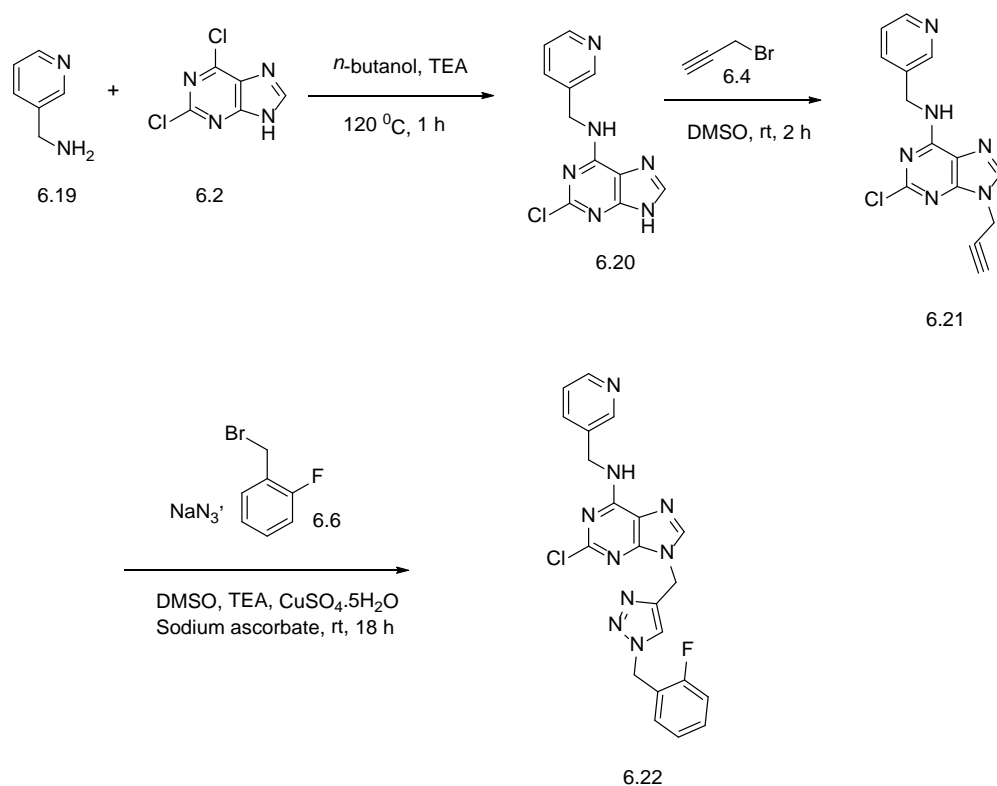


Figure 6.6. Synthesis of pyridyl ring derivative of purine-based fluoroalkyl triazole.

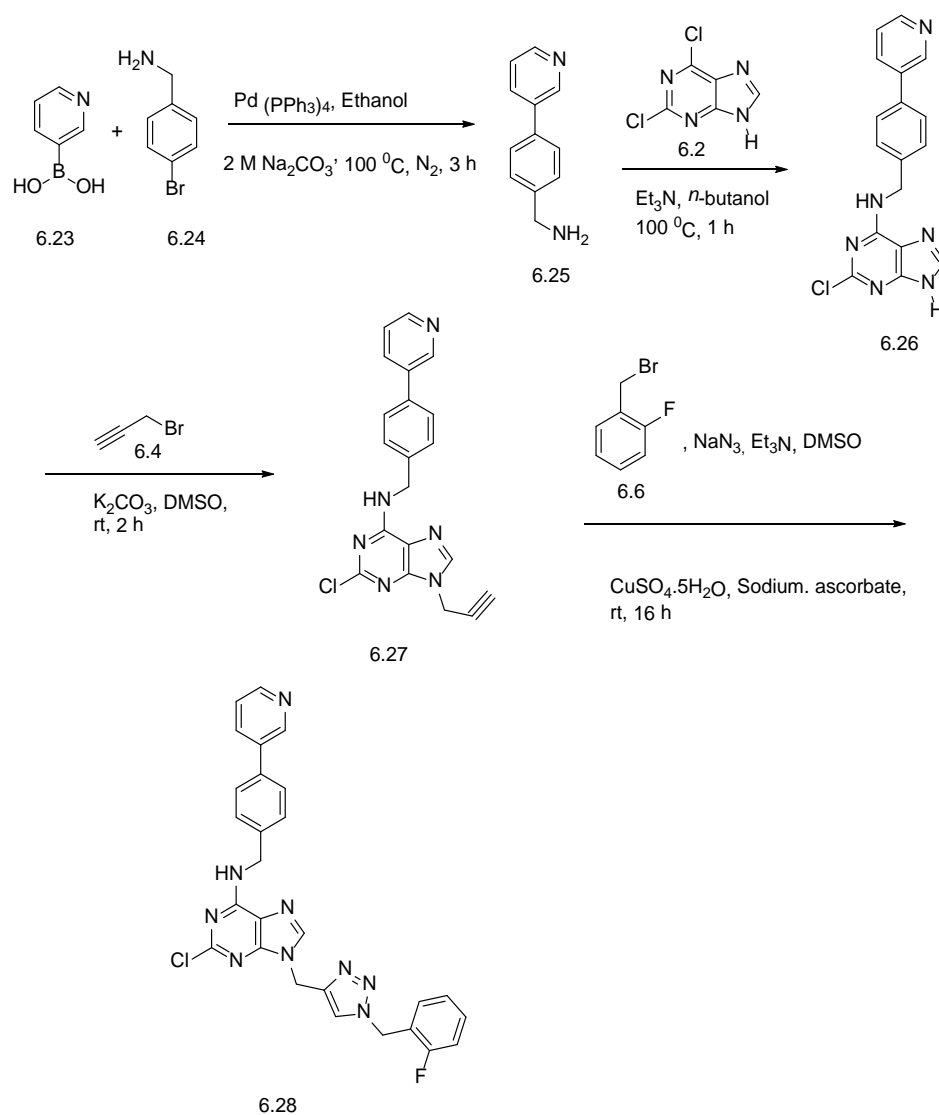


Figure 6.7. Synthesis of biarylmethylamine derivative of purine-based fluoroalkyl triazole.

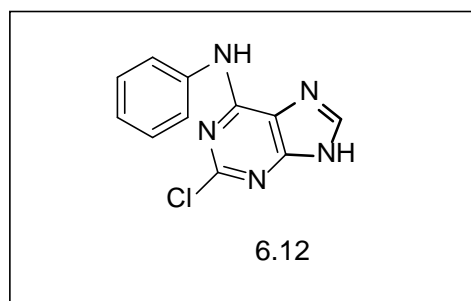
6.3. EXPERIMENTAL

6.3.1. Material and Methods. All reagents were purchased from commercial sources and used as received. Column chromatography was carried out using Merck 60, 230-400 mesh. Thin layer chromatography was carried out using silica gel coated

polyester backed sheets. The ^1H , ^{13}C NMR and ^{19}F NMR spectrum for CDCl_3 and DMSO-d_6 solutions were obtained on an INOVA-Varian 400 MHz spectrometer at 400, 100, and 376 MHz respectively. The ^1H NMR, ^{13}C NMR chemical shifts are referenced to the residual solvents signals or the internal TMS ($\delta = 0.0$). The ^{19}F chemical shifts are referenced to the internal CFCl_3 ($\delta^{19}\text{F} = 0.0$).

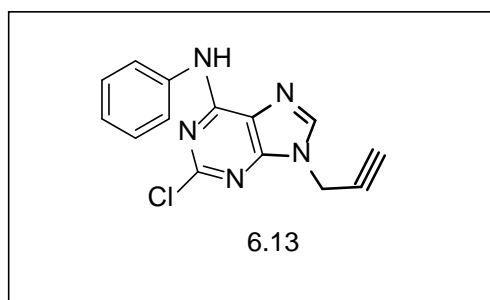
6.3.2. Synthesis and Properties of Products. Synthetic methods and characterization of prepared compounds are discussed below.

2-chloro-N-phenyl-9H-purin-6-amine (6.12).²⁸²



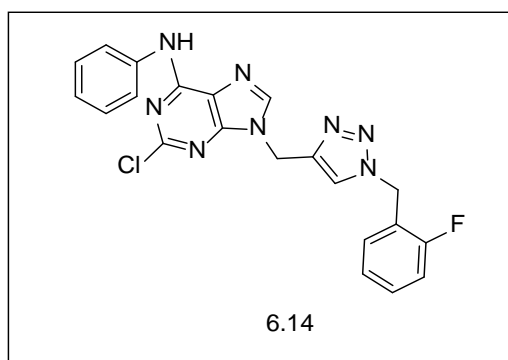
Compound **6.12** was prepared according to literature procedure. Briefly, to a suspension of 2,6 dichloropurine **6.2** (2.42 g, 12.80 mmol) in n-propanol (40 mL), aniline (2.0 g, 21.50 mmol), and DIPEA (2.76 g, 21.36 mmol) were added at rt. The reaction mixture was stirred at 100 $^{\circ}\text{C}$ for 4 h. After completion of reaction confirmed by ^1H NMR, the resulting yellow precipitate was filtered and washed with n-propanol (20 mL) and water (50 mL) to obtain compound **6.12** (2.0 g, 78%) as a yellow colored solid. mp: 289-293 $^{\circ}\text{C}$ (not completely melted, decomposed at 350 $^{\circ}\text{C}$). The compound was sufficiently pure by crude ^1H NMR and used in the next step without further purification.

2-chloro-N-phenyl-9-(prop-2-yn-1-yl)-9H-purin-6-amine (6.13).



To a solution of compound **6.12** (2.0 g, 8.19 mmol) in DMSO (20 mL), potassium carbonate (1.07 g, 12.25 mmol), and propargyl bromide **6.4** (1.07 g, 8.99 mmol) were added at rt. The reaction mixture was stirred at for 2 h at rt. After completion of reaction confirmed by ^1H NMR, water (80 mL) was added to the reaction mixture and resulting precipitate was filters and air dried overnight to obtain impure compound **6.13** (2.0 g, 87%). Finally compound **6.13** (2.0 g) was purified in acetone: hexane (1:4) to obtain compound **6.13** (1.2 g) as a cream colored solid. mp: 194-196 $^{\circ}\text{C}$. The compound was sufficiently pure by crude ^1H NMR and used in the next step without further purification.

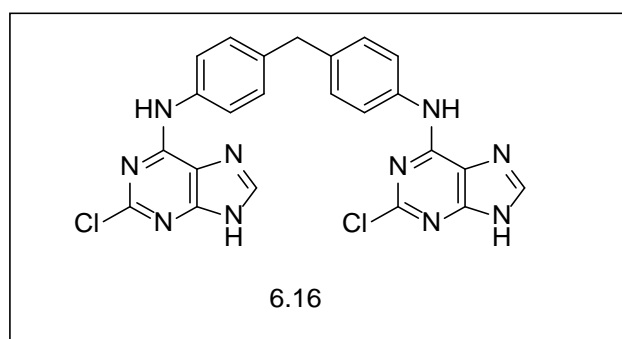
2-chloro-9-((1-(2-fluorobenzyl)-1H-1,2,3-triazol-4-yl)methyl)-N-phenyl-9H-purin-6-amine (6.14).



To a solution of sodium azide (0.225 g, 3.46 mmol) in DMSO (15 mL), 2-fluorobenzyl bromide **6.6** (0.621 g, 3.28mmol) was added at rt and reaction mixture was stirred for 30 min at rt. After 30 min, compound **6.13** (0.9 g, 3.17 mmol), triethylamine

(0.097 g, 30 mol%), CuSO₄·5H₂O (0.238 g, 30 mol%), and sodium ascorbate (0.378 g, 60 mol%) were added at room temperature and the reaction was stirred for 18 h at rt. After completion of reaction confirmed by ¹H NMR, the reaction mixture was poured in to 70 mL ice cold water and the resulting precipitate was filtered and washed with dilute ammonium hydroxide solution (5 x 50 mL) and water (250 mL) to obtain compound **6.14** (1.13g, 82%) as an off-white solid. mp: 98-105 °C. ¹H NMR (400 MHz, DMSO-d₆) δ 10.29 (br s, 1H, -NH-Ar), 8.37 (br s, 1H, -CH-purine), 8.18 (s, 1H, -CH-triazole), 7.81 (d, J = 7.88 Hz, 2H), 7.07-7.41 (m, 7H), 5.63 (s, 2H), 5.47 (s, 2H); ¹³C NMR (100 MHz, DMSO-d₆) δ 161.4, 158.9, 152.6, 152.5, 142.4, 1.8.8, 130.9, 130.9 130.8, 130.8, 128.6, 125, 124.9, 123.7, 122.8, 122.7, 121.4, 115.8, 115.6, 47.1, 47.1, 38.9, 38.4; ¹⁹F NMR (376 MHz, DMSO-d₆) δ -117.8 (dd, ¹J_{H-F} = 15 Hz, ²J_{H-F} = 7.5 Hz, 1F)

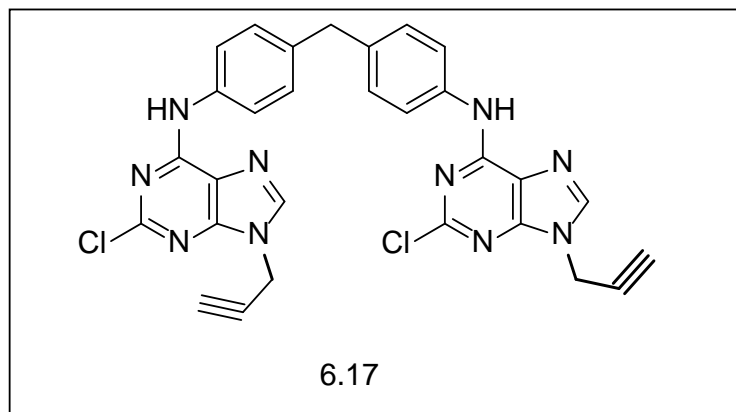
N,N'-(methylenebis(4,1-phenylene))bis(2-chloro-9H-purin-6-amine) (6.16).



To a suspension of 2,6 dichloropurine **6.2** (4.0 g, 21.16 mmol) in n-butanol (20 mL), 4,4'-methylenediamine **6.15** (2.1 g, 10.60 mmol), triethylamine (0.8 g, 7.92 mmol) were added at rt and the reaction mixture was stirred at 60 °C for 6 h. After completion of reaction confirmed by ¹H NMR, the reaction mixture was cooled to rt and the resulting precipitate was filtered and washed with methanol (10 mL) and water (20 mL) to obtain compound **6.16** as a yellow colored solid (6.47 g, 63%) mp: - (decomposition temp. 340-

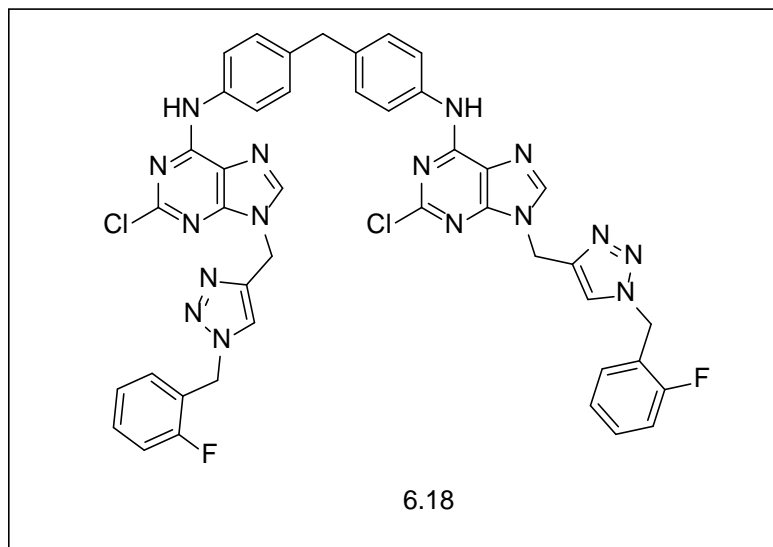
350 °C). The compound was sufficiently pure by crude ^1H NMR and used in the next step without further purification.

N,N'-(methylenebis(4,1-phenylene))bis(2-chloro-9-(prop-2-yn-1-yl)-9H-purin-6-amine) (6.17).



To a solution of compound **6.16** (2.0 g, 3.99 mmol) in DMSO (20 mL), potassium carbonate (1.21 g, 8.78 mmol), propargylbromide 3.4 (1.04 g, 8.78 mmol) were added at rt and the reaction was stirred at rt for 17 h. After completion of reaction confirmed by ^1H NMR, 100 mL water was added to the reaction mixture and the resulting precipitate was filtered, washed with water and finally purified with acetone: hexane (5:1) to obtain pure compound **6.17** (1.13 g, 50%) as a yellow colored solid. mp: - (decomposition temp. 200 °C); The compound was sufficiently pure by crude ^1H NMR and used in the next step without further purification.

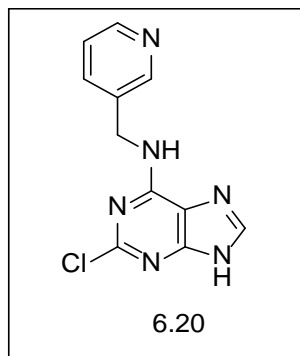
N,N'-(methylenebis(4,1-phenylene))bis(2-chloro-9-((1-(2-fluorobenzyl)-1H-1,2,3-triazol-4-yl)methyl)-9H-purin-6-amine) (6.18).



To a solution of sodium azide (0.625 g, 9.6 mmol) in DMSO (45 mL), 2-fluorobenzyl bromide **6.6** (1.64 g, 13.78 mmol) was added at rt and reaction mixture was stirred for 30 min at rt. After 30 min, compound **6.17** (2.5 g, 4.31 mmol), triethylamine (0.090 g, 30 mol%), CuSO₄·5H₂O (0.325 g, 30 mol%), and sodium ascorbate (0.514 g, 60 mol%) were added at room temperature and the reaction was stirred for 2 days at rt. After completion of reaction confirmed by ¹H NMR, the reaction mixture was poured in to 200 mL ice cold water and the resulting precipitate was filtered and washed with dilute ammonium hydroxide solution (5 x 100mL), water (500 mL) to obtain compound **6.18** (2.5 g, 66%) as an off-white solid. mp: - (decomposition temp. 200 °C). ¹H NMR (400 MHz, DMSO-d₆) δ 10.25 (br s, 2H, -NH-Ar), 8.36 (br s, 2H, -CH-purine), 8.17 (s, 2H, -CH-triazole), 7.10 -7.71 (m, 16 H), 5.63 (s, 4 H), 5.46 (s, 4H), 3.89 (s, 2H); ¹³C NMR (100 MHz, DMSO-d₆) δ 161.3, 158.9, 152.6, 152.4, 142.4, 136.8, 136.6, 130.9, 130.8, 130.7, 128.9, 128.7, 124.9, 124.8, 124.0, 122.8, 122.6, 122.0, 121.6, 115.7, 115.5, 47.1,

47.0, 38.9, 38.4; ^{19}F NMR (376 MHz, DMSO- d_6) δ -117.7 (dd, $^1J_{\text{H-F}}=15$ Hz, $^2J_{\text{H-F}}=7.5$ Hz, 2F)

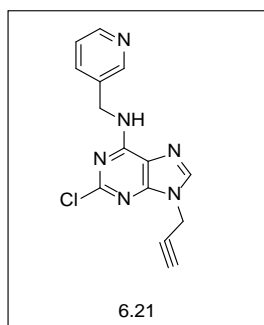
2-chloro-N-(pyridin-3-ylmethyl)-9H-purin-6-amine (6.20).



To a solution of 2,6-dichloropurine **6.2** (2 g, 10.58 mmol) in n-butanol (20 mL), triethylamine (2.67 g, 26.45 mmol) was added and the mixture was heated to 50 $^{\circ}\text{C}$. Then 3-aminomethylpyridine **6.19** (1.03 g, 9.52 mmol) was added at 50 $^{\circ}\text{C}$ and finally the reaction was heated and stirred at 120 $^{\circ}\text{C}$ for 1 h. After completion of reaction confirmed by ^1H NMR, the reaction mixture was cooled to rt and then to 0 $^{\circ}\text{C}$ using an ice-water bath. The peach colored precipitate was filtered and washed with water (20 mL) and dried under air overnight to obtain pure compound **6.20** (1.3 g, 47%). ^1H NMR (400 MHz, DMSO- d_6) δ 13.09 (br s, 1H), 8.76 (br s, 1H), 8.58 (s, 1H), 8.44-8.45 (d, 1H), 8.14 (s, 1H), 7.74-7.76 (d, $J=8$ Hz, 1H), 7.32-7.35 (t, $J=4$ Hz, 1H), 4.65 (d, 2H).

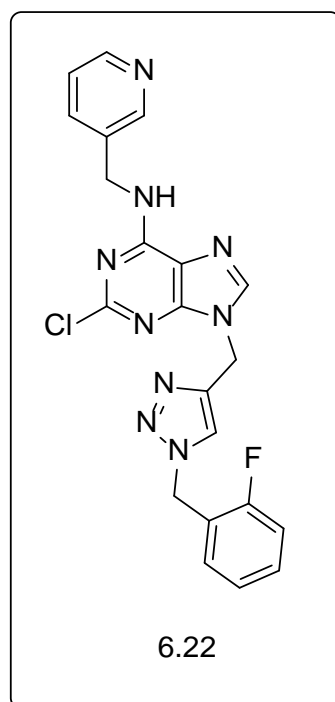
2-chloro-9-(prop-2-yn-1-yl)-N-(pyridin-3-ylmethyl)-9H-purin-6-amine (6.21).

To a solution of compound **6.20** (1.2 g, 4.6 mmol) in DMSO (10 mL), potassium carbonate (0.953 g, 6.9 mmol), propargyl bromide **6.4** (0.603 g, 5.04 mmol) were added at rt and the reaction mixture was stirred at rt for 2 h. After completion of reaction confirmed by ^1H NMR, water was added to the reaction mixture. The resulting precipitate was collected by filtration and washed with excess water to obtain compound **6.21** as a brown solid



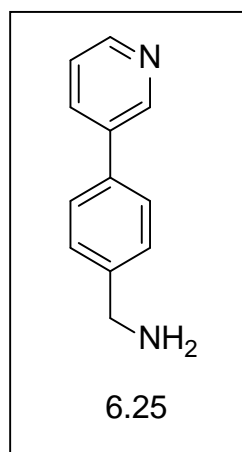
(0.960 g, 70%) Compound was further passed through silica gel column (eluent: 90%DCM: 10%MeOH) to improve the color and finally peach colored solid was obtained (0.550 g, 40%) mp. 158-161 °C; ¹H NMR (400 MHz, DMSO-d₆) δ 8.93 (br s, 1H), 8.57 (s, 1H), 8.44 (br s, 1H), 8.24 (s, 1H), 7.73-7.75 (d, J = 8 Hz, 1H), 7.33 (t, 1H), 5.01 (s, 2 H), 4.65 (d, 2H), 3.5 (s, 1H); ¹³C NMR (100 MHz, DMSO-d₆) δ 154.8, 149.04, 148.2, 140.9, 135.2, 134.6, 123.5, 77.8, 76.3, 41.0, 32.6.

2-chloro-9-((1-(2-fluorobenzyl)-1H-1,2,3-triazol-4-yl)methyl)-N-(pyridin-3-ylmethyl)-9H-purin-6-amine (6.22).



To a solution of sodium azide (0.120 g, 1.85 mmol) in DMSO (10 mL), 2-fluorobenzylbromide **6.6** (0.315 g, 1.66 mmol) was added and stirred at rt for 30 min. After 30 min., compound **6.21** (0.5 g, 1.67 mmol), triethylamine (0.05 g, 30 mol%), CuSO₄·5H₂O (0.120 g, 30 mol%), sodium ascorbate (0.2 g, 60 mol%) were added and the reaction was stirred for 18 h at rt. After completion of reaction confirmed by ¹H NMR, the reaction mixture was poured in to ice cold water (50 mL) and the resulting precipitate was filtered, washed with dilute NH₄OH (30 mL x5), finally washed with water and air dried overnight to obtain pure peach colored compound **6.22** (0.530 g, 70%) mp. 172-175 °C; ¹H NMR (400 MHz, DMSO-d₆) δ 8.9 (br s, 1H), 8.64-8.70 (br s, 2H), 8.44 9s, 1H), 8.15 (s, 1H), 7.75 (s, 1H), 7.21-7.39 (m, 5H), 5.63 (s, 2H), 5.41 (s, 2H), 4.65 (s, 2H); ¹³C NMR (100 MHz, DMSO-d₆) δ 161.3, 158.8, 154.8, 153.1, 148.1, 142.4, 141.5, 135.1, 130.8, 130.7, 130.6, 124.9, 124.8, 123.9, 122.7, 122.6, 115.7, 115.5, 47, 46.9, 41.1; ¹⁹F NMR (376 MHz, DMSO-d₆) δ -117.8 (s, 1F).

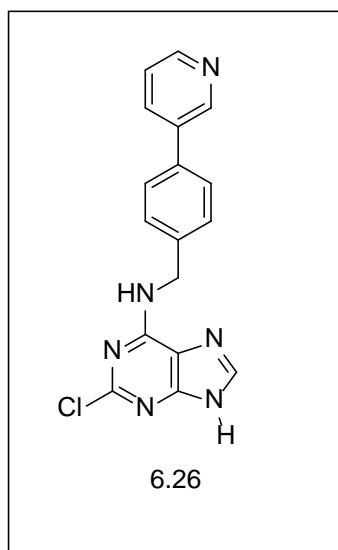
(4-(pyridin-3-yl)phenyl)methanamine (6.25).²⁸⁴



To a solution of 4-bromobenzylamine **6.24** (5 g, 26.88 mmol) in ethanol (50 mL), 3-pyridinylboronic acid **6.23** (4 g, 32.5 mmol), Pd (PPh₃)₄ (0.650 g, 0.56 mmol), 2 M sodium carbonate (27 mL) were added at room temperature under nitrogen atmosphere.

After addition, reaction mixture was heated to reflux for 3 h. After completion of reaction confirmed by TLC, reaction mixture was filtered through celite and was washed with dichloromethane. Filtrate was evaporated under reduced pressure and the residue was chromatographed on silica gel. (eluent: DCM:MeOH (90:10) to obtain compound **6.25** (2.6 g, 53 %) as a yellow colored solid. mp: 41-43 °C; ¹H NMR (400 MHz, CDCl₃) δ 8.80 (m, 1H), 8.55 (m, 1H), 7.84 (m, 1H), 7.53 (d, J=8.1 Hz, 2 H), 7.40 (d, J=8 Hz, 2H), 7.33 (m, 1H), 3.90 (s, 2 H), 1.65 (s, 2H); ¹³C NMR (100 MHz, CDCl₃) δ 148.5, 148.4, 143.3, 136.5, 134.3, 128, 127.4, 123.6, 46.2.

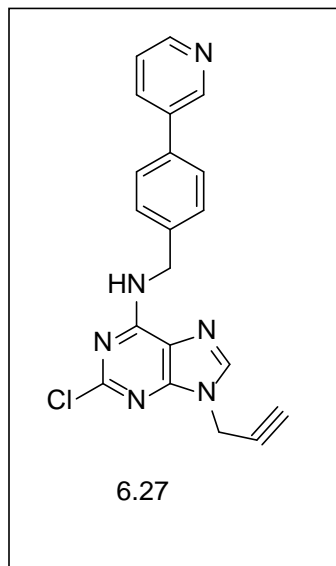
2-chloro-N-(4-(pyridin-3-yl)benzyl)-9H-purin-6-amine (6.26).



To a solution of 2, 6 dichloropurine **6.2** (1.54 g, 8.15 mmol) in n-butanol (15 mL), compound **6.25** (1.5 g, 8.15 mmol), triethylamine (1.32 g, 13.09 mmol) were added at rt and the reaction mixture was heated to 100 °C for 1 h. The resulting precipitate was filtered and washed with cold methanol and water. The solid was dried overnight under air to obtain compound **6.26** (2.16 g, 79%) as a peach colored solid. mp: 250-258 °C (decomposes); ¹H NMR (400 MHz, DMSO) δ 12.53 (br s, 1H), 8.86 9s, 1H), 8.71 (br s, 1 H), 8.55 (d, J=8 Hz, 1 H), 8.15 (s, 1 H), 8.04 (d, J=8 Hz), 7.69 (m, 2 H), 7.44 (m, 3 H),

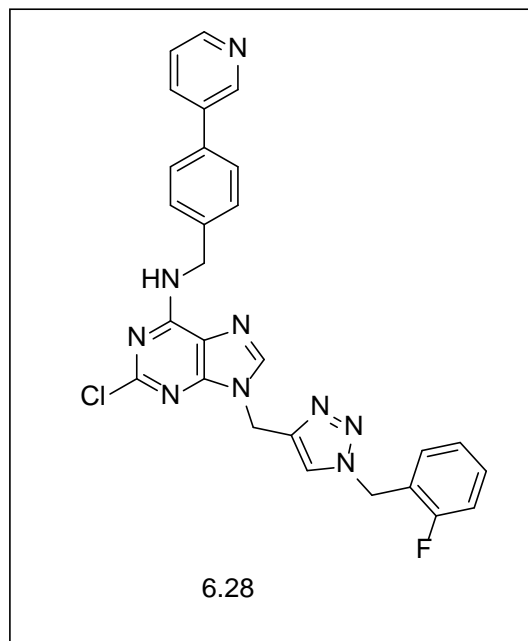
4.7 (s, 2 H); ^{13}C NMR (100 MHz, DMSO) δ 152.9, 148.4, 147.6, 140.1, 139.4, 135.7, 135.3, 133.9, 128.1, 126.8, 123.8, 42.

2-chloro-9-(prop-2-yn-1-yl)-N-(4-(pyridin-3-yl)benzyl)-9H-purin-6-amine
(6.27).



To a solution of compound **6.26** (1.5 g, 4.45 mmol) DMSO (15 mL), potassium carbonate (0.921 g, 6.67 mmol), and propargyl bromide **6.4** (0.580 g, 4.87 mmol) were added at rt. The reaction mixture was stirred at rt for 2h. After completion of reaction confirmed by TLC, 75 mL water was added to the reaction mixture and resulting precipitate was filtered, air dried overnight and finally triturated with ether to obtain compound **6.27** (1.5 g, 89%) as a light brown solid. mp: 169-172 $^{\circ}\text{C}$; ^1H NMR (400 MHz, DMSO) δ 8.97 (bs, 1H), 8.86 (s, 1H), 8.55 (d, J=8 Hz, 1 H), 8.25 (s, 1H), 8.04 (d, J=8 Hz), 7.69 (m, 2 H), 7.45 (m, 3 H), 5.02 (s, 2H), 4.71 (d, J=8 Hz, 2H), 3.51 (s, 1H); ^{13}C NMR (100 MHz, DMSO) δ 154.9, 153.3, 149.5, 148.4, 147.6, 140.9, 139.3, 135.7, 135.3, 134, 128.1, 126.9, 123.8, 118.1, 77.9, 76.3, 42.9, 32.6.

2-chloro-9-((1-(2-fluorobenzyl)-1H-1,2,3-triazol-4-yl)methyl)-N-(4-(pyridin-3-yl)benzyl)-9H-purin-6-amine (6.28).



To a solution of sodium azide (0.191 g, 2.93 mmol) in DMSO (15 mL), 2-fluorobenzyl bromide **6.6** (0.505 g, 2.67 mmol) was added at rt and reaction mixture was stirred for 30 min at rt. After 30 min, compound **3.27** (1.0 g, 2.67 mmol), triethylamine (0.081 g, 30 mol %), CuSO₄·5H₂O (0.2 g, 30 mol %), and sodium ascorbate (0.317 g, 60 mol %) were added at room temperature and the reaction was stirred for 18 h at rt. After completion of reaction confirmed by ¹H NMR, the reaction mixture was poured in to 75 mL ice cold water and the resulting precipitate was filtered, washed with dilute ammonium hydroxide (100 mL), water (150 mL) and air dried overnight. Finally the compound was triturated with ether to obtain compound **6.28** (1.0 g, 71%) as a light brown solid. mp: 192-195 °C; ¹H NMR (400 MHz, DMSO) δ 8.92 (bs, 1H), 8.24 (s, 1H), 8.16 (s, 1H), 8.04 (d, J= 4 Hz, 1H), 7.67 (m, 2H), 7.39-7.47 (m, 4H), 7.19-7.31 (m, 3 H), 5.63 (s, 2H), 5.42 (s, 2H), 4.69 (s, 2H); ¹³C NMR (100 MHz, DMSO) δ 161.3, 158.8,

154.9, 142.4, 139.3, S13.9, 130.8, 130.7, 128.1, 126.8, 124.8, 124.8, 123.9, 122.8, 122.6, 115.7, 155.5, 46.9, 46.9, 42.8, 38.2; ^{19}F NMR (376 MHz, DMSO) δ -117.8 (s, 1F)

6.3.3. NMR Spectra of the Products. The ^1H NMR, ^{13}C NMR, and ^{19}F NMR spectra of the products are shown in Figures 6.8- 6.28.

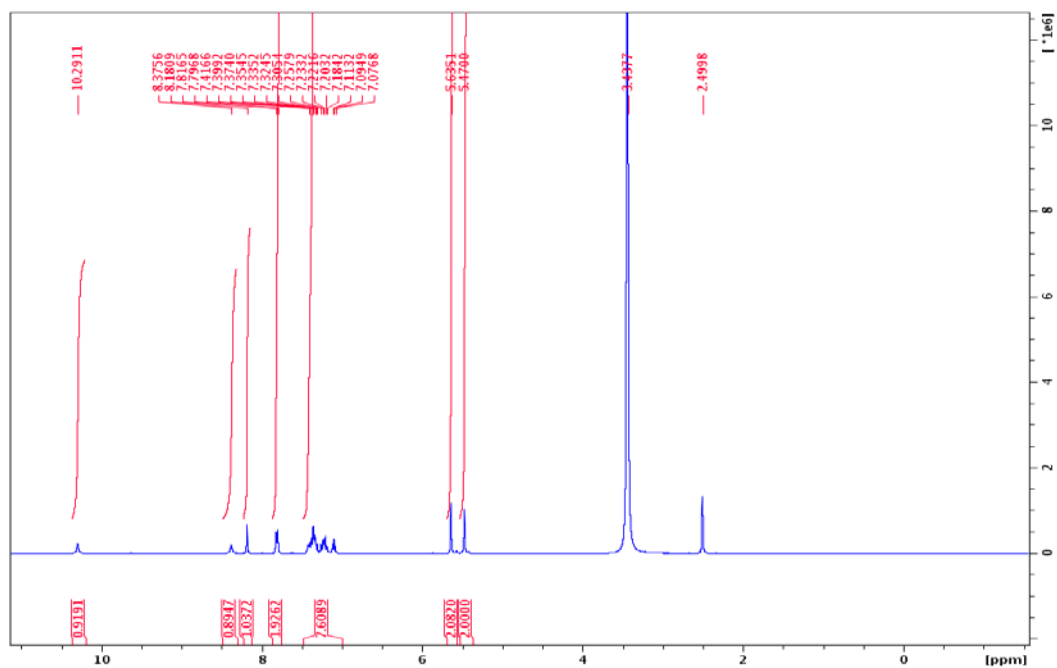
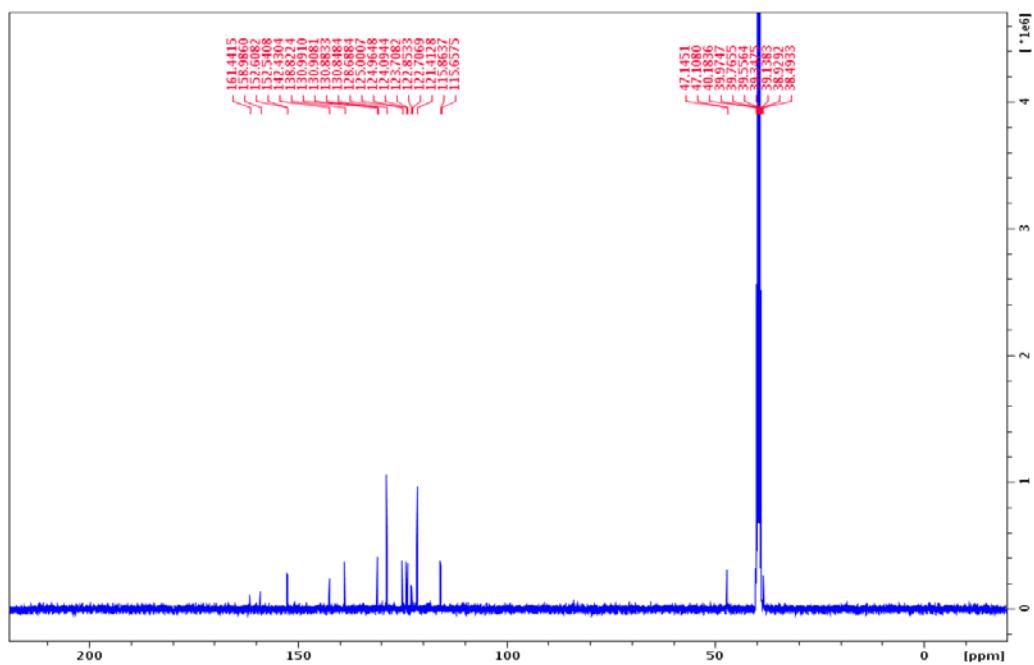
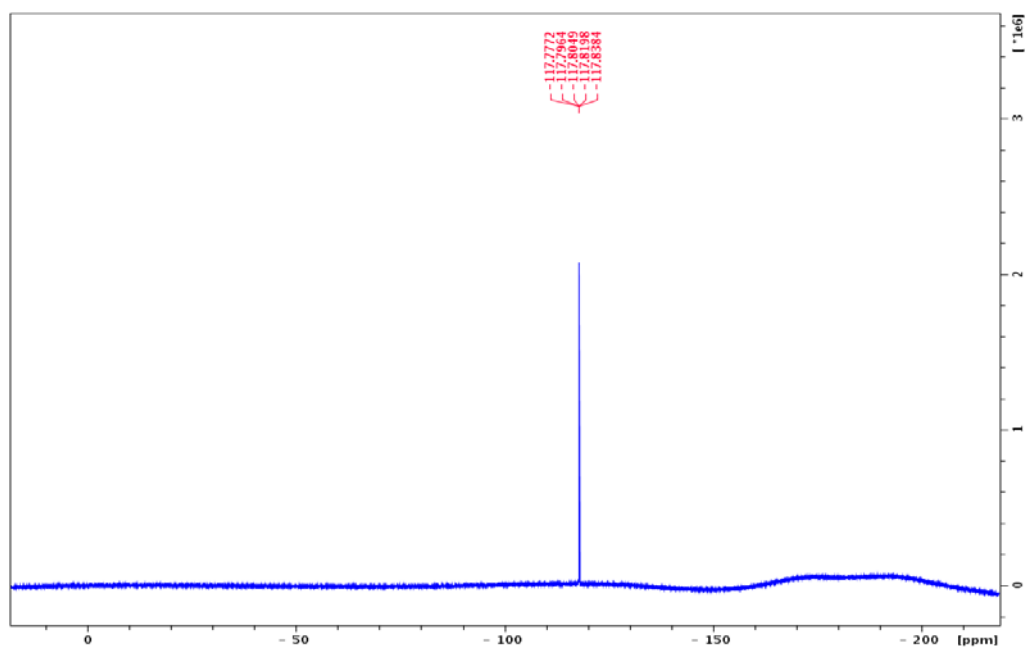


Figure 6.8. ^1H NMR spectrum of compound 6.14.

Figure 6.9. ^{13}C NMR spectrum of compound 6.14.Figure 6.10. ^{19}F NMR spectrum of compound 6.14.

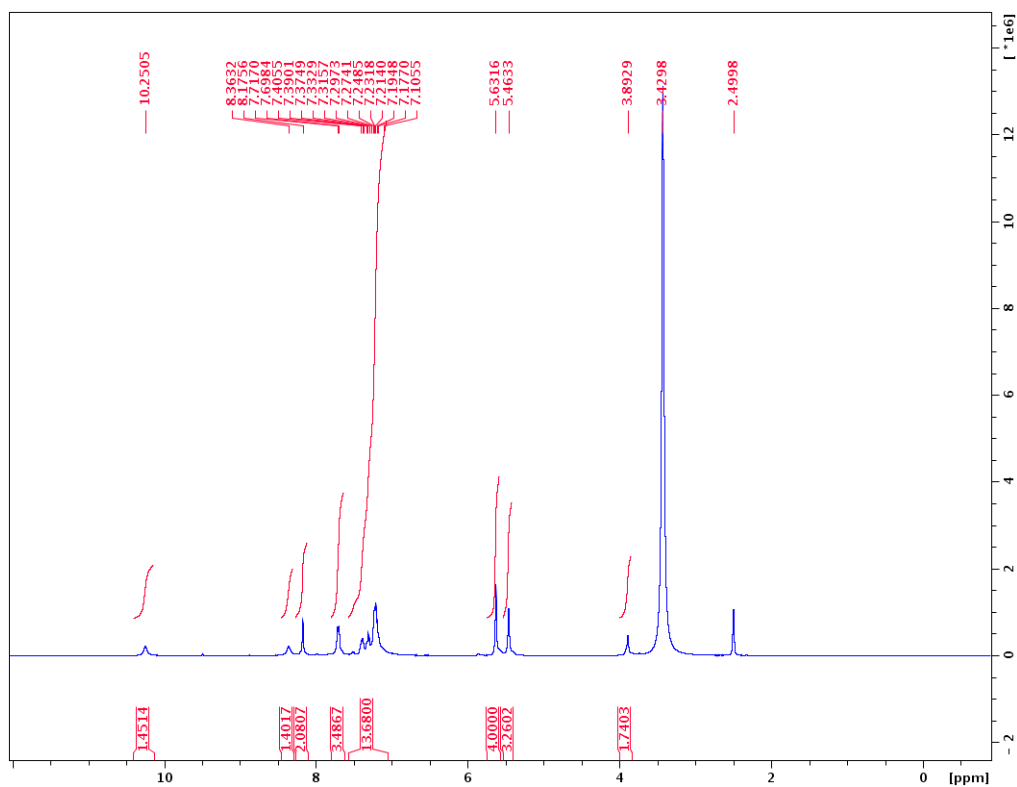


Figure 6.11. ^1H NMR spectrum of compound 6.18.

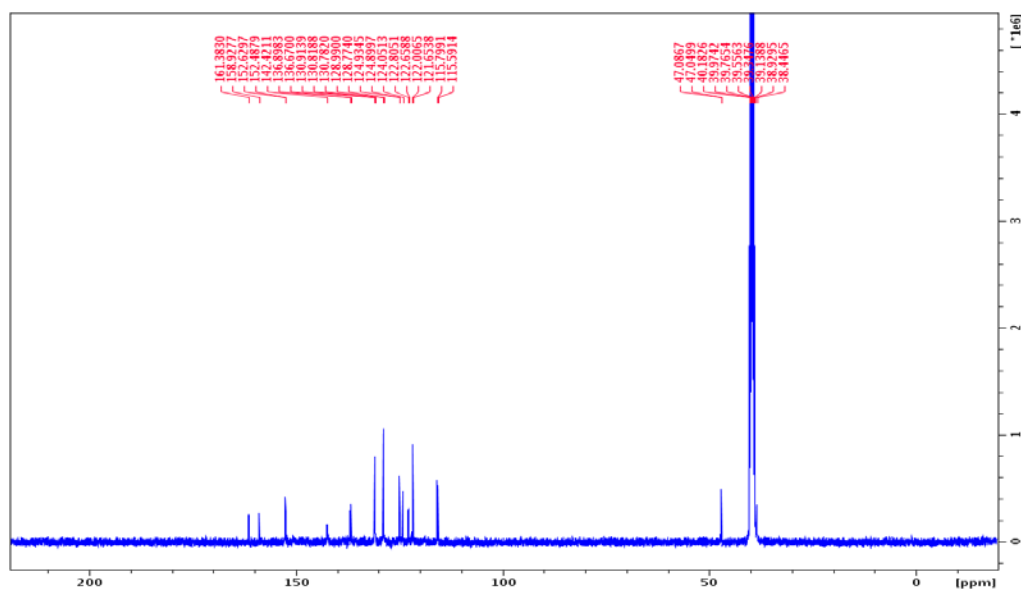


Figure 6.12. ^{13}C NMR spectrum of compound 6.18.

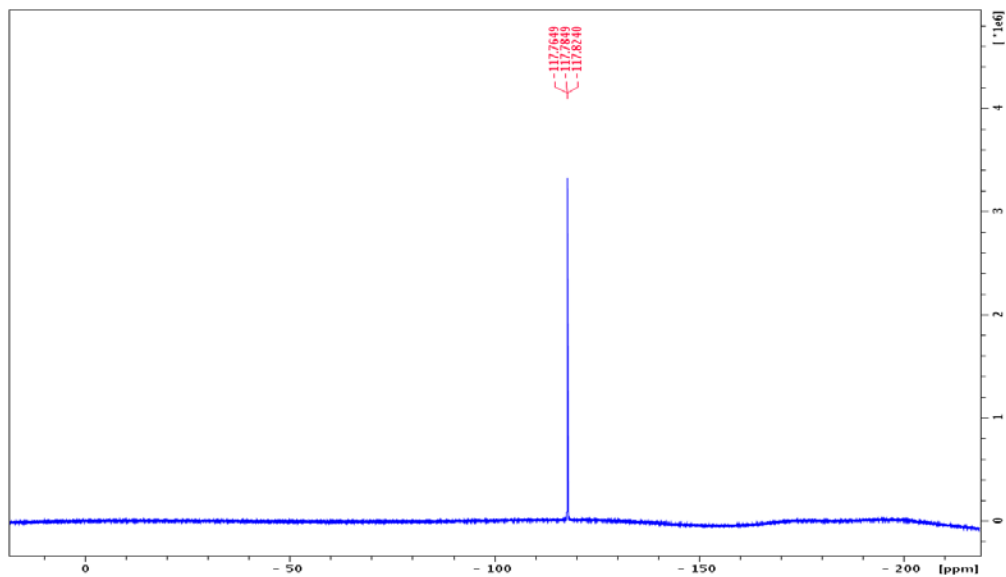


Figure 6.13. ^{19}F NMR spectrum of compound 6.18.

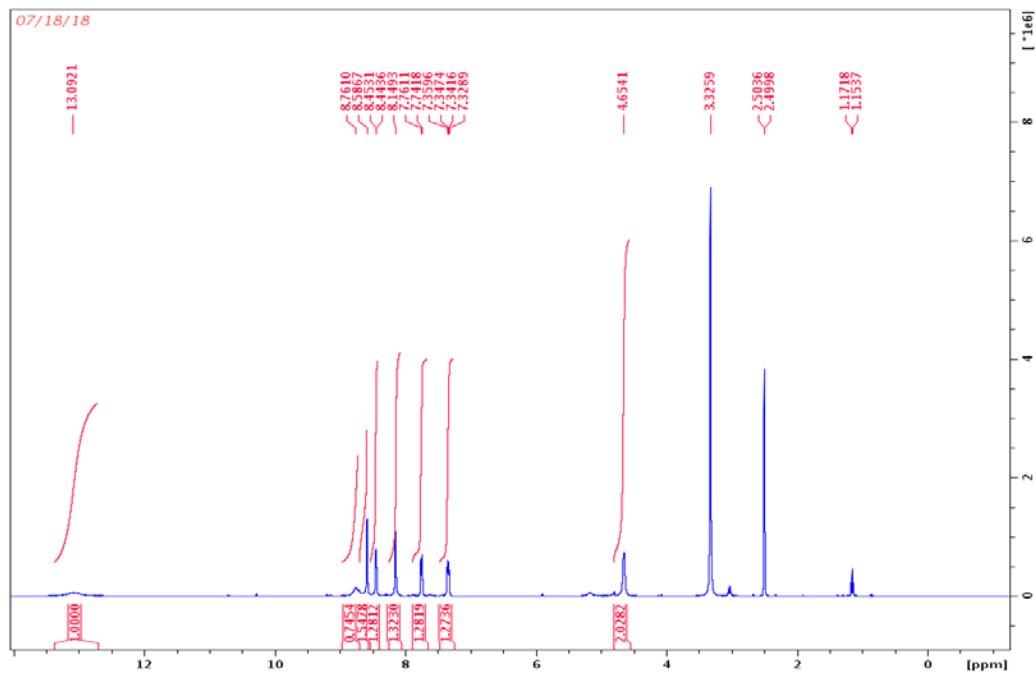


Figure 6.14. ^1H NMR spectrum of compound 6.20.

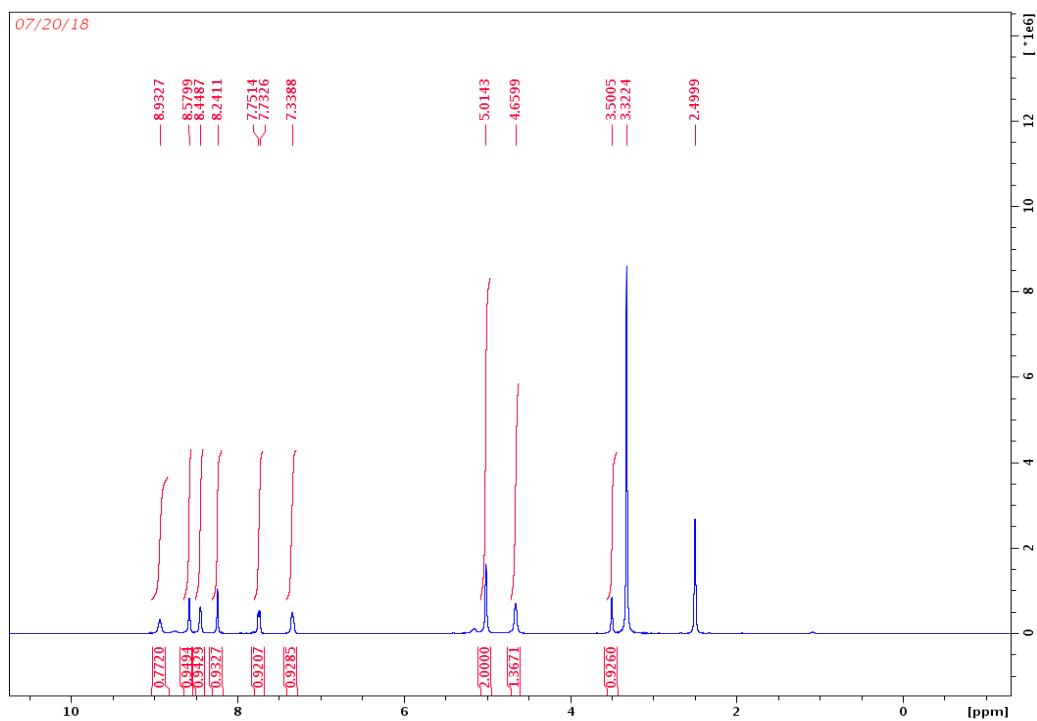


Figure 6.15. ^1H NMR spectrum of compound 6.21.

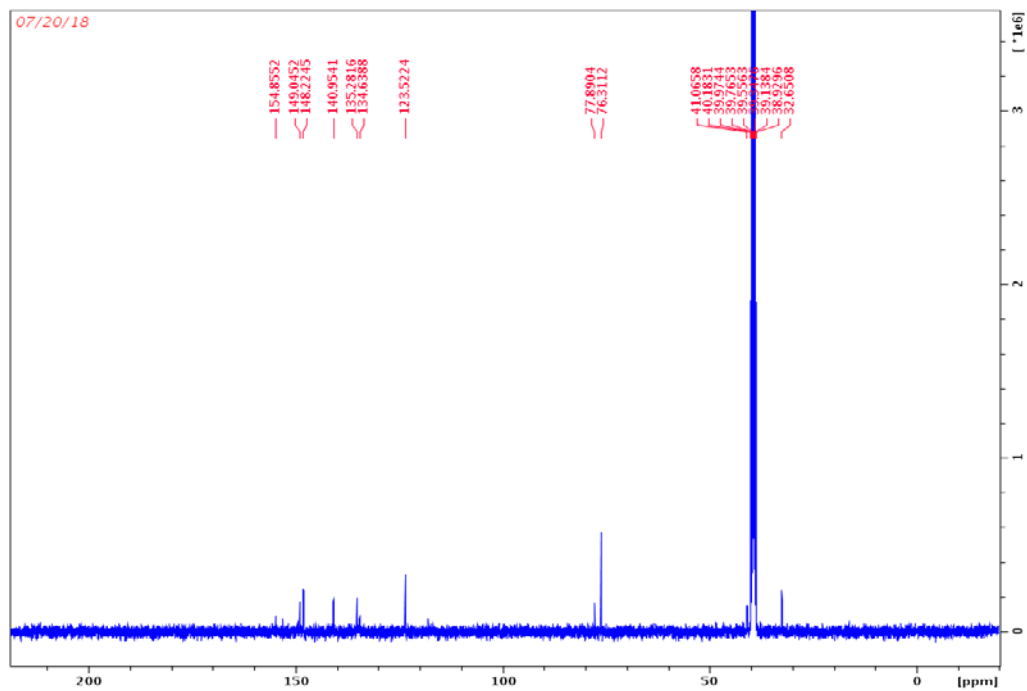


Figure 6.16. ^{13}C NMR spectrum of compound 6.21.

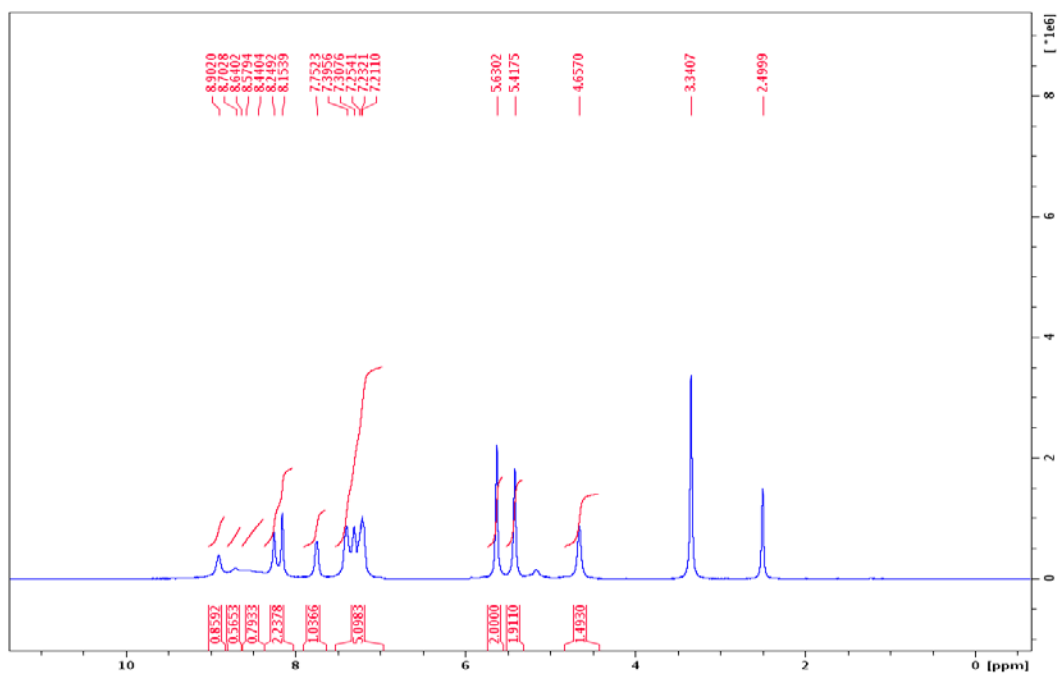


Figure 6.17. ^1H NMR spectrum of compound 6.22.

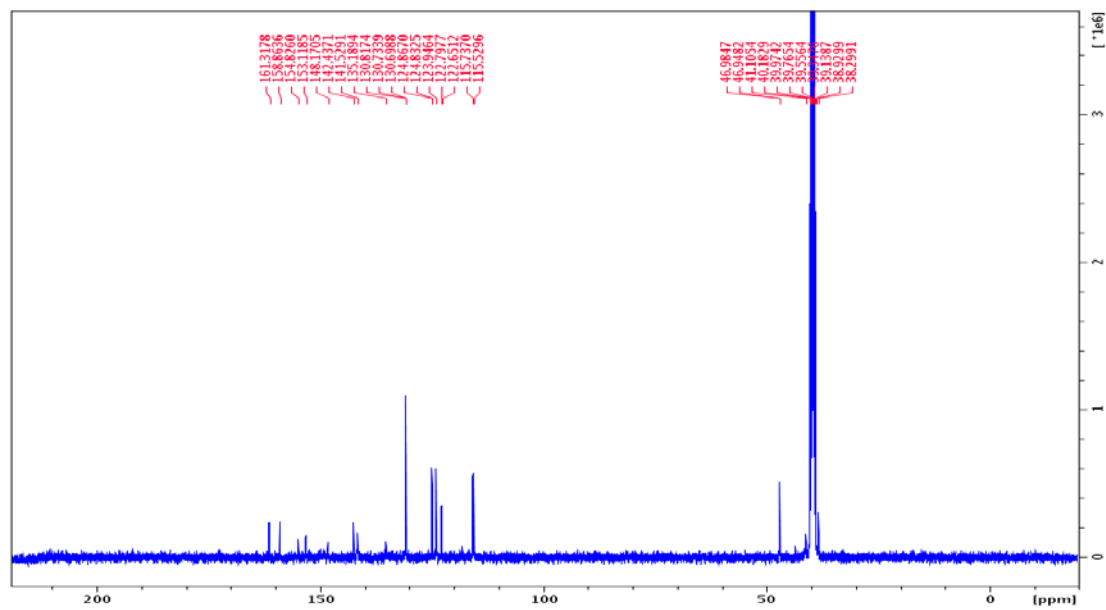
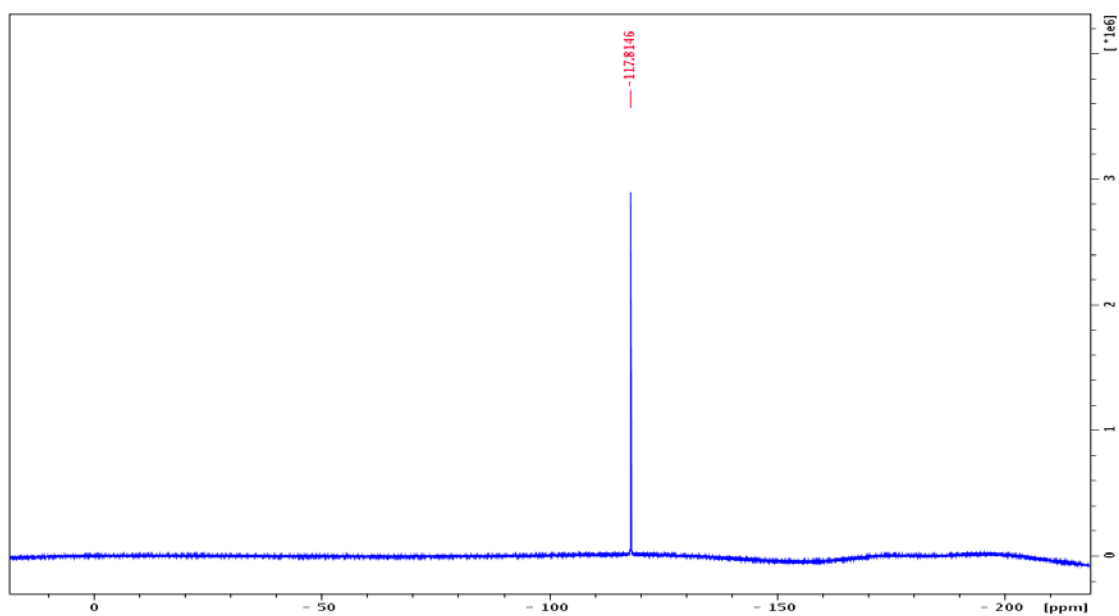
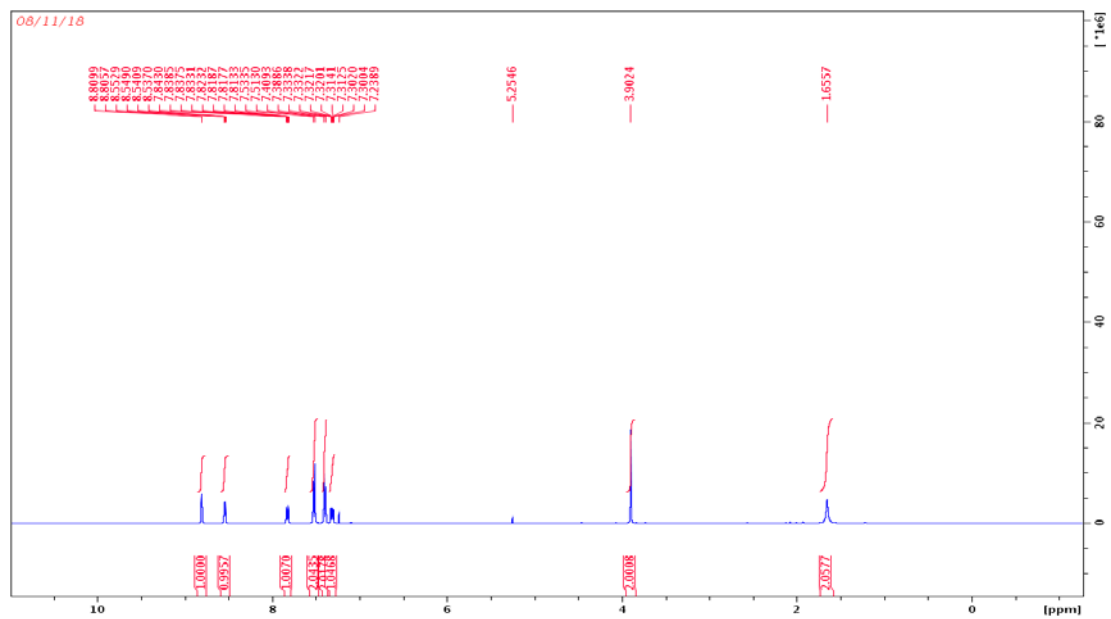
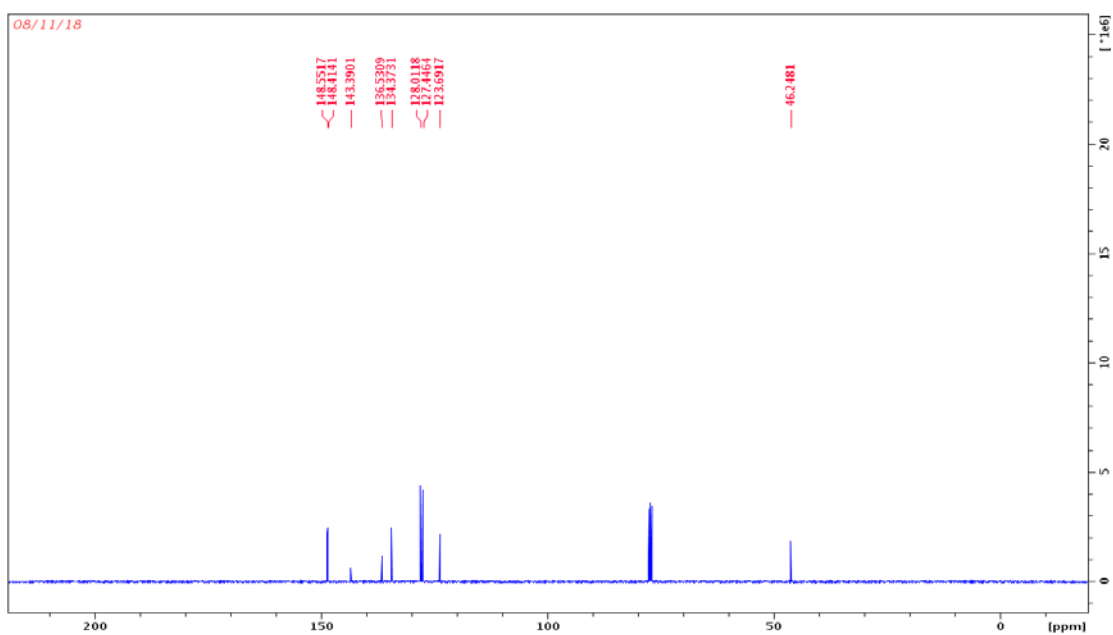
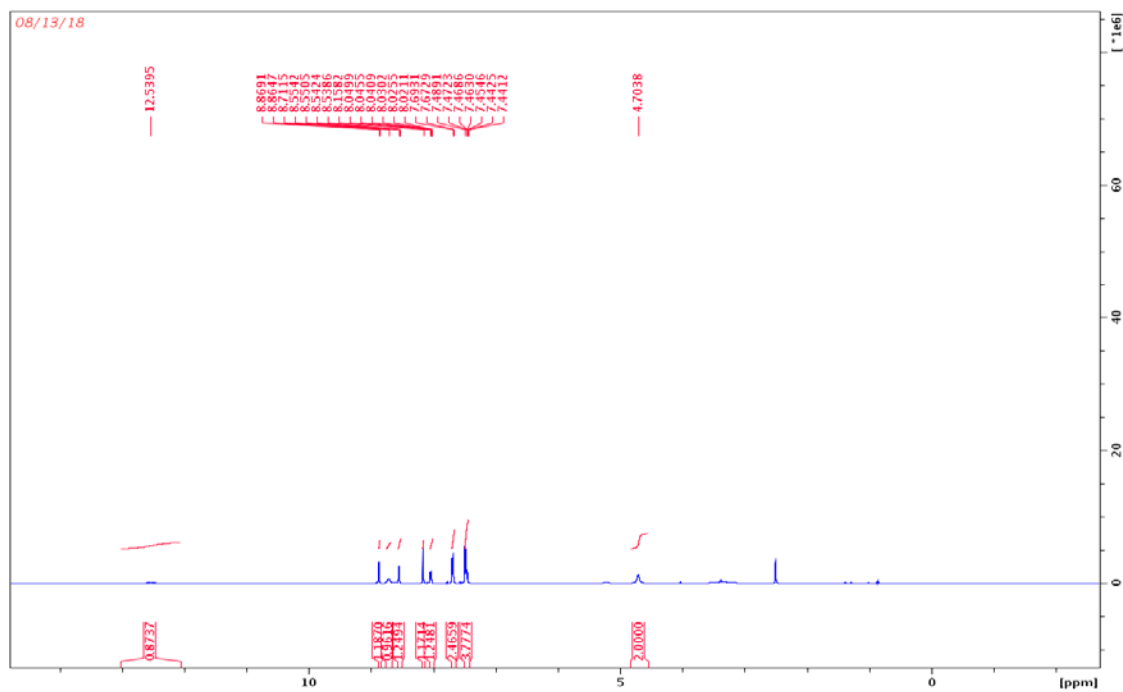


Figure 6.18. ^{13}C NMR spectrum of compound 6.22.

Figure 6.19. ^{19}F NMR spectrum of compound 6.22.Figure 6.20. ^1H NMR spectrum of compound 6.25.

Figure 6.21. ^{13}C NMR spectrum of compound 6.25.Figure 6.22. ^1H NMR spectrum of compound 6.26.

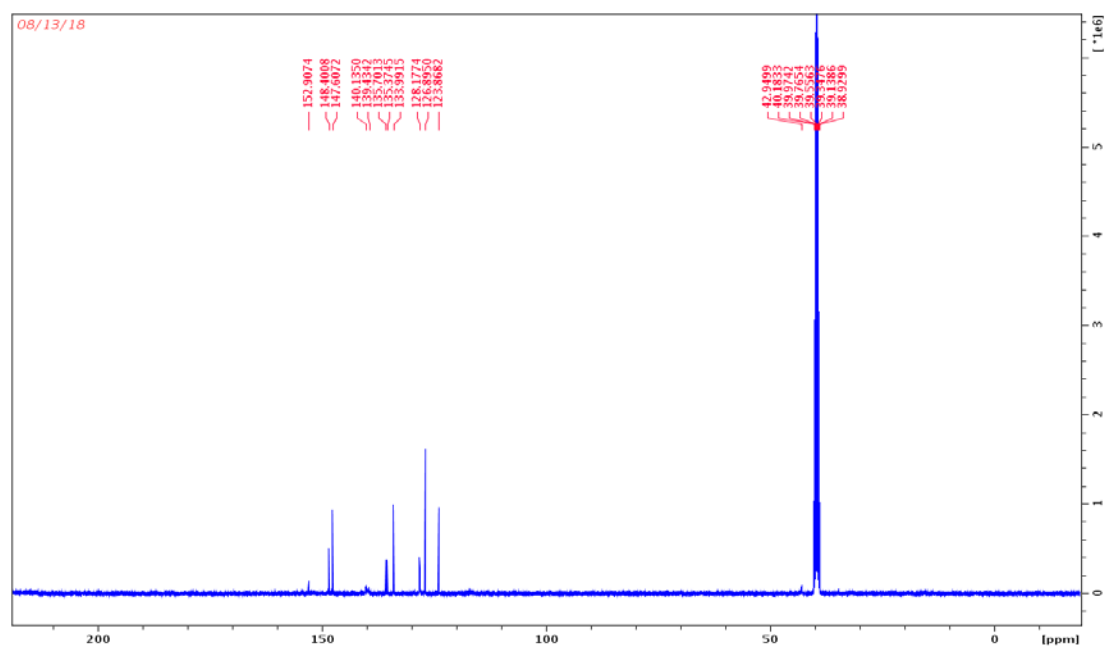


Figure 6.23. ^{13}C NMR spectrum of compound 6.26.

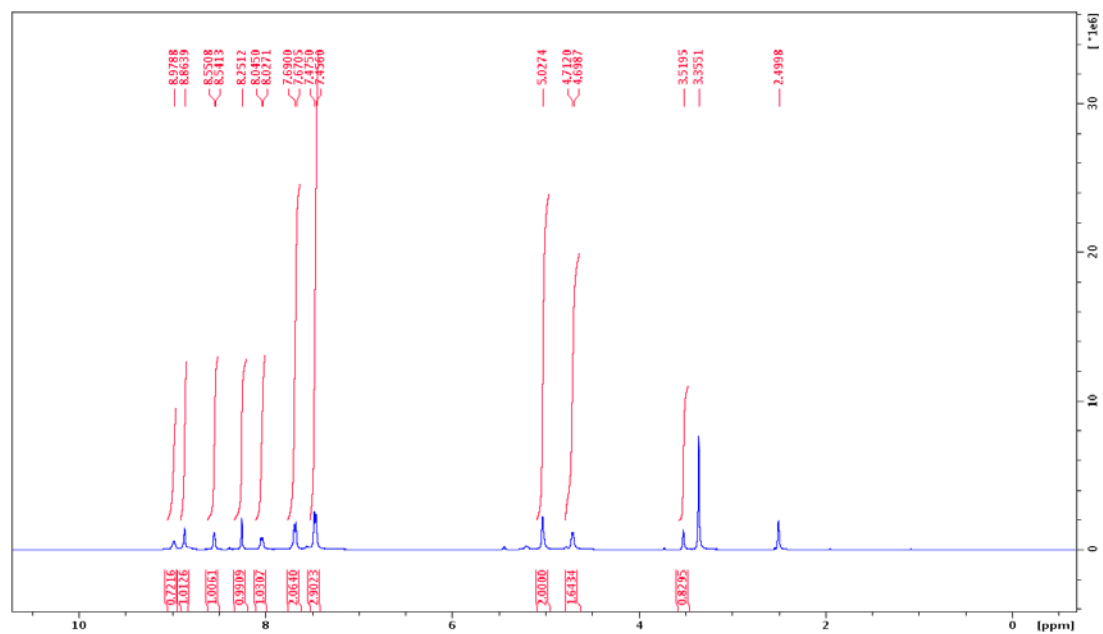


Figure 6.24. ^1H NMR spectrum of compound 6.27

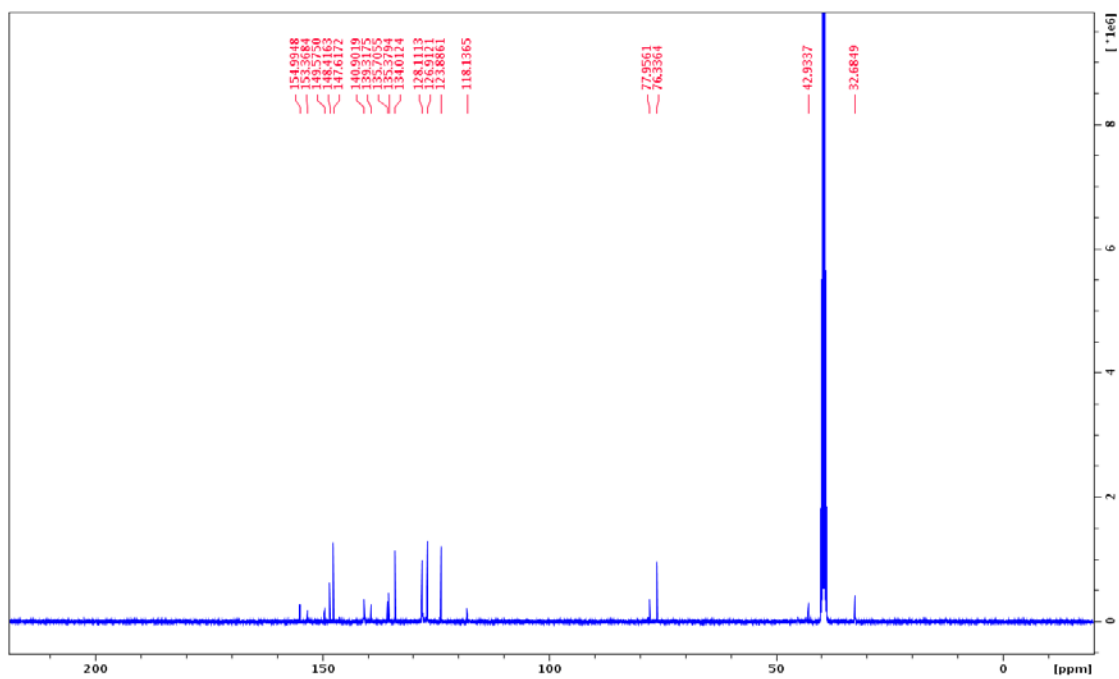


Figure 6.25. ^{13}C NMR spectrum of compound 6.27.

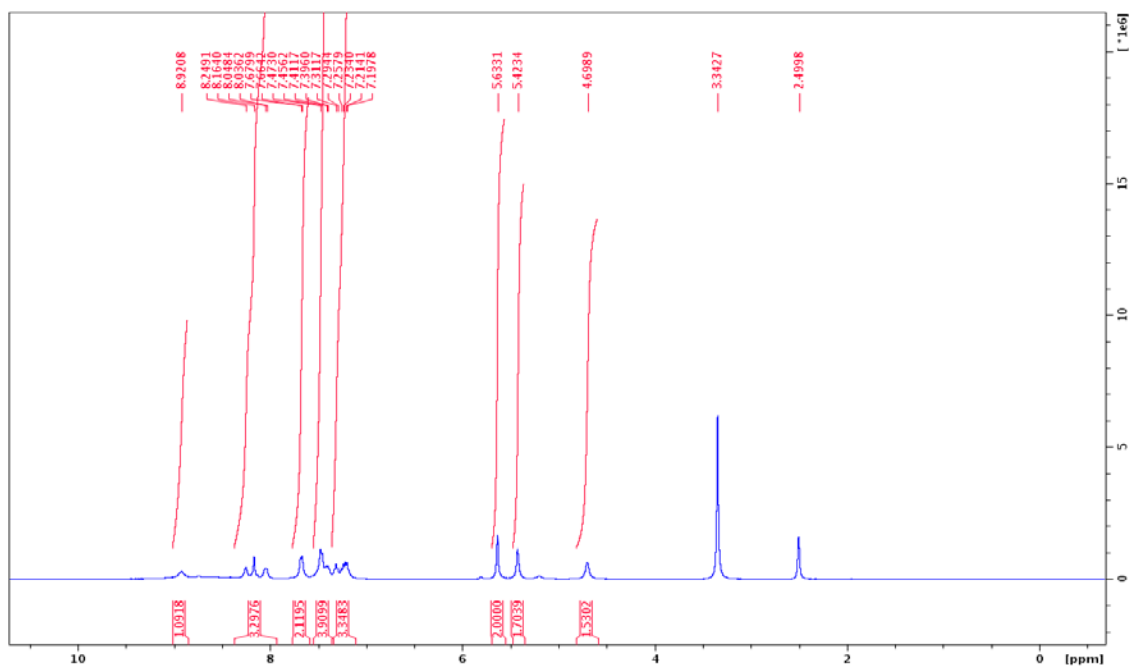


Figure 6.26. ^1H NMR spectrum of compound 6.28.

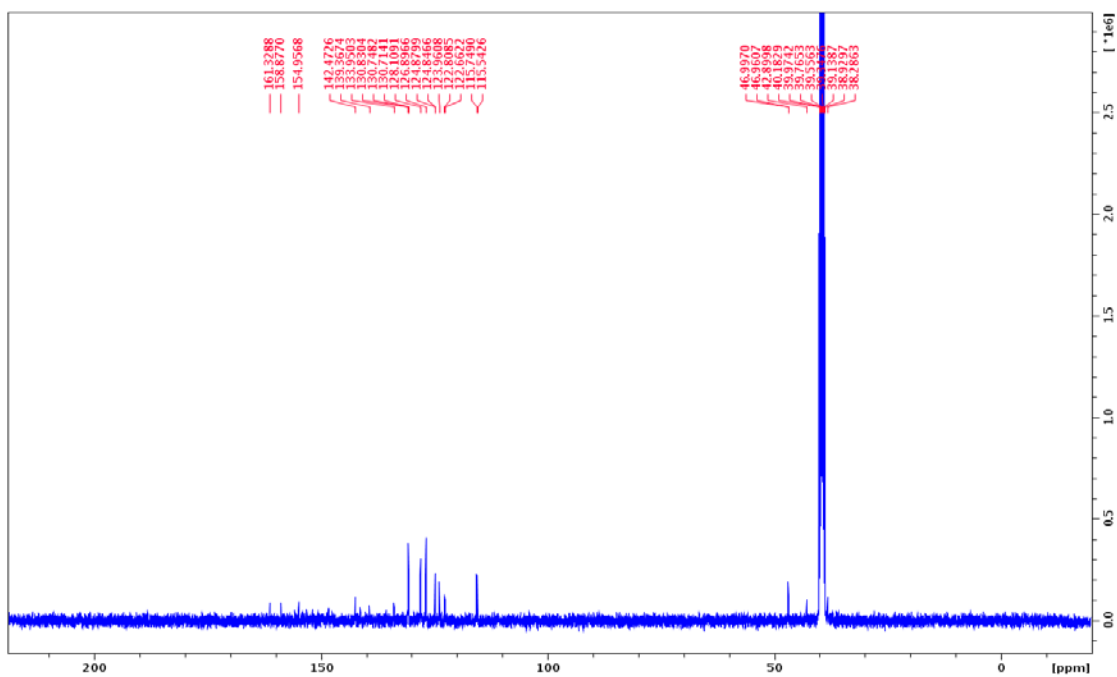


Figure 6.27. ^{13}C NMR spectrum of compound 6.28.

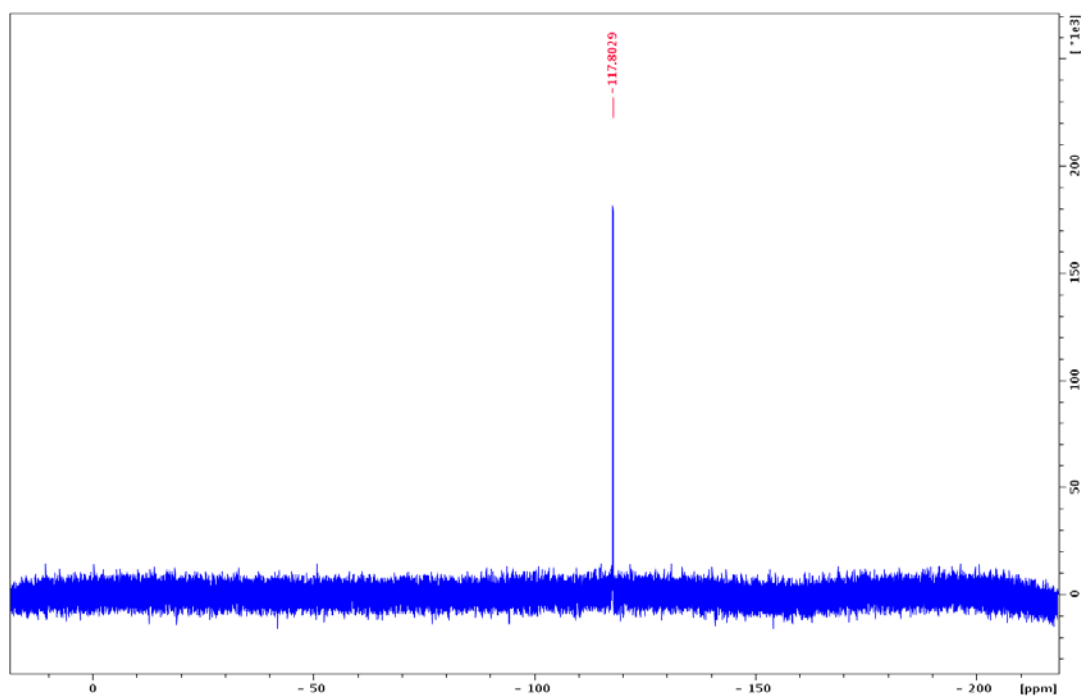


Figure 6.28. ^{19}F NMR spectrum of compound 6.28.

7. CONCLUSION

N-phenacylthiazolium bromide (PTB), N-phenacylmethylimidazolium halides, their dimeric versions and other derivatives such as morpholine, benzylamine, nitrobenzene, catechol, phloroglucinol and polyethylene glycol (PEG) were synthesized to investigate their inhibitory effects on the formation of AGEs by ^{13}C NMR spectroscopy. Dehydroascorbic acid (DHA) was chosen as a model dicarbonyl compound for this study, which was prepared in situ by oxidation of ascorbic acid. PTB was able to trap DHA in situ to form PTB-DHA adduct, as shown by ^{13}C NMR, UV-vis, and fluorescence spectroscopy studies. ^{13}C NMR study showed that the rate of DHA adduct formation with these novel compounds was faster than that of the thiazolium compound PTB. ^{13}C NMR, UV-vis, and fluorescence spectroscopy techniques were used as convenient analytical probes for following the progress of Maillard reactions, we have demonstrated the substantial AGE-inhibitory effects of citric acid and polyphenolic antioxidants such as EGCG, ferulic acid, phloroglucinol, resorcinol, catechol, acetic acid, benzoic acid, hydroxybenzoic acids, ethanol and phenol in D-glucose/ leucine or benzylamine Maillard reaction model system. Citric acid was found to be most effective among all the polyphenolic antioxidants but all other polyphenolic compounds are also potentially useful as AGE-inhibitors in food storage and processing as well as in pharmaceutical applications.

We have developed a novel photoredox catalyzed *gem*-difluorination of 1,3 dithiolanes to form *gem*-difluoromethylene compounds by using a cheap and readily available photocatalyst 9-fluorenone in the presence of visible light (household bulb 13W CFL). This reaction requires mild conditions and is applicable to *gem*-difluorination

of variously substituted diaryl 1,3-dithiolanes. We also have developed the NHC-catalyzed trifluoromethylation of aromatic aldimines, using the in situ generated sterically crowded NHC catalyst. Various aromatic N-tosylaldimines with electron-withdrawing as well as electron-donating groups on the aryl ring undergo facile trifluoromethylation in the presence of the NHC-**1**. Further optimization of the reaction conditions are in progress in our laboratory toward expanding the scope of the NHC-catalyzed trifluoromethylations.

We have synthesized novel purine-based fluoroalkyl triazole derivatives as potential cyclin-dependent kinase (CDK) inhibitors, based on the earlier reported parent purine-based triazole. Four different derivatives including aniline, methylenedianiline (dimeric version), 3-aminomethylpyridine and biarylmethylamine were synthesized by efficient synthetic methods with high purity and yields. The structural characterization and purity of these compounds was established by ^1H - and ^{13}C -NMR spectroscopy.

REFERENCES

1. Engelen, L.; Stehouwer, C. D. A.; Schalkwijk, C. G., Current therapeutic interventions in the glycation pathway: evidence from clinical studies. *Diabetes, Obes. Metab.* **2013**, *15* (8), 677-689.
2. Thornalley, P. J.; Langborg, A.; Minhas, H. S., Formation of glyoxal, methylglyoxal and 3-deoxyglucosone in the glycation of proteins by glucose. *Biochem. J.* **1999**, *344* (1), 109-116.
3. Negre-Salvayre, A.; Coatrieux, C.; Ingueneau, C.; Salvayre, R., Advanced lipid peroxidation end products in oxidative damage to proteins. Potential role in diseases and therapeutic prospects for the inhibitors. *Br. J. Pharmacol.* **2008**, *153* (1), 6-20.
4. Fu, M.-X.; Requena, J. R.; Jenkins, A. J.; Lyons, T. J.; Baynes, J. W.; Thorpe, S. R., The advanced glycation end product, N ϵ -(carboxymethyl)lysine, is a product of both lipid peroxidation and glycoxidation reactions. *J. Biol. Chem.* **1996**, *271* (17), 9982-6.
5. Liang, T.; Neumann, C. N.; Ritter, T., Introduction of Fluorine and Fluorine-Containing Functional Groups. *Angew. Chem., Int. Ed.* **2013**, *52* (32), 8214-8264.
6. Sessler, C. D.; Rahm, M.; Becker, S.; Goldberg, J. M.; Wang, F.; Lippard, S. J., CF₂H, a Hydrogen Bond Donor. *J. Am. Chem. Soc.* **2017**, *139* (27), 9325-9332.
7. Koperniku, A.; Liu, H.; Hurley, P. B., Mono- and Difluorination of Benzylic Carbon Atoms. *Eur. J. Org. Chem.* **2016**, *2016* (5), 871-886.
8. Xia, J.-B.; Ma, Y.; Chen, C., Vanadium-catalyzed C(sp³)-H fluorination reactions. *Org. Chem. Front.* **2014**, *1* (5), 468-472.
9. Fujiwara, Y.; Dixon, J. A.; Rodriguez, R. A.; Baxter, R. D.; Dixon, D. D.; Collins, M. R.; Blackmond, D. G.; Baran, P. S., A New Reagent for Direct Difluoromethylation. *J. Am. Chem. Soc.* **2012**, *134* (3), 1494-1497.
10. Li, W.; Zhu, X.; Mao, H.; Tang, Z.; Cheng, Y.; Zhu, C., Visible-light-induced direct C(sp³)-H difluoromethylation of tetrahydroisoquinolines with the in situ generated difluoroenolates. *Chem. Commun. (Cambridge, U. K.)* **2014**, *50* (56), 7521-7523.
11. Xia, J.-B.; Zhu, C.; Chen, C., Visible Light-Promoted Metal-Free C-H Activation: Diarylketone-Catalyzed Selective Benzylic Mono- and Difluorination. *J. Am. Chem. Soc.* **2013**, *135* (46), 17494-17500.

12. West, J. G.; Bedell, T. A.; Sorensen, E. J., The Uranyl Cation as Visible-Light Photocatalyst for C(sp³)-H Fluorination. *Angew. Chem., Int. Ed.* **2016**, *55* (31), 8923-8927.
13. Reddy, V. P.; Perambuduru, M.; Mehta, J., N-Heterocyclic Carbene-Catalyzed Trifluoromethylation of Aromatic N-Tosylaldimines. *Top. Catal.* **2018**, *61* (7-8), 699-703.
14. Gagosz, F.; Zard, S. Z., A Direct Approach to α -Trifluoromethylamines. *Org. Lett.* **2003**, *5* (15), 2655-2657.
15. Begue, J. P.; Bonnet-Delpon, D.; Mesureur, D.; Nee, G.; Wu, S. W., The Wittig reaction of perfluoro acid derivatives: access to fluorinated enol ethers, enamines, and ketones. *J. Org. Chem.* **1992**, *57* (14), 3807-14.
16. Wu, M.; Cheng, T.; Ji, M.; Liu, G., Ru-Catalyzed Asymmetric Transfer Hydrogenation of α -Trifluoromethylimines. *J. Org. Chem.* **2015**, *80* (7), 3708-3713.
17. Dilman, A. D.; Levin, V. V., Nucleophilic Trifluoromethylation of C=N Bonds. *Eur. J. Org. Chem.* **2011**, (5), 831-841.
18. Levin, V. V.; Dilman, A. D.; Belyakov, P. A.; Struchkova, M. I.; Tartakovsky, V. A., Nucleophilic trifluoromethylation of imines under acidic conditions. *Eur. J. Org. Chem.* **2008**, (31), 5226-5230.
19. Song, J. J.; Tan, Z.; Reeves, J. T.; Gallou, F.; Yee, N. K.; Senanayake, C. H., N-Heterocyclic Carbene Catalyzed Trifluoromethylation of Carbonyl Compounds. *Org. Lett.* **2005**, *7* (11), 2193-2196.
20. Du, G.-F.; Xing, F.; Gu, C.-Z.; Dai, B.; He, L., N-heterocyclic carbene-catalyzed pentafluorophenylation of aldehydes. *RSC Adv.* **2015**, *5* (45), 35513-35517.
21. Kano, T.; Sasaki, K.; Konishi, T.; Mii, H.; Maruoka, K., Highly efficient trialkylsilylcyanation of aldehydes, ketones, and imines catalyzed by a nucleophilic N-heterocyclic carbene. *Tetrahedron Lett.* **2006**, *47* (27), 4615-4618.
22. Sharma, S.; Singh, J.; Ojha, R.; Singh, H.; Kaur, M.; Bedi, P. M. S.; Nepali, K., Design strategies, structure activity relationship and mechanistic insights for purines as kinase inhibitors. *Eur. J. Med. Chem.* **2016**, *112*, 298-346.
23. Reddy, V. P.; Nair, N. G.; Smith, M. A.; Kudo, W. Preparation of purine-based triazoles as protein kinase inhibitors. WO2012051296A2, **2012**.
24. Reddy, P. V.; Nair, N. G.; Smith, M. A.; Kudo, W. Purine-based triazoles. US8969556B2, **2015**.

25. Nair, N.; Kudo, W.; Smith, M. A.; Abrol, R.; Goddard, W. A., III; Reddy, V. P., Novel purine-based fluoroaryl-1,2,3-triazoles as neuroprotecting agents: Synthesis, neuronal cell culture investigations, and CDK5 docking studies. *Bioorg. Med. Chem. Lett.* **2011**, *21* (13), 3957-3961.
26. Tamanna, N.; Mahmood, N., Food processing and Maillard reaction products: effect on human health and nutrition. *Int. J. Food Sci.* **2015**, *526762/1-526762/7*.
27. Salahuddin, P.; Rabbani, G.; Khan, R. H., The role of advanced glycation end products in various types of neurodegenerative disease: a therapeutic approach. *Cell. Mol. Biol. Lett.* **2014**, *19* (3), 407-437.
28. Uribarri, J.; del, C. M. D.; de, I. M. M. P.; Filip, R.; Gugliucci, A.; Menini, T.; Luevano-Contreras, C.; Macias-Cervantes, M. H.; Garay-Sevilla, M. E.; Markowicz, B. D. H.; Sampaio, G. R.; Medrano, A.; Portero-Otin, M.; Rojas, A.; Wrobel, K.; Wrobel, K., Dietary advanced glycation end products and their role in health and disease. *Adv Nutr* **2015**, *6* (4), 461-73.
29. Forbes, J. M.; Cooper, M. E.; Oldfield, M. D.; Thomas, M. C., Role of advanced glycation end products in diabetic nephropathy. *J. Am. Soc. Nephrol.* **2003**, *14* (Suppl. 3), S254-S258.
30. Ulrich, P.; Cerami, A., Protein glycation, diabetes, and aging. *Recent Prog. Horm. Res.* **2001**, *56*, 1-21.
31. Ahmed, N., Advanced glycation endproducts-role in pathology of diabetic complications. *Diabetes Res. Clin. Pract.* **2005**, *67* (1), 3-21.
32. Stitt, A.; Gardiner, T. A.; Anderson, N. L.; Canning, P.; Frizzell, N.; Duffy, N.; Boyle, C.; Januszewski, A. S.; Chachich, M.; Baynes, J. W.; Thorpe, S. R., The AGE inhibitor pyridoxamine inhibits development of retinopathy in experimental diabetes. *Diabetes* **2002**, *51* (9), 2826-2832.
33. Chellan, P.; Nagaraj, R. H., Early glycation products produce pentosidine cross-links on native proteins: novel mechanism of pentosidine formation and propagation of glycation. *J. Biol. Chem.* **2001**, *276* (6), 3895-3903.
34. Baynes, J. W.; Thorpe, S. R., Role of oxidative stress in diabetic complications: a new perspective on an old paradigm. *Diabetes* **1999**, *48* (1), 1-9.
35. Thornalley, P. J.; Minhas, H. S., Rapid hydrolysis and slow α,β -dicarbonyl cleavage of an agent proposed to cleave glucose-derived protein cross-links. *Biochem. Pharmacol.* **1999**, *57* (3), 303-307.
36. Baynes, J. W., Role of oxidative stress in development of complications in diabetes. *Diabetes* **1991**, *40* (4), 405-12.

37. Hunt, J. V.; Bottoms, M. A.; Mitchinson, M. J., Oxidative alterations in the experimental glycation model of diabetes mellitus are due to protein-glucose adduct oxidation. Some fundamental differences in proposed mechanisms of glucose oxidation and oxidant production. *Biochem. J.* **1993**, *291* (2), 529-35.
38. Wolff, S. P.; Dean, R. T., Glucose autoxidation and protein modification. The potential role of 'autoxidative glycosylation' in diabetes. *Biochem. J.* **1987**, *245* (1), 243-50.
39. Poulsen, M. W.; Hedegaard, R. V.; Andersen, J. M.; de Courten, B.; Bugel, S.; Nielsen, J.; Skibsted, L. H.; Dragsted, L. O., Advanced glycation endproducts in food and their effects on health. *Food Chem. Toxicol.* **2013**, *60*, 10-37.
40. Ahmed, M. U.; Thorpe, S. R.; Baynes, J. W., Identification of N ϵ -carboxymethyllysine as a degradation product of fructoselysine in glycated protein. *J. Biol. Chem.* **1986**, *261* (11), 4889-94.
41. Xue, J.; Rai, V.; Singer, D.; Chabierski, S.; Xie, J.; Reverdatto, S.; Burz, D. S.; Schmidt, A. M.; Hoffmann, R.; Shekhtman, A., Advanced Glycation End Product Recognition by the Receptor for AGEs. *Structure (Cambridge, MA, U. S.)* **2011**, *19* (5), 722-732.
42. Indurthi, V. S. K.; Leclerc, E.; Vetter, S. W., Interaction between glycated serum albumin and AGE-receptors depends on structural changes and the glycation reagent. *Arch. Biochem. Biophys.* **2012**, *528* (2), 185-196.
43. Teodorowicz, M.; van, N. J.; Savelkoul, H.; Teodorowicz, M.; Savelkoul, H.; van, N. J., Food Processing: The Influence of the Maillard Reaction on Immunogenicity and Allergenicity of Food Proteins. *Nutrients* **2017**, *9* (8).
44. Weli, H. K.; Akhtar, R.; Chang, Z.; Li, W.-W.; Cooper, J.; Yang, Y., Advanced glycation products' levels and mechanical properties of vaginal tissue in pregnancy. *Eur. J. Obstet. Gynecol. Reprod. Biol.* **2017**, *214*, 78-85.
45. Byun, K.; Yoo, Y. C.; Son, M.; Lee, J.; Jeong, G.-B.; Park, Y. M.; Salekdeh, G. H.; Lee, B., Advanced glycation end-products produced systemically and by macrophages: A common contributor to inflammation and degenerative diseases. *Pharmacol. Ther.* **2017**, *177*, 44-55.
46. Soman, S.; Raju, R.; Sandhya, V. K.; Advani, J.; Khan, A. A.; Harsha, H. C.; Prasad, T. S. K.; Sudhakaran, P. R.; Pandey, A.; Adishesha, P. K., A multicellular signal transduction network of AGE/RAGE signaling. *J Cell Commun Signal* **2013**, *7* (1), 19-23.
47. Lin, J.-A.; Wu, C.-H.; Lu, C.-C.; Hsia, S.-M.; Yen, G.-C., Glycative stress from advanced glycation end products (AGEs) and dicarbonyls: An emerging biological factor in cancer onset and progression. *Mol. Nutr. Food Res.* **2016**, *60* (8), 1850-1864.

48. Manigrasso, M. B.; Juranek, J.; Ramasamy, R.; Schmidt, A. M., Unlocking the biology of RAGE in diabetic microvascular complications. *Trends Endocrinol. Metab.* **2014**, *25* (1), 15-22.
49. Lin, J.-A.; Wu, C.-H.; Yen, G.-C., Perspective of Advanced Glycation End Products on Human Health. *J. Agric. Food Chem.* **2018**, *66* (9), 2065-2070.
50. Giannoukakis, N., Pyridoxamine BioStratum. *Curr. Opin. Invest. Drugs (Thomson Sci.)* **2005**, *6* (4), 410-418.
51. Rahbar, S.; Yerneni, K. K.; Scott, S.; Gonzales, N.; Lalezari, I., Novel Inhibitors of Advanced Glycation Endproducts (Part II). *Mol. Cell Biol. Res. Commun.* **2000**, *3* (6), 360-366.
52. Rahbar, S.; Figarola, J. L., Novel inhibitors of advanced glycation endproducts. *Arch. Biochem. Biophys.* **2003**, *419* (1), 63-79.
53. Williams, M. E., Clinical studies of advanced glycation end product inhibitors and diabetic kidney disease. *Curr Diab Rep* **2004**, *4* (6), 441-6.
54. Peng, X.; Ma, J.; Chen, F.; Wang, M., Naturally occurring inhibitors against the formation of advanced glycation end-products. *Food Funct.* **2011**, *2* (6), 289-301.
55. Nagai, R.; Murray, D. B.; Metz, T. O.; Baynes, J. W., Chelation: a fundamental mechanism of action of AGE inhibitors, AGE breakers, and other inhibitors of diabetes complications. *Diabetes* **2012**, *61* (3), 549-559.
56. Chandra, K. P.; Shiwalkar, A.; Kotecha, J.; Thakkar, P.; Srivastava, A.; Chauthaiwale, V.; Sharma, S. K.; Cross, M. R.; Dutt, C., Phase I clinical studies of the advanced glycation end-product (AGE)-breaker TRC4186: Safety, tolerability and pharmacokinetics in healthy subjects. *Clin. Drug Invest.* **2009**, *29* (9), 559-575.
57. Joshi, D.; Gupta, R.; Dubey, A.; Shiwalkar, A.; Pathak, P.; Gupta, R. C.; Chauthaiwale, V.; Dutt, C., TRC4186, a Novel AGE-breaker, Improves Diabetic Cardiomyopathy and Nephropathy in Ob-ZSF1 Model of Type 2 Diabetes. *J. Cardiovasc. Pharmacol.* **2009**, *54* (1), 72-81.
58. Wolffenbuttel, B. H. R.; Boulanger, C. M.; Crijns, F. R. L.; Huijberts, M. S. P.; Poitevin, P.; Swennen, G. N. M.; Vasana, S.; Egan, J. J.; Ulrich, P.; Cerami, A.; Levy, B. I., Breakers of advanced glycation end products restore large artery properties in experimental diabetes. *Proc. Natl. Acad. Sci. U. S. A.* **1998**, *95* (8), 4630-4634.
59. Vasana, S.; Zhang, X.; Zhang, X.; Kapurniotu, A.; Bernhagen, J.; Teichberg, S.; Basgen, J.; Wagle, D.; Shih, D.; Terlecky, I.; Bucala, R.; Cerami, A.; Egan, J.; Ulrich, P., An agent cleaving glucose-derived protein crosslinks in vitro and in vivo. *Nature* **1996**, *382* (6588), 275-8.

60. Nakagawa, T.; Yokozawa, T.; Terasawa, K.; Shu, S.; Juneja, L. R., Protective Activity of Green Tea against Free Radical- and Glucose-Mediated Protein Damage. *J. Agric. Food Chem.* **2002**, *50* (8), 2418-2422.
61. Lee, G. Y.; Jang, D. S.; Lee, Y. M.; Kim, J. M.; Kim, J. S., Naphthopyrone glucosides from the seeds of *Cassia tora* with inhibitory activity on advanced glycation end products (AGEs) formation. *Arch Pharm Res* **2006**, *29* (7), 587-90.
62. Morimitsu, Y.; Yoshida, K.; Esaki, S.; Hirota, A., Protein glycation inhibitors from thyme (*Thymus vulgaris*). *Biosci., Biotechnol., Biochem.* **1995**, *59* (11), 2018-21.
63. Bousova, I.; Martin, J.; Jahodar, L.; Dusek, J.; Palicka, V.; Drsata, J., Evaluation of in vitro effects of natural substances of plant origin using a model of protein glycooxidation. *J. Pharm. Biomed. Anal.* **2005**, *37* (5), 957-962.
64. Matsuda, H.; Wang, T.; Managi, H.; Yoshikawa, M., Structural requirements of flavonoids for inhibition of protein glycation and radical scavenging activities. *Bioorg. Med. Chem.* **2003**, *11* (24), 5317-5323.
65. Wu, C.-H.; Yen, G.-C., Inhibitory effect of naturally occurring flavonoids on the formation of advanced glycation endproducts. *J. Agric. Food Chem.* **2005**, *53* (8), 3167-3173.
66. Lo, C.-Y.; Li, S.; Tan, D.; Pan, M.-H.; Sang, S.; Ho, C.-T., Trapping reactions of reactive carbonyl species with tea polyphenols in simulated physiological conditions. *Mol. Nutr. Food Res.* **2006**, *50* (12), 1118-1128.
67. Caballero, F.; Gerez, E.; Batlle, A.; Vazquez, E., Preventive aspirin treatment of streptozotocin induced diabetes: blockage of oxidative status and reversion of heme enzymes inhibition. *Chem.-Biol. Interact.* **2000**, *126* (3), 215-225.
68. Malik, N. S.; Meek, K. M., The inhibition of sugar-induced structural alterations in collagen by aspirin and other compounds. *Biochem. Biophys. Res. Commun.* **1994**, *199* (2), 683-6.
69. Van Boekel, M. A. M.; Van den Bergh, P. J. P. C.; Hoenders, H. J., Glycation of human serum albumin: inhibition by Diclofenac. *Biochim. Biophys. Acta, Protein Struct. Mol. Enzymol.* **1992**, *1120* (2), 201-4.
70. Rahbar, S.; Natarajan, R.; Yerneni, K.; Scott, S.; Gonzales, N.; Nadler, J. L., Evidence that pioglitazone, metformin and pentoxifylline are inhibitors of glycation. *Clin. Chim. Acta* **2000**, *301* (1-2), 65-77.
71. Al-Abed, Y.; Mitsuhashi, T.; Li, H.; Lawson, J. A.; FitzGerald, G. A.; Founds, H.; Donnelly, T.; Cerami, A.; Ulrich, P.; Bucala, R., Inhibition of advanced glycation end product formation by acetaldehyde: role in the cardioprotective effect of ethanol. *Proc. Natl. Acad. Sci. U. S. A.* **1999**, *96* (5), 2385-2390.

72. Vasan, S.; Foiles, P.; Founds, H., Therapeutic potential of breakers of advanced glycation end product-protein crosslinks. *Arch. Biochem. Biophys.* **2003**, *419* (1), 89-96.
73. Candido, R.; Forbes, J. M.; Thomas, M. C.; Thallas, V.; Dean, R. G.; Burns, W. C.; Tikellis, C.; Ritchie, R. H.; Twigg, S. M.; Cooper, M. E.; Burrell, L. M., A Breaker of Advanced Glycation End Products Attenuates Diabetes-Induced Myocardial Structural Changes. *Circ. Res.* **2003**, *92* (7), 785-792.
74. Forbes, J. M.; Yee, L. T. L.; Thallas, V.; Lassila, M.; Candido, R.; Jandeleit-Dahm, K. A.; Thomas, M. C.; Burns, W. C.; Deemer, E. K.; Thorpe, S. M.; Cooper, M. E.; Allen, T. J., Advanced glycation end product interventions reduce diabetes-accelerated atherosclerosis. *Diabetes* **2004**, *53* (7), 1813-1823.
75. Susic, D.; Varagic, J.; Ahn, J.; Frohlich, E. D., Crosslink breakers: a new approach to cardiovascular therapy. *Curr Opin Cardiol* **2004**, *19* (4), 336-40.
76. Sajithlal, G. B.; Chithra, P.; Chandrakasan, G., Effect of curcumin on the advanced glycation and crosslinking of collagen in diabetic rats. *Biochem. Pharmacol.* **1998**, *56* (12), 1607-1614.
77. Forbes, J. M.; Soulis, T.; Thallas, V.; Panagiotopoulos, S.; Long, D. M.; Vasan, S.; Wagle, D.; Jerums, G.; Cooper, M. E., Renoprotective effects of a novel inhibitor of advanced glycation. *Diabetologia* **2001**, *44* (1), 108-114.
78. Wilkinson-Berka, J. L.; Kelly, D. J.; Koerner, S. M.; Jaworski, K.; Davis, B.; Thallas, V.; Cooper, M. E., ALT-946 and aminoguanidine, inhibitors of advanced glycation, improve severe nephropathy in the diabetic transgenic (mREN-2)27 rat. *Diabetes* **2002**, *51* (11), 3283-3289.
79. Cooper, G. J. S., Therapeutic potential of copper chelation with triethylenetetramine in managing diabetes mellitus and Alzheimer's disease. *Drugs* **2011**, *71* (10), 1281-1320.
80. Uriu-Adams, J. Y.; Keen, C. L., Copper, oxidative stress, and human health. *Mol. Aspects Med.* **2005**, *26* (4-5), 268-298.
81. Zheng, Y.; Li, X.-K.; Wang, Y.; Lu, C., The Role of Zinc, Copper and Iron in the Pathogenesis of Diabetes and Diabetic Complications: Therapeutic Effects by Chelators. *Hemoglobin* **2008**, *32* (1-2), 135-145.
82. Oboh, G.; Ademiluyi, A. O.; Agunloye, O. M.; Ademosun, A. O.; Ogunsakin, B. G., Inhibitory Effect of Garlic, Purple Onion, and White Onion on Key Enzymes Linked with Type 2 Diabetes and Hypertension. *J. Diet. Suppl.* **2018**, Ahead of Print.

83. Adefegha, S. A.; Oyeleye, S. I.; Oboh, G., Distribution of phenolic contents, antidiabetic potentials, antihypertensive properties, and antioxidative effects of soursop (*Annona muricata* L.) Fruit Parts In Vitro. *Biochem. Res. Int.* **2015**, 347673/1-347673/8.
84. Thornalley, P. J., Use of aminoguanidine (Pimagedine) to prevent the formation of advanced glycation endproducts. *Arch. Biochem. Biophys.* **2003**, 419 (1), 31-40.
85. Freedman, B. I.; Wuerth, J. P.; Cartwright, K.; Bain, R. P.; Dippe, S.; Hershon, K.; Mooradian, A. D.; Spinowitz, B. S., Design and baseline characteristics for the aminoguanidine Clinical Trial in Overt Type 2 Diabetic Nephropathy (ACTION II). *Control Clin Trials* **1999**, 20 (5), 493-510.
86. Vaitkevicius, P. V.; Lane, M.; Spurgeon, H.; Ingram, D. K.; Roth, G. S.; Egan, J. J.; Vasam, S.; Wagle, D. R.; Ulrich, P.; Brines, M.; Wuerth, J. P.; Cerami, A.; Lakatta, E. G., A cross-link breaker has sustained effects on arterial and ventricular properties in older rhesus monkeys. *Proc. Natl. Acad. Sci. U. S. A.* **2001**, 98 (3), 1171-1175.
87. Asif, M.; Egan, J.; Vasam, S.; Jyothirmayi, G. N.; Masurekar, M. R.; Lopez, S.; Williams, C.; Torres, R. L.; Wagle, D.; Ulrich, P.; Cerami, A.; Brines, M.; Regan, T. J., An advanced glycation endproduct cross-link breaker can reverse age-related increases in myocardial stiffness. *Proc. Natl. Acad. Sci. U. S. A.* **2000**, 97 (6), 2809-2813.
88. Peppas, M.; Brem, H.; Cai, W.; Zhang, J.-G.; Basgen, J.; Li, Z.; Vlassara, H.; Uribarri, J., Prevention and reversal of diabetic nephropathy in db/db mice treated with alagebrium (ALT-711). *Am. J. Nephrol.* **2006**, 26 (5), 430-436.
89. Kim, T.; Spiegel, D. A., The Unique Reactivity of N-Phenacyl-Derived Thiazolium Salts Toward α -Dicarbonyl Compounds. *Rejuvenation Res.* **2013**, 16 (1), 43-50.
90. Dominianni, S. J.; Yen, T. T., Oral hypoglycemic agents. Discovery and structure-activity relationships of phenacylimidazolium halides. *J. Med. Chem.* **1989**, 32 (10), 2301-6.
91. Richardson, M. A.; Furlani, R. E.; Podell, B. K.; Ackart, D. F.; Haugen, J. D.; Melander, R. J.; Melander, C.; Basaraba, R. J., Inhibition and breaking of advanced glycation end-products (AGEs) with bis-2-aminoimidazole derivatives. *Tetrahedron Lett.* **2015**, 56 (23), 3406-3409.
92. Furlani, R. E.; Richardson, M. A.; Podell, B. K.; Ackart, D. F.; Haugen, J. D.; Melander, R. J.; Basaraba, R. J.; Melander, C., Second generation 2-aminoimidazole based advanced glycation end product inhibitors and breakers. *Bioorg. Med. Chem. Lett.* **2015**, 25 (21), 4820-4823.

93. Al-Ghorbani, M.; Begum, A. B.; Zabiulla; Mamatha, S. V.; Khanum, S. A., Piperazine and morpholine: synthetic preview and pharmaceutical applications. *J. Chem. Pharm. Res.* **2015**, *7* (5), 281-301.
94. Polshettiwar, V.; Varma, R. S., Greener and expeditious synthesis of bioactive heterocycles using microwave irradiation. *Pure Appl. Chem.* **2008**, *80* (4), 777-790.
95. Chrysselis, M. C.; Rekka, E. A.; Kourounakis, P. N., Hypocholesterolemic and Hypolipidemic Activity of Some Novel Morpholine Derivatives with Antioxidant Activity. *J. Med. Chem.* **2000**, *43* (4), 609-612.
96. Park, M.-O.; Lee, K. C., PEGylation: Novel technology to enhance therapeutic efficacy of proteins and peptides. *Yakche Hakhoechi* **2000**, *30* (2), 73-83.
97. Greenwald, R. B., PEG drugs: an overview. *J. Controlled Release* **2001**, *74* (1-3), 159-171.
98. Becker, R.; Dembek, C.; White, L. A.; Garrison, L. P., The cost offsets and cost-effectiveness associated with pegylated drugs: a review of the literature. *Expert Rev Pharmacoecon Outcomes Res* **2012**, *12* (6), 775-93.
99. Greenwald, R. B.; Gilbert, C. W.; Pendri, A.; Conover, C. D.; Xia, J.; Martinez, A., Drug Delivery Systems: Water Soluble Taxol 2'-Poly(ethylene glycol) Ester Prodrugs-Design and in Vivo Effectiveness. *J. Med. Chem.* **1996**, *39* (2), 424-31.
100. Greenwald, R. B.; Pendri, A.; Conover, C. D.; Lee, C.; Choe, Y. H.; Gilbert, C.; Martinez, A.; Xia, J.; Wu, D.; Hsue, M.-M., Camptothecin-20-PEG ester transport forms: the effect of spacer groups on antitumor activity. *Bioorg. Med. Chem.* **1998**, *6* (5), 551-562.
101. Greenwald, R. B.; Pendri, A.; Conover, C.; Gilbert, C.; Yang, R.; Xia, J., Drug Delivery Systems. 2. Camptothecin 20-O-Polyethylene Glycol Ester Transport Forms. *J. Med. Chem.* **1996**, *39* (10), 1938-40.
102. Tsuge, O.; Kanemasa, S.; Takenaka, S., Stereochemical study on 1,3-dipolar cycloaddition reactions of heteroaromatic N-ylides with symmetrically substituted cis and trans olefins. *Bull. Chem. Soc. Jpn.* **1985**, *58* (11), 3137-57.
103. Gandasegui, M. T.; Alvarez-Builla, J., Synthesis of new disubstituted azolium ylides. *Heterocycles* **1990**, *31* (10), 1801-9.
104. Ferguson, G. P.; VanPatten, S.; Bucala, R.; Al-Abed, Y., Detoxification of Methylglyoxal by the Nucleophilic Bidentate, Phenylacetylthiazolium Bromide. *Chem. Res. Toxicol.* **1999**, *12* (7), 617-622.

105. Sero, L.; Calard, F.; Sanguinet, L.; Levillain, E.; Richomme, P.; Seraphin, D.; Derbre, S., Synthesis and evaluation of naphthoic acid derivatives as fluorescent probes to screen advanced glycation end-products breakers. *Bioorg. Med. Chem. Lett.* **2012**, *22* (21), 6716-6720.
106. Song, Y. n.; Lin, X.; Kang, D.; Li, X.; Zhan, P.; Liu, X.; Zhang, Q., Discovery and characterization of novel imidazopyridine derivative CHEQ-2 as a potent CDC25 inhibitor and promising anticancer drug candidate. *Eur. J. Med. Chem.* **2014**, *82*, 293-307.
107. Pan, G.; Ma, Y.; Yang, K.; Zhao, X.; Yang, H.; Yao, Q.; Lu, K.; Zhu, T.; Yu, P., Total synthesis of (\pm)-Anastatins A and B. *Tetrahedron Lett.* **2015**, *56* (30), 4472-4475.
108. Huigens, R. W., III; Reyes, S.; Reed, C. S.; Bunders, C.; Rogers, S. A.; Steinhauer, A. T.; Melander, C., The chemical synthesis and antibiotic activity of a diverse library of 2-aminobenzimidazole small molecules against MRSA and multidrug-resistant *A. baumannii*. *Bioorg. Med. Chem.* **2010**, *18* (2), 663-674.
109. Ma, L.; Xie, C.; Ma, Y.; Liu, J.; Xiang, M.; Ye, X.; Zheng, H.; Chen, Z.; Xu, Q.; Chen, T.; Chen, J.; Yang, J.; Qiu, N.; Wang, G.; Liang, X.; Peng, A.; Yang, S.; Wei, Y.; Chen, L., Synthesis and Biological Evaluation of Novel 5-Benzylidenethiazolidine-2,4-dione Derivatives for the Treatment of Inflammatory Diseases. *J. Med. Chem.* **2011**, *54* (7), 2060-2068.
110. McGuinness, D. S.; Cavell, K. J., Donor-Functionalized Heterocyclic Carbene Complexes of Palladium(II): Efficient Catalysts for C-C Coupling Reactions. *Organometallics* **2000**, *19* (5), 741-748.
111. Hubbard, S. C.; Jones, P. B., Ionic liquid soluble photosensitizers. *Tetrahedron* **2005**, *61* (31), 7425-7430.
112. Kumar, A.; Srivastava, S.; Gupta, G., Cascade [4 + 1] annulation via more environmentally friendly nitrogen ylides in water: synthesis of bicyclic and tricyclic fused dihydrofurans. *Green Chem.* **2012**, *14* (12), 3269-3272.
113. Khlebnikov, A. F.; Tomashenko, O. A.; Funt, L. D.; Novikov, M. S., A simple approach to pyrrolylimidazole derivatives by azirine ring expansion with imidazolium ylides. *Org. Biomol. Chem.* **2014**, *12* (34), 6598-6609.
114. Karipcin, F.; Ucan, H. I.; Karatas, I., Binuclear and mononuclear cobalt(II), nickel(II) and copper(II) complexes of 4,4'-bis(alkylaminoisonitrosoacetyl)diphenylmethane derivatives. *Transition Met. Chem. (Dordrecht, Neth.)* **2002**, *27* (8), 813-817.
115. Zhu, Y.; Zhao, Y.; Wang, P.; Ahmedna, M.; Ho, C.-T.; Sang, S., Tea Flavanols Block Advanced Glycation of Lens Crystallins Induced by Dehydroascorbic Acid. *Chem. Res. Toxicol.* **2015**, *28* (1), 135-143.

116. Varma, S. D.; Richards, R. D., Ascorbic acid and the eye lens. *Ophthalmic Res.* **1988**, *20* (3), 164-73.
117. Nemet, I.; Monnier, V. M., Vitamin C Degradation Products and Pathways in the Human Lens. *J. Biol. Chem.* **2011**, *286* (43), 37128-37136, S37128/1-S37128/3.
118. Cheng, R.; Lin, B.; Lee, K. W.; Ortwerth, B. J., Similarity of the yellow chromophores isolated from human cataracts with those from ascorbic acid-modified calf lens proteins: evidence for ascorbic acid glycation during cataract formation. *Biochim. Biophys. Acta, Mol. Basis Dis.* **2001**, *1537* (1), 14-26.
119. Lund, M. N.; Ray, C. A., Control of Maillard Reactions in Foods: Strategies and Chemical Mechanisms. *J. Agric. Food Chem.* **2017**, *65* (23), 4537-4552.
120. Martin, F. L.; Ames, J. M., Formation of Strecker Aldehydes and Pyrazines in a Fried Potato Model System. *J. Agric. Food Chem.* **2001**, *49* (8), 3885-3892.
121. Stadler, R. H.; Blank, I.; Varga, N.; Robert, F.; Hau, J.; Guy, P. A.; Robert, M.-C.; Riediker, S., Food chemistry: Acrylamide from Maillard reaction products. *Nature (London, U. K.)* **2002**, *419* (6906), 449-450.
122. Reddy, V. P.; Beyaz, A., Inhibitors of the Maillard reaction and AGE breakers as therapeutics for multiple diseases. *Drug Discovery Today* **2006**, *11* (13 & 14), 646-654.
123. Reddy, V. P.; Obrenovich, M. E.; Atwood, C. S.; Perry, G.; Smith, M. A., Involvement of Maillard reactions in Alzheimer disease. *Neurotoxic. Res.* **2002**, *4* (3), 191-209.
124. Dyer, D. G.; Blackledge, J. A.; Thorpe, S. R.; Baynes, J. W., Formation of pentosidine during nonenzymic browning of proteins by glucose. Identification of glucose and other carbohydrates as possible precursors of pentosidine in vivo. *J. Biol. Chem.* **1991**, *266* (18), 11654-60.
125. Wolff, S. P.; Jiang, Z. Y.; Hunt, J. V., Protein glycation and oxidative stress in diabetes mellitus and ageing. *Free Radical Biol. Med.* **1991**, *10* (5), 339-52.
126. Reddy, V. P.; Zhu, X.; Perry, G.; Smith, M. A., Oxidative Stress in Diabetes and Alzheimer's Disease. *J. Alzheimer's Dis.* **2009**, *16* (4), 763-774.
127. Ahmed, M.; Frye, E. B.; Degenhardt, T. P.; Thorpe, S. R.; Baynes, J. W., Nε-(carboxyethyl)lysine, a product of the chemical modification of proteins by methylglyoxal, increases with age in human lens proteins. *Biochem. J.* **1997**, *324* (2), 565-570.
128. Choe, E.; Min, D. B., Mechanisms of antioxidants in the oxidation of foods. *Compr. Rev. Food Sci. Food Saf.* **2009**, *8* (4), 345-358.

129. Mathew, A. G.; Parpia, H. A. B., Food browning as a polyphenol reaction. *Advan. Food Res.* **1971**, *19*, 75-145.
130. Nicolas, J. J.; Richard-Forget, F. C.; Goupy, P. M.; Amiot, M.-J.; Aubert, S. Y., Enzymic browning reactions in apple and apple products. *Crit. Rev. Food Sci. Nutr.* **1994**, *34* (2), 109-57.
131. Nagai, R.; Nagai, M.; Shimasaki, S.; Baynes, J. W.; Fujiwara, Y., Citric acid inhibits development of cataracts, proteinuria and ketosis in streptozotocin (type 1) diabetic rats. *Biochem. Biophys. Res. Commun.* **2010**, *393* (1), 118-122.
132. Wu, C.-H.; Yeh, C.-T.; Shih, P.-H.; Yen, G.-C., Dietary phenolic acids attenuate multiple stages of protein glycation and high-glucose-stimulated proinflammatory IL-1 β activation by interfering with chromatin remodeling and transcription in monocytes. *Mol. Nutr. Food Res.* **2010**, *54* (Suppl. 2), S127-S140.
133. Choudhury, R.; Srail, S. K.; Debnam, E.; Rice-Evans, C. A., Urinary excretion of hydroxycinnamates and flavonoids after oral and intravenous administration. *Free Radical Biol. Med.* **1999**, *27* (3/4), 278-286.
134. Bhuiyan, M. N. I.; Mitsuhashi, S.; Sigetomi, K.; Ubukata, M., Quercetin inhibits advanced glycation end product formation via chelating metal ions, trapping methylglyoxal, and trapping reactive oxygen species. *Biosci., Biotechnol., Biochem.* **2017**, *81* (5), 882-890.
135. Gao, X.; Lin, X.; Li, X.; Zhang, Y.; Chen, Z.; Li, B., Cellular antioxidant, methylglyoxal trapping, and anti-inflammatory activities of cocoa tea (*Camellia ptilophylla* Chang). *Food Funct.* **2017**, Ahead of Print.
136. Tan, D.; Lo, C.-Y.; Shao, X.; Wang, Y.; Sang, S.; Shahidi, F.; Ho, C.-T., Trapping of methylglyoxal by tea polyphenols. *Nutraceutical Sci. Technol.* **2009**, *8* (Tea and Tea Products), 245-254.
137. Wang, M.; Zhang, X.; Zhong, Y. J.; Perera, N.; Shahidi, F., Antiglycation activity of lipophilized epigallocatechin gallate (EGCG) derivatives. *Food Chem.* **2016**, *190*, 1022-1026.
138. Okada, Y.; Ishimaru, A.; Suzuki, R.; Okuyama, T., A new phloroglucinol derivative from the brown alga *Eisenia bicyclis*: potential for the effective treatment of diabetic complications. *J. Nat. Prod.* **2004**, *67* (1), 103-105.
139. Silvan, J. M.; Assar, S. H.; Srey, C.; Dolores del Castillo, M.; Ames, J. M., Control of the Maillard reaction by ferulic acid. *Food Chem.* **2011**, *128* (1), 208-213.

140. Mildner-Szkudlarz, S.; Siger, A.; Szwengiel, A.; Przygonski, K.; Wojtowicz, E.; Zawirska-Wojtasiak, R., Phenolic compounds reduce formation of N ϵ -(carboxymethyl)lysine and pyrazines formed by Maillard reactions in a model bread system. *Food Chem.* **2017**, *231*, 175-184.
141. Matiacevich, S. B.; Pilar Buera, M., A critical evaluation of fluorescence as a potential marker for the Maillard reaction. *Food Chem.* **2005**, *95* (3), 423-430.
142. Crasci, L.; Lauro, M. R.; Puglisi, G.; Panico, A., Natural antioxidant polyphenols on inflammation management: Anti-glycation activity vs metalloproteinases inhibition. *Crit. Rev. Food Sci. Nutr.* **2017**, Ahead of Print.
143. Zhang, F.-L.; Gao, H.-Q.; Shen, L., Inhibitory effect of GSPE on RAGE expression induced by advanced glycation end products in endothelial cells. *J. Cardiovasc. Pharmacol.* **2007**, *50* (4), 434-440.
144. Zhang, X.; Chen, F.; Wang, M., Antioxidant and Antiglycation Activity of Selected Dietary Polyphenols in a Cookie Model. *J. Agric. Food Chem.* **2014**, *62* (7), 1643-1648.
145. Zhang, X.; Hu, S.; Chen, F.; Wang, M., Treatment of proteins with dietary polyphenols lowers the formation of AGEs and AGE-induced toxicity. *Food Funct.* **2014**, *5* (10), 2656-2661.
146. Sang, S.; Shao, X.; Bai, N.; Lo, C.-Y.; Yang, C. S.; Ho, C.-T., Tea polyphenol (-)-epigallocatechin-3-gallate: a new trapping agent of reactive dicarbonyl species. *Chem. Res. Toxicol.* **2007**, *20* (12), 1862-1870.
147. Sheng, Z.; Gu, M.; Hao, W.; Shen, Y.; Zhang, W.; Zheng, L.; Ai, B.; Zheng, X.; Xu, Z., Physicochemical Changes and Glycation Reaction in Intermediate-Moisture Protein-Sugar Foods with and without Addition of Resveratrol during Storage. *J. Agric. Food Chem.* **2016**, *64* (24), 5093-5100.
148. Shantharam, C. S.; Suyoga Vardhan, D. M.; Suhas, R.; Channe Gowda, D., Design and synthesis of amino acids-conjugated heterocycle derived ureas/thioureas as potent inhibitors of protein glycation. *Russ. J. Bioorg. Chem.* **2014**, *40* (4), 443-454.
149. Isanbor, C.; O'Hagan, D., Fluorine in medicinal chemistry: A review of anticancer agents. *J. Fluorine Chem.* **2006**, *127* (3), 303-319.
150. Ismail, F. M. D., Important fluorinated drugs in experimental and clinical use. *J. Fluorine Chem.* **2002**, *118* (1-2), 27-33.
151. Begue, J.-P.; Bonnet-Delpon, D., Recent advances (1995-2005) in fluorinated pharmaceuticals based on natural products. *J. Fluorine Chem.* **2006**, *127* (8), 992-1012.

152. Purser, S.; Moore, P. R.; Swallow, S.; Gouverneur, V., Fluorine in medicinal chemistry. *Chem. Soc. Rev.* **2008**, *37* (2), 320-330.
153. O'Hagan, D., Understanding organofluorine chemistry. An introduction to the C-F bond. *Chem. Soc. Rev.* **2008**, *37* (2), 308-319.
154. Hagmann, W. K., The Many Roles for Fluorine in Medicinal Chemistry. *J. Med. Chem.* **2008**, *51* (15), 4359-4369.
155. Mueller, K.; Faeh, C.; Diederich, F., Fluorine in Pharmaceuticals: Looking Beyond Intuition. *Science (Washington, DC, U. S.)* **2007**, *317* (5846), 1881-1886.
156. Kirk, K. L., Selective fluorination in drug design and development: an overview of biochemical rationales. *Curr. Top. Med. Chem. (Sharjah, United Arab Emirates)* **2006**, *6* (14), 1447-1456.
157. Bohm, H.-J.; Banner, D.; Bendels, S.; Kansy, M.; Kuhn, B.; Muller, K.; Obst-Sander, U.; Stahl, M., Fluorine in medicinal chemistry. *Chembiochem* **2004**, *5* (5), 637-43.
158. Wang, J.; Sanchez-Rosello, M.; Acena, J. L.; del Pozo, C.; Sorochinsky, A. E.; Fustero, S.; Soloshonok, V. A.; Liu, H., Fluorine in Pharmaceutical Industry: Fluorine-Containing Drugs Introduced to the Market in the Last Decade (2001-2011). *Chem. Rev. (Washington, DC, U. S.)* **2014**, *114* (4), 2432-2506.
159. Maienfisch, P.; Hall, R. G., The importance of fluorine in the life science industry. *Chimia* **2004**, *58* (3), 93-99.
160. Li, Y., Molecular Design of Photovoltaic Materials for Polymer Solar Cells: Electronic Energy Levels and Broad Absorption. *Acc. Chem. Res.* **2012**, *45* (5), 723-733.
161. Kirsch, P.; Hahn, A., Liquid crystals based on hypervalent sulfur fluorides: Exploring the steric effects of ortho-fluorine substituents. *Eur. J. Org. Chem.* **2005**, (14), 3095-3100.
162. Kassis, C. M.; Steehler, J. K.; Betts, D. E.; Guan, Z.; Romack, T. J.; DeSimone, J. M.; Linton, R. W., XPS Studies of Fluorinated Acrylate Polymers and Block Copolymers with Polystyrene. *Macromolecules* **1996**, *29* (9), 3247-54.
163. Berger, R.; Resnati, G.; Metrangolo, P.; Weber, E.; Hulliger, J., Organic fluorine compounds: a great opportunity for enhanced materials properties. *Chem. Soc. Rev.* **2011**, *40* (7), 3496-3508.
164. Cametti, M.; Crousse, B.; Metrangolo, P.; Milani, R.; Resnati, G., The fluorous effect in biomolecular applications. *Chem. Soc. Rev.* **2012**, *41* (1), 31-42.

165. Babudri, F.; Farinola, G. M.; Naso, F.; Ragni, R., Fluorinated organic materials for electronic and optoelectronic applications: the role of the fluorine atom. *Chem. Commun. (Cambridge, U. K.)* **2007**, (10), 1003-1022.
166. Guittard, F.; Taffin de Givenchy, E.; Geribaldi, S.; Cambon, A., Highly fluorinated thermotropic liquid crystals: an update. *J. Fluorine Chem.* **1999**, *100* (1-2), 85-96.
167. Littich, R.; Scott, P. J. H., Novel Strategies for Fluorine-18 Radiochemistry. *Angew. Chem., Int. Ed.* **2012**, *51* (5), 1106-1109.
168. Miller, P. W.; Long, N. J.; Vilar, R.; Gee, A. D., Synthesis of ¹¹C, ¹⁸F, ¹⁵O, and ¹³N radiolabels for positron emission tomography. *Angew. Chem., Int. Ed.* **2008**, *47* (47), 8998-9033.
169. Cai, L.; Lu, S.; Pike, V. W., Chemistry with [¹⁸F]fluoride ion. *Eur. J. Org. Chem.* **2008**, (17), 2853-2873.
170. Ametamey, S. M.; Honer, M.; Schubiger, P. A., Molecular Imaging with PET. *Chem. Rev. (Washington, DC, U. S.)* **2008**, *108* (5), 1501-1516.
171. Gouverneur, V.; Seppelt, K., Introduction: Fluorine Chemistry. *Chem. Rev. (Washington, DC, U. S.)* **2015**, *115* (2), 563-565.
172. Theodoridis, G., Fluorine-containing agrochemicals: an overview of recent developments. *Adv. Fluorine Sci.* **2006**, *2* (Fluorine and the Environment: Agrochemicals, Archaeology, Green Chemistry & Water), 121-175.
173. Zareba, K. M., Dronedarone: a new antiarrhythmic agent. *Drugs Today* **2006**, *42* (2), 75-86.
174. Emsley, J., Very strong hydrogen bonding. *Chem. Soc. Rev.* **1980**, *9* (1), 91-124.
175. Welch, J. T., Advances in the preparation of biologically active organofluorine compounds. *Tetrahedron* **1987**, *43* (14), 3123-97.
176. Shimizu, M.; Hiyama, T., Modern synthetic methods for fluorine-substituted target molecules. *Angew. Chem., Int. Ed.* **2005**, *44* (2), 214-231.
177. Dilman, A. D.; Levin, V. V., Difluorocarbene as a Building Block for Consecutive Bond-Forming Reactions. *Acc. Chem. Res.* **2018**, *51* (5), 1272-1280.
178. Tozer, M. J.; Herpin, T. F., Methods for the Synthesis of gem-Difluoromethylene Compounds. *Tetrahedron* **1996**, *52* (26), 8619-8683.
179. Kuroboshi, M.; Kanie, K.; Hiyama, T., Oxidative desulfurization-fluorination: a facile entry to a wide variety of organofluorine compounds leading to novel liquid-crystalline materials. *Adv. Synth. Catal.* **2001**, *343* (3), 235-250.

180. York, C.; Prakash, G. K. S.; Olah, G. A., Synthetic methods and reactions. 196. Desulfuration fluorination using nitrosonium tetrafluoroborate and pyridinium poly(hydrogen fluoride). *Tetrahedron* **1996**, *52* (1), 9-14.
181. Reddy, V. P.; Alleti, R.; Perambuduru, M. K.; Welz-Biermann, U.; Buchholz, H.; Prakash, G. K. S., gem-Difluorination of 2,2-diaryl-1,3-dithiolanes by Selectfluor and pyridinium polyhydrogen fluoride. *Chem. Commun. (Cambridge, U. K.)* **2005**, (5), 654-656.
182. Turkman, N.; An, L.; Pomerantz, M., One-pot desulfurative-fluorination-bromination. synthesis of 2,5-dibromo-3-(1,1-difluoroalkyl)thiophenes. *Org. Lett.* **2010**, *12* (19), 4428-4430.
183. Kiryanov, A. A.; Seed, A. J.; Sampson, P., Synthesis and stability of 2-(1,1-difluoroalkyl) thiophenes and related 1,1-difluoroalkyl benzenes: fluorinated building blocks for liquid crystal synthesis. *Tetrahedron* **2001**, *57* (27), 5757-5767.
184. Prakash, G. K. S.; Hoole, D.; Reddy, V. P.; Olah, G. A., Synthetic methods and reactions. 187. Simplified preparation of α,α -difluorodiphenylmethanes from benzophenone 1,3-dithiolanes with sulfur chloride and pyridinium polyhydrogen fluoride. *Synlett* **1993**, (9), 691-3.
185. Ie, Y.; Nitani, M.; Aso, Y., Synthesis, properties, and structures of difluoromethylene-bridged coplanar p-terphenyl and its aryl-capped derivatives for electron-transporting materials. *Chem. Lett.* **2007**, *36* (11), 1326-1327.
186. Kuroboshi, M.; Hiyama, T., Synthesis of perfluoroalkyl-substituted arenes by oxidative desulfurization-fluorination. *J. Fluorine Chem.* **1994**, *69* (2), 127-8.
187. Sondej, S. C.; Katzenellenbogen, J. A., Gem-Difluoro compounds: a convenient preparation from ketones and aldehydes by halogen fluoride treatment of 1,3-dithiolanes. *J. Org. Chem.* **1986**, *51* (18), 3508-13.
188. Geary, G. C.; Hope, E. G.; Singh, K.; Stuart, A. M., Electrophilic fluorination using a hypervalent iodine reagent derived from fluoride. *Chem. Commun. (Cambridge, U. K.)* **2013**, *49* (81), 9263-9265.
189. Ilchenko, N. O.; Tasch, B. O. A.; Szabo, K. J., Mild Silver-Mediated Geminal Difluorination of Styrenes Using an Air- and Moisture-Stable Fluoroiodane Reagent. *Angew. Chem., Int. Ed.* **2014**, *53* (47), 12897-12901.
190. Bouvet, S.; Pegot, B.; Diter, P.; Marrot, J.; Magnier, E., Oxidative desulfurization-fluorination reaction promoted by [bdmim][F] for the synthesis of difluorinated methyl ethers. *Tetrahedron Lett.* **2015**, *56* (13), 1682-1686.

191. Belhomme, M.-C.; Besset, T.; Poisson, T.; Pannecoucke, X., Recent Progress toward the Introduction of Functionalized Difluoromethylated Building Blocks onto C(sp²) and C(sp) Centers. *Chem. - Eur. J.* **2015**, *21* (37), 12836-12865.
192. Fier, P. S.; Hartwig, J. F., Copper-Mediated Difluoromethylation of Aryl and Vinyl Iodides. *J. Am. Chem. Soc.* **2012**, *134* (12), 5524-5527.
193. Prakash, G. K. S.; Ganesh, S. K.; Jones, J.-P.; Kulkarni, A.; Masood, K.; Swabeck, J. K.; Olah, G. A., Copper-mediated difluoromethylation of (hetero)aryl iodides and β -styryl Halides with tributyl(difluoromethyl)stannane. *Angew. Chem., Int. Ed.* **2012**, *51* (48), 12090-12094.
194. Gu, Y.; Leng, X.; Shen, Q., Cooperative dual palladium/silver catalyst for direct difluoromethylation of aryl bromides and iodides. *Nat. Commun.* **2014**, *5*, 5405.
195. Krishnamoorthy, S.; Kar, S.; Kothandaraman, J.; Prakash, G. K. S., Nucleophilic difluoromethylation of aromatic aldehydes using trimethyl(trifluoromethyl)silane (TMSCF₃). *J. Fluorine Chem.* **2018**, *208*, 10-14.
196. Romero, N. A.; Nicewicz, D. A., Organic Photoredox Catalysis. *Chem. Rev. (Washington, DC, U. S.)* **2016**, *116* (17), 10075-10166.
197. Xia, J.-B.; Zhu, C.; Chen, C., Visible light-promoted metal-free sp³-C-H fluorination. *Chem. Commun. (Cambridge, U. K.)* **2014**, *50* (79), 11701-11704.
198. Ventre, S.; Petronijevic, F. R.; MacMillan, D. W. C., Decarboxylative Fluorination of Aliphatic Carboxylic Acids via Photoredox Catalysis. *J. Am. Chem. Soc.* **2015**, *137* (17), 5654-5657.
199. Wu, X.; Meng, C.; Yuan, X.; Jia, X.; Qian, X.; Ye, J., Transition-metal-free visible-light photoredox catalysis at room-temperature for decarboxylative fluorination of aliphatic carboxylic acids by organic dyes. *Chem. Commun. (Cambridge, U. K.)* **2015**, *51* (59), 11864-11867.
200. Ma, J.-j.; Yi, W.-b.; Lu, G.-p.; Cai, C., Transition-metal-free C-H oxidative activation: persulfate-promoted selective benzylic mono- and difluorination. *Org. Biomol. Chem.* **2015**, *13* (10), 2890-2894.
201. Douglas, J. J.; Nguyen, J. D.; Cole, K. P.; Stephenson, C. R. J., Enabling novel photoredox reactivity via photocatalyst selection. *Aldrichimica Acta* **2014**, *47* (1), 15-25.
202. Prier, C. K.; Rankic, D. A.; MacMillan, D. W. C., Visible Light Photoredox Catalysis with Transition Metal Complexes: Applications in Organic Synthesis. *Chem. Rev. (Washington, DC, U. S.)* **2013**, *113* (7), 5322-5363.

203. Olah, G. A.; Wang, Q.; Prakash, G. K. S., Synthetic methods and reactions. 170. Boron trifluoride monohydrate, a highly efficient catalyst for thioacetalization. *Catal. Lett.* **1992**, *13* (1-2), 55-60.
204. Zhang, K.; An, J.; Su, Y.; Zhang, J.; Wang, Z.; Cheng, T.; Liu, G., Amphiphilic Hyperbranched Polyethoxysiloxane: A Self-Templating Assembled Platform to Fabricate Functionalized Mesostructured Silicas for Aqueous Enantioselective Reactions. *ACS Catal.* **2016**, *6* (9), 6229-6235.
205. Hopkins, C. R., ACS Chemical Neuroscience Molecule Spotlight on Begacestat (GSI-953). *ACS Chem. Neurosci.* **2012**, *3* (1), 3-4.
206. Egami, H.; Kawamura, S.; Miyazaki, A.; Sodeoka, M., Trifluoromethylation Reactions for the Synthesis of β -Trifluoromethylamines. *Angew. Chem., Int. Ed.* **2013**, *52* (30), 7841-7844.
207. Li, X.; Su, J.; Liu, Z.; Zhu, Y.; Dong, Z.; Qiu, S.; Wang, J.; Lin, L.; Shen, Z.; Yan, W.; Wang, K.; Wang, R., Synthesis of Chiral α -Trifluoromethylamines with 2,2,2-Trifluoroethylamine as a "Building Block". *Org. Lett.* **2016**, *18* (5), 956-959.
208. Fuchigami, T.; Ichikawa, S., Electrolytic Reactions of Fluoroorganic Compounds. 14. Regioselective Anodic Methoxylation of N-(Fluoroethyl)amines. Preparation of Highly Useful Fluoroalkylated Building Blocks. *J. Org. Chem.* **1994**, *59* (3), 607-15.
209. Takaya, J.; Kagoshima, H.; Akiyama, T., Mannich-Type Reaction with Trifluoromethylated N,O-Hemiacetal: Facile Preparation of β -Amino- β -trifluoromethyl Carbonyl Compounds. *Org. Lett.* **2000**, *2* (11), 1577-1579.
210. Xu, Y.; Dolbier, W. R., Jr., Synthesis of Trifluoromethylated Amines Using 1,1-Bis(dimethylamino)-2,2,2-trifluoroethane. *J. Org. Chem.* **2000**, *65* (7), 2134-2137.
211. Crousse, B.; Narizuka, S.; Bonnet-Delpon, D.; Begue, J.-P., First stereoselective synthesis of cis 3-CF₃-aziridine-2-carboxylates. A route to new (trifluoromethyl) α -functionalized β -amino acids. *Synlett* **2001**, (5), 679-681.
212. Ohkura, H.; Handa, M.; Katagiri, T.; Uneyama, K., Diastereoselective Synthesis of S-tert-Butyl- β -(trifluoromethyl)isocysteine. *J. Org. Chem.* **2002**, *67* (8), 2692-2695.
213. Fustero, S.; Navarro, A.; Pina, B.; Soler, J. G.; Bartolome, A.; Asensio, A.; Simon, A.; Bravo, P.; Fronza, G.; Volonterio, A.; Zanda, M., Enantioselective Synthesis of Fluorinated α -Amino Acids and Derivatives in Combination with Ring-Closing Metathesis: Intramolecular π -Stacking Interactions as a Source of Stereocontrol. *Org. Lett.* **2001**, *3* (17), 2621-2624.

214. Kawano, Y.; Kaneko, N.; Mukaiyama, T., Lewis base-catalyzed perfluoroalkylation of carbonyl compounds and imines with (perfluoroalkyl)trimethylsilane. *Bull. Chem. Soc. Jpn.* **2006**, *79* (7), 1133-1145.
215. Pooput, C.; Dolbier, W. R., Jr.; Medebielle, M., Nucleophilic Perfluoroalkylation of Aldehydes, Ketones, Imines, Disulfides, and Diselenides. *J. Org. Chem.* **2006**, *71* (9), 3564-3568.
216. Wang, H.; Zhao, X.; Li, Y.; Lu, L., Solvent-controlled asymmetric Strecker reaction: stereoselective synthesis of α -trifluoromethylated α -amino acids. *Org. Lett.* **2006**, *8* (7), 1379-1381.
217. Zhang, Y.-Q.; Liu, J.-D.; Xu, H., Copper(II)-catalyzed trifluoromethylation of N-aryl imines. *Org. Biomol. Chem.* **2013**, *11* (37), 6242-6245.
218. Rubiales, G.; Alonso, C.; Martinez de Marigorta, E.; Palacios, F., Nucleophilic trifluoromethylation of carbonyl compounds and derivatives. *ARKIVOC (Gainesville, FL, U. S.)* **2014**, (2), 362-405, 44 pp.
219. Prakash, G. K. S.; Mogi, R.; Olah, G. A., Preparation of Tri- and Difluoromethylated Amines from Aldimines Using (Trifluoromethyl)trimethylsilane. *Org. Lett.* **2006**, *8* (16), 3589-3592.
220. Prakash, G. K. S.; Mandal, M.; Olah, G. A., Nucleophilic trifluoromethylation of N-tosyl aldimines. *Synlett* **2001**, (1), 77-78.
221. Pilcher, A. S.; Ammon, H. L.; DeShong, P., Utilization of Tetrabutylammonium Triphenylsilyldifluoride as a Fluoride Source for Nucleophilic Fluorination. *J. Am. Chem. Soc.* **1995**, *117* (18), 5166-7.
222. Medebielle, M.; Dolbier, W. R., Jr., Nucleophilic difluoromethylation and trifluoromethylation using tetrakis(dimethylamino)ethylene (TDAE) reagent. *J. Fluorine Chem.* **2008**, *129* (10), 930-942.
223. Xu, W.; Dolbier, W. R., Jr., Nucleophilic Trifluoromethylation of Imines Using the CF₃I/TDAE Reagent. *J. Org. Chem.* **2005**, *70* (12), 4741-4745.
224. Kawano, Y.; Fujisawa, H.; Mukaiyama, T., Lewis base-catalyzed trifluoromethylation of aldimines with (trifluoromethyl)trimethylsilane. *Chem. Lett.* **2005**, *34* (3), 422-423.
225. Kawano, Y.; Mukaiyama, T., Diastereoselective trifluoromethylation of chiral N-(tolylsulfinyl)imines in the presence of lewis bases. *Chem. Lett.* **2005**, *34* (7), 894-895.
226. Mizuta, S.; Shibata, N.; Sato, T.; Fujimoto, H.; Nakamura, S.; Toru, T., Tri-tert-butylphosphine is an efficient promoter for the trifluoromethylation reactions of aldehydes, ketones, imides and imines. *Synlett* **2006**, (2), 267-270.

227. Fukuda, Y.; Maeda, Y.; Kondo, K.; Aoyama, T., Strecker reaction of aldimines catalyzed by a nucleophilic N-heterocyclic carbene. *Synthesis* **2006**, (12), 1937-1939.
228. Fukuda, Y.; Maeda, Y.; Ishii, S.; Kondo, K.; Aoyama, T., An N-heterocyclic carbene as a nucleophilic catalyst for cyanosilylation of aldehydes. *Synthesis* **2006**, (4), 589-590.
229. Song, J. J.; Gallou, F.; Reeves, J. T.; Tan, Z.; Yee, N. K.; Senanayake, C. H., Activation of TMSCN by N-Heterocyclic Carbenes for Facile Cyanosilylation of Carbonyl Compounds. *J. Org. Chem.* **2006**, *71* (3), 1273-1276.
230. Suzuki, Y.; Abu Bakar, M. D.; Muramatsu, K.; Sato, M., Cyanosilylation of aldehydes catalyzed by N-heterocyclic carbenes. *Tetrahedron* **2006**, *62* (17), 4227-4231.
231. Wang, Y.; Xing, F.; Gu, C.-Z.; Li, W.-J.; He, L.; Dai, B.; Du, G.-F., N-heterocyclic carbene-catalyzed fluorinated silyl-Reformatsky reaction of aldehydes with difluoro (trimethylsilyl) acetate. *Tetrahedron* **2017**, *73* (30), 4501-4507.
232. Arduengo, A. J., III; Krafczyk, R.; Schmutzler, R.; Craig, H. A.; Goerlich, J. R.; Marshall, W. J.; Unverzagt, M., Imidazolylidenes, imidazolinyliidenes and imidazolidines. *Tetrahedron* **1999**, *55* (51), 14523-14534.
233. Sharghi, H.; Hosseini-Sarvari, M.; Ebrahimpourmoghaddam, S., A novel method for the synthesis of N-sulfonyl aldimines using AlCl₃ under solvent-free conditions. *ARKIVOC (Gainesville, FL, U. S.)* **2007**, (15), 255-264.
234. Kraiem, J.; Ghedira, D.; Ollevier, T., Hydrogen peroxide/dimethyl carbonate: a green system for epoxidation of N-alkylimines and N-sulfonylimines. One-pot synthesis of N-alkyloxaziridines from N-alkylamines and (hetero)aromatic aldehydes. *Green Chem.* **2016**, *18* (18), 4859-4864.
235. Vlahos, C. J.; McDowell, S. A.; Clerk, A., Kinases as therapeutic targets for heart failure. *Nat. Rev. Drug Discovery* **2003**, *2* (2), 99-113.
236. Strebhardt, K., Multifaceted polo-like kinases: drug targets and antitargets for cancer therapy. *Nat. Rev. Drug Discovery* **2010**, *9* (8), 643-660.
237. Sawyers, C. L., Rational therapeutic intervention in cancer: kinases as drug targets. *Curr Opin Genet Dev* **2002**, *12* (1), 111-5.
238. Gust, T.; von Bonin, A. In *Kinases as drug targets in inflammation: in vitro and in vivo target validation and expression profiling*, Transworld Research Network: 2007; pp 31-49.

239. Cohen, P.; Alessi, D. R., Kinase Drug Discovery - What's Next in the Field? *ACS Chem. Biol.* **2013**, *8* (1), 96-104.
240. Catapano, L. A.; Manji, H. K., Kinases as drug targets in the treatment of bipolar disorder. *Drug Discovery Today* **2008**, *13* (7/8), 295-302.
241. Brehm, K., Protein kinases as drug targets in the treatment of alveolar echinococcosis. *Drug Discovery Infect. Dis.* **2014**, *5* (Protein Phosphorylation in Parasites), 357-373.
242. Merritt, C.; Silva, L. E.; Tanner, A. L.; Stuart, K.; Pollastri, M. P., Kinases as Druggable Targets in Trypanosomatid Protozoan Parasites. *Chem. Rev.* (Washington, DC, U. S.) **2014**, *114* (22), 11280-11304.
243. Kini, S. G.; Garg, V.; Prasanna, S.; Rajappan, R.; Mubeen, M., Protein Kinases as Drug Targets in Human and Animal Diseases. *Curr. Enzyme Inhib.* **2017**, *13* (2), 99-106.
244. Ferguson, F. M.; Gray, N. S., Kinase inhibitors: the road ahead. *Nat. Rev. Drug Discovery* **2018**, *17* (5), 353-377.
245. Sontag, J.-M.; Sontag, E., Protein phosphatase 2A dysfunction in Alzheimer's disease. *Front Mol Neurosci* **2014**, *7*, 16.
246. Sontag, J.-M.; Nunbhakdi-Craig, V.; White, C. L., 3rd; Halpain, S.; Sontag, E., The protein phosphatase PP2A/B α binds to the microtubule-associated proteins Tau and MAP2 at a motif also recognized by the kinase Fyn: implications for tauopathies. *J Biol Chem* **2012**, *287* (18), 14984-93.
247. Visser, R.; Landman, E. B. M.; Goeman, J.; Wit, J. M.; Karperien, M., Sotos syndrome is associated with deregulation of the MAPK/ERK-signaling pathway. *PLoS One* **2012**, *7* (11), e49229.
248. Singh, S.; Gupta, P. D., Deregulation of intermediate filament protein phosphorylation leads to pathogenesis: a review. *Biomed. Lett.* **1999**, *59* (231), 27-32.
249. Shukla, V.; Skuntz, S.; Pant, H. C., Deregulated Cdk5 Activity Is Involved in Inducing Alzheimer's Disease. *Arch. Med. Res.* **2012**, *43* (8), 655-662.
250. Saito, T.; Hisanaga, S.-i., Synaptic function of CDK5 and its deregulation in neurodegenerative diseases. *Jikken Igaku* **2013**, *31* (2, Zokan), 265-270.
251. Lu, K. P., Pinning down cell signaling, cancer and Alzheimer's disease. *Trends Biochem. Sci.* **2004**, *29* (4), 200-209.

252. Jeon, G. S.; Kim, K. Y.; Hwang, Y. J.; Jung, M.-K.; An, S.; Ouchi, M.; Ouchi, T.; Kowall, N.; Lee, J.; Ryu, H., Deregulation of BRCA1 Leads to Impaired Spatiotemporal Dynamics of γ -H2AX and DNA Damage Responses in Huntington's Disease. *Mol. Neurobiol.* **2012**, *45* (3), 550-563.
253. Zhang, J.; Yang, P. L.; Gray, N. S., Targeting cancer with small molecule kinase inhibitors. *Nat. Rev. Cancer* **2009**, *9* (1), 28-39.
254. Wu, P.; Nielsen, T. E.; Clausen, M. H., FDA-approved small-molecule kinase inhibitors. *Trends Pharmacol. Sci.* **2015**, *36* (7), 422-439.
255. Cruz, J. C.; Tsai, L.-H., Cdk5 deregulation in the pathogenesis of Alzheimer's disease. *Trends Mol. Med.* **2004**, *10* (9), 452-458.
256. Malumbres, M., Cyclin-dependent kinases. *Genome Biol* **2014**, *15* (6), 122.
257. Wagey, R. T. E.; Krieger, C., Abnormalities of protein kinases in neurodegenerative diseases. *Prog. Drug Res.* **1998**, *51*, 133-183.
258. Shchemelinin, I.; Sefc, L.; Necas, E., Protein kinases, their function and implication in cancer and other diseases. *Folia Biol (Praha)* **2006**, *52* (3), 81-100.
259. Botta, M., New Frontiers in Kinases: Special Issue. *ACS Med. Chem. Lett.* **2014**, *5* (4), 270.
260. Fedorov, O.; Mueller, S.; Knapp, S., The (un)targeted cancer kinome. *Nat. Chem. Biol.* **2010**, *6* (3), 166-169.
261. Wu, P.; Nielsen, T. E.; Clausen, M. H., Small-molecule kinase inhibitors: an analysis of FDA-approved drugs. *Drug Discovery Today* **2016**, *21* (1), 5-10.
262. Druker, B. J.; Talpaz, M.; Resta, D. J.; Peng, B.; Buchdunger, E.; Ford, J. M.; Lydon, N. B.; Kantarjian, H.; Capdeville, R.; Ohno-Jones, S.; Sawyers, C. L., Efficacy and safety of a specific inhibitor of the BCR-ABL tyrosine kinase in chronic myeloid leukemia. *N. Engl. J. Med.* **2001**, *344* (14), 1031-1037.
263. Steelman, L. S.; Pohnert, S. C.; Shelton, J. G.; Franklin, R. A.; Bertrand, F. E.; McCubrey, J. A., JAK/STAT, Raf/MEK/ERK, PI3K/Akt and BCR-ABL in cell cycle progression and leukemogenesis. *Leukemia* **2004**, *18* (2), 189-218.
264. Winter, G. E.; Rix, U.; Carlson, S. M.; Gleixner, K. V.; Grebien, F.; Gridling, M.; Mueller, A. C.; Breitwieser, F. P.; Bilban, M.; Colinge, J.; Valent, P.; Bennett, K. L.; White, F. M.; Superti-Furga, G., Systems-pharmacology dissection of a drug synergy in imatinib-resistant CML. *Nat. Chem. Biol.* **2012**, *8* (11), 905-912.
265. Panjarian, S.; Iacob, R. E.; Chen, S.; Engen, J. R.; Smithgall, T. E., Structure and Dynamic Regulation of Abl Kinases. *J. Biol. Chem.* **2013**, *288* (8), 5443-5450.

266. Sharma, S.; Mehndiratta, S.; Kumar, S.; Singh, J.; Bedi, P. M. S.; Nepali, K., Purine analogues as kinase inhibitors: A review. *Recent Pat. Anti-Cancer Drug Discovery* **2015**, *10* (3), 308-341.
267. Sala, M.; Kogler, M.; Plackova, P.; Mejdrova, I.; Hrebabecky, H.; Prochazkova, E.; Strunin, D.; Lee, G.; Birkus, G.; Weber, J.; Mertlikova-Kaiserova, H.; Nencka, R., Purine analogs as phosphatidylinositol 4-kinase III β inhibitors. *Bioorg. Med. Chem. Lett.* **2016**, *26* (11), 2706-2712.
268. Lee, A. D.; Ren, S.; Lien, E. J., Purine analogs as CDK enzyme inhibitory agents: A survey and QSAR analysis. *Prog. Drug Res.* **2001**, *56*, 155-193.
269. Konstantopoulos, N.; Marcuccio, S.; Kyi, S.; Stoichevska, V.; Castelli, L. A.; Ward, C. W.; Macaulay, S. L., A purine analog kinase inhibitor, calcium/calmodulin-dependent protein kinase II inhibitor 59, reveals a role for calcium/calmodulin-dependent protein kinase II in insulin-stimulated glucose transport. *Endocrinology* **2007**, *148* (1), 374-385.
270. Kolodziej, M.; Goetz, C.; Di Fazio, P.; Montalbano, R.; Ocker, M.; Strik, H.; Quint, K., Roscovitine has anti-proliferative and pro-apoptotic effects on glioblastoma cell lines: a pilot study. *Oncol. Rep.* **2015**, *34* (3), 1549-1556.
271. Gray, N. S.; Wodicka, L.; Thunnissen, A.-M. W. H.; Norman, T. C.; Kwon, S.; Espinoza, F. H.; Morgan, D. O.; Barnes, G.; LeClerc, S.; Meijer, L.; Kim, S.-H.; Lockhart, D. J.; Schultz, P. G., Exploiting chemical libraries, structure, and genomics in the search for kinase inhibitors. *Science (Washington, D. C.)* **1998**, *281* (5376), 533-538.
272. Hisanaga, S.-i.; Endo, R., Regulation and role of cyclin-dependent kinase activity in neuronal survival and death. *J. Neurochem.* **2010**, *115* (6), 1309-1321.
273. Endo, R.; Saito, T.; Asada, A.; Kawahara, H.; Ohshima, T.; Hisanaga, S.-I., Commitment of 1-Methyl-4-phenylpyridinium Ion-induced Neuronal Cell Death by Proteasome-mediated Degradation of p35 Cyclin-dependent Kinase 5 Activator. *J. Biol. Chem.* **2009**, *284* (38), 26029-26039.
274. Lopes, J. P.; Oliveira, C. R.; Agostinho, P., Neurodegeneration in an A β -induced model of Alzheimer's disease: the role of Cdk5. *Aging Cell* **2010**, *9* (1), 64-77.
275. Zheng, Y.-L.; Amin, N. D.; Hu, Y.-F.; Rudrabhatla, P.; Shukla, V.; Kanungo, J.; Kesavapany, S.; Grant, P.; Albers, W.; Pant, H. C., A 24-Residue Peptide (p5), Derived from p35, the Cdk5 Neuronal Activator, Specifically Inhibits Cdk5-p25 Hyperactivity and Tau Hyperphosphorylation. *J. Biol. Chem.* **2010**, *285* (44), 34202-34212.

276. Helal, C. J.; Kang, Z.; Lucas, J. C.; Gant, T.; Ahlijanian, M. K.; Schachter, J. B.; Richter, K. E. G.; Cook, J. M.; Menniti, F. S.; Kelly, K.; Mente, S.; Pandit, J.; Hosea, N., Potent and cellularly active 4-aminoimidazole inhibitors of cyclin-dependent kinase 5/p25 for the treatment of Alzheimer's disease. *Bioorg Med Chem Lett* **2009**, *19* (19), 5703-7.
277. Akue-Gedu, R.; Debiton, E.; Ferandin, Y.; Meijer, L.; Prudhomme, M.; Anizon, F.; Moreau, P., Synthesis and biological activities of aminopyrimidyl-indoles structurally related to meridianins. *Bioorg. Med. Chem.* **2009**, *17* (13), 4420-4424.
278. Helal, C. J.; Kang, Z.; Lucas, J. C.; Gant, T.; Ahlijanian, M. K.; Schachter, J. B.; Richter, K. E. G.; Cook, J. M.; Menniti, F. S.; Kelly, K.; Mente, S.; Pandit, J.; Hosea, N., Potent and cellularly active 4-aminoimidazole inhibitors of cyclin-dependent kinase 5/p25 for the treatment of Alzheimer's disease. *Bioorg. Med. Chem. Lett.* **2009**, *19* (19), 5703-5707.
279. Oumata, N.; Bettayeb, K.; Ferandin, Y.; Demange, L.; Lopez-Giral, A.; Goddard, M.-L.; Myriantopoulos, V.; Mikros, E.; Flajolet, M.; Greengard, P.; Meijer, L.; Galons, H., Roscovitine-Derived, Dual-Specificity Inhibitors of Cyclin-Dependent Kinases and Casein Kinases 1. *J. Med. Chem.* **2008**, *51* (17), 5229-5242.
280. Otyepka, M.; Bartova, I.; Kriz, Z.; Koca, J., Different Mechanisms of CDK5 and CDK2 Activation as Revealed by CDK5/p25 and CDK2/Cyclin A Dynamics. *J. Biol. Chem.* **2006**, *281* (11), 7271-7281.
281. Bettayeb, K.; Sallam, H.; Ferandin, Y.; Popowycz, F.; Fournet, G.; Hassan, M.; Echaliier, A.; Bernard, P.; Endicott, J.; Joseph, B.; Meijer, L., N-&N, a new class of cell death-inducing kinase inhibitors derived from the purine roscovitine. *Mol. Cancer Ther.* **2008**, *7* (9), 2713-2724.
282. Zatloukal, M.; Gemrotova, M.; Dolezal, K.; Havlicek, L.; Spichal, L.; Strnad, M., Novel potent inhibitors of *A. thaliana* cytokinin oxidase/dehydrogenase. *Bioorg. Med. Chem.* **2008**, *16* (20), 9268-9275.
283. Wilson, S. C.; Atrash, B.; Barlow, C.; Eccles, S.; Fischer, P. M.; Hayes, A.; Kelland, L.; Jackson, W.; Jarman, M.; Mirza, A.; Moreno, J.; Nutley, B. P.; Raynaud, F. I.; Sheldrake, P.; Walton, M.; Westwood, R.; Whittaker, S.; Workman, P.; McDonald, E., Design, synthesis and biological evaluation of 6-pyridylmethylaminopurines as CDK inhibitors. *Bioorg. Med. Chem.* **2011**, *19* (22), 6949-6965.
284. Denton, T. T.; Zhang, X.; Cashman, J. R., 5-Substituted, 6-Substituted, and Unsubstituted 3-Heteroaromatic Pyridine Analogues of Nicotine as Selective Inhibitors of Cytochrome P-450 2A6. *J. Med. Chem.* **2005**, *48* (1), 224-239.

VITA

Jatin Mehta was born in 1980 in Haryana, India. He received his primary, middle, and high school education in Ambala City, India. He received his Bachelor's Degree in Science (Chemistry, Botany, and Zoology) from Kurukshetra University in June 2002 and a Master's degree in Industrial Chemistry, with first division, in June 2004 from Kurukshetra University, India. In January 2013, Jatin joined the Missouri University of Science and Technology (M S&T) to pursue his Ph.D. He was also a Teaching Assistant in the Department of Chemistry at M S&T. In December 2018, Jatin received his Ph.D. in Chemistry from Missouri University of Science and Technology, under the direction of Dr. V. Prakash Reddy.